Université de Neuchâtel **Institut de Géologie**

Formation and transport of CH_4 and CO_2 in deep peatlands

Isotope geochemical analysis and numerical modelling based on field research at the Etang de la Gruère Bog in Switzerland

Thèse

Présentée à la Faculté des Sciences de l'Université de Neuchâtel (Suisse)
pour l'obtention du grade de

Docteur ès Sciences

par

BERND EILRICH

2002

Jury:

PROF. KARL B. FÖLLMI (Neuchâtel) *directeur de thèse*
DR. PHILIPP STEINMANN (Neuchâtel) co-*directeur de thèse*

PROF. STEPHEN J. BURNS (Amherst, Massachusetts)
PROF. JEAN-MICHEL GOBAT (Neuchâtel)
DR. MARKUS LEUENBERGER (Berne)

TABLE OF CONTENTS

© B. Eilrich, 2002
All rights reserved.

1 FOREWORD

1.1 Structure of this manuscript

The main results of research are presented in three papers, which constitute the body of this thesis. They focus on the pore water geochemistry of the Etang de la Gruère Bog and on its implications for microbial methanogenic pathways and gas transport in peatlands.
An introductory **chapter (2)** states the objective of this study and explains the significance of peatland carbon mineralisation and methanogenesis. Current developments in this field of research are briefly reviewed to address the open questions. The following chapters reflect the course of the investigation with fieldwork, laboratory analysis, modelling and interpretation. The field site with its geological and climatological characteristics is presented in **chapter 3**. **Chapter 4** describes the methods applied in the field and in the laboratory. Particular emphasis is put on those methods and instruments, which have especially been designed or adapted for deep peat pore water research and have been used by the author of this study. Results, which have not been included in the papers, are presented in **chapter 5**.
The three papers bear the most important outcome of this study. They are incorporated in **chapter 6** and appear in a non-finalised version. Some information may occur more than one time, especially in the introductions and discussions. Some general conclusions **(chapter 7)** are intended to bring the various implications of these three studies together and indicate, where further research is needed. The summary of this thesis, given in **chapter 8** in English, French and German language, is followed by the acknowledgements and references **(chapters 9 and 10)**. Tables containing analytical data and additional information are provided in the appendices.

1.2 Context of this work

A wide range of biological, geochemical and hydrological issues have already been studied at the Etang de la Gruère, one of Switzerland's largest remaining peat bogs. Among other scientists, the main applicant for this research project (P. Steinmann, Neuchâtel University) investigated the Etang de la Gruère for his PhD thesis. Dr. Steinmann's studies focussed on the geochemistry of peat and pore water. The here presented research can be seen as a continuation of his work, broadening certain aspects of peat pore water chemistry and addressing new questions, while inevitably neglecting others. It represents a pluridisciplinary approach involving partners from the Geochemical and Environmental Analysis Group at the Geological Institute and the Microbiology Laboratory at the Botanical Institute of Neuchâtel University as well as the Stable Isotope Laboratories of the Geological Institute and of the Division of Climate and Environmental Physics at the Physics Institute of Bern University.

1.3 Financial support

This research project has been funded by the Swiss National Sciences Foundation (SNF), grants nos. 21-55630.98 and 20-63841.00. A 12.5 % assistant position within the Institute of Geology has been made available to the author since February 2000. The IGBP poster award on the occasion of the "First Swiss Global Change Day" helped financing the author's participation at the Goldschmidt 2000 Conference in Oxford, UK.

2 INTRODUCTION

This study deals with peatland geochemistry. It is based on field research at the Etang de la Gruère Bog (EGr) in Switzerland and focuses on methane (CH_4) and carbon dioxide (CO_2) formation and transport in the lower peat layers, the so-called catotelm. Both CO_2 and methane are important greenhouse gases.

2.1 Ombrotrophic and minerotrophic mires

Bogs such as EGr receive their water and nutrient supply solely from the atmosphere (precipitation, dust). They are also referred to as "ombrotrophic" or "ombrogenous" mires (gr. ombros = rain). **Fen peats**, by contrast, are predominantly fed by mineral-rich water, e.g. ground water or river water, and are therefore sometimes named "minerotrophic" or "minerogenous" mires. Table 2-1 summarises the similarity and differences of these two major peatland types.

Table 2-1: Summary of major bog and fen characteristics according to Maltby and Proctor (1997) and IPCC (1996).

	fen peat (minerotrophic)	**bog (ombrotrophic)**
habitat	waterlogged	waterlogged
water and solute supply	predominantly ground water	atmospheric input
average depth	generally <2 m	between 2 and 12 m in most cases
mineral content	relatively high	very low
ash content	high (10 % and more)	low (ca. 3 %)
pH in near surface pore waters	7 - 8	3 - 4.5
C : N ratio	<20	>30
C : P ratio	<100 in most cases	>1000 in most cases

Bogs can further be subdivided into two different types, blanket bogs and raised bogs (Fig. 2-1). **Blanket bogs** extend over the landscape like a blanket and consist of relatively thin peat, which follows the underlying topography. **Raised bogs** such as the EGr are gently domed areas of acid peat, which develop typically over fen peats of filled-in lake basins, over coastal flats or river floodplains (Maltby and Proctor, 1997). It is interesting to note that by weight, a raised bog in its upper fresh part may be up to 98 % water and only 2 % solid peat[1] (IPCC, 1996). Blanket bogs are rather more solid with up to 85 % water.[2]

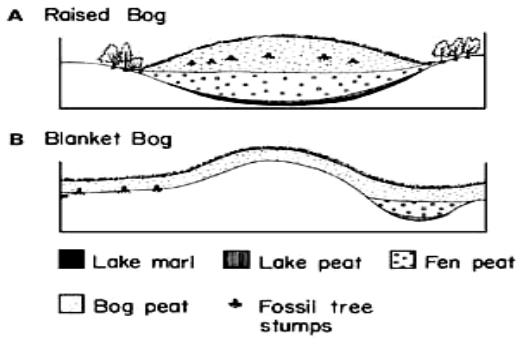

Fig. 2-1: Schematic illustration of the two major bog types. Type A corresponds to the investigated convex-shape part of the Etang de la Gruère Bog and may reach a thickness of several meters. Type B is relatively thin (<1 m in most cases) and much more frequent at low altitudes. So-called "Atlantic blanket bogs" below 200 m asl. are distinguished from "mountain blanket bogs" above 200 m asl. (according to IPCC, 1996).

[1] A raised peat bog may hence contain fewer solids than, for example, milk.
[2] This great volume of water is held within the dead *Sphagnum* fragments. The ability to retain water is one of the properties, which makes *Sphagnum* peat a prized horticultural material (IPCC, 1996).

2.2 Occurrence of peatlands in general …

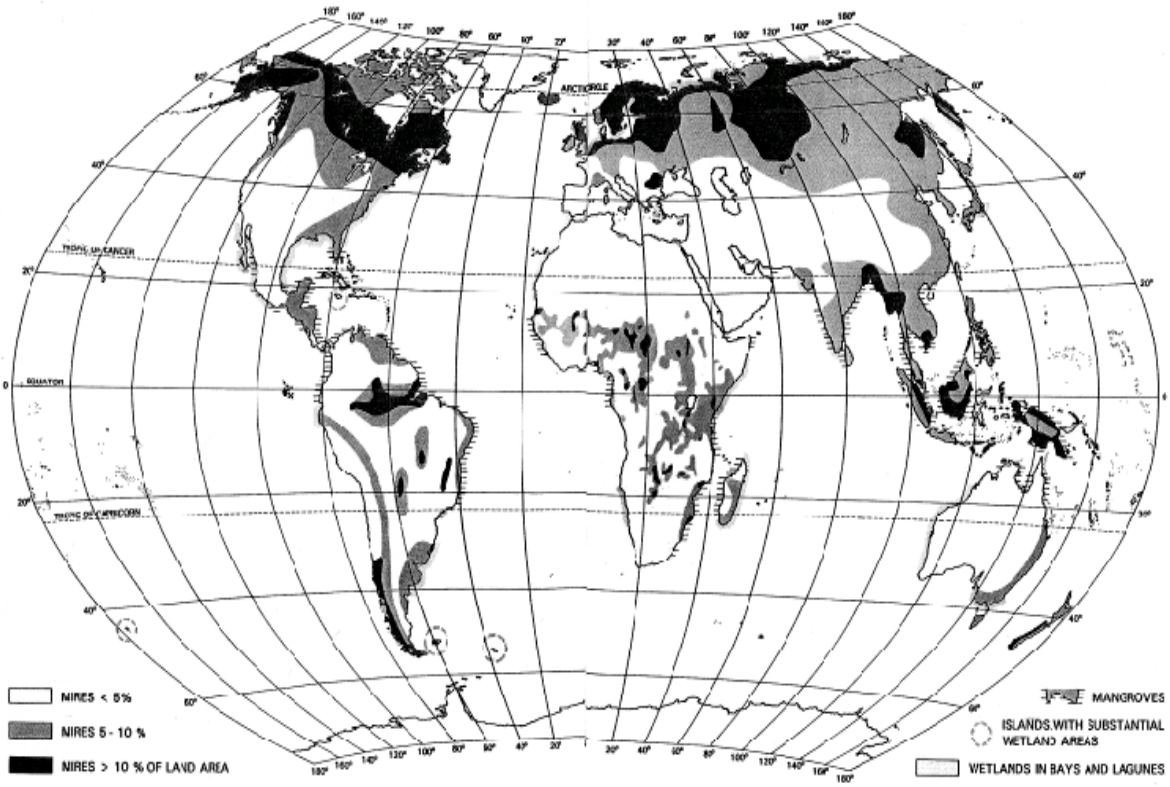

Fig. 2-2: Map showing the global distribution of peatlands (mires with a minimum peat thickness of 30 cm; according to Lappalainen, 1997). In this figure, however, the percentage of remaining peatlands in northern Central Europe is overestimated (K. Föllmi - pers. comm.).

Fig. 2-2 shows the global distribution of "peatlands" in a wide sense, i.e. including also marshlands, gleysols, tundra soils, fluvisols and other histosols (peat soils), yet, no swamps are included, such as those at the mouths of the rivers Guadalquivir in Spain and Nile in Egypt. A map showing the location of important mires in Switzerland is given in Fig. 2-3. Estimates of the total area of the World's peatlands (bogs and fens only) vary considerably from about 1.1 (Bülow, 1929; Nikonow and Sluka, 1964) and ca. 5 (Kivinen and Pakarinen, 1981) to 6 million km^2 (Maltby, 1988). One reason for this large variation is certainly the age of the estimates and the problems encountered when doing such a global survey (lack of detailed information about remote areas, use and availability of survey methods, e.g. aerial and satellite imagery). Another reason is the still ongoing loss of peatlands, e.g. by transformation in agricultural soils (e.g. Dungan, 1990; Inisheva 2000). The basic problem, however, is to distinguish areas where the peat layer is 30 cm at minimum from areas just covered by wetland vegetation (floodplains, coastal lagoons, mangroves, swamps). On this basis, a detailed and more recent analysis is provided by Lappalainen (1997), who estimated the global peatland area at 3,985,000 km^2. This area represents about 3 % of the Earth's total ice-free land surface. The global peatlands contain some 5 to $6*10^{12}$ t of wet peat (Lappalainen, 1997).

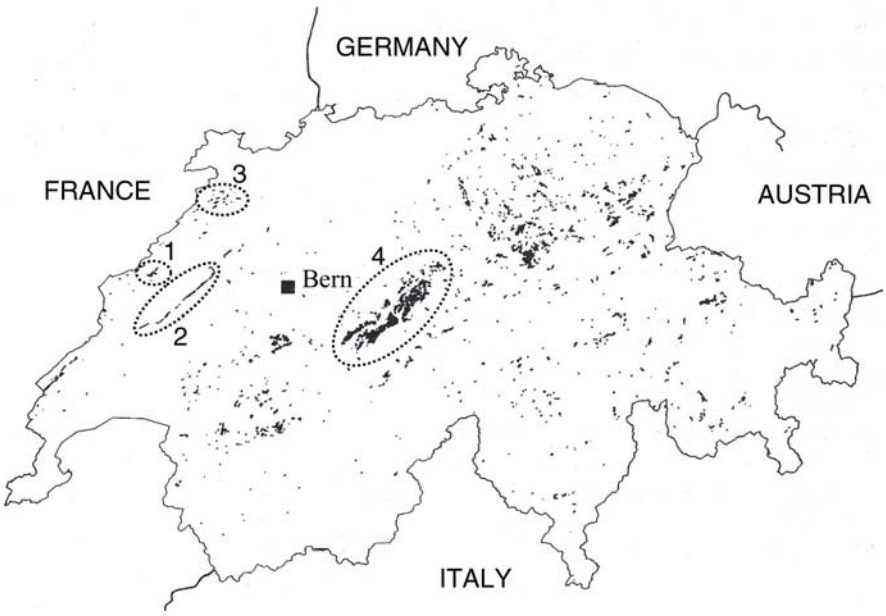

Fig. 2-3: Distribution of mires of national importance in Switzerland (according to Küttel, 1997).
1 - Vallée de Sagne;
2 - Along the southeastern shore of Lake Neuchâtel;
3 - Franches Montagnes;
4 - Berner Oberland and central Switzerland north of Lake Thun and Lake Brienz.

… and of ombrotrophic mires in particular

As ombrotrophic mires (bogs) are entirely dependent on atmospheric input for their water and nutrient supply, they only develop in humid regions without seasonally too pronounced deficits in precipitation[3]. Hence they occur predominantly in temperate latitudes (generally between 50 to 70° N, in mountainous regions also further south) in Europe, Asia, western North America and somewhat further south in eastern North America (Maltby and Proctor, 1997; Malterer, 1997; Rubec, 1997). Along with fen peats, these ombrotrophic mires are often referred to as "northern hemisphere peatlands" (e.g. Fung, et al., 1991), because their occurrence is very much restricted in the southern hemisphere due to the absence of landmass in the corresponding latitudes.[4] The northern limit for accumulation of deep peat in ombrotrophic mires is probably set by declining primary production and longer frost periods at high latitudes. The extensive subarctic and low-arctic peatlands are generally shallower, more acidic and nutrient-poor (Gore, 1983; Whigham et al., 1993). The southern and eastern limits of northern hemisphere peatlands are probably determined by the maximum tolerable summer water deficit, at which net accumulation of peat can take place (Maltby and Proctor, 1997). An example for huge northern hemisphere peatlands is the west Siberian Great Vasjugan Bog (cf. Fig. 3-7), from which pore water samples have been obtained in the course of this study (cf. chapters 3.2, 11.AI-3, and 11.AII-14). The Great Vasjugan Bog is the world's largest coherent mire. It covers an area of more than 50,000 km^2 (Inisheva et al., 2000).

Ombrotrophic mires do also occur in tropical regions, e.g. in Amazonia, Equatorial Africa and Southeast Asia (Fig. 2-2). Tropical bogs are primarily distinct from northern peatlands by vegetation. Usually, they are tree-covered, their pore water chemistry and ash (non-organic matter) content, however, clearly indicate ombrotrophic origin. Domed bogs, e.g. near Riau on the Indonesian island of Sumatra, may reach 10 m or more of peat thickness (Rieley et al., 1997).

[3] In turn, carbon isotopes in bog plants may be used as climatic indicators (Ménot and Burns, 2001).
[4] Some smaller peatlands, however, can be found on the South Island of New Zealand (Dobson, 1979), the Falkland Islands and southern Patagonia (Rabassa et al., 1997) for instance.

2.3 Acrotelm and catotelm

Each bog reveals its individual peat stratigraphy (layering) with specific characteristics for the fibric matrix, the degree of decomposition and compaction, the hydraulic conductivity, the ash (i.e. non-organic matter) content, and so forth. Despite the multitude of individual characteristics, two principal zones are usually common to all bogs. The upper zone is called the **acrotelm** or the root-zone[5]. The acrotelm is a thin layer, generally only some 30 cm deep. It consists of fibres of predominantly *Sphagnum* (e.g. *Sphagnum fuscum*, *Sphagnum magellanicum*) mosses, which are largely still alive, often in upright position and colourful with red, yellows and ochre. Rainwater can move relatively rapidly through this layer. The water level and the degree of oxygenation in this zone are subject to seasonal change. The zone below the acrotelm comprising the bulk of the peat and reaching to the ground of the bog is known as the **catotelm**. The catotelm is generally much thicker than the acrotelm and always water-saturated. It consists of often significantly decomposed peat, where individual plant stems have collapsed under the weight of mosses above them and have produced an amorphous, dark-coloured fibric mass of plant fragments. Water movement through this amorphous peat is slow - typically much less than 0.1 m per day (IPCC, 1996). In consequence of water saturation and organic matter decomposition, the catotelm is permanently anaerobic.

2.4 Geochemistry of ombrotrophic mires

Ombrotrophic mires are extremely low in nutritive elements. This is a direct consequence of the conditions of formation and particularly true for nitrogen (N) and phosphorus (P); cf. Table 2-1. Aerts et al. (1992) showed that in natural remote bogs N is limiting to plant growth, while in bogs closer to areas, which are more influenced by human activity and predominantly by agriculture, the limiting nutritive element is P.

Potassium (K) is another major nutrient for plants and animals and also tightly cycled. Typically, K concentrations are highest in the active vegetation zone at the top of the bog. Absolute concentrations, however, are low (<1 $mg*l^{-1}$, cf. Table 2-2) and fluctuate more widely during the seasons and from bog to bog than other major elements such as sodium (Na), magnesium (Mg), and calcium (Ca) (Maltby and Proctor, 1997). As can be inferred from Table 2-2, the concentrations of all major elements are very variable from place to place, although the absolute concentrations are small compared to other fresh water systems. Due to low pH as well as abundant dissolved organic matter (and hence increased solubility and complexation), bog waters are enriched in elements like aluminium (Al), manganese (Mn) and iron (Fe) relative to "normal" freshwaters (Ramann, 1895; Shotyk, 1997). The relative abundance of Fe in mire surface waters is often apparent as iridescent, 'oily' film of chalybeate ('containing iron') waters, which have come in contact with air (cf. Shotyk, 1988). This phenomenon has been reported in numerous publications (e.g. Dachnowski, 1912; Puustjärvi, 1952, Armstrong and Boatman, 1967).

[5] The term "root-zone" is misleading, because in strict biological sense *Sphagnum* mosses, which are the most important plant species in raised mires, do not have roots. Their stems continue to grow at the surface during peat accumulation and may be as long as 30 - 40 cm below the surface. Alike other typical peatland plants, they have well developed aerenchyma, allowing oxygen to diffuse down from the above ground parts (Crum, 1984). An example for a widespread bog plant with roots is *Eriophorum*.

In near surface bog waters, chloride, bicarbonate, and sulphate[6] are the major inorganic anions (Maltby and Proctor, 1997). Some 10 to 30 %[7] of the total anion charge is accounted for by the dissolved organic matter, e.g. humic, fulvic, or carboxylic acids (Maltby and Proctor, 1997). Most investigations show low but relative constant chloride concentrations in the order of 0.2 - 1 mg*l^{-1} (Steinmann and Shotyk, 1997a, Wind-Mulder and Vitt, 2000). Chloride concentrations in peat bogs can be up to 10 times higher than in rainwater because of mixing of the bog pore water with nearby ground waters (Steinmann and Shotyk, 1994; cf. Table 2-2). Below the acrotelm, nitrate (NO_3^-), sulphate (SO_4^{2-}) and phosphate (PO_4^{3-}) concentrations are rapidly diminishing to virtually zero, yet may again increase towards the ground (Brown, 1985; Steinmann, 1995). There is no general rule for the concentration change in the peat bog profile. While the Mn concentration is usually decreasing with depth (Shotyk, 1986) due to precipitation at the top under less reducing conditions ("redox recycling"), the Mg and Ca concentrations are generally increasing with depth (e.g. Steinmann, 1995). At EGr, the average concentration increase from pore waters at 0.5 m depth to pore waters at 5 m depth, is about 2 fold for Na, 5 fold for K, 50 fold for Ca, and 100 fold for Mg (cf. chapter 5.1). The main reason for this concentration increase is an increased influence of the substratum (clays and marls at EGr; cf. chapter 3.1.2) on the bog pore water chemistry.
Moreover, at the time when the deeper peat layers formed, these were situated much closer to the substratum and in touch with mineral rich ground waters ("fen peat", cf. chapter 2.1). Peat layers in the lower bog may therefore still show "fen conditions" (Shotyk et al., 2001) and continue to be an ion source for the peat pore water. The groundwater represents another important source, from which ions may derive by mixing and diffusion (McKenzie et al., 2002).

Table 2-2: Chemical composition of bog surface waters versus typical freshwaters (modified from Shotyk, 1989a).

Constituent	Typical freshwater	Typical bog surface water	Selected bog surface waters	
			Inisheva et al. (2000)	according to Shotyk (1989a)
Na (mg/l)	7.2[a]; 0.14[m]	2 - 5[f]	0.6	0.3[i]
K (mg/l)	1.4[a]; 0.09[m]	<1[f]	n.i.	0.2[i]
Mg (mg/l)	3.7[a]; 0.04[m]	0.5 - 1[f]	1.6	0.3[i]
Ca (mg/l)	14.7[a]; 0.36[m]	0.5 - 1[f]	1.9	0.7[i]
Al (µg/l)	50[b]	300 - 1500[g]	n.i.	280[j]
Fe (µg/l)	40[b]	100 - 6000[g]	n.i.	440[j]
Mn (µg/l)	8[b]	30 - >1000[g,h]	n.i.	30[h]
Cl^- (mg/l)	5.8[a]; 0.3[m]	0.2 - 1[k]	n.i.	n.i.
HCO_3^- (mg/l)	53.0[a]	0 - 5.5[g]	3.6	0[d]
SO_4^{2-} (mg/l)	2.9[c]; 2.15[m]	0.1 - 5[g]	0.5	n.i.
Total N_{aq} (mg/l)	>1.4[c]; >2.5[m]	0.5 - 2[g]	>0.7	n.i.
DOC (mg/l)	ca. 10[d]	25 - 75[d]	n.i.	25 - 75[d]
O_{2aq} (mg/l)	9 (at T = 25 °C)[d]	0 (subsurface)[d]	n.i.	0 (subsurface)[d]
pH	ca. 7.5[e]; 4.96[m]	3.5 - 4.5[f]	4.0	ca. 4[d]

[6] The sulphate concentrations in bog pore waters are however often overestimated as a consequence of organic sulphide oxidation in the sample. Sulphate concentration analysis carried out directly after sampling for this study showed only minor (<150 ppb) concentrations, which declined rapidly with depth (cf. chapter 11.AII).
[7] Oxidation effects during sample taking and storage potentially lead to an overestimation of the sulphate concentration and may, in turn, cause an underestimation of the dissolved organic matter concentration. The analysis of bog pore water sampled with particular care (e.g. sampling under a nitrogen atmosphere) demonstrated that the share of dissolved organic matter in the total anion charge could be as high as 80 % (Steinmann and Shotyk, 1997a).

[a] World average river water (Berner and Berner, 1987)
[b] Typical freshwater composition (Drever, 1997)
[c] Likens et al. (1977) in Drever (1982)
[d] Shotyk (1989)
[e] Calculated from $[HCO_3^-]$ assuming $pCO_2 = 10^{-3.0}$ bar
[f] Maltby and Proctor (1987)
[g] Shotyk (1988)
[h] Shotyk (1987)
[i] Gorham et al. (1985)
[j] Urban et al. (1987)
[k] Wind-Mulder and Witt (2000)
[m] Average chemical composition of wet deposition at Payerne, 1985-1991 (EMPA 1985-1991; in Steinmann and Shotyk, 1994)
n.i. not indicated

2.5 Principal physical transport processes of chemical species in bog pore water

2.5.1 Pore water advection

Advection is defined as the bulk movement of a fluid, e.g. due to pressure or density contrasts (Krauskopf and Bird, 1995). In hydrogeology, advection is often associated with the transport of a non-reactive, conservative contaminant, or tracer, in a porous medium at a velocity equal to the average groundwater velocity (Piteau Associates, 1993). For peatlands, the term advection has a slightly different meaning: When rainwater falls on a bog or when snow and ice melt, the water at the surface increases the hydrostatic pressure in the pore water column and the water will start to flow downwards (and to a certain degree also sidewards) through the permeable pore space until a new hydrostatic equilibrium is attained. The flow field is determined by the hydraulic gradients and the hydraulic conductivities. The downward flow of water through the pores is called **pore water advection**. Advective species transport in peat bogs is usually unidirectional from up to down. There are however important exceptions, where transport is upward directed due to pore water tension (e.g. Siegel et al., 1995). The location in the bog (a central location, for example, or near the margins), the degree of curvature of the raised part of the bog, and hydrological parameters such as the ratio of the vertical and the horizontal hydraulic conductivity, determine how much water will flow downwards and to the sides (cf. chapter 5.2.5 and Fig. 5-16). Individual and very complex flow direction may occur in every bog.

When pore water moves down due to advection, its chemical load (ions, colloids, dissolved gas) is also transported to greater depths. The rate of pore water advection depends primarily on the amount of precipitation, the peat's hydraulic conductivity, permeability, thickness, as well as the bog's lateral extension and its confinements, which may be more or less watertight. Pore water temperature patterns at EGr (cf. chapter 5.2.2 and Fig. 5-17) indicate pore water advection rates of about 1 to 3 cm per day.

2.5.2 Molecular diffusion

Diffusion is defined as the intermixing of atoms and/or molecules of solids, liquids and gases, where the atoms or molecules of a certain type move from an area of high concentration to an area of low concentration (Vogt and Wargo, 1993). Fick's first law describes the rate of

diffusion of a substance across a surface element, as given by a formula expressing the proportionality between diffusion flux J [mol*m*s^{-1}] and concentration gradient dC/dx. In this equation, J = -D dC/dx, where D [m^2*s^{-1}] is the diffusion coefficient (Harcourt, 2002). Fick's first law is often used to quantify the diffusive flux of molecules in liquid systems (e.g. Makhov and Bazhin, 1999). Most dissolved gases such as sulphur hexafluoride (SF_6) and methane, are transported by **molecular diffusion** (Van Bodegom et al., 2001; Van Bodegom and Scholten, 2001), while for other gases, such as CO_2 ("carbonate equilibrium"), ion diffusion plays an important or, as for instance in the case of hydrochloric acid gas (HCl), virtually the only role. For ion diffusion, the charge balance should also be considered (cf. chapter 4.3.2). In a technical sense, peatlands can be regarded as a suspension of solid matter (the peat matrix) in water. In contrast to advection, which is restricted to relatively large interconnected pore space, diffusion also occurs in fine pore space. It is hence much more influenced by molecule-scale electrostatic effects as in "open" media. For a more exact estimate of diffusive transport in porous media, again, the charge balance should also be taken into account (cf. Steinmann, 1995).

2.5.3 Ebullition

Gas species in peatlands may also be transported in the gas phase by bubbles. In theory, bubbles form, when the pressure of all gas species dissolved in the pore water (i.e. the sum of their partial pressures) exceeds the confining hydrostatic pressure. In practice, this is not always the case (see below). The relationship between the concentration of a dissolved gas species and its corresponding partial pressure is given by Henry's law, which states that the pressure in a co-existing gas phase is directly proportional to the concentration of the gas in the solution (Harcourt, 2002). The equilibrium constant ("Henry's law constant") K_H [M*bar^{-1}) = C(gas)/p(gas), where C(gas) is the concentration of this gas in solution and p(gas) is the partial pressure of an ideal gas. Sander (1999) provides a comprehensive list of Henry constants for numerous chemical compounds. Bubble formation and transport are commonly described as **ebullition**. As it is generally the case for advection, ebullitive species transport is unidirectional. Yet in contrast to the latter, it is upward directed due to the buoyancy of gas bubbles in water.

Often, a considerable over-saturation of the pore water with gas species occurs (Abegg and Anderson, 1997; Siegel et al., 1997). This means that the total partial pressure of the dissolved gas species exceeds the confining hydrostatic pressure without bubble formation. Gas over-saturation is particularly pronounced in porous media (e.g. in the lower catotelm of EGr up to 1.8 times; cf. chapter 6.4.4.3 and chapter 11.AIII-Goldschmidt'00-Fig.2a), where the pore walls impede bubble growth. The bubble formation in porous media is very complex and many factors (e.g. the maximum possible bubble size, effects of surface tension, replacement of the liquid by gas, re-equilibration of the gas content during bubble movement) need to be taken into account (cf. Chanton et al., 1989b). In laboratory experiments (incubation of peat soils) carried out by Lansdown et al. (1992), the ebullitive flux of methane was more than 15 times larger than the diffusive flux.

2.6 Peatlands and greenhouse gas emission

Greenhouse gas emissions to the atmosphere and concentration variations are often seen in relation to human activity (Table 2-3). For the global greenhouse gas budget however, natural emissions, in particular of CO_2 and CH_4, are very important. In case of CH_4, peatlands represent the largest single natural source (Fig. 2-4) - cf. chapters 2.6 and 2.7.

Table 2-3: Examples of greenhouse gases that are affected by human activities (according to IPCC, 2001).

	Pre-industrial conc.	**Concen-tration in 1998**	**Rate of concentration change** (calculated over the period 1990 - 1999)	**Atmos-pheric lifetime**	**Radiative forcing** due to change in abundance [W*m^{-2}]	**Global warming potential**	
						Time horizon 20 yrs	Time horizon 100 yrs
CO_2 (Carbon dioxide)	ca. 280 ppm	365 ppm	1.5[a] ppm/yr	5 - 200[c] yr	1.46	1	1
CH_4 (Methane)	ca. 700 ppb	1745 ppb	7.0[b] ppb/yr	12[d] yr	0.48	62	23
N_2O (Nitrous Oxide)	ca. 270 ppb	314 ppb	0.8 ppb/yr	114[d] yr	0.15	275	296
CFC-11 (Chlorofluoro-carbon-11)	zero	268 ppt	-1.4 ppt/yr	45 yr	0.07	6300	4600
HCF-23 (Hydrofluoro-carbon-23)	zero	14 ppt	0.55 ppt/yr	260 yr	0.002	9400	12000
CF_4 (Perfluoro-methane)	ca. 40 ppt	80 ppt	1 ppt/yr	>50,000 yr	0.003	3900	5700

a Rate has fluctuated between 0.9 and 2.8 ppm/yr over the period 1990 - 1999
b Rate has fluctuated between 0 and 13 ppb/yr over the period 1990 - 1999
c No single lifetime can be defined for CO_2 because of different rates of uptake by different removal processes.
d The lifetime has been defined as an “adjustment time” that takes into account the indirect effect of the gas on its own residence time.

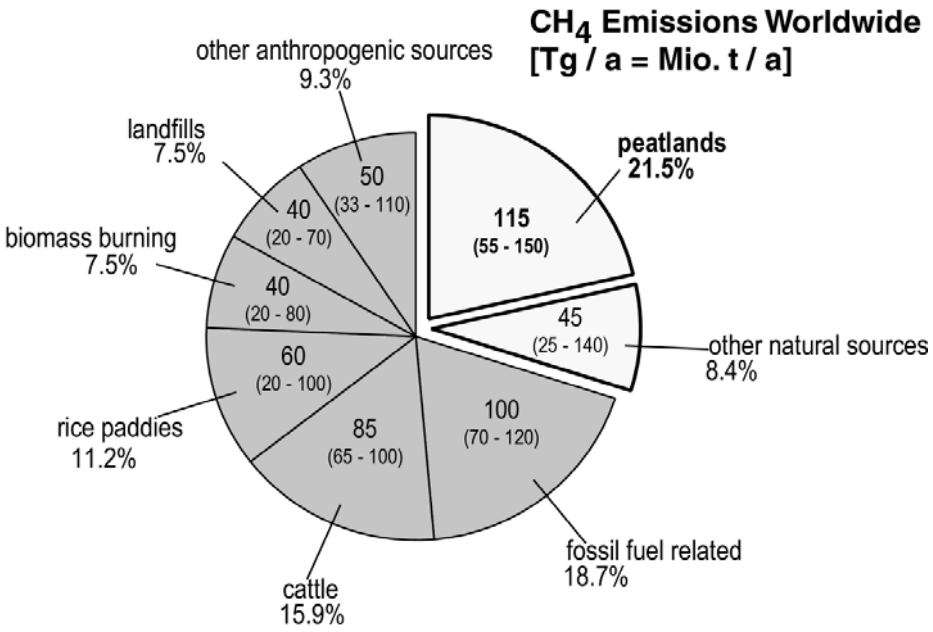

Fig. 2-4: Contributions of different sources to the global methane emissions to the atmosphere. Natural sources are represented on light grey, anthropogenic sources on dark grey background; estimates according to Houghton et al. (1995).

Peatlands not only produce but also consume large quantities of greenhouse gases. 300 - 455 Pg (10^9 t) of carbon have accumulated since the last glacial period (Sjörs, 1981; Gorham, 1991), corresponding to 20 - 30 % of the global soil carbon pool and 40 - 60 % of the carbon stored in atmospheric CO_2. The average long-term carbon accumulation rate is 20 - 30 g $C*m^{-2}*y^{-1}$ (Turunen and Tolonen, 1997). This number differs mainly with respect to the geographic location. Generally, it is smaller (12.1 - 23.7 g $C*m^{-2}*y^{-1}$) in northern Siberian mires with long frost periods (e.g. Turunen et al., 2001). The average carbon accumulation rate is about 10 % of the average annual net primary production (307 g $C*m^{-2}*y^{-1}$; Gorham, 1991). Despite the carbon dioxide emissions, peatlands therefore represent a major sink for atmospheric CO_2 in the long term.

According to a study conducted by Alm et al. (1999), daily winter CO_2 fluxes for different peat lands ranged from 0.16 to 0.49 g $C*m^{-2}*d^{-1}$, whereas summer fluxes could be 5 times as high. With respect to CH_4 methane emissions to the atmosphere (cf. Fig. 2-4), peatlands are a major source[8] (e.g. Bartlett and Harriss, 1993; Lelieveld et al., 1998; IPCC, 2001). Other, yet relatively modest, greenhouse gas emissions from peatlands include nitrogen oxides (NO_x) and in particular dinitrogen oxide (N_2O; "laughing gas"), as well as halomethanes ($C(HX)_4$) (cf. Davidson, 1991). An analysis of gases emitted from peatlands is given in Table 2-4.

[8] "Wetlands", a more general term, which includes also mires with less than 30 cm peat thickness (Lappalainen, 1997) and other waterlogged soils as for example floodplains, coastal lagoons, mangroves, swamps, rice paddies, represent *the* major source of methane to the atmosphere. This is even the case, when both natural and anthropogenic sources are considered (e.g. Hein et al., 1997; Houwelling et al., 1999; cf. Fig. 2-4).

Table 2-4: Composition of "marsh gas" for different European and North American mires. The high discrepancy between early and recent study may not only be attributed to the different mires investigated but also to the technical development of chemical analysis.

	Früh and Schröter (1904)	Rigg et al. (1927)	Alm et al. (1999)	
			winter*	summer*
Component	**%**	**%**	**%**	**%**
CH_4	57.1 - 91.8	9.4 - 37.4	0.6 - 8.4	1.7 - 8.0
CO_2	3.4 - 20.3	43.9 - 62.2	91.6 - 99.4	92.0 - 98.3
H_2	0.2 - 6.4	n.a.	n.d.	n.d.
CO	0.6 - 1.8	n.a.	n.d.	n.d.

* calculated from flux data; total CH_4 and CO_2 = 100%
n.a. not available
n.d. not detected

At present, northern hemisphere peatlands indirectly have a negative radiative forcing effect, i.e. they 'cool the atmosphere', because CO_2 uptake by plant growth and organic matter accumulation compensates for the warming effect of peatland CH_4 emissions (Martikainen, 1997). The level of the water table in the peatland is of outstanding importance for the actual greenhouse gas emissions from mires and, in turn, for the potential feedback of peatlands to global and regional climatic change. A possible lowering of the water level as a consequence of reduced rainfall or higher evapotranspiration, for instance, would, within a few months and years already, increase the CO_2 and N_2O emissions (Kettunen et al., 1996; Nykanen et al., 1998), but reduce the CH_4 release (Moore and Knowles, 1989, 1990; Freeman et al., 1993; Martikainen et al., 1993). According to Nykanen et al. (1997), lowering the water table in a boreal mire by only 1 cm, would increase the CO_2-C release by 10 $g*m^{-2}*y^{-1}$. A fundamental, yet very recent object of research is the question, how peatland gas production will change in response to global warming. Incubation experiments carried out so far show for most peatland types increasing methane (and CO_2) production at higher temperatures (Updegraff et al., 1998).

2.7 Methane emissions from peatlands

Recent estimates for the global methane release from peatlands to the atmosphere range from 145 Tg/a (Houwelling et al., 1999) to 237 Tg/a (Hein et al., 1997) and make up for more than 80 % of all natural and about 25 to 40 % of the total, i.e. natural and anthropogenic, emissions (cf. Fig. 2-4; IPCC, 2001). The total amount of methane emitted from northern hemisphere peatlands is estimated at 35 or 38 Tg (10^{12} g) per year (Fung et al., 1991; Bartlett and Harriss, 1993, respectively). Northern peatlands contribute hence to about one third to the total natural wetland source.

Most of the pioneering studies (e.g. Panikov et al., 1993) concerned with methane emission from peatlands try to explain the methane emission only in respect to the bulk area of the peat. There is now an increasing number of very specific investigations, for example concerned with the seasonal methane fluxes: According to Alm et al. (1999), for instance, summer fluxes of methane from the bog surface may be up to 15 times higher than winter fluxes. Other studies are concerned with the contribution of single peatland plants to CH_4 emissions (e.g. Frenzel and Rudolph, 1998), the effect of temperature (e.g. Crill et al., 1994) or major

inorganic ions (e.g. Dise and Verry, 2001) on peatland methane production. Methane emissions may vary very much from peatland to peatland. The reported fluxes range from <1 to 3200 mg CH_4 $m^{-2}*d^{-1}$ (Shotyk, 1989b; Bubier et al., 1993; Glenn et al., 1993; Roulet et al., 1994; Shannon and White, 1994; Martikainen et al., 1995; Alm et al., 1999). The actual methane production in the peat is however higher, as important quantities of methane are oxidised in the acrotelm (e.g. Sundh et al., 1995) or in plant stems (Frenzel and Rudolph, 1998) and hence not emitted into the atmosphere. During the last years, scientists were able to isolate a range of acidophilic methane-oxidising bacteria from northern peatlands (Dedysh et al., 1998). Oxidation rates may range from ca. 30 to 50 % of the methane produced (Holgate 1990; Frenzel and Karofeld, 2000). In some rare cases and depending very much on the watertable, up to 100 % and more of the methane are oxidised. Methane concentrations in the uppermost part of the acrotelm may then fall below atmospheric levels (ca. 2 ppm) leading to CH_4 flow from the atmosphere into the peat (Martikainen et al., 1995; Roulet and Moore, 1995).

2.8 How does methane form in peatlands?

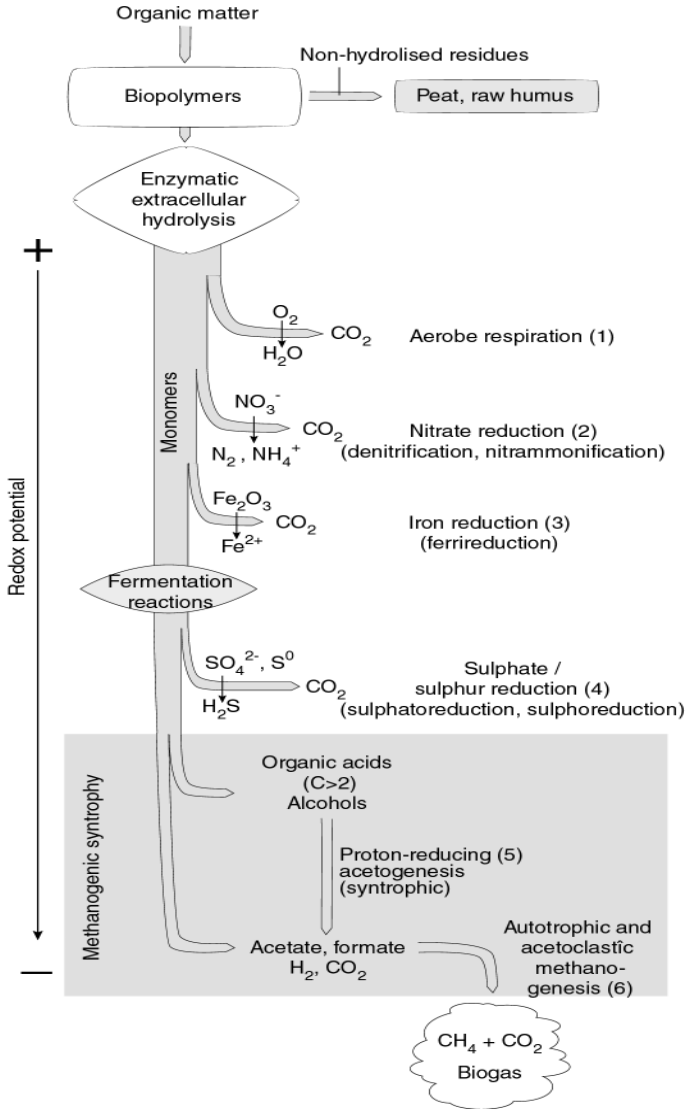

Fig. 2-5: Successive reductions during the aerobic-anaerobic transition. After aerobic respiration (1) has exhausted available oxygen, anaerobic denitrifying bacteria (2), facultative and iron-reducing bacteria (3) reduce nitrate and iron, with a concomitant lowering of the redox potential of the medium. Fermentation reactions can take place, giving rise to metabolites (alcohols, organic acids) that can be utilised by obligate anaerobic bacteria. The sulphate and sulfur-reducers occur first (4). The 'climax' stage of methanogenic syntrophy (5 and 6) produces marsh gas, a mixture of methane and carbon dioxide. It is produced only at the end of the process, if oxidisable substrates are still available (according to Gobat et al., 1998).

- CO_2 reduction and acetate splitting -

While the actual emission calculations are widely acknowledged, the occurrence and relative importance of biochemical pathways that lead to methane formation ("methanogenesis") in wetlands are still vividly debated (e.g. Hornibrook et al., 1997; Waldron et al., 1998).

Methane is an end product of anaerobic decomposition processes in peatlands. Methanogenesis only becomes a competitive microbial metabolic process in the absence of oxidation processes with molecular oxygen and other potential electron acceptors (e.g. NO_3^-; Fe^{3+}; SO_4^{2-}), which yield more energy ("reduction séquentielle", Gobat et al., 1998; cf. Fig. 2-5).

Two major methanogenic pathways are distinguished: CO_2 reduction and methylotrophism. **CO_2 reduction** is a microbial metabolic process, where CO_2 (or HCO_3^-) is converted into methane. The necessary electrons predominantly derive from oxidation of H_2. Methylotrophic bacteria by contrast catabolise organic compounds that contain methyl groups (e.g. methanol, ethanol, dimethyl sulphide, methylated amines). The methyl groups are reduced to CH_4 using electrons from oxidation of other methyl groups or from hydrogen. **Acetoclastic methanogenesis** is a special case of methylotrophism, as the electrons used for reduction of the acetate's methyl group derive from its carboxyl group, which is oxidised to CO_2 (Boone et al., 1993). The study of concentration patterns and the carbon stable isotope composition of CH_4 (and co-existing CO_2) is not only a powerful tool to identify and to evaluate the various sources of methane in the environment (cf. Cicerone and Oremland, 1988), but also to characterise the microbial methanogenic processes (e.g. Whiticar et al., 1986). This is the major objective of this thesis.

The following questions are therefore addressed:

- What are the **concentrations** of acetate and other volatile fatty acids (VFA) such as formate and propionate in the catotelm of the Etang de la Gruère Bog? How and why are these concentrations changing during the seasons? Are these changes reflected in the methane concentration patterns? Confer **chapter 6.1**.

- Given the **isotopic evidence**, is there a significant shift in the methanogenic pathway with time or with depth? To our knowledge, this is the first investigation of peat methanogenic processes up to 6 m below ground surface. How do the results correlate to studies at other bogs and what are the possible reasons for the discrepancies? Confer **chapter 6.2**.

- What are agreements and disagreements, when the observed concentration patterns and interpretations are tested in a **numerical model**? Confer **chapter 6.4**.

3 THE STUDY SITES

3.1 Etang de la Gruère (EGr)

The principal site of field research for this study is the Etang de la Gruère peat bog (EGr) in NW Switzerland. It has been chosen for the following reasons:

- Availability of background information: The EGr field site had already been very well studied and considerable information on biological, hydrological and geochemical aspects are available. In the following, some examples of earlier research work at EGr with focus on different fields of research are given: Paleobotany and palynology (Joray, 1942), conservation (Büttigkofer, 1942), peatland ecology (Feldmeyer-Christe, 1990), peat pore water geochemistry (e.g. Steinmann, 1995; Steinmann and Shotyk, 1997a, Steinmann et al., 1998) and peat chemistry (Steinmann and Shotyk, 1997b), age dating of peat and atmospheric lead deposition (Shotyk et al., 1998; Shotyk et al., 2001), peat pore water carbon stable isotopes (Steinmann et al., 2000), peat pore water hydrology (McKenzie et al., 2002), and lithogenic trace metals (Shotyk et al., 2001). In addition, F. Roos from Bern University currently carries out a research project about heavy metal, especially Hg, deposition in the peat record (scientific direction by W. Shotyk from Heidelberg University), which allowed the use of similar field instrumentation and the exchange of data, samples, and information.

- Thickness of the peat layer: Since it has been the aim to study also the pore water chemistry of the deeper acrotelm, a bog with sufficiently thick peat was indispensable. At the EGr study site, the peat thickness exceeds 6 m. This thickness of peat deposition exceeds that of most boreal bogs (3 - 4 m; Maltby and Proctor, 1997). In addition, the selected site is characteristic for the EGr Bog as well as for other boreal peat bogs with respect to surface vegetation and peat matrix.

- Location and accessibility: The EGr can easily be reached by car. The distance from Neuchâtel and hence from the laboratory facilities is just about 50 km. This proved to be particularly important for determining instable organic acid concentrations as quickly as possible.

In general understanding, the term “Etang de la Gruère” denotes by far more the artificial lake (fr. étang = pond, small lake) than the peat complex around it (Fig. 3-1). Therefore, the usage of “Etang de la Gruère Bog” is a viable alternative to address exclusively the raised mire, i.e. not the lake nor the relatively small swamp, fen, and transitional zones being present at the Etang de la Gruère as well. For simplification, however, the mere topographic name (or “EGr” in abbreviation) will also be used in this study to designate the bog.

Fig. 3-1: Photograph showing a part of the Etang de la Gruère

The Etang de la Gruère has been included in several Swiss Federal Inventories of Mires of National Importance: Inventory of Raised and Transitional Mires, 1991 (Mire no. 2; cf. Grünig et al., 1984); Inventory of Fen-Mires, 1994 (Mire no. 1312; cf. OFEP, 2000); Inventory of Particularly Beautiful Mires, 1996 (Mire no. 7; cf. OFEP 2000).

While in older literature (especially in documents written between the 16th and the 19th century; cf. Mulhauser, 1996) "Etang de la Gruère" is mostly written with a "y" ("Gruyère"), this soft-sounding, unaspirated letter often drops out in more recent writing to avoid confusion with the Gruyère Region in the Swiss Canton of Fribourg.
Etymologically, two different explanations are given for the name of the site: "Gruère" (or "Gruyère") has been the historic term for a woodland domain under the patronage of a local lordship (Mulhauser, 1996). The second explanation (Wermeille, 1998) relates "Gruère" to the German word "Grütze" (groats), a rather general name for several products ground in a mill. The Etang de la Gruère Lake has first been dammed in middle of the 17th century to supply waterpower for a mill, which was in use for more than 300 years (from about 1650 to 1952; cf. Mulhauser, 1996).

3.1.1 Physiographical setting

The Federal-Reserve EGr lies in the Franches Montagnes, which is a karstic plateau within the Folded Jura in NW Switzerland (Fig. 3-2). The EGr lake and peat bog is located 4 km SE of Saignelégier around 100 m N of the Road Saignelégier-Tramelan (Fig. 3-3).

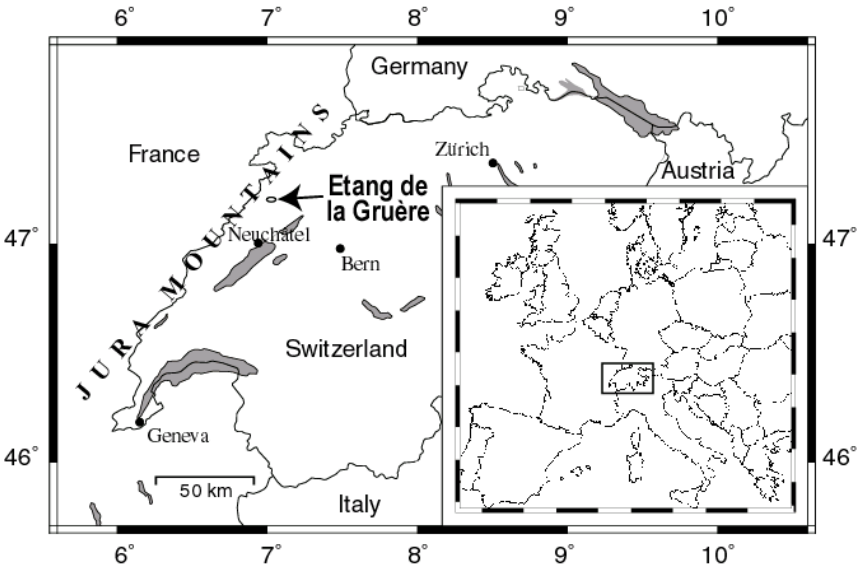

Fig. 3-2: Location of the Etang de la Gruère in Northwest Switzerland's Jura Mountains.

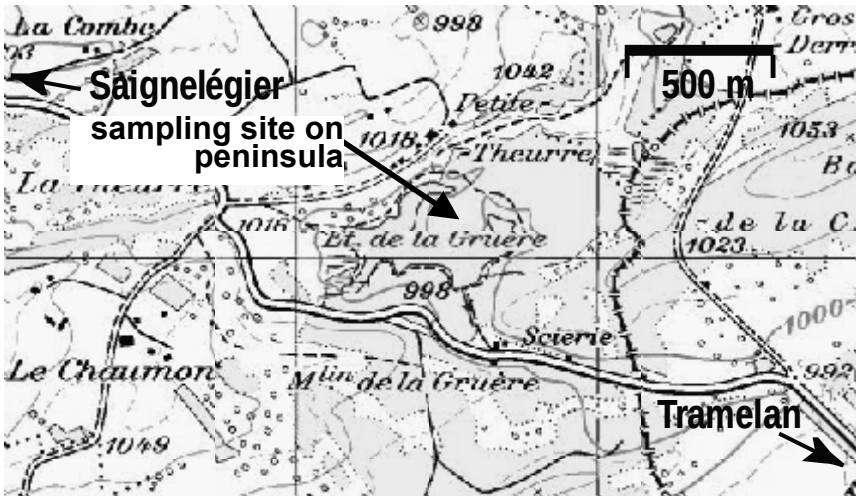

Fig. 3-3: Swiss topographic map 50 (scale 1 : 50,000): Detail of the Etang de la Gruère region.

The bog covers a total area of 22.5 ha on a remarkably domed peninsula and the lake margins (Fig. 3-4). The elevation of the bog is approximately 1000 m asl. (994 to 1002 m). The surrounding hillocks are 20 to 50 m higher (cf. Fig. 3-3). The elevation above sea level of the Franches Montagnes ranges between ca. 500 m (banks of the river Doubs) and ca. 1100 m ("Sur le Peu") with wide peneplain sections at about 1000 m asl.. The plateau is open towards N and W, whereas towards SE, it is flanked by two consecutive mountain chains, the Montagne du Droit (1263 m) and the Chasseral (1607 m).

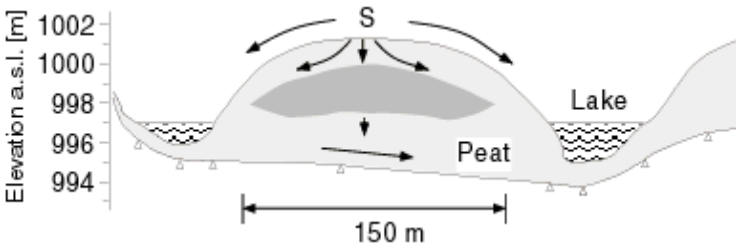

Fig. 3-4: Vertical cross-section of the Etang de la Gruère peat bog. The arrows indicate the assumed water flow regime (cf. chapter 5.2.5). The "S" marks the location of the main sampling site. The shaded area in the middle of the peninsula refers to a zone with increased peat decomposition (after Steinmann and Shotyk, 1997a).

Most of the EGr Bog is covered by a loose spruce and pine tree forest with *Pinus unicata* prevailing. The sampling site lies in an open part ("Oeil de l'Etang de la Gruère") almost in the middle of the domed peninsula (cf. Fig. 3-3). The open part shows faint development of hummocks and hollows. Its surface vegetation is dominated by *Sphagnum magellanicum* in the hollows and *Sphagnum rubellum* on the hummocks (Feldmeyer-Christe, 1990).

3.1.2 Geological setting

The EGr peat complex formed in a local depression, where organic matter has accumulated since the end of the Pleistocene and throughout the entire Holocene. Radiocarbon age dating indicates first peat formation at ca. 12,370 ^{14}C years (about 14,500 years BP, Shotyk et al., 1998). The substrate is clay derived from Oxfordian (lowest Upper Jurassic) clays and marls. As pollen-based dating of the clays did not yield ages older than 12,000 years (Joray, 1942), reworking of the clays and marls is assumed (Steinmann, 1995). Reworking of clays and marls may occur as a result of the movements of local ice-sheets or by flowing water over a frozen karstic ground during and at the end of times of glaciation. The Oxfordian clays occur in the core of the "Les Bois-Paturatte" anticline and are confined by more resistant "Argovian" (lower Upper Jurassic, yet, strictly speaking not a chronostratigraphic unit) marly limestones (Forkert, 1932). The underlying "Dalle nacrée" (massive slab-shaped limestone) is exposed in a culmination of the anticline (Gros Bois Derrière) about one kilometre to the WNW (Steinmann, 1995).

The local depression in which the EGr is situated has an ellipsoidal shape and a length of ca. 900 m, a width of 200 - 300 m, and an average depth of about 30 m (cf. Fig. 3-3). Its long axis strikes almost 60° (i.e. ENE) and thus parallels the major folding of the Jura Mountains. Secondary overprinting by local glaciation during the last ice age, however, cannot be excluded. Yet so far, no direct evidence for glaciation (e.g. local, kar-like glacier deposits) has been found (Mulhauser, 1996). There is, however, indirect evidence that peat formation followed a period of glaciation at the EGr: Basal clays still contain carbonate and hence had probably not been subject to intense weathering (Joray, 1942) as would be the case for substratum marls exposed to moderately warm climate. The age dating indicates that the accumulation of organic matter could have started directly upon melting of the glacier ice and formation of the periglacial, non-artificial, EGr lake.

3.1.3 Climate

The EGr region is characterised by a humid, temperate zone mountain climate. Long-term climatological data (Fig. 3-5) refer to the international standardised 30 years' average (MeteoSwiss Costumer Service, Zürich) of values measured for the time period from 1961 to 1990 at Saignelégier (ca. 4 km WNW' of EGr - precipitation) and La Chaux-de-Fonds (ca. 20 km SW' of EGr - temperature) meteorological stations (MeteoSwiss Costumer Service, Zürich): Temperature variation (annual mean 5.8 °C) shows continental influence, with a daily mean temperature of 15 °C in the warmest (July) and of -5 °C in the coldest month (January). Precipitation, however, is high (annual mean 1511 mm) due to the elevation above sea level and the Franche Montagne's exposition in the luff of predominant northwesterly winds. Typically, a snow-cover is present for a period of 80 to 120 days per year.

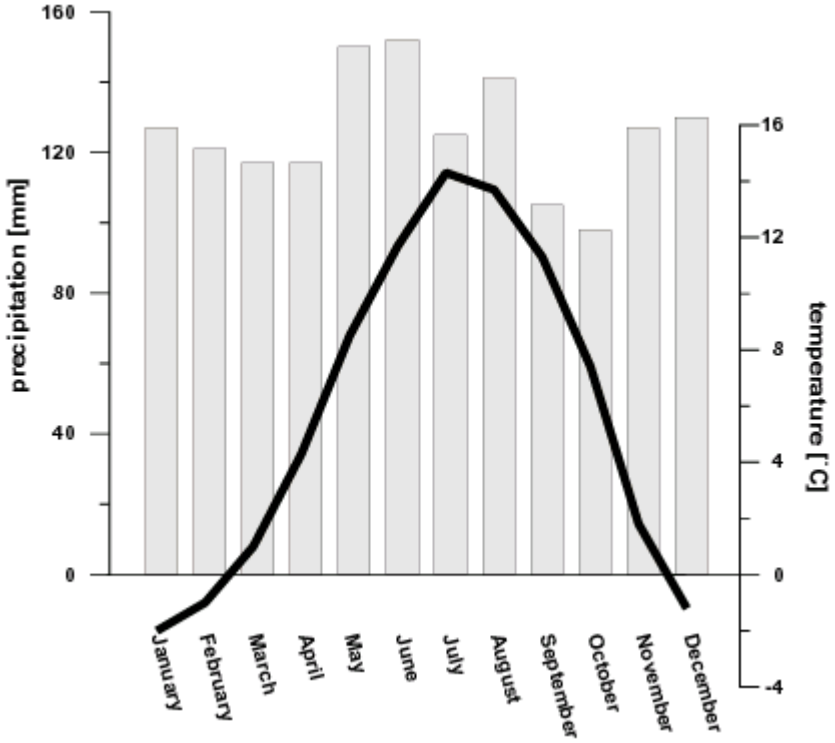

Fig. 3-5: Mean monthly precipitation and temperature for the time period from 1961 to 1990 measured at the MeteoSwiss meteorological stations (precipitation: Saignelégier; temperature: La Chaux-de-Fonds) in the Franches Montagnes region. For the Saignelégier meteorological station, which is closer to the field site (cf. text), the 30 year temperature average was not available (data from MeteoSwiss Costumer Service, Zürich).

3.1.4 Peat characteristics

An account on the history of peat deposition at the EGr and the biological diversity of the different peat-forming plants is given by Steinmann (1995).

Fig. 3-6 schematically shows the peat stratigraphy at the sampling site along with the pH profile and ash contents. Low pH values of 4.5 and below near the bog's surface for both, the pore waters and the solid matrix are typical for raised ombrogenic peat lands. Similar values are, for example, reported for a large number of peat bogs in North America, northern Europe (Shotyk, 1988), and Siberia (Inisheva et al., 2000). At the Etang de la Gruère, pore water pH values increase steadily with depth. After a relative gentle increase to about 3.5 m (ca. pH 5.5) below ground surface, the pH increase is more pronounced in the lower catotelm and the bog pore water's pH gets close to neutral values at about 6 m (ca. pH 6.5) below ground surface. Steinmann (1995), observed the same trend, yet with even slightly lower pH values in the upper catotelm (above ca. 3 m depth). The strong pH increase in the lower bog can be explained by mixing of pore waters derived from the substratum (carbonate minerals in marly

clays and marls - cf. chapter 3.1.2). In the study presented here, comparable relative pH patterns have been observed for all measurement series (cf. chapter 5.2.1), absolute pH values for the pore water in the lower catotelm were however consistently lower than those reported by Steinmann (1995). A significant seasonal variation of the pH at EGr was not observed (chapter 5.2.1). The pH values for peat suspended in deionised water were lower than those for the pore water. The difference is particularly large for the lower catotelm what again highlights the influence of the substratum on the peat pore water.

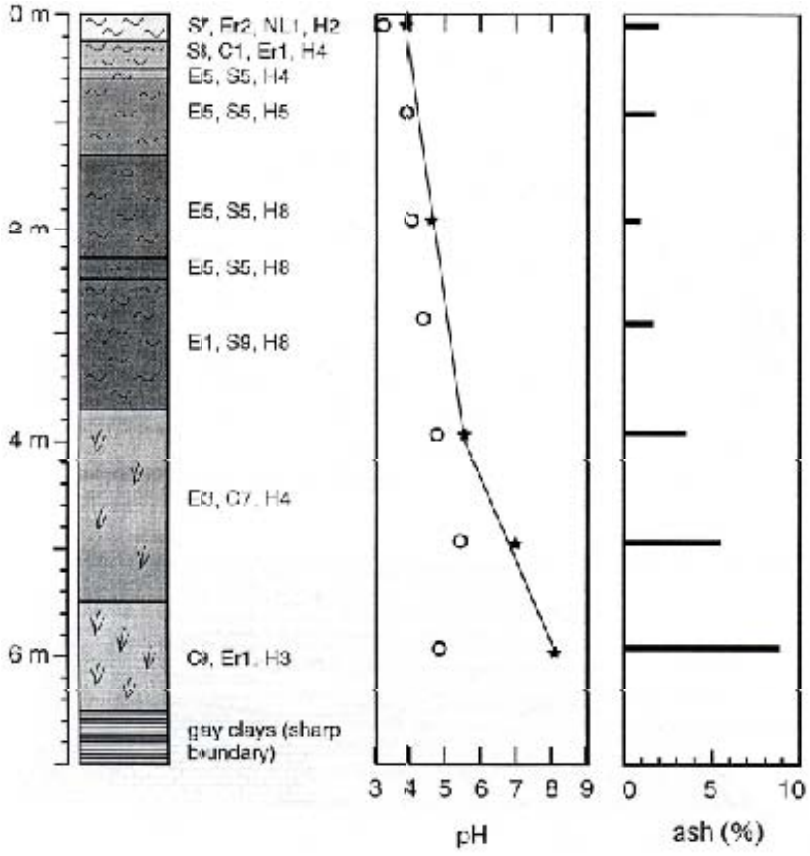

Fig. 3-6: Peat stratigraphy at the coring site (EGr) along with the pH profile and the ash contents. Filled stars in the pH profile refer to pH values of pore waters, open circles refer to pH values of peat suspended in deionised water. S: Sphagnum peat, Er: Eriophorum peat, C: Carex peat, NL: remains of shrubby plants. The H-values (e.g. "H8") refer to the "Von Post scale" of humification (from Steinmann, 1995).

The ash content in peat is a measure for the share of the peat's mineral (i.e. the non-organic matter) content. According to Steinmann (1995), the ash content at EGr generally increases with depth and reaches an average value of almost 9 wt-% at the base of the bog reflecting the early bog forming conditions. On the other hand, this means an organic matter content of over 90 wt-% and even more than 95 wt-% in the first ca. 4 m of the bog. There are in the EGr bog distinct (cm scale) layers with a considerably higher mineral content of up to 30 wt-% (P. Steinmann - pers. comm.).

The degree of humification (cf. Fig. 3-6) is conveniently expressed by descriptive classification according to the "Von Post scale" (Von Post and Granlund, 1925). Changes in peat land vegetation, in climate and / or the accumulation rate of organic matter influence humification. At EGr, a zone of more decomposed peat (H8, according to the Von Post humification scale) is situated between 130 and 370 cm (Steinmann, 1995). Accordingly, the vertical hydraulic conductivity of this zone is much lower than above and below (10^{-4} cm/s; McKenzie et al., 2002; cf. chapter 5.2.5). The possible implications of the peat structure for the pore water chemistry and turnover of chemical species are discussed in chapters 6.1 and 6.4.4.

3.2 Other field sites

Work on the two further field sites, the "Tourbière de la Chaux-des-Breuleux" in Switzerland and the "Vasjugan Bog" in Russia, is the result of cooperation with scientists from other institutions working on related issues, i.e. the Microbiology Laboratory of the Biological Institute at Neuchâtel University and the Tomsk-based Russian Academy of Agricultural Sciences' Institute of Peat, respectively.

The Tourbière de la Chaux-des-Breuleux is situated in the Franches Montagne Region about 3 km south of EGr in Switzerland's northwest Jura Mountains. The average elevation of the bog above sea level is about 990 m. The other physiographical and climatological aspects of that site are also very similar to EGr. For a detailed description of the Tourbière de la Chaux-des-Breuleux, cf. Maeder (2000).

The Vasjugan Bog (Fig. 3-7) is situated in the southern part of West Siberia between the cities of Omsk, Novosibirsk, and Tomsk. It is the world's largest coherent bog covering 50,000 square kilometres of lowlands between the Ob and Irtysh Rivers. It has an average depth of 3 to 4 meters and contains ca. 19 * 10^9 t of peat, i.e. 16 % of the total peat reserves in West Siberia (Inisheva et al., 2000). Scientific research conducted with respect to the Vasjugan Bog has mainly concentrated on peat amelioration and potential agricultural use. An enormous effort has been made to regionally classify and characterise the different mire types. A detailed peat stratigraphy is therefore available for various representative sites.

The Vasjugan Bog's elevation above sea level ranges from ca. 50 to 95 m. The climate is strongly continental with short, warm summers and long, extremely cold winters. The average annual precipitation varies from 700 to 850 mm. For a detailed description of the Vasjugan Bog, cf. Inisheva et al. (2000).

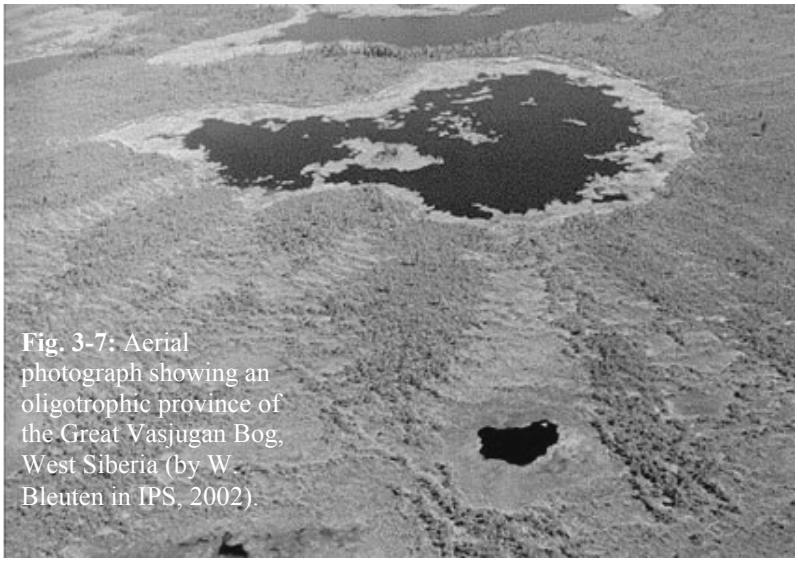

Fig. 3-7: Aerial photograph showing an oligotrophic province of the Great Vasjugan Bog, West Siberia (by W. Bleuten in IPS, 2002).

4 METHODS

4.1 Sampling of bog pore waters

Pore water samples were obtained in situ with plexiglass diffusion chambers ("peepers"; cf. Steinmann and Shotyk, 1996), which allow diffusion between the bog pore water and the liquid in the chamber. Figs. 4-1a and 4-1b show the two different types of peepers used for pore water sampling near the surface (Type A) and in the deeper bog (Type B).

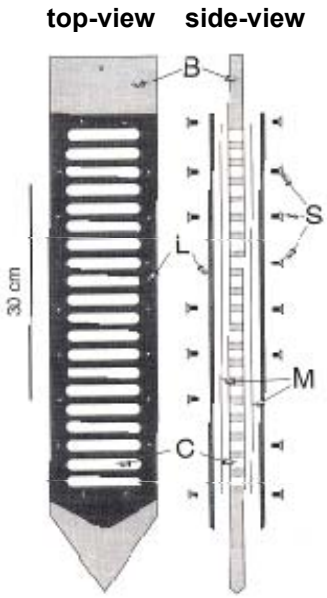

Fig. 4-1a (right): Illustration of peeper Type A.
Peeper Type A consists of a 2 x 15 x 70 cm thick plexiglass body (*B*) with chambers (*C*). Membrane filters (*M*) are held in place by 0.5 cm thick plexiglass lids (*L*) and nylon screws (*S*) (from Steinmann and Shotyk, 1996).

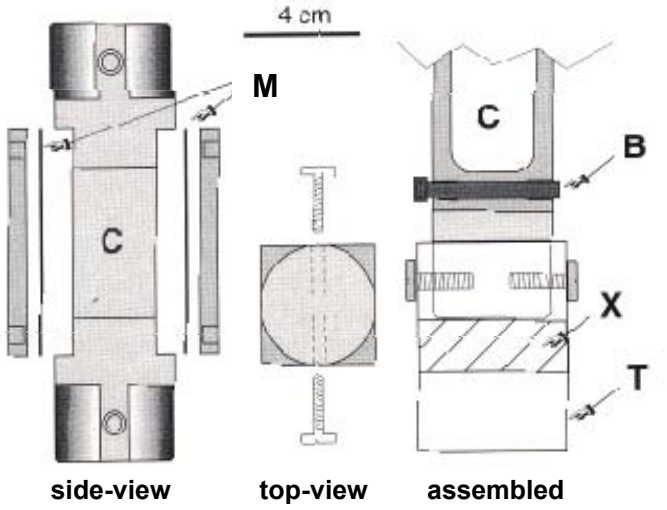

Fig. 4-1b (left): Illustration of peeper Type B.
Peeper Type B is a single chamber (C) cut from a 15 cm long plexiglass bar (4 x 4 cm). Membrane filters (*M*) are held in place by plexiglass lids (*L*) fixed with cable binders (*B*). The polypropylene connecting tubes (*T*) are sealed against the interior (*X*) to prevent the introduction of O_2 or near-surface waters, when the peepers are installed (from Steinmann and Shotyk, 1996).

The peepers had been designed for an earlier fieldwork at EGr. A. Steinmann from Schötz (Switzerland) and technicians of the University of Bern (Switzerland) manufactured the peeper sets. They were used by P. Steinmann for his PhD project Steinmann (1995) at the same site and left to the author for this study. Fig. 4-2 shows schematically, how the two peeper types were installed at the EGr field site.

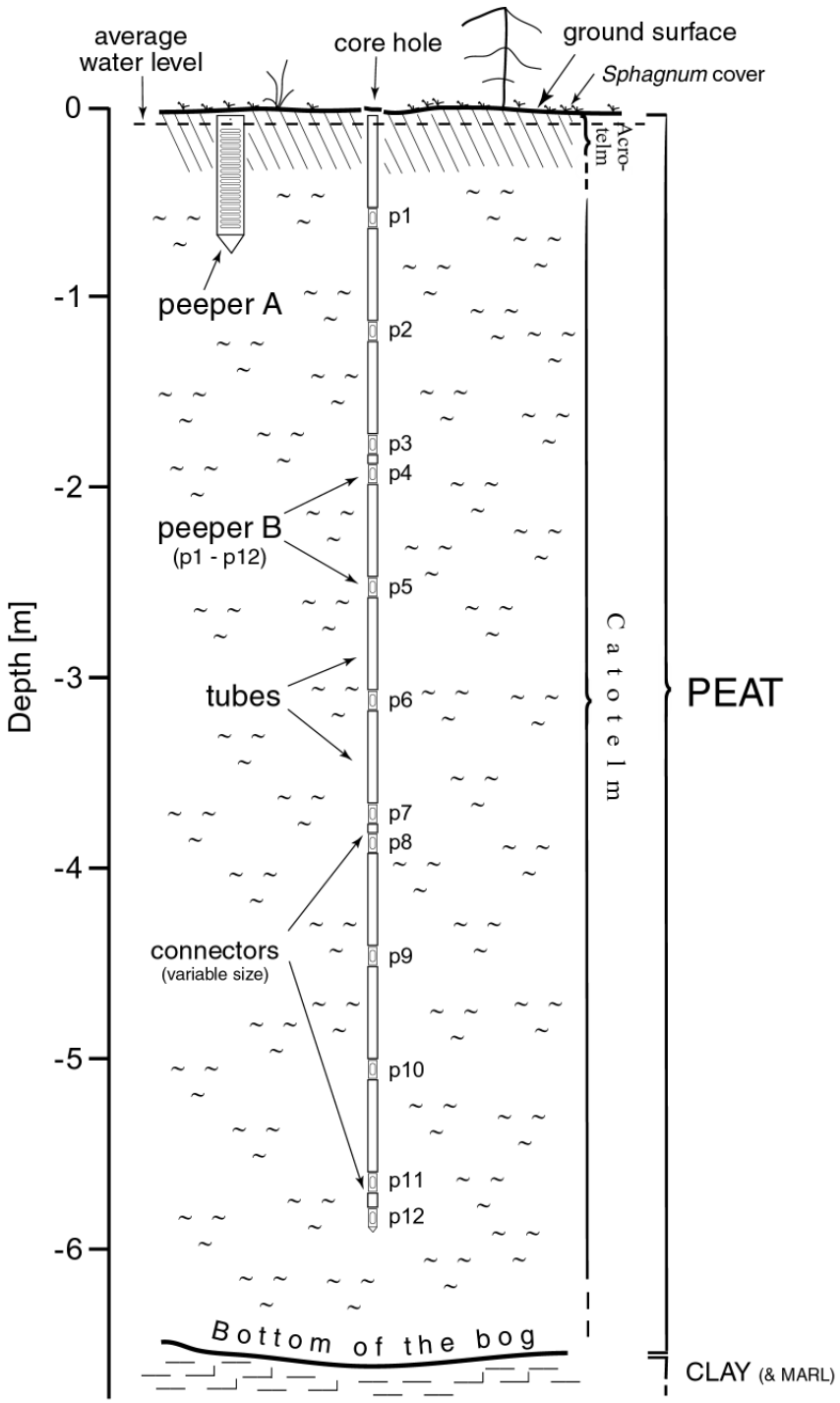

Fig. 4-2: Schematic illustration of the peeper configuration in the EGr Bog. Peeper Type A was installed as a single piece near the surface, whereas Type B peepers were connected to each other by tubes or special connectors and could be hence also be used for pore water sampling in the deep catotelm. Usually, either 11 or 12 peepers of Type B were installed for each sample series.

Shallow pore water profiles were sampled with a short, flat (2 cm thick) plexiglass body containing 20 parallel chambers (Type A, cf. Fig. 4-1a). The volume of the chambers is approximately 30 ml. Both sides of the peeper are covered with a 0.2 μm polysulfone filter membrane, which is available in rolls (Gelman, U.S.A). A 0.5 mm mesh polypropylene screen (Lanz-Anliker, Switzerland) protects the membrane against damage by wood or roots. Both the membrane and the screen are held in place by lids with a frame, which fits the chambers. The lids are fixed to the peeper chambers by nylon screws. As the total surface of the membranes covering each chamber on both sides is 30 cm^2, approximately one square centimetre of membrane per millilitre of sample volume is available for ion and molecule

exchange with the pore water. Peeper A has a total length of 75 cm. The length of the chamber assembly, however, is only 50 cm. Due to the small distance between each chamber milled into the plexiglass body, the depth resolution of this sampling technique is relatively high (ca. 2 cm). The sampling range of Type A peeper is variable and depends on the depth of insertion into the ground. In the study presented here, the sampling range was between 23 and 73 cm.

The deeper bog pore water profiles were sampled using single diffusion chambers (Type B peepers). The chambers were milled from a plexiglass bar with a quadratic 4 x 4 cm cross section (Fig. 4-1b). The chamber volume is also approximately 30 ml. As the total surface of membrane covering the chamber on both sides is ca. 25 cm^2, 0.8 cm^2 of membrane per millilitre of sample volume are available for exchange with the pore water. Alike Type A, the chambers of peeper Type B are covered by a filter membrane (0.2 µm polysulfone membrane; produced by Schleicher & Schuell, Germany), a polypropylene screen (mesh size 0.5 mm; Lanz-Anliker, Switzerland) to prevent damage of the membrane and a plexiglass lid. Nylon cable binders are used to attach the lids at the two sides of each chamber.
On the field site, the single Type B diffusion chambers were linked to each other with polypropylene tubes (ca. 50 cm long) and connectors (variable length from 5 to 14 cm). Nylon screws were used for fixing the tubes or connectors to the peepers (cf. Fig. 4-1b). The depth resolution of this sampling technique varied between 14 and 60 cm depending on the configuration of chambers, tubes and connectors. Since up to 12 diffusion chambers could be linked at a time, the depth range of the Type B peepers was from ca. 50 to 590 cm below ground surface. Two such sets of Type B peepers (with 12 and 11 diffusion chambers, respectively) were available and were alternately installed in the bog.

Prior to the first use in the field, all plexiglass parts had been leached in 10 % nitric acid and then extensively washed with deionised water. Before each field campaign, all plexiglass parts were leached another time in 10 % nitric acid and then extensively rinsed with deionised water. At the end of each sampling campaign the peepers and lids were thoroughly washed, first with tap water, then with deionised water, before being stored in sealed polyethylene boxes in the laboratory.
In the morning before each sampling campaign, all components used were carefully rinsed with deionised water. The filling procedure was different for the two peeper types and was performed in the laboratory in Neuchâtel: Peeper Type A was first put, the open side up, in a plexiglass box constructed for this purpose. Deionised and degassed water (electrical resistivity >17 Ω/m) was poured into the box, until the peeper chambers were entirely filled. Then, the membrane, screen and lid were mounted on the upper side. Finally, the box was completely filled with deionised and degassed water and sealed for transport.

As for peeper Type B, the diffusion chambers were first provisionally closed on the lower side by pressing a moistened membrane (plus screen and lid) gently against the chamber. Subsequently, the chamber was filled with deionised and degassed water and then carefully covered on the upper side with the membrane to avoid trapping air bubbles in the chamber. Afterwards, the lids were fixed on both sides with cable binders. For transport, the so-prepared peepers were stored in deionised (resistivity >17 Ω/m) and degassed water in a sealed polyethylene container. In order to degas (deaerate) the deionised water nitrogen (99.995 vol-%) was injected for 30 to 40 minutes into a slim receptacle containing deionised water, allowing the bubbles to ascent in a long water column. In particular, this was necessary to remove the potentially remaining dissolved oxygen from the peeper liquid.

Upon arrival on the field site (and usually after sampling and removal of the previous set of peepers), the new peepers were installed. For peeper Type A, a rectangular (ca. 4 x 20 cm) and about 80 cm deep hole was cut into the peat using different knifes and an axe. The peeper set was then installed as shown in Fig. 4-2 and covered with the original sod.
For peeper Type B, no new hole was necessary, as a pre-existent core hole drilled for an earlier research project (cf. Steinmann, 1995) could be used. On the field site, the diffusion chambers were linked to each other using the polyethylene tubes and connectors shown in Fig. 4-2. Set up of the peeper configuration and installation into the ground was done progressively and in vertical position by screwing each time the appropriate part of the configuration to those already installed in the ground hole (Fig. 4-3). The tubes were plugged with silicone-clad rubber stoppers to prevent introduction of air (O_2) or larger volumes of near surface waters at depth. In addition, a certain degree of buoyancy could hence be maintained. The buoyancy effect slowed the drowning of the assembly down and thus reduced the risk of component loss and of the hole being blocked. Upon completion of the set up, the hole was covered with the original sod.

Fig. 4-3: Installation of a new set of Type B peepers. Field assistant: M. Gurk (photograph by U. Helg).

The peepers usually remained for five to seven weeks in the bog, what is largely sufficient for the chamber liquid to equilibrate with the pore water in the peat (Steinmann and Shotyk, 1996). The peepers were removed from the peat using a small chain, which was drawn through a hole at the top of the peeper (Type A) or at the top of the uppermost tube (Type B). The peepers were removed from the bog at once (Type A) or, in case of Type B, by progressively, one by one, dismembering the diffusion chambers from the assembly. As the hole narrowed considerably, even within a relatively short time interval of few weeks, due to lateral pressure, pulling out of the peepers sometimes proved to be outright difficult. This was particularly the case for the long, 12 diffusion chambers comprising configuration of peeper Type B.

Latex gloves (rinsed with deionised water) were used, whenever the diffusion chambers had to be touched for filling, sealing, fixation and sampling (Fig. 4-4). For sampling, new, sterilised, single use material including standard syringes, needles and vacutainers was used (cf. Fig. 4-4). The needles had a wide orifice to reduce low pressure and potential degassing, when the samples were taken. Vacutainers are evacuated and sealed glass-tubes, widely used for blood sampling. The vacutainers chosen for pore water sampling had a guaranteed evacuated volume of 7 ml (total volume 8.2 ml) and a silicone-clad poly-buthylene rubber seal.

Fig. 4-4: Sampling of a peeper Type B. The liquid in the peeper chamber is transferred into a vacutainer using a standard plastic syringe (photograph by U. Helg).

Liquid and gaseous ("headspace") phase in the vacutainer: The total volume of the vacutainers used is 8.2 ml. Under normal atmospheric pressure conditions, the minimum vacuum guaranteed by the manufacturer is 7 ml. Tests have shown that the actual evacuated volume is often considerably higher, between 7 and 8 ml in most cases. For all measurements, the volume ratio of liquid and gaseous phase was kept constant (5 and 3.2 ml, respectively).

Upon removal of the peepers from the peat, one side of the diffusion chamber was rinsed with deionised water to remove peat fibres from membrane and screen. 10 or 20 ml standard plastic syringes were then carefully positioned at the screen slit for penetration of the chamber membrane. The syringes were supplied with wide orifice pipette tips (diameter ca. 2 mm) to reduce the suction force and hence the low pressure when drawing up the sample. The pore water samples were slowly drawn up into the syringes to prevent bubble formation.
The pipette tip was subsequently exchanged for a steel needle. Four vacutainers were filled with 5 ml of sample liquid each, for the CH_4 concentration sample and its duplicate as well as for the ^{13}C-CH_4 and the ^{13}C-DIC sample. After again exchanging the steel needle for a wide orifice pipette tip, another 7 ml of sample liquid were drawn up into the syringe for pH determination and ion chromatography analysis. The remaining approximately 3 ml of chamber liquid were drawn up into a separate syringe for DOC analysis. The two syringes were subsequently plugged to prevent degassing and kept together with the vacutainers in a cold box for transport. Chemical analysis of the samples for pH and anions was carried out in the evening upon arrival at the laboratory in Neuchâtel.

Two different vacutainer types had been tested for potential contamination by methane or other gases, which could interfere with the measurements (cf. chapter 4.3.3). The Becton Dickinson vacutainer (ref-no. 367615) showed no interference and was therefore chosen. A different type of vacutainer (ref-no. 368430), which was used for pore water sampling in July and September 1999, had been discarded for that reason.

4.2 Measurements of the physical properties of the EGr pore water

Parallel to pore water sampling some physical properties of the EGr Bog were determined. Primarily, these measurements concern the temperature of the pore water, the bog's surface and the air at 1.25 m above ground surface. The ground water level and the vertical hydraulic gradient were determined using piezometers. Qualitatively, the weather conditions at the time of sampling, including cloud coverage and air movement were noted as well.

4.2.1 Temperature

4.2.1.1 Manual temperature measurements

In situ pore water temperatures were determined using a commercial temperature probe. The temperature sensor has nail-like shape and a total length of ca. 20 cm. The temperature is however only measured at its 3 cm long pointed end (Fig. 4-5). The sensor was fitted to an aluminium tube and up to three extension tubes (length of each tube: 1.5 m; diameter of the interior: 1.0 cm; diameter of the exterior: 1.2 cm). The total probe length is hence 6.2 m. The probe is connected to a display via cable (length: ca. 8 m) laid in the interior of the tubes.

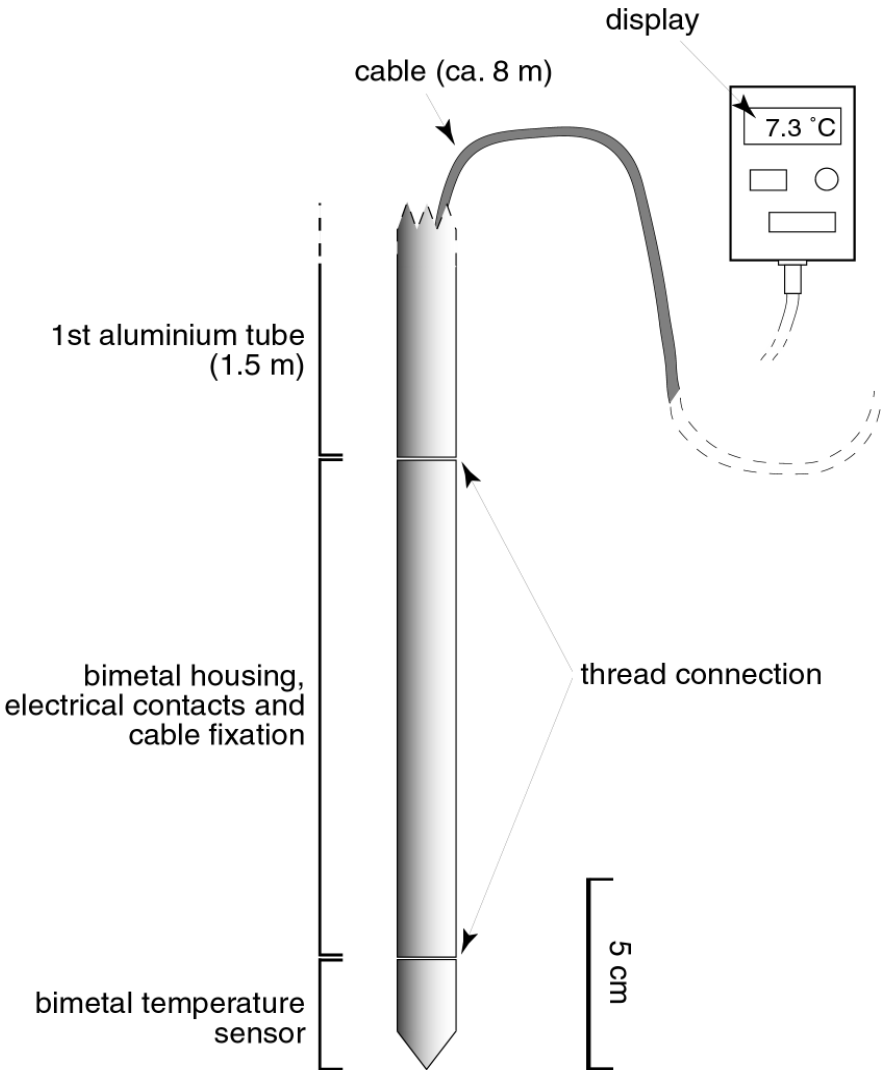

Fig. 4-5: Schematic illustration of the temperature probe used for measuring the pore water temperature at EGr. Screwing up to 3 aluminium extension tubes to the probe allows measuring pore water temperatures to a maximum depth of 6.2 m.

The readings were taken to the first decimal (1/10 °C). In case of skipping readings between two decimal values the arithmetic mean was noted; e.g. 8.25 °C for readings skipping between 8.2 and 8.3 °C. The relative standard deviation $\sigma[n-1]$ for the measurements is ca. 0.022 (n = 20). Preliminary tests have shown that the maximum divergence of the sensor reading, when compared to standard ethanol thermometer reading and a second electronic temperature sensor reading, is less than 0.05 K for the relevant temperature range between 5 and 25 °C. It should be noted, that the instrument is relatively sluggish to adjust to new temperatures, although this does not impede the measurements. The equilibration time of the sensor depends on the relative temperature change and hence on the previous temperature measured. For a temperature change smaller than 3 K, which was the case for most EGr bog pore water measurements, the equilibration time of the sensor is below 10 s. For higher temperature changes (occurring exclusively in the upper bog parts, at the surface and in the air), up to 30 s and in extreme cases up to several minutes had to be allowed until the instrument's reading became stable. The EGr pore water temperature was measured in the main sampling hole after removal of the peepers. About one hour was allowed for the water temperature stratification in the hole to re-establish after the artificial turbulences caused by the removal of the peepers. Control temperature measurements from an undisturbed site (ca. 2 m south of the sampling hole) have been in agreement with those made at the main sampling site. The observed differences were equal or below 0.1 °C.

4.2.1.2 Automatic temperature recording

In October and November 1999, a data logger (1200 Series "Squirrel", Grant Systems U.K.) was used for automatic temperature recording. For this purpose, it was equipped with four bimetal temperature sensors. The bimetal sensors were fixed with adhesive tape at different depths (0.4, 1, 1.95 and 3.3 m below ground surface) to the tubes connecting the Type B peepers. The sensors were then connected to the data logger, which contains a battery for power supply, a calculation and a memory unit. The data logger remained at the bog's surface in a lockable plastic box, which had been wrapped in a partly perforated plastic bag in order to prevent moisture from entering the device. The Squirrel was programmed to take readings every 15 minutes and to store the arithmetic mean of the temperature readings taken for each sensor over 24 hours. The Squirrel can be used at temperatures between -30 and +65 °C and with a relative (not condensing) humidity of up to 95 %. The precision of the temperature recordings of the Squirrel had not been determined, but appeared "high", when the Squirrel was tested under laboratory conditions. For unknown reasons, data storage ended on November 20th, 1999 already, although the data logger worked normally without significant battery discharge. It was removed from the field on November 26th, 1999. For temperature sensor 2 (installed at 1 m depth), no data at all could be retrieved from the logger. Due to these technical problems and due to the fact that the obtained profiles showed very regular, predictable trends (cf. chapter 5.2.6), it was decided not to recommence the automatic recordings.

4.2.2 Water level and vertical hydraulic gradient

The water level at EGr was measured before sampling at the site of peeper installation. It is expressed in cm below ground surface. From time to time the ground water level was also controlled at a hole ca. 2 m south of the sampling location cored more recently in July 2000. Water level measurements at the sampling site and at the control site yielded no significant (≤3cm) differences.

The vertical hydraulic gradient of the EGr Bog has been controlled using piezometers, which had already been installed at the site for an earlier hydrological study (McKenzie et al., 2002). Piezometers are tubes, which are installed in vertical position in the ground. They have different lengths and a wall perforation at different depths. At the bottom, they are sealed to prevent peat from entering. At EGr, four piezometer nests had been installed and controlled by J. McKenzie and other hydrogeologists for their study. The piezometer nest used in study presented here, is situated ca. 2.5 m SW of the sampling site. It consists of a large, completely perforated PVC tube with an approximate diameter of 4 cm and three smaller PVC tubes of 1.1 cm in diameter and screen lengths of 5 to 10 cm. The length of the piezometers varies between 200 and 600 cm (McKenzie et al., 2002). The wall perforation begins at 150, 250 and 550 cm, respectively. Chason and Siegel (1986) describe further technical details and the underlying hydrological principles of the method. For this study, the piezometers were only used to control, whether the direction of the bog water flow was downward (as it should usually be the case) or upward directed. The readings are discussed in chapter 5.2.4.

Other hydrological observations discussed in chapter 5.2.5 refer to a publication by McKenzie et al. (2002) and are based on piezometers at different locations at the crest and flanks of the EGr Bog. The readings obtained by McKenzie et al. (2002) were analysed using the Hvorslev method (Hvorslev, 1951), which incorporates the lag time of the water level recovery in the piezometer to calculate the horizontal hydraulic conductivity. The vertical hydraulic conductivity was measured from falling head tests on sealed peat cores in a Darcy apparatus (Freeze and Cherry, 1979). The horizontal hydraulic conductivity was determined by slug and bail tests.

4.3 Chemical analysis of bog pore waters

4.3.1 Determination of pH

The pH value of the pore water samples was determined directly upon arrival from the field. This was important to minimise the effects of pH relevant chemical, biochemical and physical reactions: The pH value of the sample increases, as volatile organic acids (e.g. acetic acid) evaporate or decompose. Tests for acetic acid, which represents the dominant low-molecular weight organic acid in bog pore water (cf. Steinmann and Shotyk, 1997a), have shown that concentrations decline rapidly within a few days after sampling. Biochemical degradation of the DOC in the peeper liquid, for example, may lower the pH of the sample, as CO_2 and organic acids are formed. Dissolution of CO_2 (H_2CO_3* formation) and dissociation of organic acids increase the hydronium (H_3O^+) concentration of the sample. Bubble formation, by contrast, leads to CO_2 loss and hence to a shift of the carbonate equilibrium towards higher pH values.

For pH determination, 1 to 2 ml of sample liquid were taken from the syringe and transferred into small glass test tubes commonly used for centrifuging. These tubes were chosen as they have a diameter, which is only slightly larger than that of the pH sensor (1 and 0.8 cm, respectively) and a comparable bottom curvature. They represent ideal receptacles of pH measurement, when only very little volumes of liquid (<2 ml) are disposable. Prior to use, the test tubes had been rinsed out with deionised water and stored in a closed cupboard.

The sensor used for pH measurements is a combined glass electrode (Metrohm, Switzerland; product-no. 6.0233.100) for a pH range from 0 to 14. The hemispherical indicator electrode has a glass membrane with a resistance from 150 to 400 MΩ. The diaphragma of the reference electrode (Ag/AgCl) is ground-joint and has a KCl electrolyte concentration of 3 M. Before starting the pH measurements, the pH sensor had been adjusted to the sample temperature (22 °C) and calibrated for the relevant pH range (4.5 to 6.5) with pH 4 and pH 7 buffered standard solutions (Merck). The precision of the measurements during the time-span of concern after calibration has been determined by measuring 10 times the buffered standard solutions for pH 4 and 7 with similar volumes of liquid in the same glass test tubes and in the same way as for the samples. The relative standard deviation is below 0.025 for pH 4 and below 0.02 for pH 7.

Change in pH probe handling

Before September 2000, the measurements had been made separately for each sample. After having taken each reading, the probe was rinsed and suspended in KCl solution. The overview of the results, obtained by then (cf. chapter 5.2.1), showed that the probe did not completely re-adjust to the pH range of the EGr samples, especially, when these were below pH 5. Since September 2000, far more consistent results could be obtained by measuring the entire series in row without suspending the probe in the KCl solution after each measurement. As rinsing of the probe also caused significant pH change, the probe has ever since only been carefully dabbed with soft tissue between each measurement.

4.3.2 Ion chromatography of organic-rich waters from peatlands

Ion chromatography of bog pore waters played a major role in this study. Most of the conclusions drawn in chapters 6.1, 6.2, and 7 are based on concentration values obtained by ion-chromatography or related to them. This is particularly the case for acetate (as well as the anions of other low-weight organic acids: propionate, formate, lactate) and DIC ("total carbonate", i.e. H_2CO_3*, HCO_3^-, and CO_3^{2-}). Ion chromatography is based on the principle that different ions have different retention times (Fig. 4-6), when they run through ion

exchange resin. It is therefore possible to separate the ions and to determine their respective concentrations by integration of the conductivity change their arrival provokes at a detector. Modern ion chromatography has become a standard analytical tool for many areas of hydrochemical research and allows precise and sensitive measurements on relatively small sample quantities. Given the limited volume of sample liquid from peeper chambers (ca. 8 ml were at disposition for ion analysis), this aspect should be stressed.
Due to the high content of organic, e.g. humic and fulvic acids in bog pore waters (up to 80 % of all ions; Steinmann and Shotyk, 1997a), whose concentrations were not determined, a charge balance of anions and cations would not be useful and has therefore not been attempted in this study.

4.3.2.1 Anions

The EGr bog pore water samples were analysed for the following dissolved anions: chloride (Cl^-), acetate (CH_3COO^-), and total carbonate ($H_2CO_3^* + HCO_3^- + CO_3^{2-}$). Some samples have also been analysed for phosphate (PO_4^{3-}), nitrate (NO_3^-) and sulphate (SO_4^{2-}) among those, as was expected, only sulphate showed significant concentrations in the uppermost parts of the bog. The formate ($CHOO^-$) peak has been evaluated for the January 2000 sample series but then omitted due to small concentrations, which further decreased rapidly with depth of the sample. Lactate ($C_3H_5O_3^-$) and propionate ($CH_3CH_2COO^-$), by contrast, were measured for all series from January 2000 to August 2001. Fig. 4-7 shows ion chromatograms for some typical anion standards and samples measured.

The concentrations of these anions were determined using a Dionex DX-500 ion chromatograph equipped with IonPak AS/AG 11-HC columns and an EG 40 eluent generator. The eluent is produced electrochemically by electrolysis of deionised, filtered and degassed water and subsequent cation exchange (K^+ replaces H_3O^+). The EG 40 allows running an eluent concentration gradient with an isocratic pump. Although this instrument is combined with an auto sampler, samples had to be injected manually to prevent degassing of the sample liquid in the vials (and hence false values for DIC and, to a minor extent, for acetate as well). When injecting manually, high molecular weight dissolved organic carbon (DOC, e.g. humic acids) was removed by mounting cartridges ("Onguard-P Cartridges, Dionex, Switzerland) with adsorptive filling (polyvinylpyrrolidone polymer), between the syringe outlet and the inlet of the ion chromatograph. The cartridge protected the IC column from being loaded with high molecular weight DOC. This helps to increase the lifetime of the column and reduce the cost of analysis. For each sample a new cartridge was used. Before use, the cartridges had to be moistened with deionised water, which was pressed through them at low flow rates (<1 ml per minute) in order to prevent the formation of channels in the polyvinylpyrrolidone powder. The cartridges were then rinsed with 1 to 2 ml of the sample liquid to avoid erroneous measurements as a consequence of sample dilution with the deionised water.

Approximately 2 ml of sample liquid were loaded manually into the loop for each measurement. This volume is largely sufficient to purge the loop (loop volume 50 µl). The sample in the loop is subsequently injected into the eluent flow and hence passes the column. The pressure was between 2500 and 3000 psi (approximately 17.2 and 20.6 MPa). A gradient method was used similar to the one described by Steinmann and Shotyk (1995). The initial eluent concentration of 2 mM KOH was increased to 25 mM between 8 to 10 minutes after start of the analysis and the chromatography stops after 20 minutes. The eluent flow rate was 1.5 ml per minute.

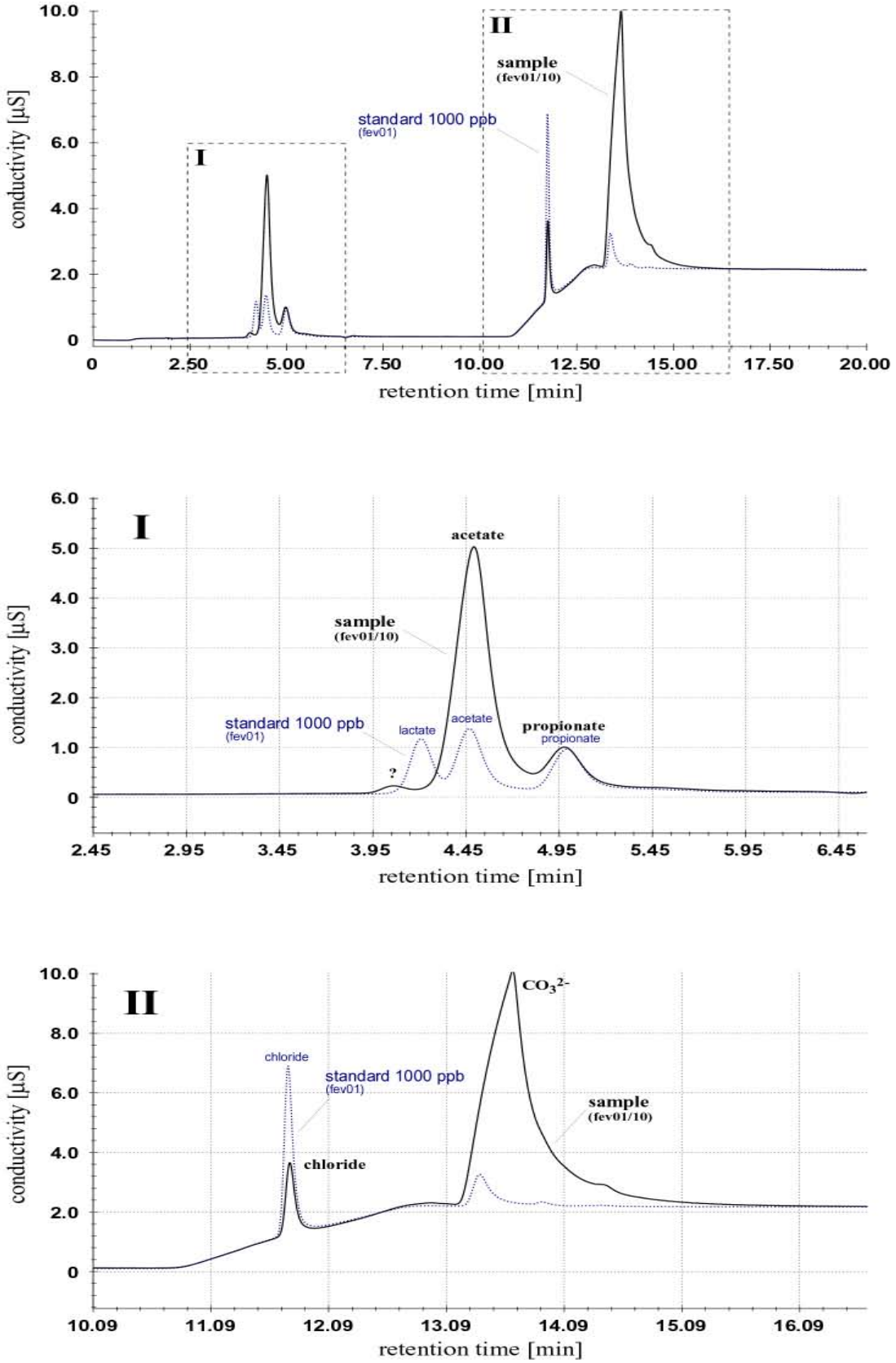

Fig. 4-6: Overlay plots of standard and sample ion chromatograms can be used to identify the ions based on retention time and peak shape. The detail (I) of the anion chromatogram shows that the first peak of the sample does not correspond to the lactate peak of the standard. There is, however, as shown in detail II, an excellent correspondence between the sample and the standard peak for chloride.

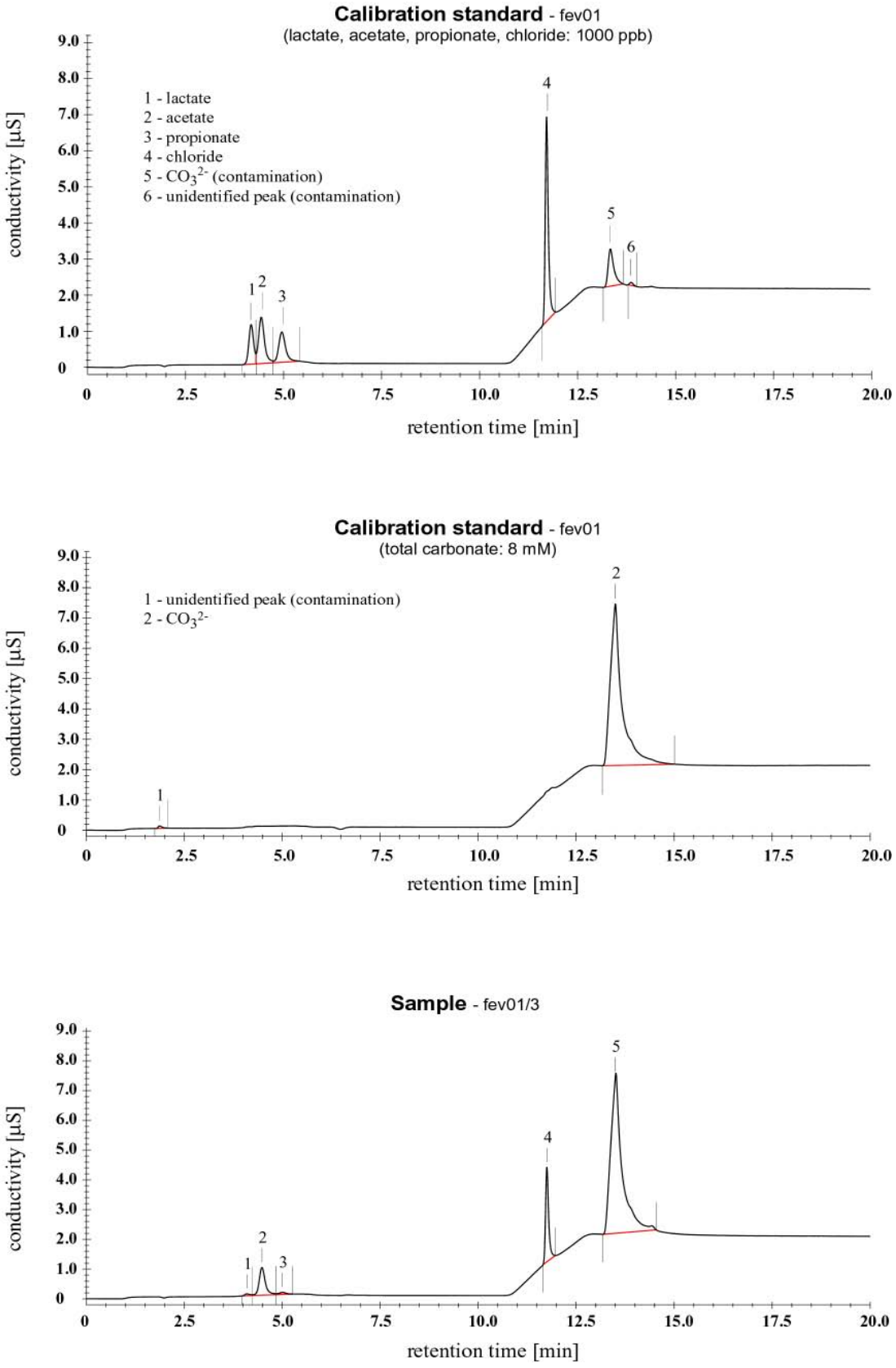

Fig. 4-7: Ion chromatograms for anion standards and samples of the EGr February 2001 sample series. The peaks in the sample were identified by comparing the retention time and the peak shape of the samples with those of the standards. The base line, which is necessary to compute the peak surface, was either drawn automatically or adapted manually to the peak shape using so-called start / stop markers.

The analytical precision of the device was determined by measuring the chloride and the acetate calibration standard 10 times. The relative standard deviation for chloride varied between 0.27 (for standard 2 corresponding to a Cl^- concentration of 100 ppb) and 0.0052 (for standard 5 corresponding to a Cl^- concentration of 3000 ppb). For acetate, the relative standard deviation varied between 1.02 (for standard 1 corresponding to a CH_3COO^- concentration of 30 ppb) and 0.011 (for standard 5 corresponding to a CH_3COO^- concentration of 3000 ppb). Calibration standard 4 (corresponding to Cl^- and organic acid concentrations of 1000 ppb) was routinely re-measured as a sample at the end of each measurement series. The reproducibility was generally good with a difference below 5 % between the value of the standard injected as sample at the end and the corresponding standard value obtained at the beginning of the measurements. Some calibration curves for the anion standards are shown in Fig. 4-9.

4.3.2.2 Cations

The EGr Bog pore water samples were analysed for the following dissolved cations: sodium (Na^+), ammonium (NH_4^+), potassium (K^+), magnesium (Mg^{2+}) and calcium (Ca^{2+}). Fig. 4-8 shows ion chromatograms for some typical cation standards and samples measured.

The concentrations of these cations were determined using a Dionex DX-120 ion chromatograph equipped with IonPak CS/CG 12A columns. The eluent used was a 22 mM solution of methanesulfonic acid (MSA) in deionised water. The sample volume for cation analysis was between 3 and 4 ml in most cases. Since early 2000, the samples had not been measured any more upon arrival from the field. Instead, they were stored in a cold room for several months in order to avoid the time consuming process of preparing and measuring each series separately. For better preservation of the samples, they had been 1 : 1 diluted with the eluent, i.e. with 22 mM MSA. No systematic difference was observed between the samples measured directly upon arrival from the field and those, which had been stored for several months. A standard isocratic method (i.e. the eluent concentration is not changed during run time) for cation analysis was applied. The run was set to stop after 10 minutes.
In contrast to anion analysis, the IC's auto-sampler could be used when measuring cation concentrations, because no volatile species were to be determined. Ca. 1.5 ml of the MSA-diluted sample liquid were injected through cartridges with adsorptive filling ("Onguard-P Cartridges, Dionex, Switzerland) and filled into standard glass vials for auto-sampler operated IC. The new sample vials were rinsed 3 times with deionised water and than 2 to 3 times with the diluted sample liquid before being filled with the sample. The volume of the sample liquid to be injected automatically was set to 250 µl. This volume is sufficient to purge the loop (loop volume 50 µl). The pressure at the pump head was between 1500 and 2000 psi (approximately 10.3 and 13.7 MPa). The eluent flow rate was usually 1.5 ml per minute. For one single series, accidentally, it was 1.3 ml per minute without noticeably impeding correct measurement.

The method applied is a standard method in cation IC analysis. Its analytical precision is high with a relative standard deviation below 2 % for concentrations between 50 ppb and 1 ppm, and below 1 % for concentrations above 1 ppm. Calibration standard 4 (corresponding to cation concentrations of 3 ppm) was routinely re-measured as a sample at the end of each measurement series. The reproducibility was excellent with a difference below 2 % between the value of the standard injected as sample at the end and the corresponding standard value obtained at the beginning of the measurements. Some calibration curves for the cation standards are shown in Fig. 4-9.

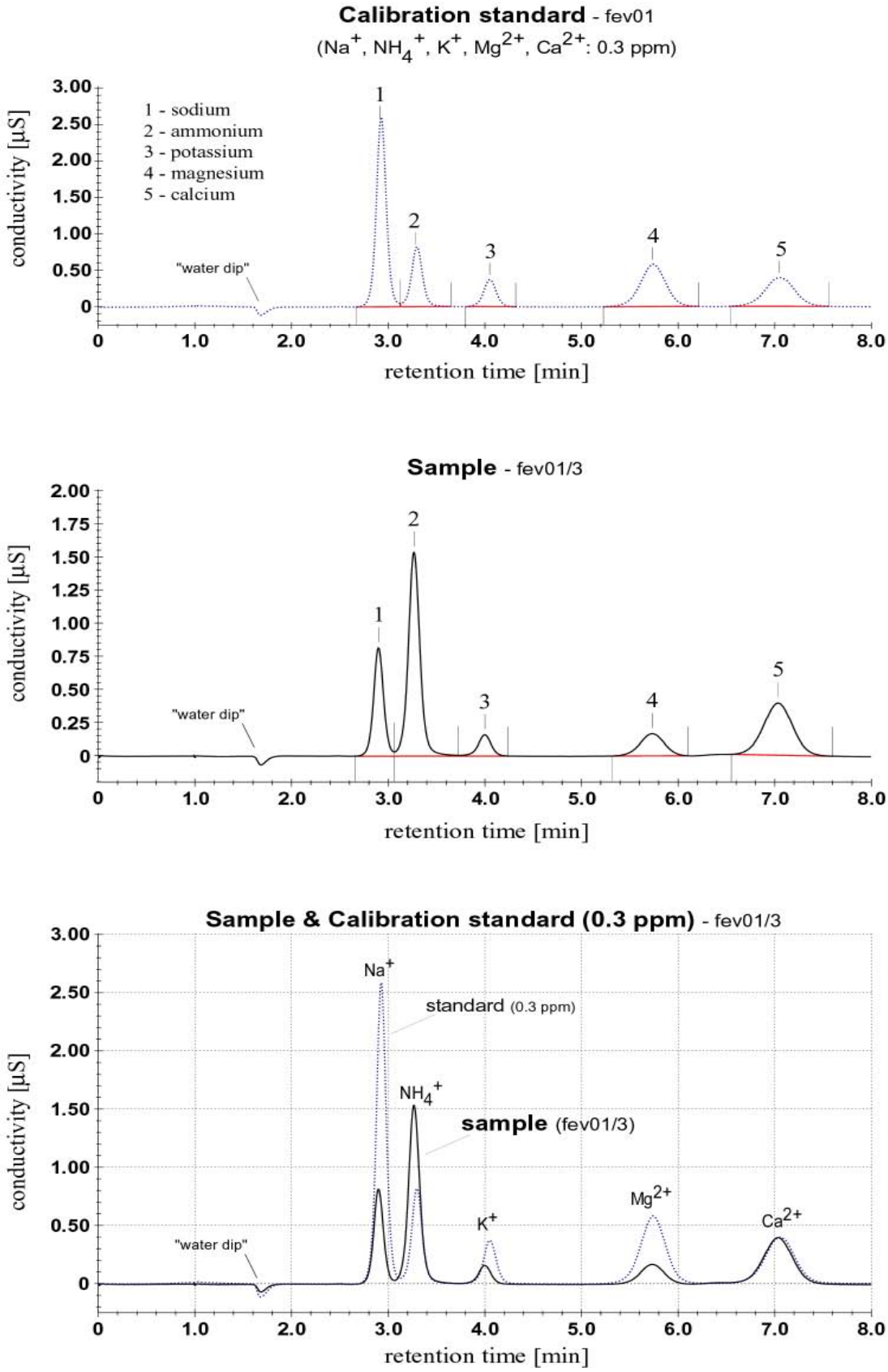

Fig. 4-8: Ion chromatograms for cation standards and samples of the EGr February 2001 sample series. The peaks in the sample were identified by comparing the retention time and the peak shape of the samples with those of the standards. The base line, which is necessary to compute the peak surface, was either drawn automatically or adapted manually to the peak shape using so-called start / stop markers.

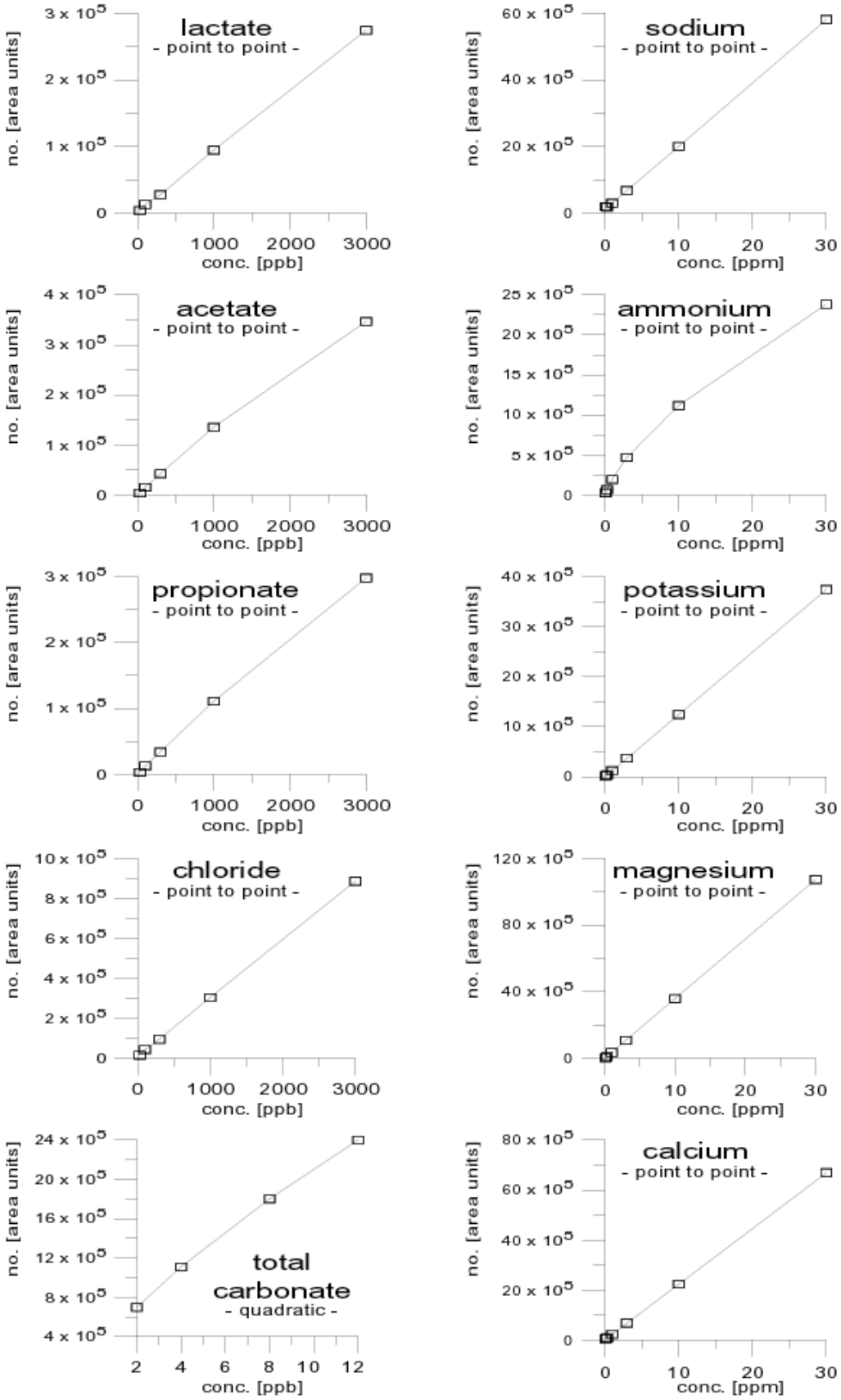

Fig. 4-9: Calibration curves of the principal standards used for ion chromatography analysis. Usually, a point-to-point calibration method was chosen for both, anions and cations. For total carbonate (DIC), however, a quadratic calibration method was chosen for best adaptation to the values of standards measured.

4.3.3 Gas chromatography and headspace gas analysis

4.3.3.1 Method

Methane concentrations were measured by gas chromatography (GC). The gas chromatograph (GC) used for headspace analysis of bog pore waters is a Perkin-Elmer 8500 microprocessor-controlled gas chromatograph equipped with a flame ionisation detector (FID). The column chosen for analysis is a HayeSep® Dip packed column (Macherey & Nagel). The sample temperature at injection was 22 °C and heating of the column was isothermal at 80 °C. While the GC's software calculated the peak areas, the conversion into concentration units and necessary corrections had to be made separately using Microsoft Excel.

For pore water CH_4 analysis, the liquid sample obtained in the field (cf. chapter 4.1) was kept in a vacutainer for one to two days to allow sufficient time for equilibration of the gas concentration in the liquid phase with the gas phase in the headspace above. For all measurements, the volume ratio of liquid and gas phase was kept constant (5 : 3.2 ml, respectively). The gas was injected using a gas-tight lockable glass syringe (Hamilton) with a total syringe volume of 2.5 ml. The volume of gas injected was 500 µl for each run.

4.3.3.2 Calibration

The calibration gas mixture ("standard") used was 1 vol-% (10,000 +/- 200 ppm) CH_4 in nitrogen gas and 100 vol-% CH_4 of a methane purity superior to 99.995 vol-%. Additional calibration standards were diluted manually by mixing the gas from the purchased standard with laboratory air within the same gas-tight lockable glass syringe as used for injection. Concerning the CH_4 concentration in the laboratory air, cf. the following chapter 4.3.3.3. The range for the standards measured was adapted to the expected concentrations of the sample. The concentrations of the standards are given in Table 4-1.

Table 4-1: Calibration standards used for pore water methane analysis and the analytical device's precision for the different standard concentrations over the entire period of analysis.

CH_4 concentration of standard [vol-%]	**number of standards measured for each series**	**average value [area units]**	**relative standard deviation for n values**	**n** (series March 2000 - August 2001)	**dilution factor**	
					100 vol-% CH_4 standard	**1 vol-% CH_4 standard**
20	0 - 1	194.40	0.162	3	5	
10	1 - 2	101.35	0.100	13	10	
5	1 - 2	51.88	0.099	14	20	
2	1 - 2	22.12	0.129	16	50	
1	1 - 2 / 2 -3	10.62 / 10.38	0.108 / 0.085	17 / 31	100	1
0.5	1 - 2	5.65	0.097	15	-	2
0.25	1 - 2	2.82	0.164	13	-	4
0.1	1 - 2	1.25	0.150	14	-	10
0.05	0 - 1	0.72	0.161	10	-	20
0.025	0 - 1	0.47	-	1	-	40

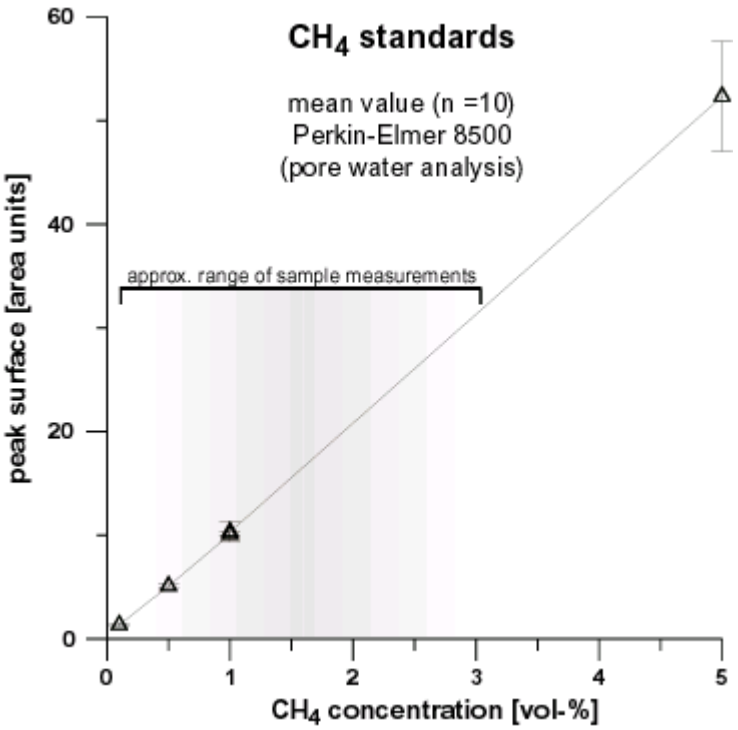

Fig. 4-10: Mean peak surface values for different concentrations of the methane standard. The measurements were repeated 10 times for each standard. The relative standard deviation is given by the error bars. A linear calibration method was used. The shaded area marks the range of the methane concentrations in the samples (cf. Table 4-2).

As shown in Table 4-1, the increase of peak surface of the CH_4 standards allowed linear calibration of the complete relevant concentration range (cf. Fig. 4-10). A drift of the standards' peak surface during the period of measurements (March 2000 - August 2001) was not observed. Evidently, the analytical precision generally decreased as the dilution factor of the calibration standards increased. The high relative standard deviations for the calibration standard analysis are a consequence of inferring analytical values over a long period of time. This does, however, not directly indicate low precision of the analytical device and the method applied. It is convenient to focus on a single series for a sufficiently large number (e.g. 10) of repeated calibration standard measurements in order to evaluate the analytical precision. As can be inferred from Table 4-2, the precision of analysis given by the relative standard deviation for repeated measurements increased with increasing concentrations. Dilution and higher dilution factors decrease the analytical precision.

Table 4-2: Determination of the analytical device's precision for the different standard concentrations - October 14th, 2000 test.

CH_4 concentration of standard [vol-%]	**number of standards measured**	**average value [area units]**	**relative standard deviation for n values**	**n** (test – October 14th, 2000)	**dilution factor**	
					100 vol-% CH_4 standard	**1 vol-% CH_4 standard**
5	10	52.33	0.099	10	20	
1	10 / 10	10.34 / 10.11	0.092 / 0.024	10 / 10	100	1
0.5	10	5.65	0.097	10	-	2
0.1	10	1.25	0.150	10	-	10

4.3.3.3 Blanks

Regular tests with blank injection showed that the CH_4 concentration of the laboratory air was generally below the detection limit of the GC (approximately 30 ppm) at the beginning of the measurements, but increased during standard preparation due to gas loss from the 100 vol-% CH_4 standard. The measured blank methane concentrations, however, were in no case significant for the accuracy of pore water CH_4 analysis. For the measurement series from March 2000 (start of GC measurements at Neuchâtel University) until August 2001, the average CH_4 peak surface of the blanks (laboratory air) was 0.13 area units corresponding to a methane concentration of ca. 70 ppm (relative standard deviation: 1.154; n = 35). Usually, even the lowest methane concentrations of the samples were over 10 times higher than the highest blank methane concentrations. Only in one extreme case, the CH_4 concentration detected in the laboratory air was ca. 260 ppm (July 2001). The lowest CH_4 concentration of the headspace gas diluted with laboratory air, however, was still more than 5 times higher (1431 ppm; July 2000).

Usually, the CH_4 concentration of blanks was determined at the beginning, at about half time (after having measured the standards), and at the end of each measurement series. Blanks obtained from virgin vacutainers gas yielded CH_4 concentrations similar to those of ambient laboratory air: Instantaneous pressure equilibration of the low-pressure samples with ambient air, when the sample was injected into the GC is the cause for the similar readings. This observation supports the results of a test by a laboratory at Joesuu University, Finland (Jukka Alm, pers. comm.) that showed that the vacutainers used since October 1999 were free of contaminations, which could interfere with the methane measurement.

4.3.3.4 Duplicates

The correlation of the analytical results of the sample and the duplicate can also be expressed by their relative standard deviation. For the gas samples measured in Neuchâtel according to the method described in chapter 4.3.3.5 (this method had been applied since June 2000), the average (arithmetic mean) relative standard deviation for all measurements is 0.104, corresponding to an average difference in concentration of the sample and the duplicate of ca. 10 %. Single relative standard deviation values for one sample and its duplicate could however be as high as 0.637 (August 2001). The low precision of the method, when only the sample / duplicate pair is considered, is primarily a consequence of the small number of duplicates (1) for each depth, thus providing only the minimal statistical base (n = 2). As n appears in the denominator of the standard deviation formula, a higher n would considerably increase precision. Yet, due to the small volume of sample liquid in the peeper chambers (30 ml), it was not possible to take more than 2 samples for CH_4 determination at each depth without neglecting other important parameters such as ion concentrations and isotopes. A statistical approach using the chi-squared distribution (E. Verecchia - pers. comm.) yielded a clear correlation between sample and duplicates (significance level >0.995). Another statistical approach based on the width of the distribution of the differences between sample and the duplicate (P. Schnegg - pers. comm.) yielded a relative error in the order of 8 % for the measurement of the sample and the duplicate. The error of the mean values is approximately 6 % (P. Steinmann - pers.comm.). A systematic error, e.g. potential degassing of the chamber liquid as the duplicate sample was always obtained after the first sample, can be excluded: In 58 % of all measurements the analytical result for the duplicates proved to be higher than for the sample. The average absolute reading of the duplicate was also slightly (by about 1 %) higher than that of the sample. A possible explanation for the higher values of duplicates with respect to the samples could be a marginally increased temperature of the pore water sample due to longer exposition in the laboratory and hence an equilibrium shift from the liquid to the gas phase.

4.3.3.5 Sample injection

In the course of methane concentration analysis, a particular pre-injection method of syringe handling was developed, which is schematically illustrated in Fig 4-11. According to this method, headspace gas is drawn up into a gas-tight injection syringe to the mark of 1 ml and the syringe is closed. In order to account for low pressure or overpressure in the headspace of the vacutainer of up to 2 bars of the headspace, another (empty) volume of 1 ml is added to the sample volume in the syringe (i.e. the piston was moved to the mark of 2 ml on the syringe scale, while the syringe remains locked). Opening of the syringe lock allowed subsequent pressure equilibration with ambient air. 0.5 ml of headspace gas are then injected into the GC (cf. Fig. 4-11).

It can be safely excluded for all samples that headspace gas pressures exceed 2 bars. Transferred headspace gas volumes for carbon stable isotope analysis (cf. chapter 4.4) indicate that the headspace gas pressure varies only between 0.75 and 1.91 bars.

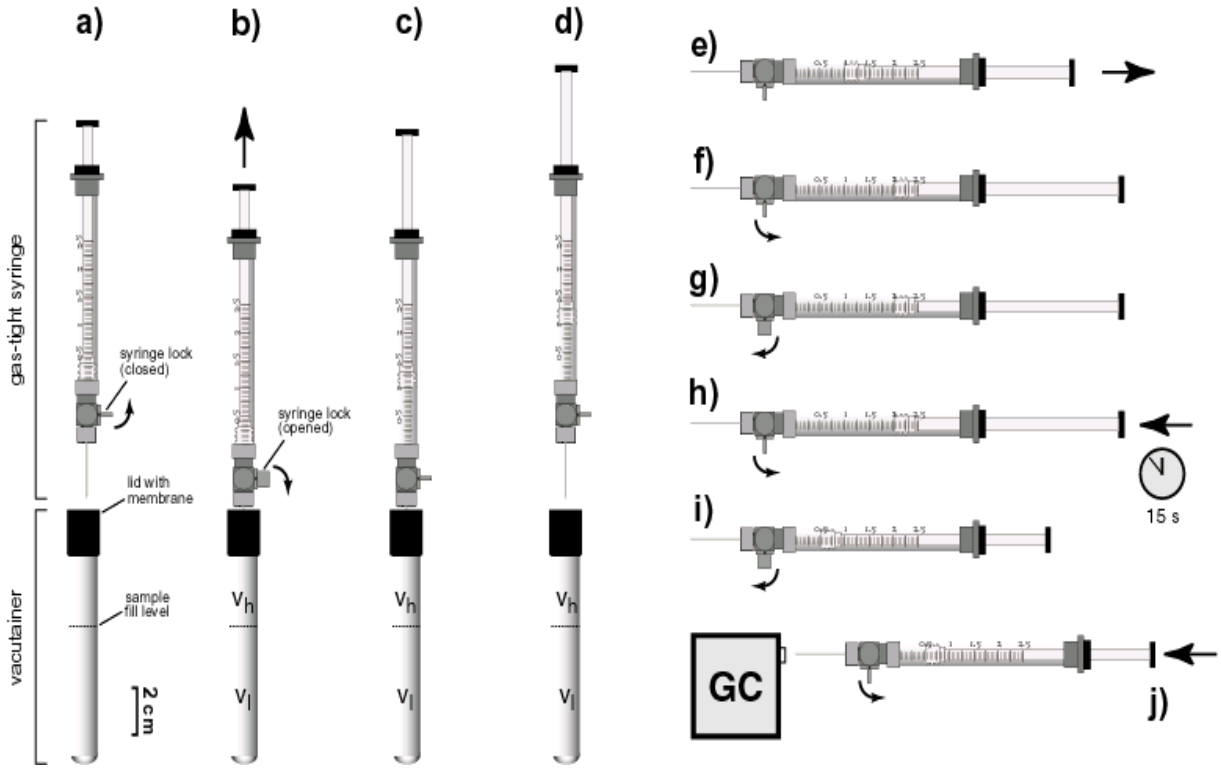

Fig. 4-11: Schematic illustration of the syringe handling procedure prior to sample injection into the gas chromatograph (*GC*). V_h denotes the headspace of the vacutainer and V_l the liquid volume. a) The syringe needle is pricked into the vacutainer headspace through the rubber septum. The syringe lock is opened. b) The piston is moved to the mark of 1 ml and c) the syringe lock is closed. d) The needle is taken out of the vacutainer. e) The piston is moved to the mark of 2 ml, while the syringe lock remains closed. The potential overpressure in the syringe may thereby expand and underpressure is obtained. f) The syringe lock is opened in order to allow pressure equilibration with ambient air. g) The syringe lock is closed again. h) After ca. 15 seconds to ensure thorough gas mixing, the piston is moved to the mark of 0.5 ml. The remaining 1.5 ml gas are vented, as the syringe lock is opened. i) The syringe lock is closed again. j) The chosen volume (0.5 ml) of gas (at atmospheric pressure) in the syringe is now ready for injection into the gas chromatograph.

4.3.3.6 Calculation of the CH_4 concentration from headspace gas analysis

Admissibility of simplification
The total quantity of methane - CH_4 (total) - in a vacutainer is the sum of the respective quantities in the gas - CH_4 (g) - and the liquid - CH_4 (l) - phase; cf. equation (1).

(1) $CH_4\,(total) = CH_4\,(g) + CH_4\,(l)$

As the methane concentration of the pore water is to be determined on the basis of the methane concentration in the headspace, it is important to show that CH_4 (l) is negligible (e.g. <5 %) with respect to CH_4 (g). Otherwise, the pore water methane concentrations would be significantly underestimated. At equilibrium conditions between the liquid and the gas phases, the CH_4 (g) quantity is the product of the methane concentration in the headspace (in terms of its molarity) and the volume of the headspace. The CH_4 (l) quantity is the product of the methane concentration in the headspace (in terms of its partial pressure), the volume of the liquid phase and the Henry Constant for methane. Equation (1) can therefore be substituted by equation (2).

(2) $CH_4\,(total) = [CH_4]_{headspace[M]} * Vtot_{headspace} + [CH_4]_{headspace[bar]} * V_l * K_{H[CH4]}$

Comparison of the two terms in equation (3) shows, that CH_4 (l) is indeed negligible with respect to CH_4 (g):

(3) $[CH_4]_{headspace[bar]} * V_l * K_{H[CH4]}) / ([CH_4]_{headspace[M]} * Vtot_{headspace}) = 0.0383$

The relationship between molarity and partial pressure units for an ideal gas at 20 °C is given by the following equation (4):

(4) $[CH_4]_{headspace[bar]} = [CH_4]_{headspace[M]} * 24.05$

It follows from equation (4), that the result of equation (3) is independent of the actual concentration and of the pressure in the headspace. The calculation of the pore water methane concentration can therefore be simplified without significantly underestimating the pore water methane concentrations.

Explanation of the symbols

CH_4 (total)	total quantity of methane in the vacutainer
$[CH_4]_{headspace[M]}$	methane concentration in the headspace in terms of its molarity
$[CH_4]_{headspace[bar]}$	methane concentration in the headspace in terms of its partial pressure
$V_{headspace}$	volume of headspace (3.2 ml)
$Vtot_{headspace}$	total headspace volume = $V_{headspace} + V_{syr}$
V_l	volume of the liquid sample (5 ml)
V_{syr}	gas volume drawn from the vacutainer into the syringe (1 ml)
$K_{H[CH4]}$	Henry's law constant for methane (e.g. $1.34*10^{-3}$ M/bar at 20 °C)

Calculation and the corrections
The methane concentration in the pore water is calculated from the measured headspace concentrations considering the volume of gas injected and correcting for the unequal volumes of liquid and headspace in the vacutainer. In addition to these corrections, the measured CH_4 concentration needs to be multiplied by 2 to correct it for dilution with the ambient air, caused

by the syringe handling described above (cf. step "e" in Fig. 4-11). The following paragraph gives an overview of the necessary calculations for correct determination of the pore water methane concentration. For simplification, the calculation is divided into three steps referring to the correction for dilution, unit change, and volume difference, respectively.

1st step: Dilution of the gas sample
Remark: Correction for a 1st dilution effect by syringe handling.
(5) C_{new} [ppm] = C_{meas} [ppm] * 2

2nd step: Adaptation of the units
Remark: Correction factor to be added for unit change.
(6) C_{new} [mM] = C_{new} [ppm] / (V_{MG20})

3rd step: Consideration of the differences in volume of the liquid and the gas phase
Remark: Correction for the different volumes of gas and liquid phase.
(7) CH_4 [mM]$_{aq}$ = C_{new} [mM] * (($V_{headspace}$ + V_{syr}) / V_l)

Explanation of the symbols

C_{meas} [ppm]	measured CH_4 concentration in ppm
C_{new} [ppm]	calculated CH_4 concentration value after first correction, in ppm
C_{new} [mM]	calculated CH_4 concentration value after first correction, in mM
CH_4 [mM]$_{aq}$	calculated CH_4 concentration for the liquid sample, in mM
V_l	volume of the liquid sample (5 ml)
V_{MG20}	molar gas volume at T = 20 °C (24.05 M^{-1})
V_{syr}	volume of gas drawn from the vacutainer into the syringe (1 ml)
$V_{headspace}$	volume of the headspace (3.2 ml) = $V_{vacutainer}$ - V_l
$V_{vacutainer}$	volume of the vacutainer (8.2 ml)

4.3.4 Dissolved organic carbon

The typical light to dark brown colour is due to humic and fulvic acids in peat bog waters. These acids and other soluble organic compounds (e.g. acetate, propionate) constitute the generally high content of dissolved organic carbon (DOC) in bog pore waters. The main source of DOC is organic matter degradation and secretion from plants and bacteria. Labile DOC is the metabolic substrate for a wide range of peatland microbial communities. The DOC concentration therefore represents an important parameter for microbial, e.g. methanogenic, turnover (cf. chapter 6.1).

Approximately 2 ml of sample liquid from the diffusion chambers were used for DOC measurement. The samples were kept in sealed plastic syringes in a cold room and in dark for the time period between sampling and analysis (1 to 5 days in most cases). The analytical device, a Dohrmann TOC DC - 190 modular organic carbon analyser, was operated by the Service cantonal de la protection de l'environnement (SCPE) of the canton Neuchâtel in Switzerland. On the day of analysis, the samples were diluted 10 times with deionised water to adapt the samples' DOC concentrations to the calibration standard used at the SCPE (4 ppm corresponding to 4 mg C/l). The selected analysis mode was NPOC ("non-purgeable organic carbon"). This means that purgeable organic carbon, e.g. volatile fatty acids or dissolved CH_4, was not measured. The detection range of the analytical device was set to 0 - 500 mg C/l. The detection limit and the precision of the analytical device are 0.2 mg C/l and +/- 0.1 mg C/l (B. Calame - pers. comm.), respectively.

Total organic carbon (TOC = DOC plus particulate organic carbon) analysis represents a determination method of organic carbon in a sample regardless of its oxidation state or biodegradability. As for the samples from EGr, the TOC content equals the DOC content, because they were filtered using the 0.2 μm membrane (cf. chapter 4.1). For the measurement of total organic carbon, the sample is exposed to an oxidising environment usually at very high temperatures (e.g. 950 °C). With complete oxidation all carbon is converted to carbon dioxide and swept into a detector by the carrier gas. The oxidation process is based on the following stoichiometry:

$$C_aH_bN_cO_d + (a + \frac{b}{4} - \frac{d}{2})O_2 \rightarrow aCO_2 + \frac{b}{2}H_2O + \frac{c}{2}N_2$$

Detection is by non-dispersive infrared analysis, i.e. the infrared light absorbed by carbon dioxide as it passes through a flow-through IR absorption cell is measured.

4.4 Mass-spectrometry of carbon stable isotopes

Carbon (atom number 6) has two stable isotopes: ^{12}C and ^{13}C. The abundance ratio of these two isotopes determines the carbon stable isotope composition. A widely used expression for stable isotope compositions is the δ-(delta)-notation, where the isotope abundance ratio of the sample is compared to the abundance ratio of the same isotopes in an internationally accepted standard and reported as a part-per-thousand (‰) difference. A high degree of intercomparability between laboratories can so be maintained. For the carbon stable isotope composition, equation 8 shows, how the δ values are calculated.

(8) $$\delta\,^{13}C\,[‰] = [(R_{smpl}/R_{std}) - 1)] * 1000$$

, where R denotes the $^{13}C/^{12}C$ abundance ratio and the subscripts denote the sample and the isotope standard.

The carbon stable isotope composition of a sample is typically reported relative to that of a primary standard that defines the zero point on the δ scale of carbon isotope abundances. Recently, Jasper (2001) defined quantitative methods for estimating molecular isotope measurements and their statistical errors (cf. also Jaspers et al., 2002). In practice, isotope laboratories use their own internal standards, which are then calibrated with internationally accepted standards. Such an international standard, for instance, is the Vienna PeeDee Belemnite (VPDB) carbonate standard from the International Atomic Energy Agency (IAEA). The measured abundance ratio for $^{13}C/^{12}C$ in the VPDB standard is 0.0124 (Kendall and Caldwell, 1998) and hence only slightly higher than the $^{13}C/^{12}C$ abundance ratio in nature (approximately 0.0111; Holleman and Wiberg, 1985).

In this study, the carbon stable isotope composition was determined for the following species:

- dissolved chemical species in the pore water of EGr (cf. chapter 11.AII)
  - CH_4, (sample series from August 1999 to August 2001)
  - DIC (sample series from August 1999 to August 2001)
  - DOC (selected sample series)
  - separated humic and fulvic acids (April 2000 sample series),
- gases emitted from EGr
  - CH_4 (September/October 2001 flux study)

CO_2 (September/October 2001 flux study),
- the peat matrix (samples from a peat core taken at the EGr site in 1998).

4.4.1 Sample preparation and storage (Pore water methane and DIC)

Pore water samples for carbon stable isotope analysis of methane (^{13}C-CH_4) and DIC (^{13}C-DIC) were obtained in the same way as for the methane concentration analysis (cf. chapter 4.1) using diffusion chambers for in situ filtration ("peepers").

For DIC carbon stable isotope analysis, 5 ml of sample liquid were transferred by syringe from the peeper into an evacuated and sealed glass tube ("vacutainer", cf. chapter 4.1). The vacutainers containing the sample liquid were then stored in a cold box and later in a cold room in dark for the time before analysis. The time period between sampling and analysis ranged from several weeks to several months, depending on the availability of the partner analytical facilities and the time schedule of the operating personnel.
Two separate vacutainers were used for transport and storage of the methane sample. The transport vacutainers (each with 5 ml of sample liquid for carbon stable isotope analysis) were usually taken out of the cold box or the cold room in the evening upon arrival from the field. Prior to further treatment, they were allowed ca. 3 - 4 hours to adapt to laboratory temperature (ca. 20 °C). A gas-tight lockable (Luer-lock) syringe was used to transfer headspace sample gas into empty storage vacutainers (see chapter 4.1 for more information on the vacutainers used). To do this, the syringe's piston was always drawn up to the mark of 5 ml, although - depending on the pressure of the headspace sample - the actual volume of gas transferred was different. The actual gas volume transferred could approximately be determined by the new piston position after having locked the syringe and removed force from the piston. Without exception, the transferred volumes were below 5 ml, yet, in particular for samples from the deeper bog, well superior to the headspace volume of 3.2 ml, indicating overpressure in the transport vacutainer. The volumes of gas transferred were noted. Upon sample gas transfer, helium gas was injected into the storage vacutainers, until atmospheric pressure was reached. The pressure equilibration is necessary in order to avoid low-pressure during the storage period or when the sample was to be taken out of the vacutainer for analysis. The volumes of helium added to the sample gas were also noted. The gas samples were stored in a cold room for the time period before analysis, which could range from several days to several months. Preliminary experiments had shown that the gas loss from the vacutainers during storage time could be neglected.

4.4.2 Pore water CH_4 carbon stable isotope analysis

The carbon stable isotope analysis of the pore water methane samples was performed by Markus Leuenberger from the Division of Climate and Environmental Physics at the Physics Institute of Bern University. M. Leuenberger's laboratory is specialized in low-volume trace gas stable isotope analysis on ice cores (e.g. Leuenberger and Siegenthaler, 1992; Lang et al., 1999; Leuenberger et al., 1999).

Depending on the methane concentration, between 100 µl and 10 ml of gas from the storage vacutainer were injected in a helium carrier gas stream. CO_2 and CO were removed from the sample gas in Ascarit and Schütze reagent traps, respectively. The sample was then dried in a $MgClO_4$ trap. Subsequently, the remaining CH_4 (as well as, potentially, the higher hydrocarbons) present in the sample was oxidised to CO_2 at 1100 °C in an oven, then frozen out using liquid nitrogen and kryo-focussed for better peak shaping. Afterwards, the sample was defrosted and via a helium carrier gas stream transferred to the isotope ratio mass-

spectrometer (ir-MS). The ir-MS used was a ThermoFinnigan MAT Delta Plus XL with several special characteristics for low-volume trace gas isotope analysis described by Leuenberger et al. (2000a) and Leuenberger et al. (2000b). It is equipped with an automated pre-GC concentration device for concentration regulation ("Precon"; for details cf. Brand, 1995). The accuracy of the absolute isotope values was relatively low (2 ‰) as the carbon stable isotope composition range of the internal laboratory CH_4 standards used for calibration was out of the range of the samples' carbon stable isotope composition. The precision, i.e. concerning the differences from sample to duplicates, however, was much higher (below 0.5 ‰ in most cases).

4.4.3 DIC carbon stable isotope analysis

DIC carbon stable isotope analysis was performed by C. Weyhenmeyer at the Isotope Laboratory of the Geological Institute of Bern University. The applied method and the technical details are similar to those described by Krishnamurthy et al. (1997) and Atekwana and Krishnamurthy (1998).

For the analysis, a septum tube (vacutainers; "vacuum serum tubes", 10 ml size, Becton Dickson & Co.) with a rubber stopper was filled with 0.5 ml of anhydrous phosphoric acid (100 % H_3PO_4), sealed and for at least 10 minutes evacuated to a pressure of less than 10^{-3} Torr (<0.133 Pa). 2 ml of the sample liquid were added to the vacutainers with a gas-tight syringe. The samples were allowed to react with the phosphoric acid in the sealed vacutainers for 2 hours at 25 °C, while they were constantly shaken. The vacutainers were subsequently attached to a needle on the vacuum line (the rubber stopper was punctured but not pierced) after which the line and needle headspace were evacuated for five minutes. Then, the rubber stopper of the sample vacutainer was pierced with the on-line needle. The gas was expanded cryogenically and the CO_2 was frozen into a glass tube ("cold finger") submersed in liquid nitrogen for five minutes. Expanding the gas cryogenically implies that there was a water trap in between the sample and the cold finger to remove all water. Then, the non-condensable gases were pumped away from the headspace of the cold finger for 15 seconds, while the CO_2 was still frozen. Afterwards, the glass tube was closed off by turning a valve. At the connected mass spectrometer (VG Prism II ir-MS), the isotope ratios of the liberated CO_2 were measured. The samples have been analysed in duplicate or triplicate where sufficient material was available. The overall analytical precision of the measurement is approximately 0.1 ‰.

4.4.4 Pore water DOC carbon stable isotope - sample preparation and storage

For ^{13}C-DOC sample preparation, the remaining pore water sample liquid of the by then analysed or transferred samples for CH_4 concentration or carbon stable isotope analysis was used. 10 to 15 ml (depending on disposable volume and DOC concentration) of each sample were filled into evaporating dishes (Schott Duran). Prior to use, the dishes had been cleaned with hydrochloric acid, rinsed out two times with deionised water and heated to 500 °C for several hours in order to prevent inorganic or organic carbon contamination. The sample liquid in the dishes was acidified with hydrochloric acid (Merck "Suprapur") until a pH of ca. 2 was reached to remove the inorganic carbon from the sample. The samples were subsequently put into an oven and kept at a temperature of 50 °C for about two days until the water had completely evaporated and the organic carbon formed a brown crust on the evaporating dishes. 5 to 6 drops of deionised water were then added to separate the desiccated

sample from the glass. This procedure yielded a concentrated suspension containing the samples' organic carbon, which was immediately transferred with glass pipettes into tin capsules. Then, the samples were again put into the oven and kept for another day at 50 °C for complete desiccation within the tin cartridges. At length, these cartridges were folded using tweezers and stored on a closed tray for transport.

4.4.5 Separation of humic and fulvic acids

Humic acids (e.g. $C_{308}H_{328}O_{90}N_5$) are high molecular weight (>2000 daltons) organic acids (Haworth, 1971). By definition, humic acids represent that fraction of humic substances, which is not soluble in water under strong acidic conditions, i.e. below pH 2 (according to Stevenson, 1985) or below pH 1 (EPCA, 2000), but is soluble at higher pH values. Fulvic acids (e.g. $C_{18}H_{40}O_8N_2$) are organic acids with a lower molecular weight (<2000 daltons). Fulvic acids represent the fraction of humic substances that is soluble in water under all pH conditions. Both, humic and fulvic acids are widespread in organic soils (e.g. Gobat et al., 1998).

In order to separate humic from fulvic acids, the sample liquid was gradually acidified with hydrochloric acid (Merck "Suprapur"), while its pH was continuously monitored with a pH-probe (cf. chapter 4.2). At pH 1, the acidification was stopped. After about 24 hours, the remaining solution (containing the fulvic acids) was separated from the precipitated organic matter (containing the humic acids) with a glass pipette. The separated samples were subsequently put into an oven and kept at a temperature of 50 °C for about two days until the water had completely evaporated and the organic carbon formed a crust on the evaporating dishes. 5 to 6 drops of deionised water were added to the desiccated sample to remove it from the glass. Concentrated suspensions containing the respective humic or fulvic acids were thus obtained and transferred into tin capsules with glass pipettes. The tin capsules were put again into the oven and kept for another day at 50 °C for complete desiccation of the samples. The capsules were then folded using tweezers and stored on a closed tray for transport.

4.4.6 Carbon stable isotope analysis of separated humic and fulvic acids

The carbon stable isotope analysis of the separated humic and fulvic acids was performed by S. Burns at the Isotope Laboratory of the Geological Institute of Bern University. The organic carbon was oxidised to CO_2 in a Carlo-Erba CHN elemental analyser and subsequently analysed for its carbon stable isotope composition in a coupled isotope ratio mass-spectrometer (ir-MS).

4.4.7 CO_2 and CH_4 carbon stable isotope analysis of gas emissions

The carbon stable isotope analysis of CH_4 and CO_2 samples from EGr gas emissions was performed by M. Leuenberger from the Division of Climate and Environmental Physics at the Physics Institute of Bern University. The analytical methods and devices correspond largely to those described above for the pore water CH_4 carbon stable isotope analysis. Minor divergences concern the volumes of sample gas used (due to the different concentrations in headspace and flux chamber samples), and, in case of CO_2, the procedure of sample separation.

4.4.8 Peat matrix carbon stable isotope analysis

Prior to this study in 1998, P. Steinmann from the Geological Institute of Neuchâtel University took a peat core at the EGr Bog. Peat samples from various depths between 0.15

and 6 m were thus obtained. The samples were ground in early 2000. The carbon stable isotope composition of the peat was determined by S. Huon from the Laboratory of Isotope Biogeochemistry at the University Pierre and Marie Curie in Paris.

4.5 Sampling of gas on the bog site

In addition to the headspace gas samples (obtained by sampling pore water in the vacutainers), gas emitted from the EGr Bog was also sampled directly. The gas samples were to be used to determine the carbon stable isotope signature of the CO_2 and methane emissions at EGr. Gas sampling (CH_4) and concentration measurements (CO_2) are needed to approximately determine the flux rates for these greenhouse gases from the surface of the EGr into the atmosphere.

4.5.1 Preparation of the field site

The site chosen for gas sampling and gas flux measurements was situated approximately 2.5 m SE of the main pore water sampling hole. The site was selected with respect to its accessibility, its surface and its presumable subsurface characteristics (plain ground, absence of nearby pools, trees and roots. Three standard sanitary polyethylene tubes (80, 80 and 30 cm long, each with an inner diameter of 19 and an out diameter of 20 cm) were installed in upright position in the bog. In order to limit the compressional impact on the ground, installation was done by rotation of the tubes driving them into the peat and using the tube walls as a cutting edge. For this purpose, the lower end of the tube walls had been given a zigzag shape and sharpened, while, at the upper end, two small holes were cut on opposite sides of the tube wall. A broomstick could thus be applied to increase the rotary leverage (Fig. 4-12), when the tubes were driven into ground. The two side holes were then plugged with plastic stoppers, while the upper end of the tube was at level with the ground surface and left open. At the upper end of the tubes, a ca. 4 cm long polyethylene ring was tightly attached at the outer tube wall. The ring ends slightly (ca. 1 cm) above the tubes and is hence situated above the bog's surface. Cylindrical receptacles could conveniently be fixed at the top of the tubes and sealed with grease to avoid gas exchange with the atmosphere (Fig. 4-13).

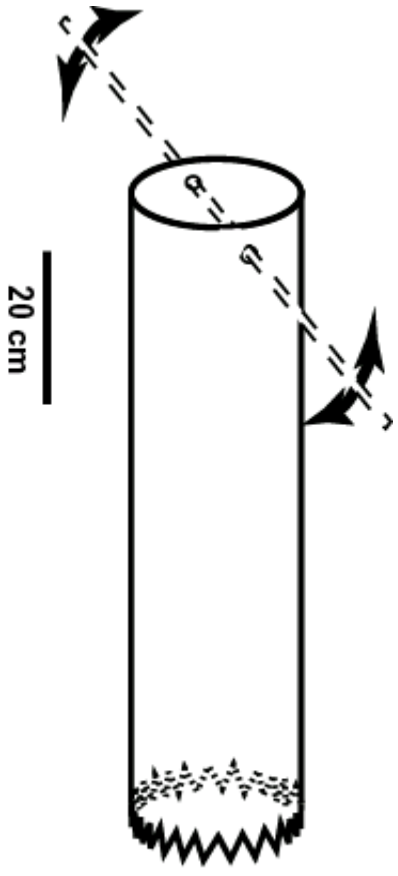

Fig. 4-12: A broomstick might be used to drive the tubes into ground (idea and design: A. Villard).

Mounting of receptacles to the tubes, purging of their a priori atmospheric gas content, set up of the detection devices as well as repeated measurement and sampling would have caused a considerable impact on the ground in direct vicinity of the chosen site, and, hence, would have inevitably disturbed the measurements. An boardwalk of ca. 2 m length as well as an access boardwalk of ca. 1.5 m length had therefore been installed at the site about 5 months before start of the CO_2 and CH_4 flux measurements. It had not only been designed to facilitate work and minimize artificial degassing effects of the soft ground, but also to reduce the impact on the bog's sensitive and protected ground vegetation.

4.5.1.1 Receptacles

The receptacles are made of plexiglass and have the same diameter as the tubes (inner diameter of 19 cm outer diameter of 20 cm) a height of ca. 29.7 cm and correspondingly volume of ca. 8420 cm^3. While the lower end (which was to be fixed at the top of the tubes) is open, the upper end is closed. The upper end has a circular hole of 1.3 cm in diameter in the middle, which was plugged with a polybuthylene rubber septum and used for sampling by syringe. The cylinders are also equipped with a small hose (inner diameter 1 mm; length ca. 2.5 m), which connects the receptacles' interior to the outside (cf. Fig. 4-13). It is therefore possible to maintain atmospheric pressure in the inside, while, at the same time keeping the influence of air movement and air exchange at minimum.

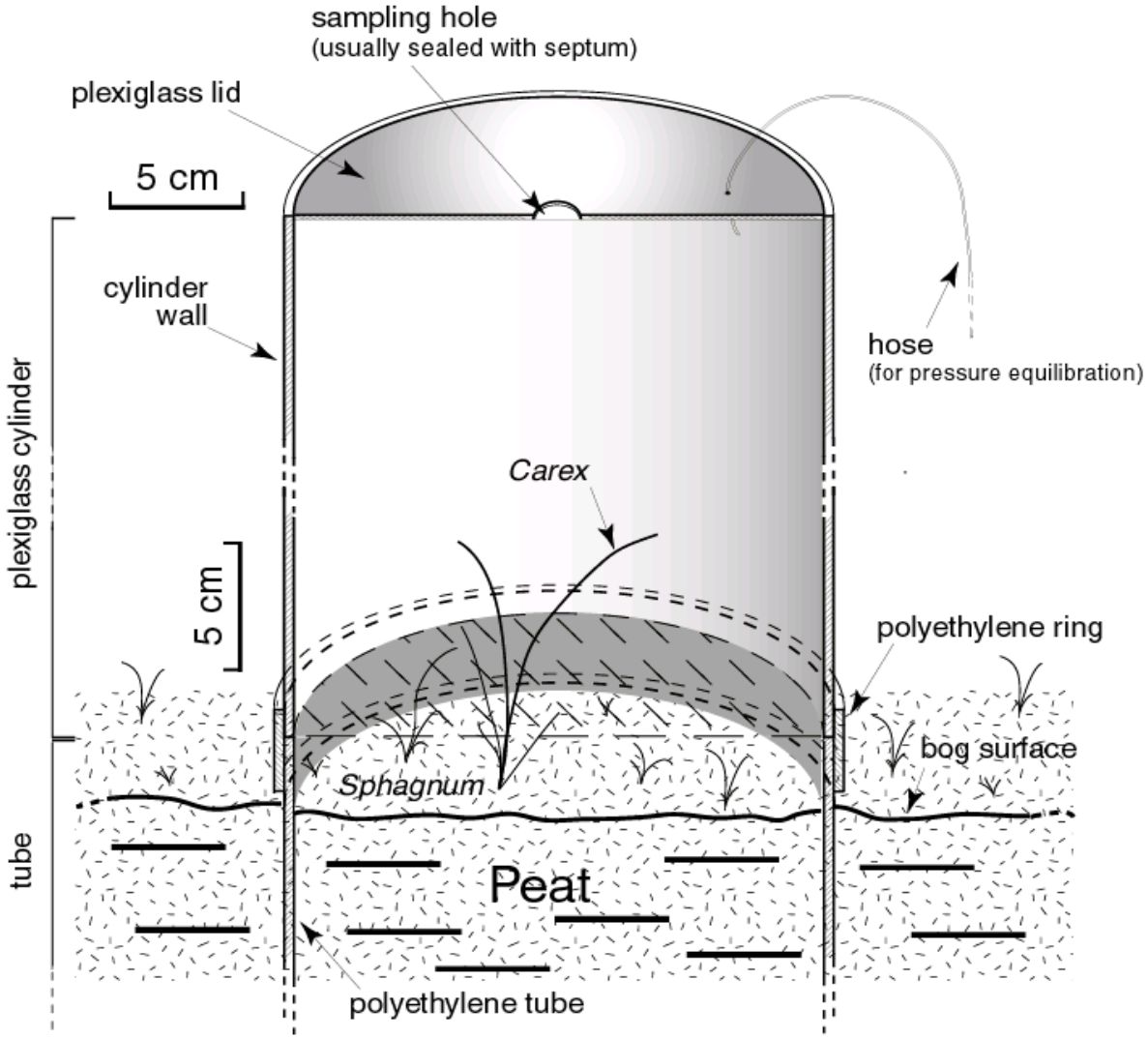

Fig. 4-13: Schematic illustration showing a vertical profile view of a tube with the gas receptacle (plexiglass cylinder) at its top. For gas-tightness, grease is put between the upper wall margin of tube and the lower wall margin of the receptacle. The length of the hose is about 2.5 m.

4.5.1.2 Purging of the receptacles

Before mounting the plexiglass cylinders on the tube ends, attempts were made to purge them with nitrogen in order to remove the atmospheric CO_2. This was necessary for the carbon

stable isotope measurements on the CO_2 emitted from the ground. These attempts turned out to be unsatisfactory: atmospheric CO_2 at considerable amounts re-entered the cylinders, when they were eventually shifted towards the tubes and while being mounted. To overcome this problem, liquid nitrogen was cautiously poured through the central hole at the top of the cylinder. Most of the liquid nitrogen would evaporate immediately without reaching the ground of the cylinders and create an overpressure that drives gas (through the same central hole) out of the cylinder. By this method, the remaining CO_2 concentration in the cylinders could be drastically decreased to less than 5 ppm in most cases. It should be noted, that the effects accompanying direct usage of liquid nitrogen (considerable temporary temperature change, slight kryogenic effects on the ground vegetation) could potentially affect the gas flux from the bog. It should, however, not influence the carbon stable isotope composition of the CO_2 from the ground.

4.5.2 Gas sampling

Gas samples were taken for CH_4 concentration analysis as well as CH_4 and CO_2 carbon stable isotope analysis. For this purpose, 10 ml of gas were drawn up through the septum into a gas-tight, lockable syringe. The gas was transferred into the vacutainers described in chapter 4.1. The amount of gas transferred was 5 ml for each sample for CH_4 concentration analysis. For isotope analysis, the vacutainers were completely filled with the sample, i.e. 7 to 8 ml of gas were transferred depending on the actual vacuum in the vacutainers. The gas samples were kept in a cold box for transport and storage. The time period between sampling and analysis varied from one day to several months. Tests for vacutainers filled with known gas concentrations showed no or only minor leakage for this time period. The maximum (CH_4) concentration decrease observed after four months was below 10 %.

4.6 Gas flux measurements

The measurement of the net methane flux across the water / atmosphere interface is based on the static chamber method described by Moore and Roulet (1991). The cylinders, which served as receptacles for the gas emissions from the ground, are described in chapter 4.5.1.1.
A portable infrared analyser was used for the CO_2 concentration measurements. Although portable flame ionisation detectors (FID) exist, it appeared more convenient to do the methane analysis using a stationary GC at the University of Neuchâtel. This was mainly for financial reasons. Samples for CH_4 concentration determination were usually taken directly upon CO_2 measurement. The measurements were carried out at increasing time intervals for all three cylinders, starting ca. 2 minutes after fixation and sealing of each cylinder on the tube. The flux measurements lasted for 3 to 4 hours and were repeated several times in summer and autumn 2001. For CH_4, the determined concentrations in most cases did not allow the calculation of a gas flux. Preliminary measurements of the CH_4 flux (one of them over two days) were carried out in 2000, yet did not yield reliable results either.

4.6.1 CO_2

The gas analyser used to measure the carbon dioxide concentration is a PP Systems WMA-2 rugged CO_2 analyser / controller. The detection method ("linearised, non-dispersive infrared gas analysis") is based on the quantitative absorption of characteristic infrared wavelengths by chemical compounds: In a standardised analytical environment, the absorption of a specific wavelength is proportional to the concentration of the corresponding chemical compound. The CO_2 measurement range (0 - 2000 ppmv) has been chosen according to user

requirements. For the analytical device, the precision is better than +/- 0.5 %. The linearity is +/- 1.0 %. The detection limit is below 1 ppm by volume. A gas mixture of 1000 ppm CO_2 (99.995 vol-% purity) in nitrogen was chosen for calibration. The WMA-2 analytical device does not correct automatically for optical gas density variations due to temperature, pressure, or so-called foreign gas broadening (e.g. by H_2O vapour). A correction for these effects, based on a value for the atmospheric CO_2 concentration (362 ppmv), has therefore been made after analysis. While perhaps negligible in other studies, for the study presented here, this correction proved to be particularly important with respect to air pressure differences (and hence differences in the optical gas density) due to the considerable discrepancy in altitude between the laboratory (at ca. 450 m asl.), where the calibration was made, and the EGr site (at ca. 1000 m asl.), where the measurements were made.

(9) $CO_2\ [ppmv] = R_{meas}\ [ppmv] * F_{corr}$

(10) $F_{corr} = R_{atmCalibSite} / R_{atmFieldSite}$

Explanation of the symbols

CO_2 [ppmv]	CO_2 concentration in ppm by volume
R_{meas} [ppmv]	Reading of measurement in ppm by volume
F_{corr}	Correction factor for optical density variations
$R_{atmCalibSite}$	atmospheric CO_2 concentration at the site where the analytical device was calibrated
$R_{atmFieldSite}$	atmospheric CO_2 concentration at the field site, where the CO_2 concentration was determined

The WMA-2 infrared detector was equipped with an approximately 30 cm long polypropylene pipe connected to a small needle. Sample gas was then sucked from the interior of the plexiglass cylinder through the septum and via the induction pipe into the detector. The inner diameter of the pipe was only 2.5 mm to decrease the pipe volume and hence the time lags between the start of the measurement and obtaining the correct reading. The WMA-2 was set for dynamic gas sampling, i.e. gas inflow while CO_2 detection (in contrast to the static mode in which the gas flow stops when the detection chamber is filled). The advantage of the dynamic mode is a higher accuracy of the measurement, as no sample contamination occurred. This was the case in the static mode due to pump failure. The disadvantage is higher sample consumption, and, as the gas is sucked out of the plexiglass chamber, low pressure in the chamber. This likely causes inflow of atmospheric air via the pressure equilibration outlet (cf. Fig. 4-13) into the chamber and perhaps even artificially increased gas emissions from the ground.

The gas flow (60 ml / minute) to the analytical device had been determined in the laboratory. The volume of gas removed from the plexiglass chamber during each measurement interval (30 seconds corresponding to a pumped volume of 30 ml) could therefore also be calculated. This is important to correct for the systematic error caused by the inflow of atmospheric air into the chamber after each measurement.

4.6.2 CH_4

Gas samples for CH_4 concentration measurement were taken from all three plexiglass chambers after different time intervals (cf. chapter 4.5.2).

4.6.2.1 Method

The gas chromatograph used for gas flux sample analysis of bog pore waters was a Carlo Erba 4130 connected to a packed column equipped with a flame ionisation detector (FID). An isothermal oven program was chosen and the temperature was set 80 °C. The gas was injected with a gas-tight lockable glass syringe (Hamilton) of a total volume of 500 µl. The volume of gas injected was 300 µl for each run.

4.6.2.2 Calibration

Calibration gas mixtures ("standards") with 1 ppm, 100 ppm and 10,000 ppm methane (purity superior to 99.995 %) in nitrogen were used. The calibration gas for CH_4 concentrations in between the purchased standards was mixed manually using the same gas-tight lockable glass syringe as for injection. The range for the standards was adapted to the expected concentrations of the sample (Fig. 4-14). Table 4-3 gives an overview of the standards used for most measurements.

Table 4-3: Calibration standards used for gas flux methane analysis and the analytical device's precision for the different standard concentrations

CH_4 concentration of standard [ppm]	**manual dilution? (CH_4 concentration of purchased standard used) [ppm]**	**number of standards measured**	**average value [area units]**	**relative standard deviation for n values**	**n** (October 17th, 2001)
10,000	no (10,000)	5	6,909,284	0.018	5
1000	yes (10,000)	5	3,071,710	0.043	5
500	yes (10,000)	5	1,647,498	0.090	5
250	yes (10,000)	5	749,641	0.065	5
225	yes (10,000)	3	563,119	0.153	3
200	yes (10,000)	3	520,946	0.157	3
160	yes (10,000)	2	491,713	0.109	2
140	yes (10,000)	2	383,761	0.052	2
125	yes (10,000)	3	317,818	0.219	3
100	no (100)	11	192,378	0.058	11
50	yes (100)	3	93,612	0.022	3
10	yes (100)	3	25,445	0.006	3
1	no (1)	8	15,465	0.023	3
					n (Test September 7th, 2001)
100	no (100)	14	195,848	0.030	14
1	no (1)	5	16,332	0.021	5

The increase of peak area for the relevant concentration showed a partial lack of linearity (cf. Fig. 4-14). Therefore, a point-to-point calibration method was chosen for the CH_4 concentration calculation. A drift of the standards' peak surface during the measurements and the preliminary tests (August 2001 - October 2001) was not observed. The relative standard deviations of the calibration standards reflect the error made, when the standard was diluted in the syringe. They also reflect the influence of the methane concentration in the ambient air, especially, when the standard's CH_4 concentration was very low (e.g. 1 ppm).

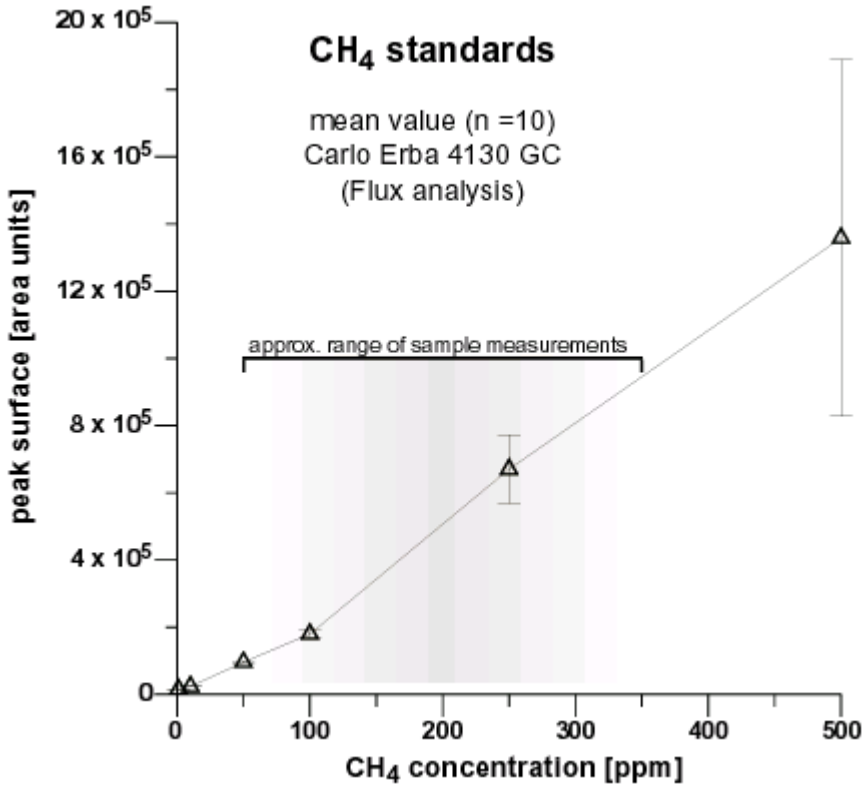

Fig. 4-14: Mean peak surface values for different concentrations of the methane standard. The measurements were repeated 10 times for each standard and the relative standard deviation is given by the error bars. A point-to-point calibration method was used. The shaded area marks the range of the methane concentrations in the samples.

4.6.2.3 Blanks

Blanks were measured at the beginning, throughout and at the end of the calibration and the sample measurements. The blanks (generally ambient laboratory air) showed a well discernable peak for methane corresponding to a concentration of ca. 0.3 ppmv (relative standard deviation: approximately 0.17; n = 17). The laboratory air did not show significant CH_4 concentration change during the measurements. Blanks taken from new, pristine vacutainers also yielded methane concentrations of ca. 0.3 ppmv (relative standard deviation: approximately 0.06; n = 5).

4.6.2.4 Corrections

The values obtained by gas chromatography analysis needed to be corrected, as the samples were transported (and stored) in vacutainers. The samples have therefore been diluted by the vacutainers' residue gas content. In case the sample volume injected into the vacutainers was inferior to the evacuated reference volume of the vacutainers (and there was hence low pressure), additional dilution by laboratory air occurred when preparing the sample for injection into the GC. The correction factor depends on the volume of sample gas injected into the vacutainers and the total volume of the vacutainers themselves.

Correction for sample dilution

(11) CH_4 [ppmv] = C_{meas} [ppmv] * (($Vtot_{vacutainer}$ + V_{syr})/ Vs)

Explanation of the symbols

C_{meas} [ppmv]	measured CH_4 concentration in ppm by volume
CH_4 [ppmv]	calculated CH_4 concentration for the gas sample in ppm by volume
Vs	volume of the sample injected into the vacutainer
$Vtot_{vacutainer}$	total volume of the vacutainer (8.2 ml)
V_{syr}	volume of gas drawn from the vacutainer into the syringe (1 ml)

The CO_2 (and CH_4) flux from the bog was then calculated from the corrected concentration values with respect to the volume of the plexiglass chambers, their ground surface, the time interval between the measurements as well as the quantitative influence of the volume of gas removed for sampling and due to its replacement by ambient air. It was assumed that only atmospheric air would compensate for the low pressure caused by sampling, and that there was no increase of gas emission from the ground.

5 HYDROLOGY AND MAJOR ELEMENTS

This chapter summarises those results of the study, which are not directly related to the methane and CO_2 concentration in the pore water of the EGr. The patterns of major element concentrations, pH, precipitation, air and pore water temperature, hydrology are described here along with their seasonal variations. With respect to most of the species and parameters mentioned, this work can be seen as the continuation of an earlier, pioneering study of the geochemistry in deep petlands (Steinmann, 1995). This study is relevant as - for the first time - results of a long-term (more than 2 years) investigation of deep peatland geochemistry are presented.

5.1 Major element concentrations and their seasonal variations

Pore water samples from the EGr were obtained using diffusion chambers ("peepers") for in situ filtration (cf. chapter 4.1). The major cations measured are sodium (Na^+), potassium (K^+), magnesium (Mg^{2+}), and calcium (Ca^{2+}). The ammonium (NH_4^+) concentration has also been determined, as it represents an important product of organic matter decomposition. Concerning the anions, the concentration of chloride (Cl^-) has been measured during the entire period of study. The concentrations of other anions, such as phosphate (PO_4^{3-}) and sulphate (SO_4^{2-}) decrease very rapidly in the acrotelm already. They have been determined for some sample series at the beginning of the study.

Typically, ombrotrophic bog pore waters have low major element concentrations (cf. chapter 2.4). The composition of bog surface waters converges at rainwater composition (Shotyk, 1988). This has been observed for different sampling methods and for a wide range of bogs at different locations and different climate zones (cf. Table 2-2). The concentrations generally decrease with distance from the bog margins towards the interior, except for those elements whose primary source is rain only (e.g. Cl^-).

Earlier, yet less continuous investigations with respect to major element concentrations at EGr (Steinmann, 1995; Steinmann and Shotyk, 1997a&b) indicate similar patterns for this bog. The pore water chemical analysis of this study confirms the earlier findings: While the absolute concentrations are low, the relative concentration increase towards the ground is pronounced. The concentration increase with depth is due to pore water mixing with the underlying strata, dissolution of dust, as well as advective and diffusive transport processes (cf. chapters 2.5.1 and 2.5.2, respectively; cf. McKenzie et al., 2002). Ions whose major direct source is rainwater (e.g. Cl^-) consequently do not show this trend. In connection with dilution from the acrotelm due to pore water advection, the processes mentioned above may have created the observed concentration patterns. Significant and repeated seasonal variations, however, are in most cases absent.

5.1.1 Sodium (Na^+)

Fig. 5-1 shows that the sodium concentrations in the pore water of EGr were generally below 1 ppm (mg/l) during the study period. Slightly higher concentrations of up to ca. 3 ppm were detected only in one series of measurements (November 2000) in the deep catotelm as well as in the upper catotelm and acrotelm. In November 2000, an additional peeper (Type A, cf. chapter 5.1.9) had been installed ca. 3.5 m SW of the main sampling hole). As the samples derived from peeper Type A were measured directly after the samples from the deep catotelm of peeper Type B, contamination during analysis can be an explanation for this singular observation. The blank measured as a sample between the two series, however, does not indicate this. The relative concentration differences observed in the course of the year are very small. No clear seasonal variation can be deduced for the EGr pore water's sodium concentration patterns. It may however be noted, that all sampled profiles showed minimum Na^+ concentrations in the upper catotelm (1 - 3 m depth).

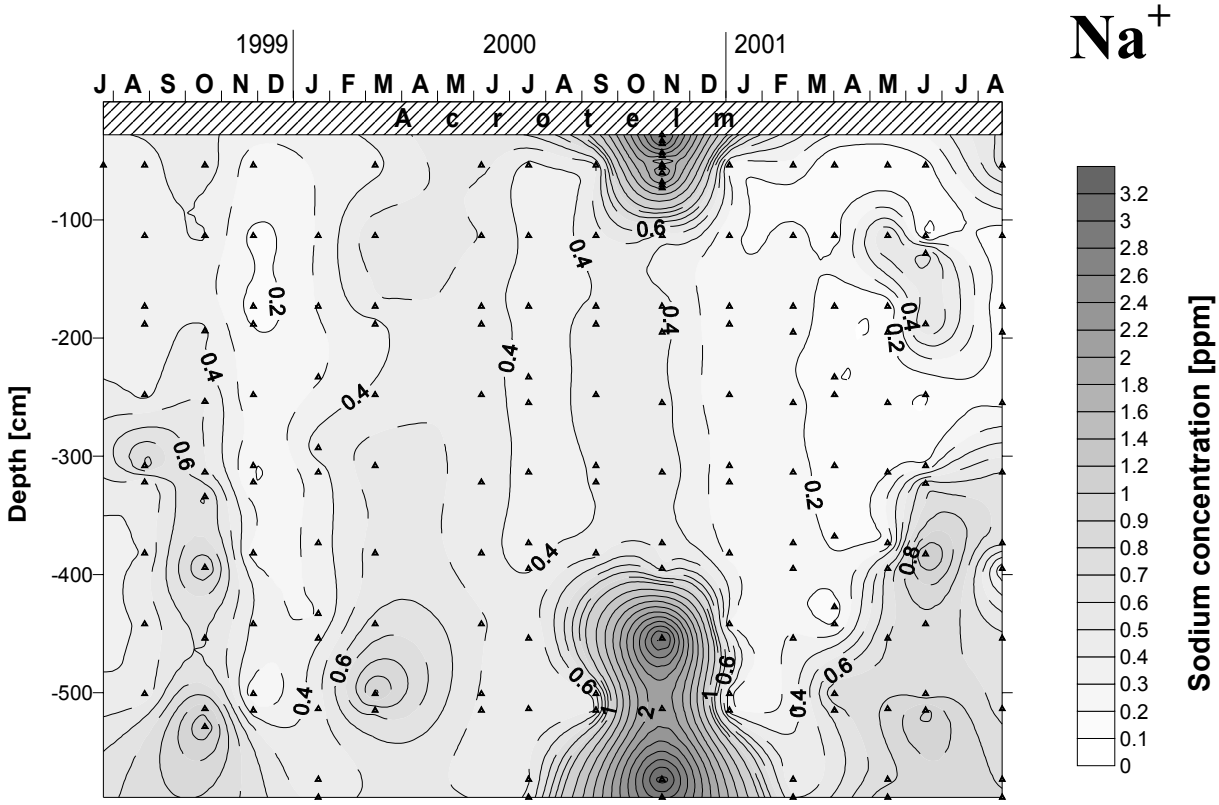

Fig. 5-1: Isopleth diagram showing the sodium pore water concentrations measured in the catotelm of EGr from July 1999 to August 2001. The triangles represent the data points.

5.1.2 Potassium (K^+)

The potassium concentration in the EGr pore water was generally below 2 ppm (Fig. 5-2). Higher concentrations (up to ca. 3.5 ppm) occurred in the deep catotelm (generally below ca. 4.5 m depth). Highest potassium concentrations were observed in the very early phase of sampling, in August 1999 with a maximum of 5.71 ppm at ca. 5 m depth. A possible explanation for this observation is given below in chapter 5.1.5.

The low potassium concentrations observed in the deep catotelm (below 4 m depth) in October 1999 are difficult to explain. Possibly, heavy rainfalls lasting from September 20th, 1999 until October 8th, 1999 (cf. Fig. 5-13) have led to the anomalously low potassium concentrations on the day of sampling (17th October 1999). A similar anomaly has been observed for calcium and, to a lesser extent, for magnesium, yet not for sodium. Sodium concentrations are relatively high in the entire bog profile in October 1999 (cf. Fig. 5-1). This indicates, that sodium in bog pore water derives mainly from rainwater. Potassium, which is intensively cycled in organic matter, may reflect potential organic matter decomposition patterns. The binding of K^+ to organic matter, however, is probably less important than its role as an electrolyte in the cell fluids (P. Steinmann - pers. comm.). Alike sodium, the potassium concentration in the pore water of EGr showed only minor changes, rarely exceeding one order of magnitude. This observation is characteristic of bogs and has already been observed in very early studies, e.g. by Ramann (1895). The data set revealed no clear seasonal variation. As in the case of sodium, it should be noted, that lowest concentrations occur for all series in the upper catotelm (1 - 3 m depth).

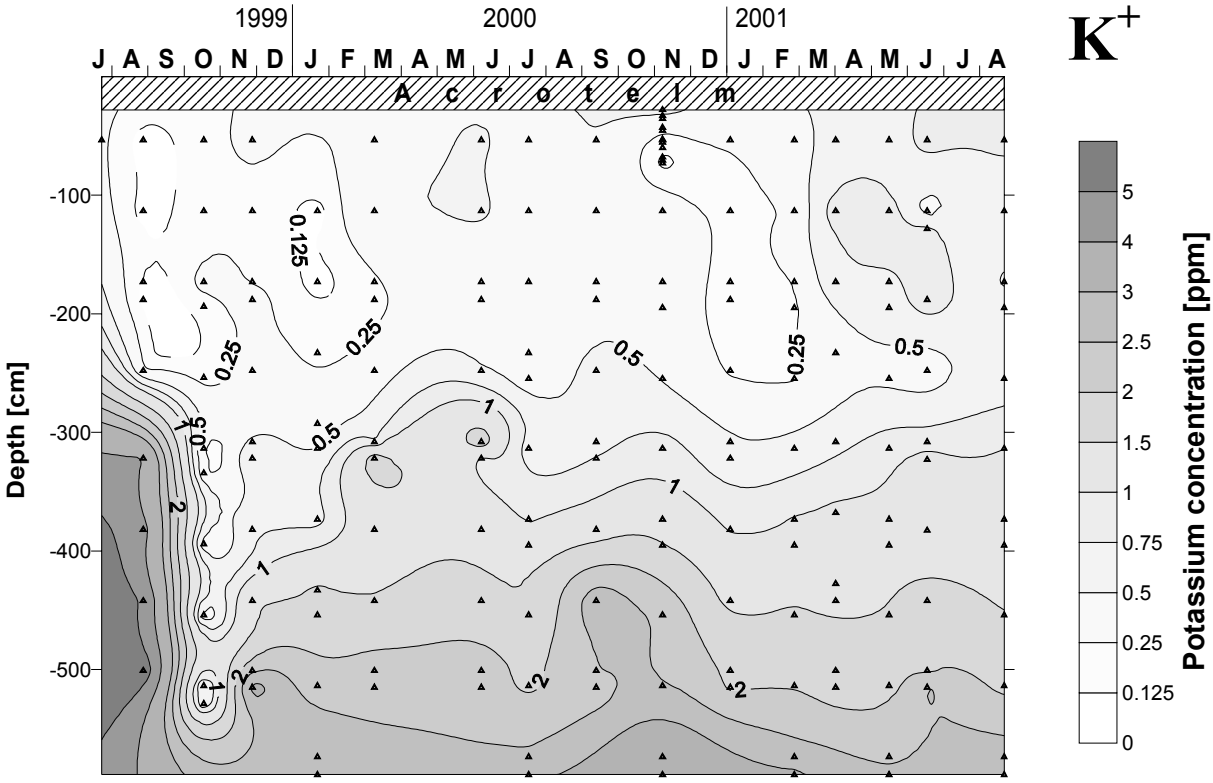

Fig. 5-2: Isopleth diagram showing the potassium pore water concentrations measured in the catotelm of EGr from July 1999 to August 2001. The triangles represent the data points.

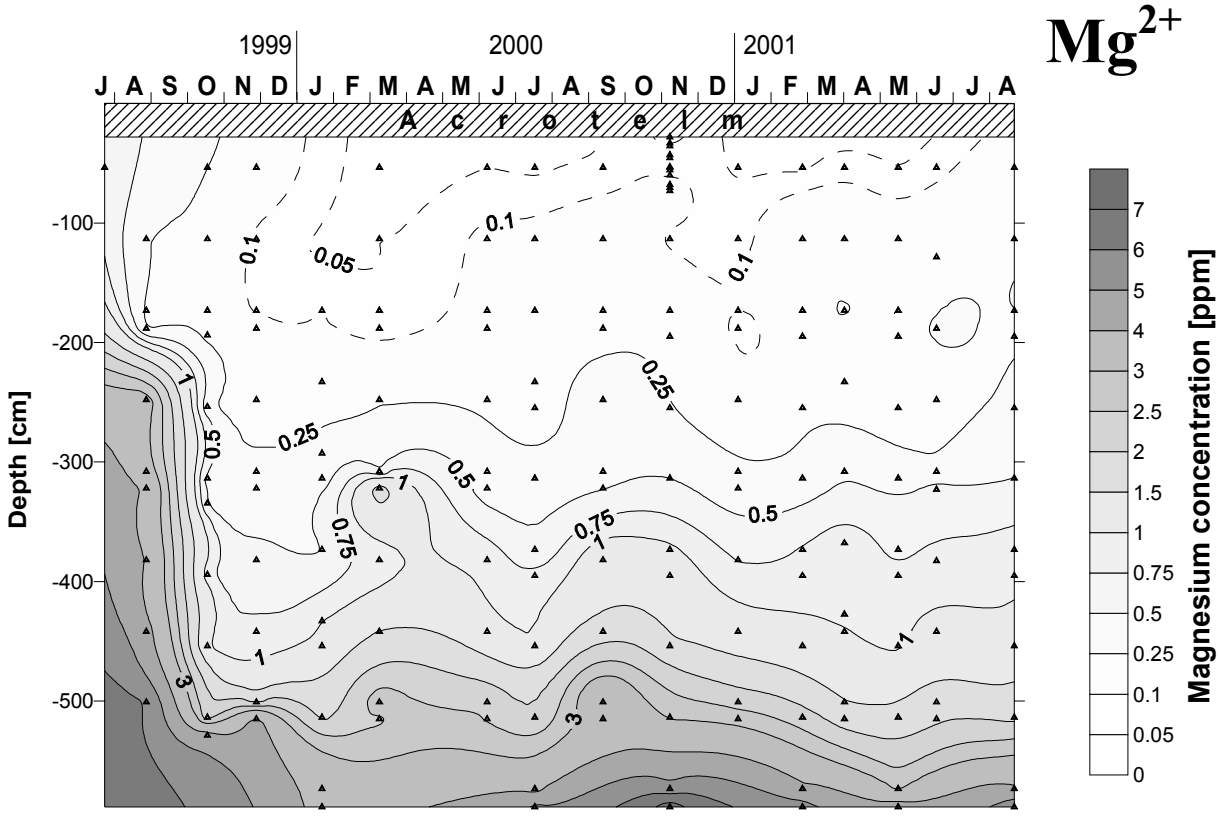

Fig. 5-3: Isopleth diagram showing the magnesium pore water concentrations measured in the catotelm of EGr from July 1999 to August 2001. The triangles represent the data points.

5.1.3 Magnesium (Mg^{2+})

Magnesium in the EGr pore water showed a clear concentration increase with depth for most samples (Fig. 5-3). The rate of increase is low in the upper catotelm (above ca. 3 m depth), but accented in the lower catotelm (below ca. 3 m depth). The absolute concentration values range from as low as 0.03 ppm at the top of the catotelm (March 2000) to up to 7.6 ppm at ca. 5.9 m depth (November 2000). For an explanation of the anomalously high magnesium concentrations measured during the very early phase of sampling (August 1999), confer chapter 5.1.5. The magnesium concentration in EGr pore water shows no significant seasonal variations.

5.1.4 Calcium (Ca^{2+})

The EGr pore water calcium concentration patterns (Fig. 5-4) are very similar to those for magnesium. The concentration increase with depth is slight for the upper catotelm (above ca. 3 m depth), but pronounced for the lower catotelm (below ca. 3 m depth). The absolute concentrations range from 0.25 ppm at the top of the catotelm to 50 - 100 ppm at the bottom at 5.9 m depth. In August 2001, they showed an exceptionally high value (213 ppm) at 5.9 m depth. As for the interpretation of anomalously high calcium concentrations measured during the very early phase of sampling (August 1999), cf. chapter 5.1.5. A seasonal variation could not be deduced for the calcium concentration in the EGr pore water.

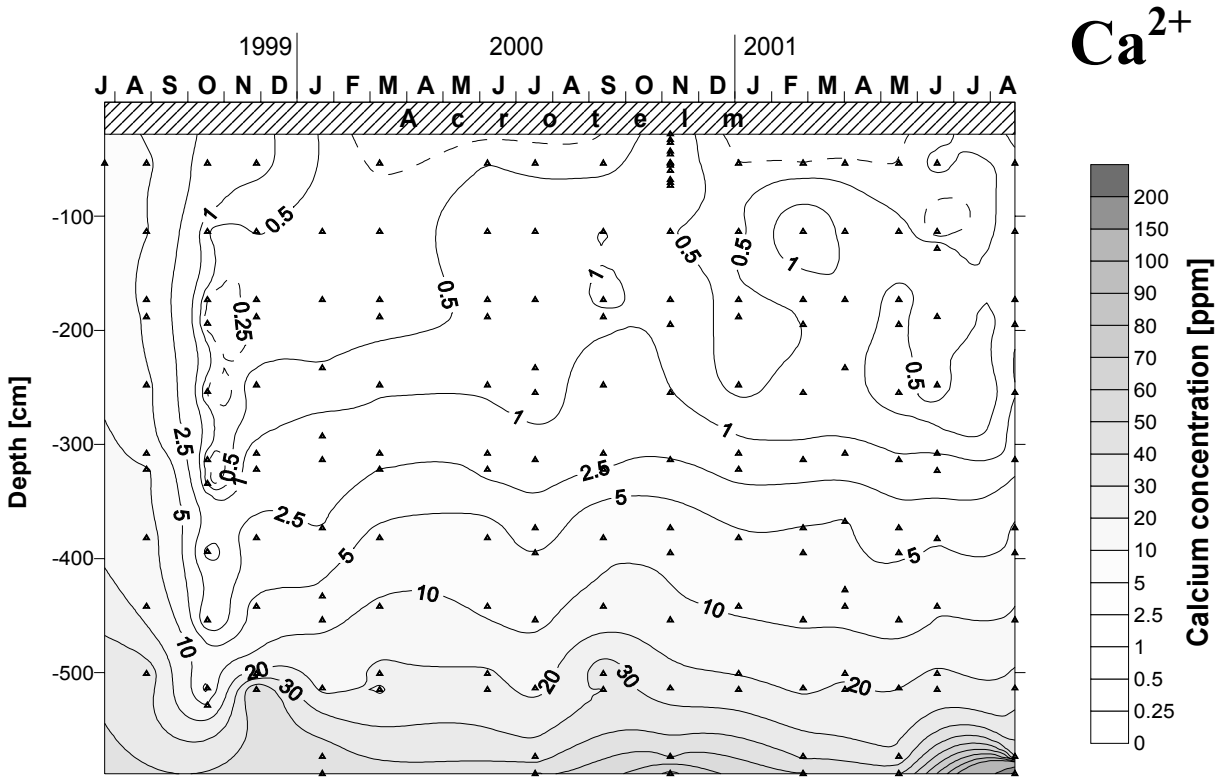

Fig. 5-4: Isopleth diagram showing the calcium pore water concentrations measured in the catotelm of EGr from July 1999 to August 2001. The triangles represent the data points.

5.1.5 Early phase of sampling - potassium, magnesium, calcium

Remarkably high K^+, Mg^{2+} and Ca^{2+} concentrations were observed in the early phase of sampling: The measurements of August 25th, 1999 yielded anomalously high Mg^{2+} and Ca^{2+} concentrations at all depth levels. For K^+, the measured concentrations of this series were particularly high below ca. 2.5 m depth and include the absolute maximum value (5.71 ppm at ca. 5 m depth). The high concentrations in the early phase of sampling are probably related to the reactivation of the sampling hole about two months before and the associated mechanical impact and the disturbances created (e.g. by squeezing pores and solids), when installing the peepers (cf. chapter 4.1). Ions, which are normally incorporated in solid organic matter (in particular K^+, Mg^{2+} and Ca^{2+}; cf. Shotyk, 1988), could have been mobilised and higher pore water concentrations are therefore observed in the analysis. Other cations such as Na^+ and NH_4^+, by contrast, are to a smaller degree associated with plant material and, hence, do not discernibly contribute to such an effect. This is also the case for the measured anions (Cl^- and CH_3COO^-). Such effects, however, have not been observed in preliminary studies, for instance, directly after the hole had been cored (P. Steinmann - pers. comm.).

5.1.6 Ammonium (NH_4^+)

In contrast to the other major ions measured at EGr, ammonium concentrations are high compared to uncontaminated ground waters (Berner and Berner, 1987). For all sample series at EGr, pore water NH_4^+ concentrations increase with depth (Fig. 5-5). In contrast to magnesium and calcium, the rate of NH_4^+ concentration increase is slightly more pronounced in the upper than in the lower catotelm. The ammonium concentrations range from ca. 0.1 ppm at 0.5 m depth to ca. 20 ppm at 5.9 m depth. During the period of study from August

1999 to August 2001, only slight concentration variations (in the order of 5 to 25 %) were observed. These do not seem to be related to seasonal temperature change.

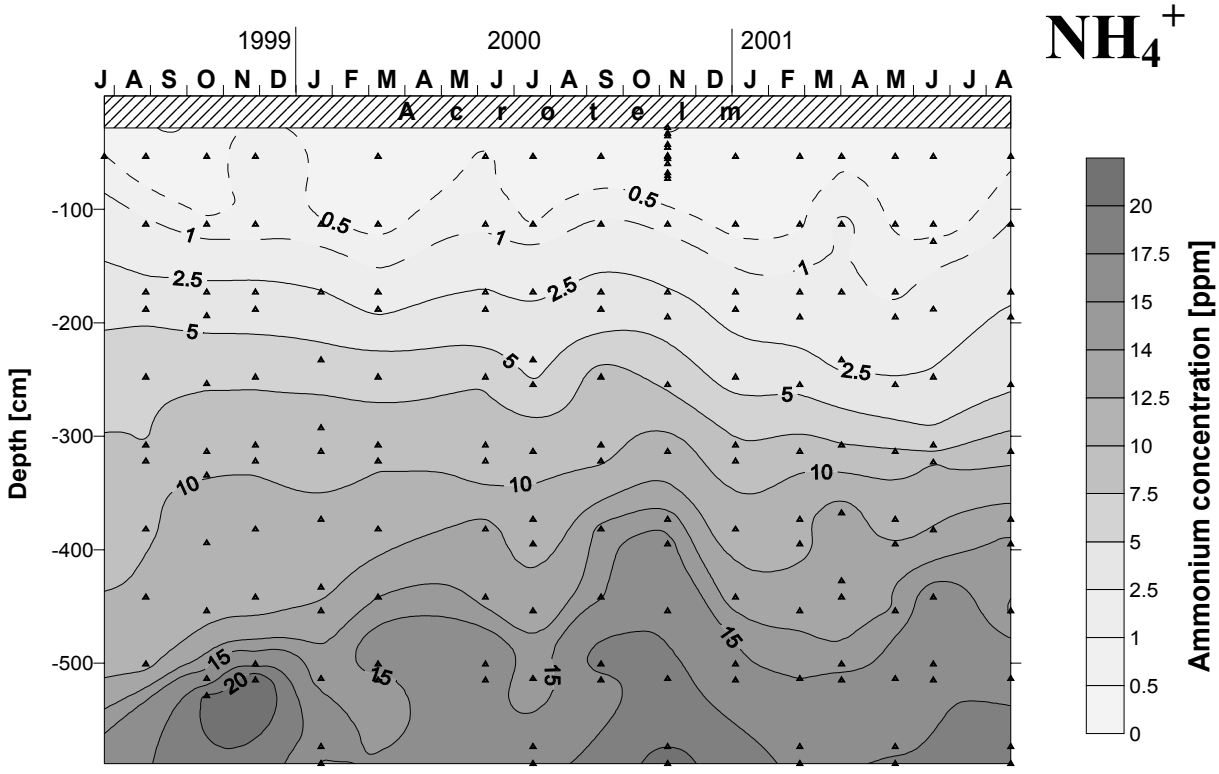

Fig. 5-5: Isopleth diagram showing the ammonium pore water concentrations measured in the catotelm of EGr from July 1999 to August 2001. The triangles represent the data points.

5.1.7 Chloride (Cl^-)

The chloride concentrations measured in the pore water of EGr during the study period ranged from ca. 230 to about 830 ppb (Fig. 5-6). These are relatively low concentrations with respect to "typical" ground waters (cf. Table2-2; Drever, 1997; Berner and Berner, 1987). While major cations (in particular K^+) showed minimum concentrations in the upper catotelm, chloride disclosed almost inverse patterns with highest concentrations between 1 and 2 m below ground surface for most sample series. This could be due to the fact that in ombrotrophic mires, the chloride input derives solely from the atmosphere. Concentrations therefore decrease only slightly with depth (e.g. by incorporation in DOC; Dahlman, 1993), whereas potassium is rapidly taken up in the acrotelm and uppermost catotelm by plants. In contrast to most cations measured, the chloride concentrations showed seasonal differences: Concentrations were by some 10 to 20 % lower in autumn and winter than in spring and summer (cf. Fig. 5-6). This is probably a consequence of the arrival of melt water in spring and increased precipitation (cf. Fig. 3-5) and evaporation in summer. The database is however too small to prove a seasonal trend.

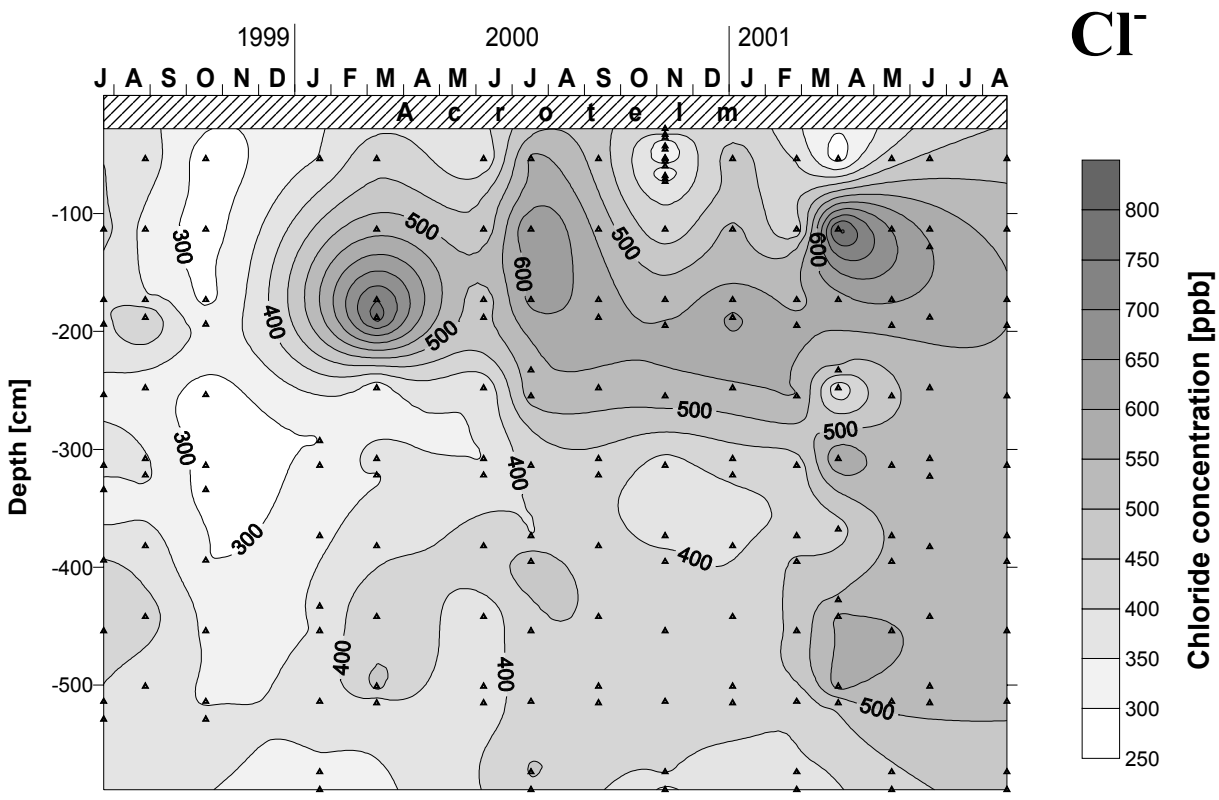

Fig. 5-6: Isopleth diagram showing the chloride pore water concentrations measured in the catotelm of EGr from July 1999 to August 2001. The triangles represent the data points.

5.1.8 Dissolved inorganic carbon (H_2CO_3*, HCO_3^-, CO_3^{2-})

The dissolved inorganic carbon (DIC) concentration of the EGr pore water generally increased with depth (Fig. 5-7). The increasing hydrostatic pressure towards the ground of the bog is one reason for the observed concentration increase, as CO_2 is more soluble at higher pressures. It may account for a linear 1.5 fold increase over the entire 6 m profile, but not for the two-fold increase observed between 1.5 and 2.5 m depth. Higher pH in the lower catotelm is another important factor for the pronounced DIC increase with depth, because it shifts the carbonate dissolution equilibrium towards HCO_3^- and CO_3^{2-}. This results in potentially higher DIC concentrations in the deep catotelm, when sufficient CO_2 is produced, e.g. by fermentation reactions or as a by-product of acetogenesis (cf. Fig. 6-1). At depths below ca. 2.5 m, the EGr pore water is already over-saturated in dissolved gases (chapter 11.AIII-Goldschmidt‘00-Fig.2a). Carbonate dissolution from the marly substrate of the bog (cf. chapter 3.1.2) and mixing of pore waters may also contribute to higher DIC concentrations in the lower part of EGr.

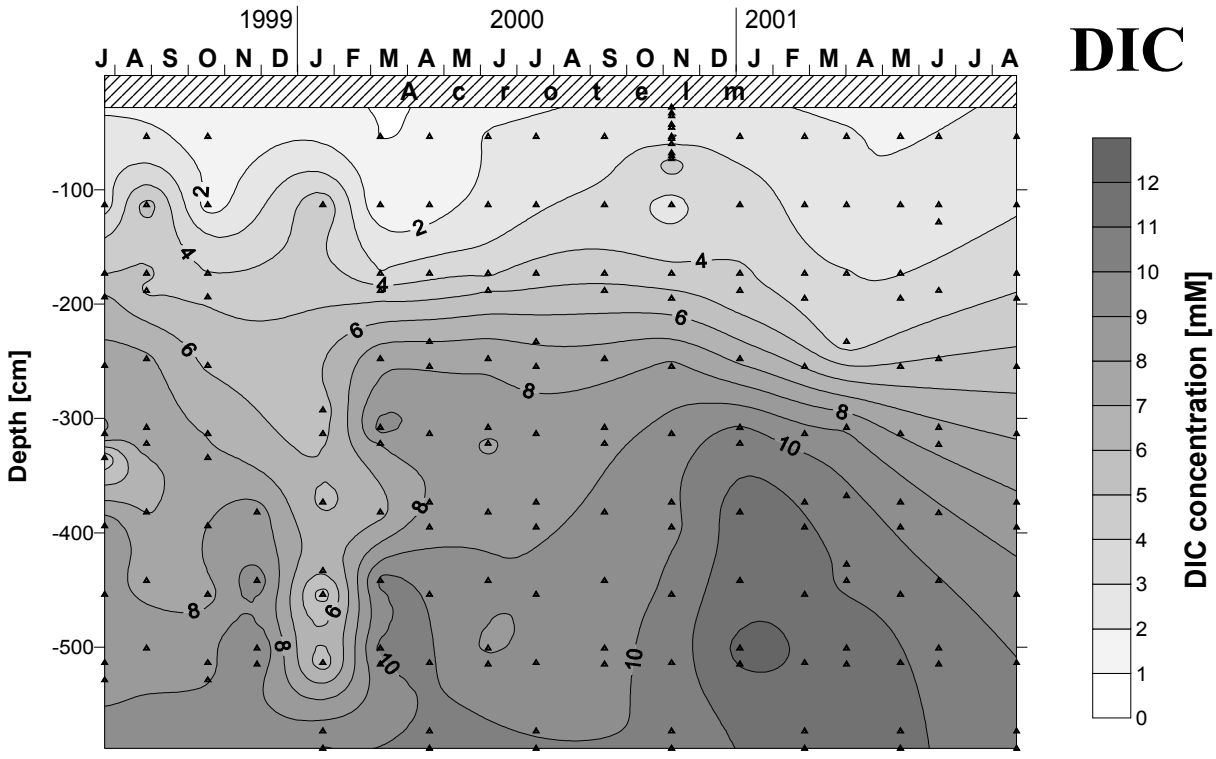

Fig. 5-7: Isopleth diagram showing the DIC pore water concentrations measured in the catotelm of EGr from July 1999 to August 2001. The triangles represent the data points.

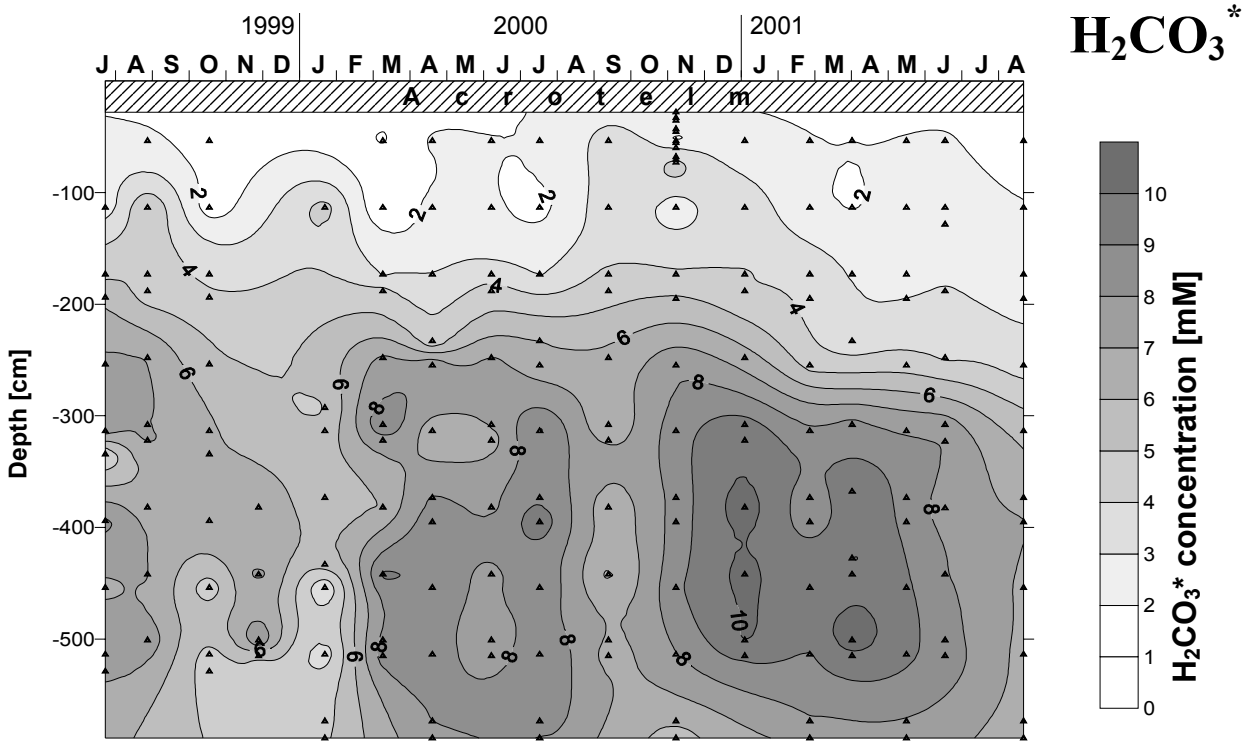

Fig. 5-8: Isopleth diagram showing the H_2CO_3* concentration in the pore water calculated for the catotelm of EGr. The calculation is based on the DIC concentrations (cf. Fig. 5-7) and the pH values (cf. Fig. 5-11) measured in the EGr pore water from July 1999 to August 2001. The triangles represent the data points.

The relatively low DIC concentration measured in the lower catotelm (below ca. 2 m) in January 2000 is perhaps an artefact and the result of gas loss from the peepers. In the January 2000, methane (cf. Fig. 6-3) similarly showed anomalously low concentrations in this depth range, although being sampled and stored in different receptacle (vacutainers instead of syringes). No indication for gas loss while sampling, however, was noted and the peeper membranes were intact. Since remarkably low acetate concentrations had been observed in November 1999 and January 2000 (cf. Fig. 6-2), a decline in microbial acetoclastic activity in the deep catotelm encroaching on CO_2 and methane production (cf. discussion in chapter 6.1) should also be considered. The January 2000 DIC anomaly is reflected by low H_2CO_3* concentrations in the deep catotelm (Fig. 5-8). For calculation of the H_2CO_3* concentration the two carbonate equilibrium constants and the corresponding pore water pH values were considered (P. Steinmann, pers. comm.).

5.1.9 November 2000 data from a different peeper (Type A)

On November 7th, 2000, pore water samples were obtained using the two different types of peepers (cf. chapter 4.1) at the same time: The long Type B peeper set was installed as usual at the main sampling hole. The short Type A peeper was installed in a newly cored hole, ca. 3.5 m SW of the main sampling hole. The analytical results for pore water samples collected with the Type A peeper generally correspond very well to the results for samples obtained with peeper Type B. The only exceptions concern the sodium concentration (cf. chapter 5.1.1) and the pH (cf. chapter 5.2.1). It is worthwhile looking at some results of the November 2000 pore water analysis for the samples obtained with peeper A separately, i.e. independently of the long-term concentrations variations shown in the isopleth diagrams in the preceding chapters.

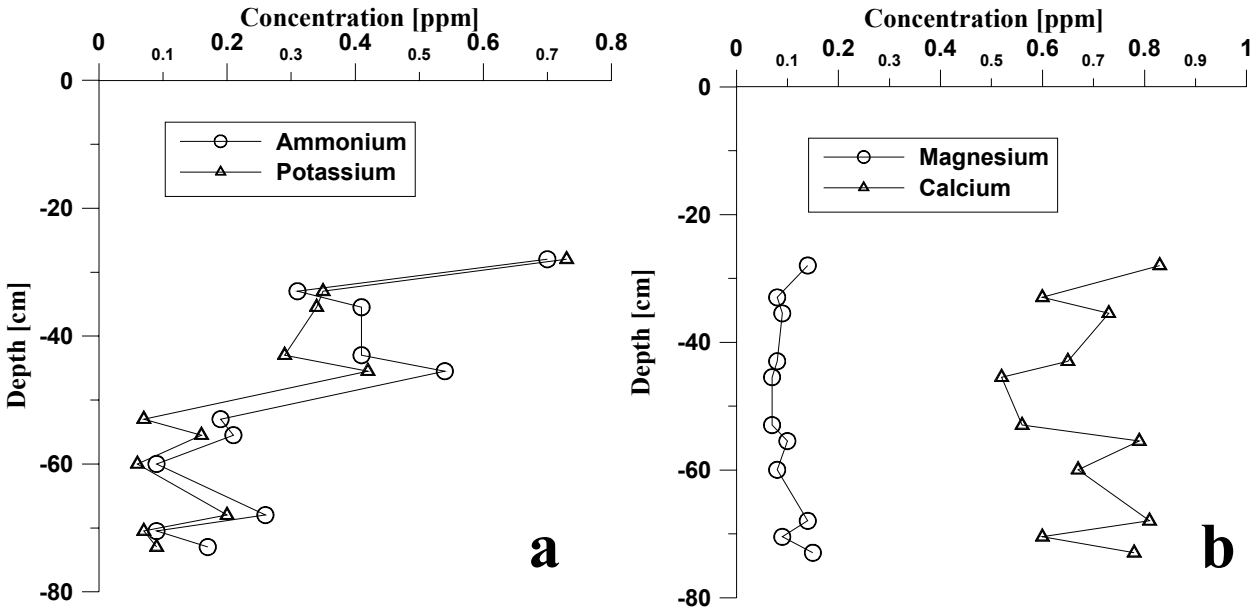

Figs. 5-9a&b: Pore water concentrations of different chemical species measured in the acrotelm and upper catotelm of EGr. The pore water samples were obtained using Type A peeper set (cf. chapter 4.1).

For ammonium and potassium (Fig. 5-9a), declining concentrations were observed in the sampled depth range between 28 and 73 cm. (The uppermost sample at 23 cm below ground surface had to be discarded as it was too close to the bog water level at that site.) This

indicates that ammonium and potassium are enriched in the shallow vegetation zone, linked to microbial activity in the upper layer, and probably actively cycled in plant organic matter. The parallel trending wiggles of the ammonium and potassium concentrations at high sample resolution (2.5 cm) further point to the presence of geochemically well distinguished and relatively thin peat layers. The magnesium and calcium concentration patterns in the upper EGr catotelm (Fig. 5-9b) support this interpretation. They show a similar parallel trend, although at first sight this might not be so evident due to the larger absolute concentration differences. The absolute concentrations of these two elements remain rather constant, when the entire range from 28 to 73 cm is considered. Apparently, their concentrations are not, or only to a minor degree, affected by vegetation.

5.2 Physiochemical, physical, and hydrological characteristics

5.2.1 pH

The pH was measured in pore water samples, which were obtained using the peepers described in chapter 4.1. Typically, the pH in peat bog water is lowest near the surface and increases downwards mainly due to the decreasing production of organic acids, pore water mixing and a change in the peat matrix composition in greater depths (Shotyk, 1988, IPCC, 1996). Near-surface EGr pore waters in a depth of ca. 10 cm have a pH of about 4.4 (Steinmann and Shotyk, 1997a). As can be inferred from Fig. 5-10, the downward pH increase observed at EGr in the study presented here, is not entirely linear, but more pronounced below ca. 4 m depth. This is very likely a consequence of pore water mixing near the bog's marly substrate. pH values at ca. 50 cm below ground surface (corresponding to the depth-level of the uppermost Type B peeper) were typically around 4.7. At 4 m depth, the pore water had a pH of approximately 5.5. Near the ground of the bog at ca. 5.9 m depth, the EGr pore water showed almost neutral pH around 6.3. The EGr pH pattern varied only little during the study period (Fig. 5-11). There is no indication for a significant seasonal dependency of the pH levels. The less regularly downward increasing pH before September 2000 can be attributed to the handling of the pH probe (cf. chapter 4.3.1).

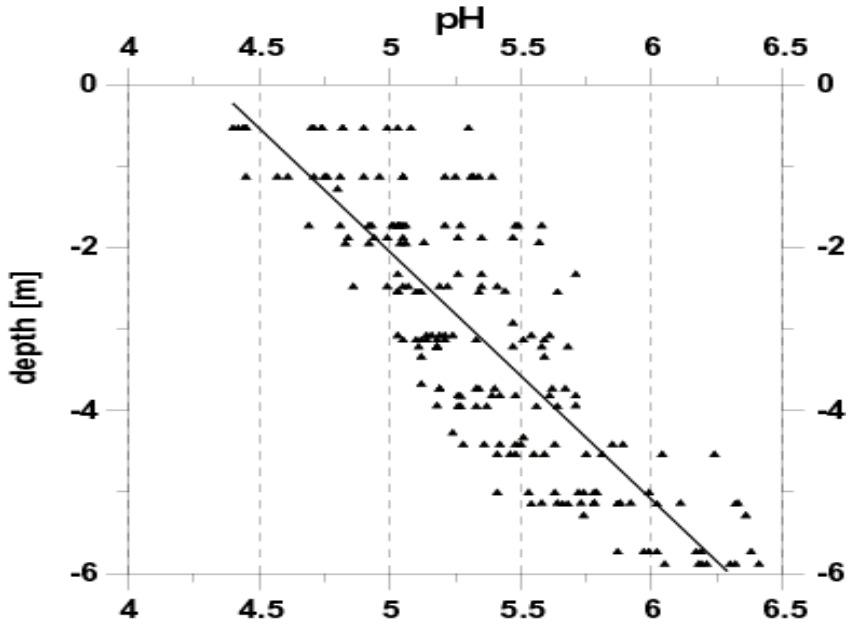

Fig. 5-10: Compilation of all pH values determined for the EGr pore water during the study period from July 1999 to August 2001.

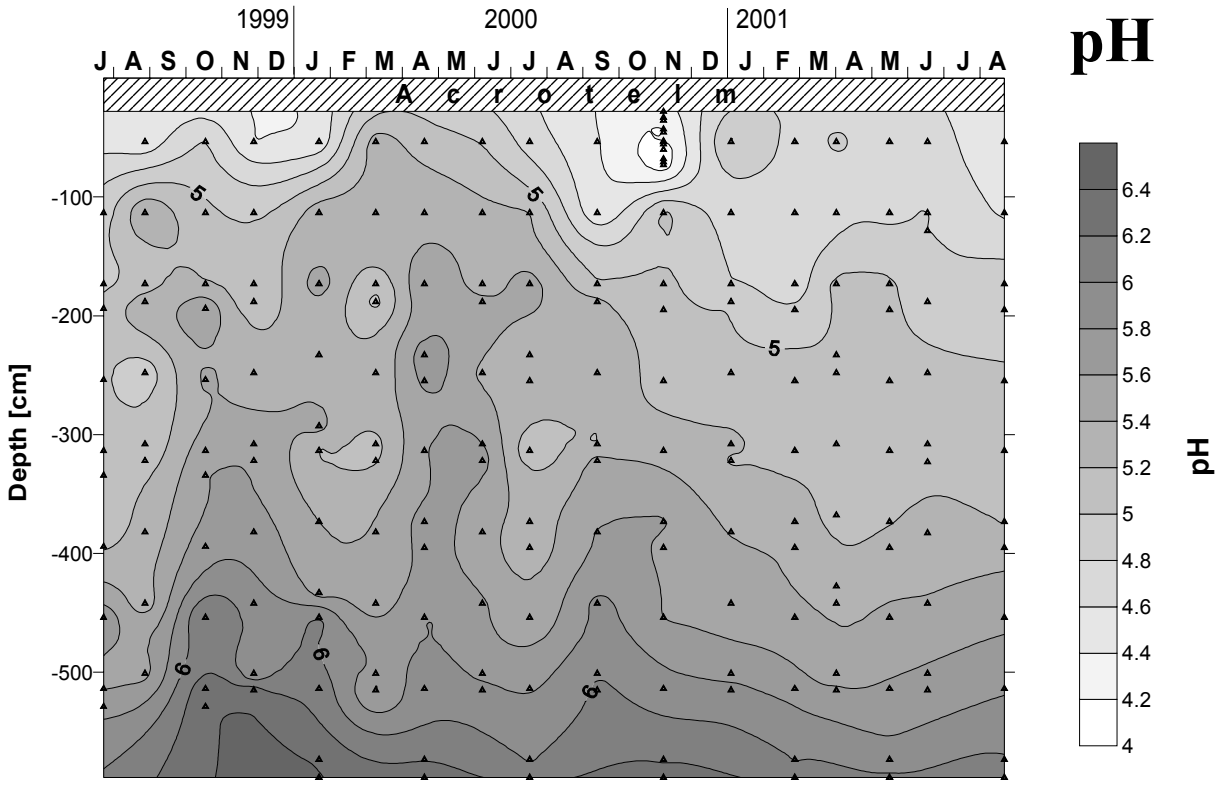

Fig. 5-11: Isopleth diagram showing the pH in the catotelm pore water of EGr during the period of measurement from July 1999 to August 2001. The triangles represent the data points.

In November 2000, pore water samples were obtained using the short peeper (Type A; cf. chapter 4.1), which had been installed in the acrotelm and upper catotelm ca. 3.5 m SW of the principal sampling hole. These samples showed considerably lower pH values than were observed in the pore water of the normally used long (Type B) peepers. At 53 cm below ground surface (corresponding to the depth at which the uppermost Type B peeper was installed), the measured pH for the peeper Type B was 4.9, while it was 4.2 for peeper Type A. This is probably not an erroneous measurement, nor should it be attributed to the different design of the two peepers (cf. Fig. 4-1a&b): The observation highlights the potential local geochemical variations in a bog and may be attributed to the microtopography-related influences of peat vegetation, permeability, microbial reactions and others. Shotyk (1988) gives examples for abrupt pH changes in peat bogs: He cites an earlier worker (Chodat, 1924), who was surprised how quickly the pH could change across the surface of a peatland. In this extreme example, Chodat (1924) had found over distances as small as 1 m that the pH could change from less than 4 to more than 7. Similar observations were made by Kotilainen (1927) and Kurz (1928). Another potential reason for different pH values at the same depth-level may be related to the shape of the sampling hole. During the course of sampling, the uppermost part of the main sampling hole (to a depth of ca. 20 cm) had widened by 2 to 3 cm. This might have caused a water conduit, which could have reached the uppermost diffusion chamber of the Type B peeper and affected (i.e. increased) the pH. If, however, this was the case, the opposite effect with more acid waters percolating from the top and hence a decrease in pH should be expected.

5.2.2 Precipitation and temperature

Precipitation and the daily mean temperature data for the period of field research were obtained from the Saignelégier meteorological station (M. Jeanbourquin/MeteoSwiss - pers. comm.) located ca. 4 km west of the EGr Bog. In the time period of concern (from June 1999 to October 2001), the monthly precipitation and the monthly mean temperatures were characteristic for the region (cf. chapter 3.1.3). By and large, they follow typical seasonal patterns (Fig. 5-12). Major climatic deviations, for instance, have been observed in July 2000, when temperatures were unusually low or in March 2001, when precipitation was unusually high. Both, the annual mean precipitation (1640 mm) and the annual mean temperature (8.1 °C) as averaged from June 1999 to Mai 2001 were significantly higher than the standardised 30 years' average from 1961 to 1990 (1511 mm and 5.8 °C, respectively - cf. chapter 3.1.3). Years with 10 % or more than the average annual precipitation are not unusual in the Franches Montagnes Region and occurred 13 times in the period from 1982 to 2001 (MeteoSwiss - pers. comm.). For temperature, the difference is particularly pronounced (2.3 °C), but can be explained by the fact the La-Chaux-de-Fonds meteorological station, where the long-term average is measured, is characterised by lower average temperatures than average temperatures at the Saignelégier station. The averaged annual mean temperature at Saignelégier meteorological station for the time period from 1990 - 2000 was 7.7 °C (M. Jeanbourquin - pers. comm.) and hence only 0.4 °C lower the average temperatures calculated for the period of field research. Moreover, "*the 1990s have been the warmest decade and 1998 the warmest year of the millennium*" (IPCC, 2001), and it is therefore not surprising that more recent annual mean temperatures reflect this and hence differ from the long-term average.

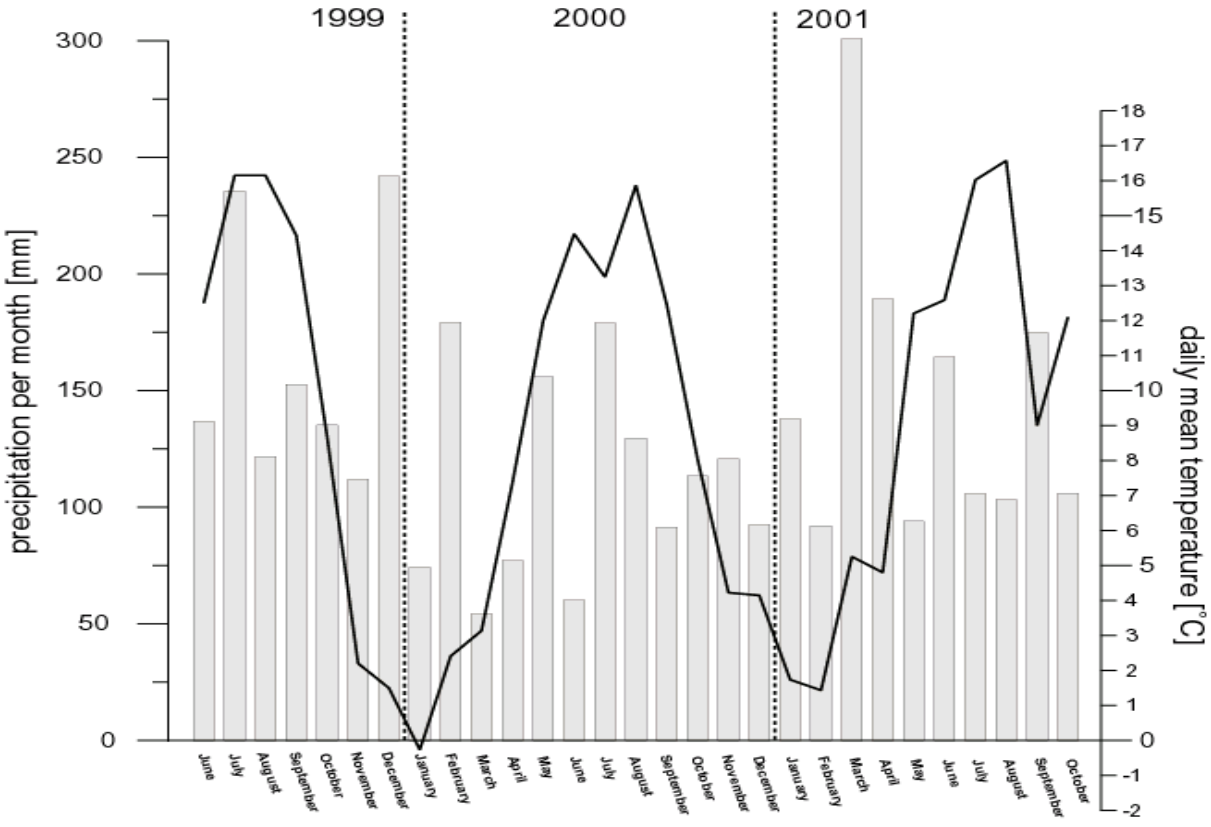

Fig. 5-12: Monthly precipitation and monthly mean temperatures at Saignelégier meteorological station (ca. 4 km west of EGr) for the time period of field measurements. The monthly values are based on daily precipitation data and three temperature (for 7.30am, 1.30pm, 7.30pm) readings per day provided by M. Jeanbourquin.

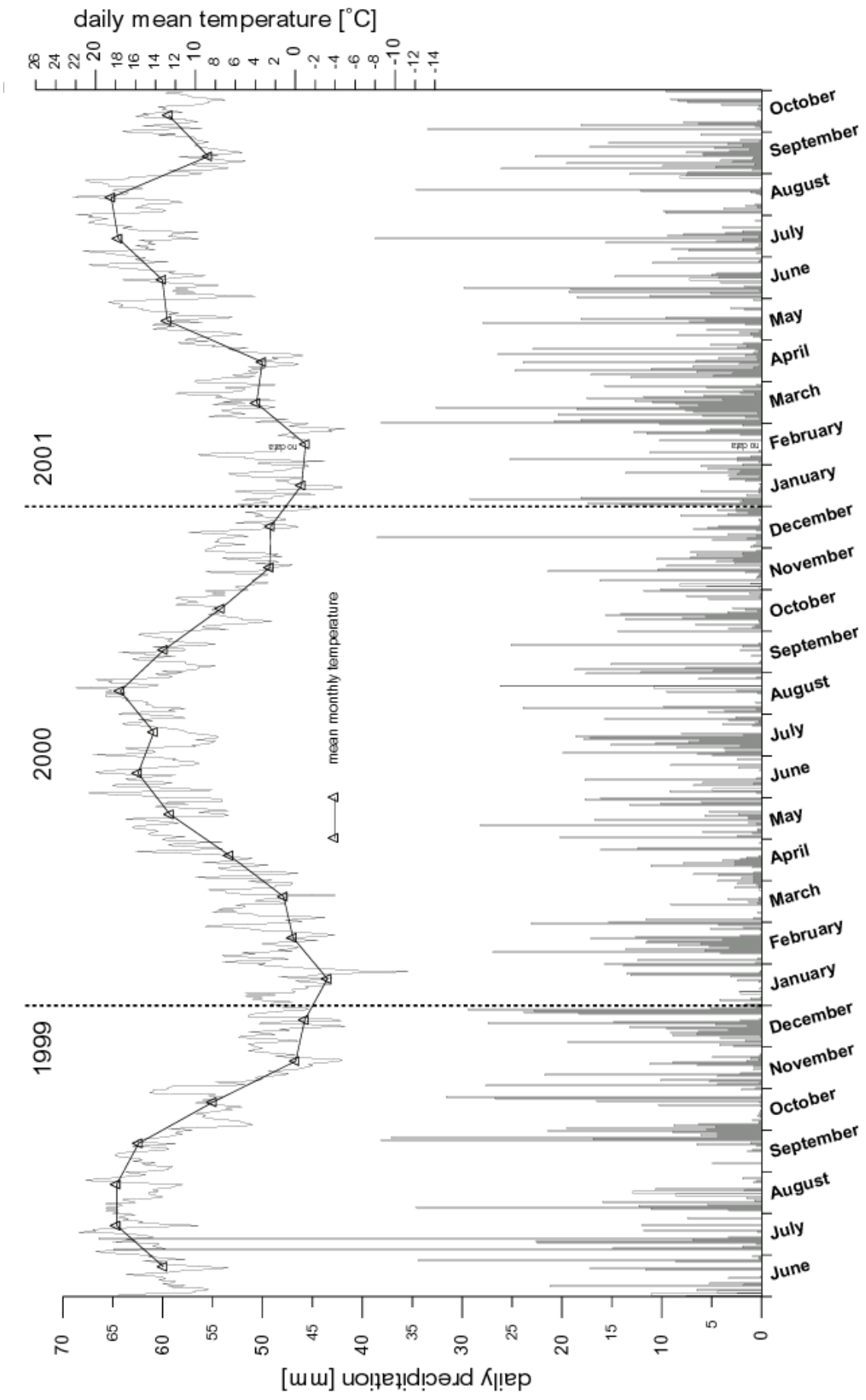

Fig. 5-13: Daily precipitation and daily mean temperatures at Saignelégier meteorological station (ca. 4 km west of EGr) for the time period of field measurements. The values are based on daily precipitation data and three daily temperature (7.30am, 1.30pm, 7.30pm) readings provided by M. Jeanbourquin (MeteoSwiss, Saignelégier).

Fig. 5-13 provides more detailed information on daily precipitation and daily mean temperatures for the time period of concern: A particular dry period was observed from August 19th to September 18th, 1999; a particular wet period, for instance, lasted from February 22nd until March 29th, 2001. The lowest daily mean temperature measured was -11.3 °C (January 25th, 2000), the highest was 22.3 °C (August 15th, 2001). Such short-term temperature changes, in particular with respect to precipitation, may have influenced some of the geochemical parameters determined. The anomalously low potassium and magnesium concentrations measured in deep parts of the EGr bog (cf. chapters 5.1.2 and 5.1.3) on October 15th, 1999, for instance, are probably a consequence of heavy rainfalls in the period from September 20th to October 8th, 1999 (cf. Fig. 5-13).

5.2.3 Water table

Fig. 5-14 shows the variations of the water table at the EGr sampling site. During the period of study from June 1999 to October 2001, the average water table was ca. 14 cm below ground surface. The depth of the water level depended primarily on the climatic regime (and predominantly on precipitation) before the measurements. The lowest water level was measured on September 12th, 2000 (21 cm below ground surface) after an entire week with relative high temperatures and virtually no precipitation. The highest water level was observed on April 2nd, 2001 (4 cm below ground surface) and can be explained by the unusually intense precipitation in the month before (cf. Fig. 5-13). The severe and almost uninterrupted rainfalls of March 2001 had also caused catastrophic flooding in several parts of Switzerland. A relative low water table in winter is the consequence of a 5 to 15 cm thick ice-cover at the surface of the EGr Bog (cf. chapter 11.AIII-EUG'01-Fig.3), effectively hampering precipitation water from entering the bog.

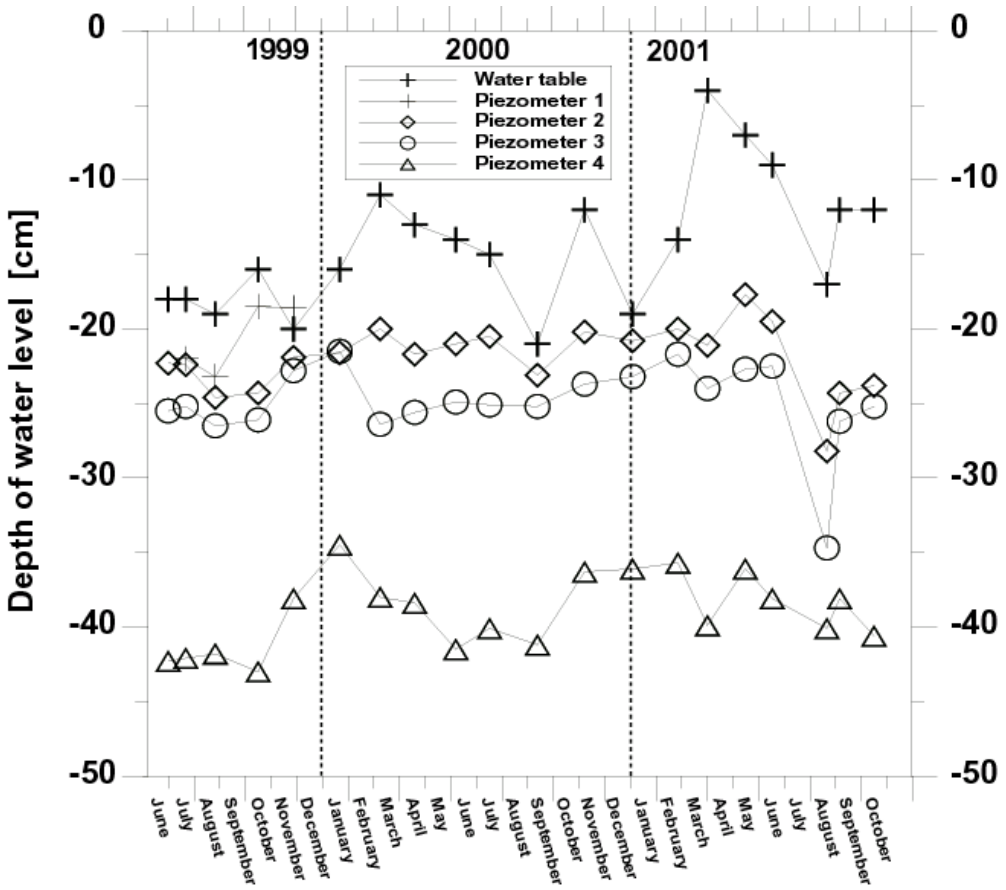

Fig. 5-14: Depth of the water table in the main sampling hole and of the water levels in the four piezometers installed at EGr ca. 2.5 m SW of the main sampling hole. The measurements at the main sampling hole were taken before removal of the peepers.

5.2.4 Piezometer data

The water levels in the 4 piezometers showed only little variation during the period of study from June 1999 to October 2001 (Fig. 5-14). Rare deflections were for example observed on January 3rd, 2000 and on August 22nd, 2001 and can be explained by the respective wet or dry periods before the measurements (cf. Fig. 5-13). The piezometer data indicate a stable downward directed water flow regime at EGr during the entire period of field research.

Fig. 5-15 shows the vertical hydraulic gradients as determined for the EGr in two depth zones, one ranging from 150 to 250 cm (i.e. between piezometer 2 and 3), and the other, from 250 to 550 cm (i.e. between piezometer 3 and 4). The average vertical hydraulic gradient is 0.030 for 150 - 250 cm depth and 0.047 for 250 - 550 cm below ground surface. The gradients are generally downward directed, except for January 2000, when a very weak upward directed gradient (-0.001) was determined. An upward hydraulic gradient causes pore water advection to stop and potentially even an upward transport of pore water (Siegel et al., 1995; McKenzie et al., 2002). This rare phenomenon coincides with the ice-cover at EGr existing in January 2000 (cf. chapter 11.AIII-EUG'01-Fig.3).

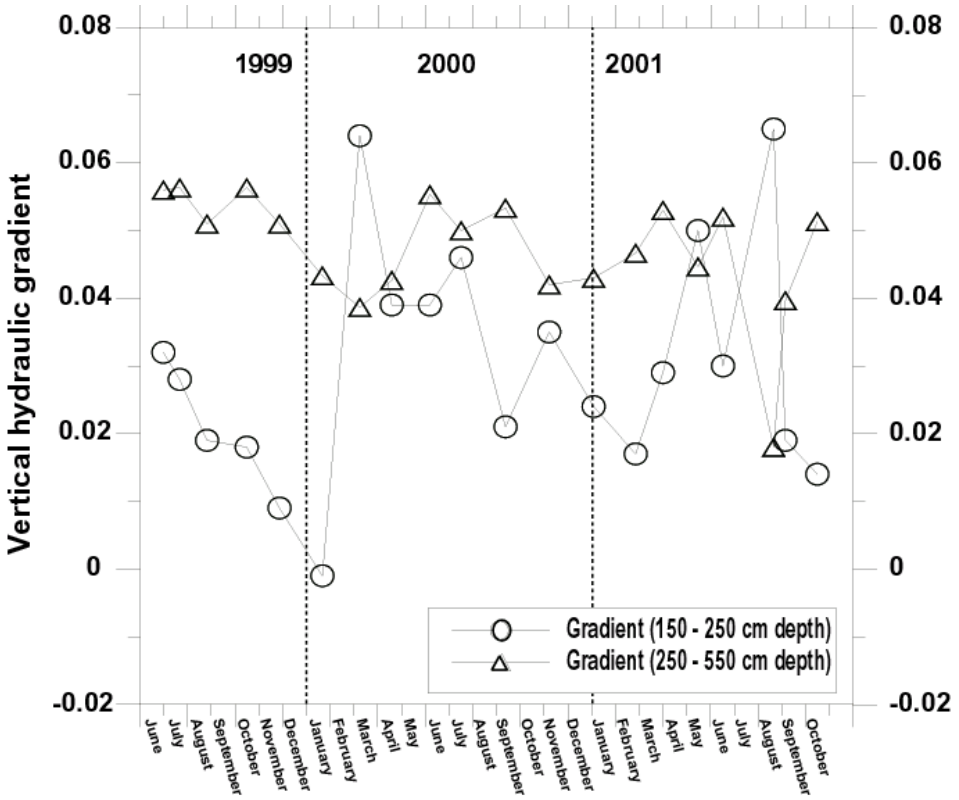

Fig. 5-15: Vertical hydraulic gradients as determined for the EGr in two depth zones, ranging from 150 to 250 cm (i.e. between piezometer 2 and 3) and from 250 to 550 cm (i.e. between piezometer 3 and 4). Except for the weak upward directed gradient (-0.001) observed in January 2000, the gradients indicated a downward directed ground water flow.

The piezometer data obtained in this study are in good agreement with the results of an earlier hydrological study at EGr. It was carried out by J. McKenzie and others and lasted from July 1st, 1997 to August 31st, 1998. In their report, McKenzie et al. (2002) have calculated an average overall downward directed gradient of 0.04 at the crest and the flanks of the bog for the time period of concern. Higher piezometer water levels and reduced vertical hydraulic gradients during winter were observed in both studies. Differences in the piezometer water levels are normal, as deflections from the seasonal trend depend very much on the effective annual precipitation. Higher vertical hydraulic gradient in the lower parts of the bog (as determined in both studies for a depth between 250 to 550 cm) may facilitate enhanced lateral

flow of the pore water above. McKenzie et al. (2002) present a possible pore water flow model, which takes also the results from measurements at other piezometer stations (e.g. at the flanks of the EGr bog) into consideration. The model shows predominant vertical pore water flow for central bog parts and at its flanks, while it is widely horizontal in between these two regions (Fig. 5-16).

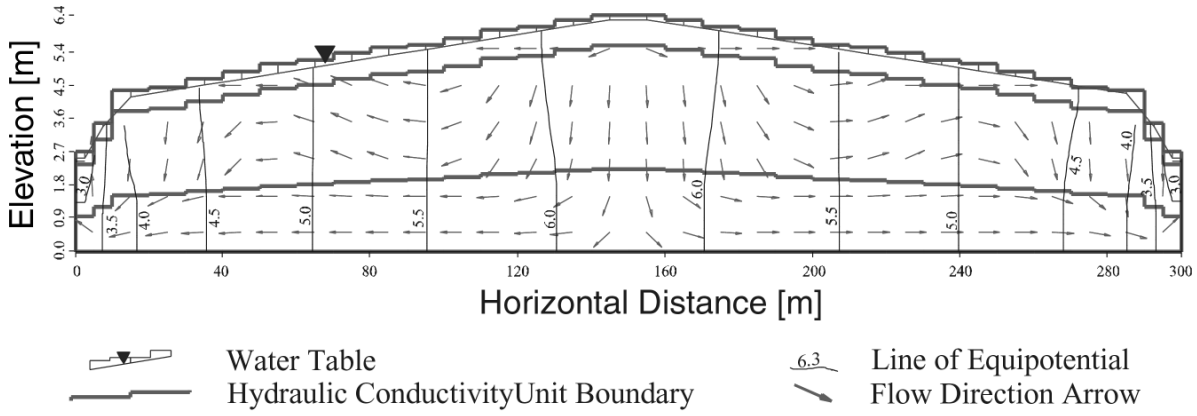

Fig. 5-16: Visual MODFLOW model for the raised bog section of EGr. The arrows indicate the direction of pore water flow. The model is based on the three hydraulic units characterised in Table 5-1 with constant values for hydraulic conductivity and thickness. The vertical and subvertical lines show the equipotential (according to McKenzie et al., 2002).

5.2.5 Other hydrological observations at EGr

Usually, the vertical hydraulic head at EGr was consistently downward directed from the upper to the lower part of the bog. Occasionally however, the hydraulic head at the bottom of the peat column was higher than that in the middle, but lower than that of the water table. Under such conditions the water moved downward from the water table and upwards from the mineral soil / peat interface towards the centre of the peat profile, which was under-pressured. McKenzie et al. (2002) argue that episodic methane ebullition (cf. Romanowiecz et al., 1993) could have caused temporarily under-pressured conditions in the centre of the peat profile, yet did not test this hypothesis.

For a better classification of different conductivity zones, McKenzie et al. (2002) subdivided the EGr bog into three layers (Table 5-1). Similar values for hydraulic conductivity have been reported from a Minnesota peatland (Chason and Siegel, 1986). These are based on the degree of humification (cf. chapter 3.1.4).

Table 5-1: Classification of hydraulic units at the EGr Bog according to McKenzie et al. (2002).

Hydraulic Unit	**Location in EGr Bog**	**Depth range [m]**	**Degree of decomposition** (according to the Von Post Scale; Von Post, 1925)	**Calibrated vertical hydraulic conductivity K_v [cm^{-1}]**	**Calibrated horizontal hydraulic conductivity K_h [cm^{-1}]**	**Calibrated anisotropy ratio (K_h/K_v)**
"3"	Top	0 - 2.2	H1 - H4	10	1	0.1
"2"	Middle	2.2 - 5.5	H8	$1*10^{-6}$	$2.51*10^{-6}$	2.51
"1"	Bottom	5.5 - 6.5	H3 - H4	$6.31*10^{-3}$	$3.16*10^{-5}$	$5.01*10^{-3}$

The weighted average of all the vertical hydraulic conductivities at EGr is $1.59*10^{-4}$ $m*s^{-1}$. The so-called anisotropy ratios (the horizontal hydraulic conductivity divided by the vertical hydraulic conductivity) for both, the top and the bottom unit of EGr are smaller than 1, which is unusually low. McKenzie et al. (2002) attribute the low anisotropy ratio to an increased vertical hydraulic conductivity as a consequence of secondary vertical pathways created by plant stems.

5.2.6 Pore water temperature

The temperature variations in EGr pore water for the time period between June 1999 and October 2001 are shown in Fig. 5-17. While temperatures in the deeper parts of the bog remained almost constant during the entire study period (less than 1 °C change below 4 m depth), the near-surface temperatures were changing considerably depending on the season: At 1 cm depth, i.e. above the water-saturated zone, measured temperatures could be as low as -0.9 °C (January 2000) or as high as 22.7 °C (August 2001). 20 cm below ground surface, i.e. in a zone, which is usually water-saturated (cf. Fig. 5-14), the readings ranged from 1.2 °C (February 2001) to 16.0 °C (August 1999 and August 2001). As can be inferred from Fig. 5-14, the water level at EGr was slightly below 20 cm in August 2000. This is probably the reason, why a particularly high peat temperature was measured then. The lowest temperature in the water-saturated zone (0.5 °C) was observed in February 2001 in a depth of 36 cm. An up to 15 cm thick ice-cover was present at the surface of the EGr Bog from late November 1999 to early March 2000 and from early December 2000 to early March 2001 (cf. chapter 11.AIII-EUG'01-Fig.3).

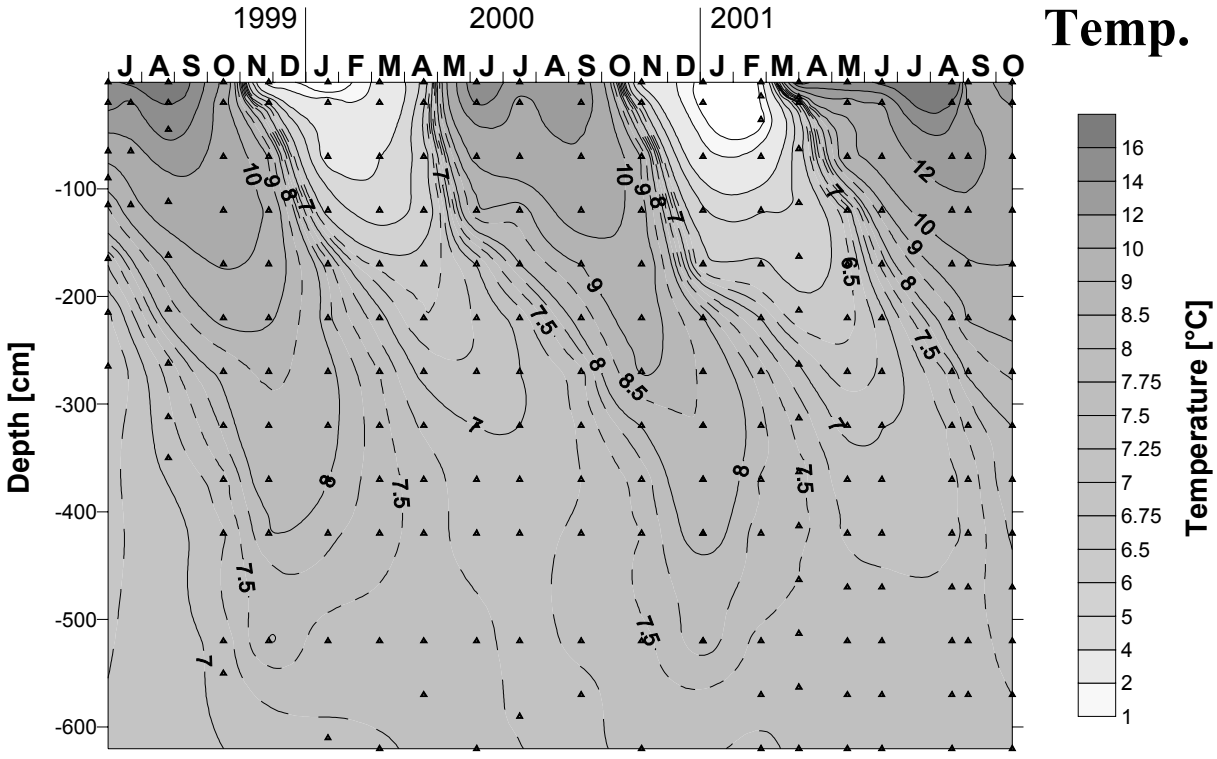

Fig. 5-17: Isopleth diagram showing the EGr pore water temperature during the period of measurement from June 1999 to October 2001. The triangles represent the data points. For details concerning the temperature measurements, confer chapter 4.2.1.1.

The oblique direction of the cigar-shaped thermo-isopleths in the time-space plot shown in Fig. 5-17 illustrates, how pore water temperature change propagates downward with time. The rate at which the water moves downward the bog can hence be estimated based on the temperature slope shown in Fig. 5-17. Pore water advection would hence be between 1.5 and 2 cm per day ($1.7*10^{-7}$ to $2.3*10^{-7}$ m/s), if it represents the only mechanism for the observed temperature patters and conductive heat flow is neglected. Preliminary temperature modelling (adaptation of species transport model - cf. chapter 6.4 - on temperature) indicates that conductive heat transport in the bog plays only a minor role. Its share is less than 1 ‰ of the heat transported by advection. The model also indicates that the heat flux due to decomposition of organic matter and microbial activity is in the same order of magnitude as conductive heat transport and can also be neglected. This implies that the bog's pore water temperature is almost exclusively dependent on the rate of advection and on the water temperature at its surface, i.e. on ambient atmospheric temperature.

From October 15th to November 20th, 1999, pore water temperatures at EGr were measured using an automated data logger ("Squirrel"; Grant Systems, UK). The Squirrel was programmed for temperature measurement every 15 minutes and a daily recording of one averaged value (cf. chapter 4.2.1.2). Expectedly, the pore water temperature observed during this time period (Fig. 5-18) decreased and its variation corresponds to the long-term patterns derived from the monthly measurements (Fig. 5-17). The automatic recording showed a slight temperature increase of ca. 0.7 °C shortly after start of the measurement. It was caused by the sluggish downward transport of warmer near-surface pore water from the preceding summer season (cf. Fig. 5-17).

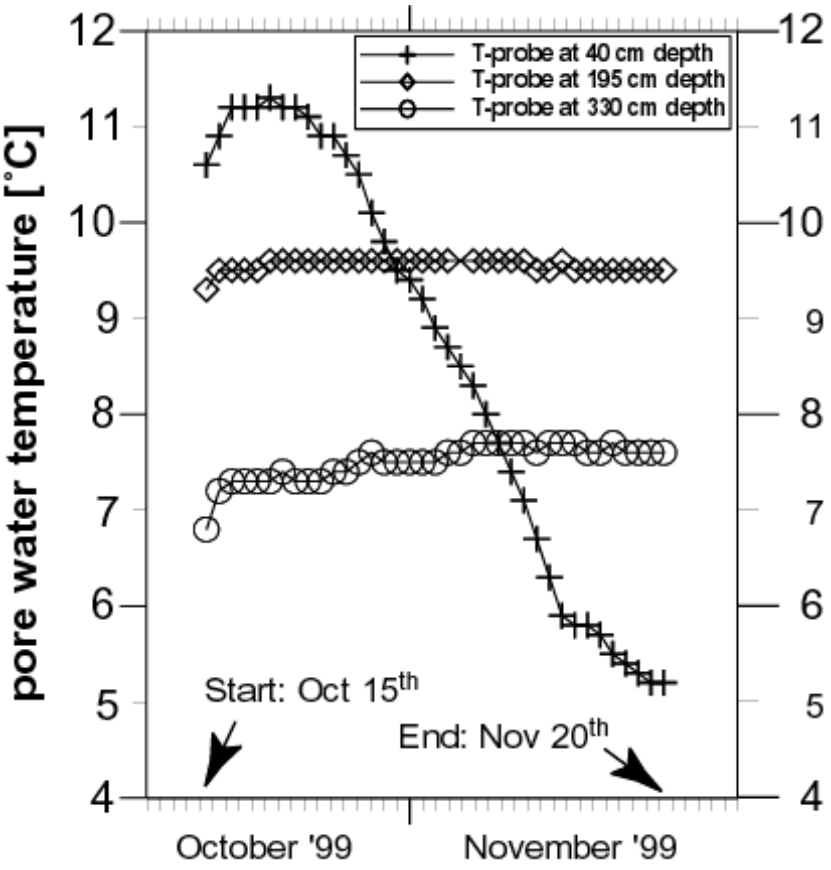

Fig. 5-18: Pore water temperatures recorded at EGr with an automated data logger ("Squirrel") for different depths (40; 195 and 330 cm below ground surface).

6 METHANE AND CO_2 IN PEATLANDS - IMPLICATIONS FROM EGR DATA

6.1 Acetate in deep peat bog environments - Seasonal variation and implications for methanogenesis: Investigation of an ombrotrophic peat bog in the Jura Mountains, Switzerland (paper in preparation)

6.1.1 Abstract

This study reports the acetate concentration patterns along with those for methane and DOC in the pore water of a deep (> 6 m) peat bog, the Etang de la Gruère (EGr) bog in Switzerland. Pore water samples were obtained in situ using diffusion chambers ("peepers") down to a depth of almost 6 m from October 1999 to August 2001. Acetate concentrations increase with depth from well below 5 µM at 0.5 m to more than 180 µM at 5 m, but then decline probably due to lateral flow of water on the ground of the bog. An acetate concentration maximum in the shallow catotelm at about 1.8 m depth has repeatedly been observed in late spring and can be related to increasing pore water temperatures in that season. The presence of two other concentration maxima at approximately 3.2 and 5 m depth is confirmed by most measurement series. As the pore water temperatures are almost depth-invariant in the deeper bog, these maxima seem to reflect the degree of peat decomposition, hydrology, and, as a consequence, the zonal distribution of microbial acetate producing and consuming communities. Significant seasonal variations (by a factor of 3 or more) occur with highest acetate concentrations in spring and early summer and lowest in autumn and early winter. The timing of these variations suggest that a) considerably increased pore water temperatures in the shallow bog and hence increased acetate production in spring and b) the downward advective transport of acetate and labile DOC in the bog pore water profile play an important role. The observed acetate concentrations, the vertical and temporal gradients prove a potential for acetogenesis and acetoclastic methanogenesis also in the deep catotelm.

6.1.2 Introduction

Estimates of methane emissions from wetlands, based on stable isotope balance models, range between 100 and 200 Tg each year, i.e. 20 to 40 % of the total methane released into the atmosphere (Cicerone and Oremland, 1988). About 35 Tg are attributed to northern hemisphere peatlands (marshland, fens and bogs) still representing a significant source of this potent greenhouse gas (Fung et al., 1991). Latest measurements indicate that yet again after a period of relative stability in the early 1990s the CH_4 concentration in the Earth's atmosphere is increasing by about 10 ppbv per year (Wuebbles and Hayhoe, 2000). As a possible explanation, enhanced CH_4 emission from northern hemisphere peatlands is currently being discussed (Wuebbles and Hayhoe, 2000).

Acetate (CH_3COO^-) represents a key-metabolite (Fig. 6-1) in the methanogenic process in wetlands (Lovely and Klug, 1982). It is formed microbially by fermentation of high molecular weight organic matter ($2CH_2O \Rightarrow CH_3COO^- + H^+$) or via synthetic acetogenic pathways involving carbon dioxide and hydrogen, $2CO_2 + 4H_2 \Rightarrow CH_3COO^- + H^+ + 2H_2O$ (cf. Conrad, 1999 and references cited therein). In acidic environments such as peat bogs, certain bacteria are capable of splitting acetate into carbon dioxide and methane ($CH_3COO^- + H^+ \Rightarrow CO_2 + CH_4$). These processes are relatively well studied in the shallow zone of peatlands and other

anoxic environments (e.g. paddy soils, marine sediments, landfills). In shallow bog environments seasonal changes in acetate concentration and possible implications for methanogenesis have been reported from various sites (Shannon and White, 1994; Shannon and White, 1996; Steinmann et al., 1998). Shannon and White (1996), for instance, report a seasonal fluctuation in the acrotelm of two Michigan bogs with acetate concentrations ranging from below 20 µM to >1000 µM and methane concentrations from below 50 µM to more than 500 µM. Highest acetate concentrations were observed in spring, whereas high methane concentrations occurred in all four seasons.

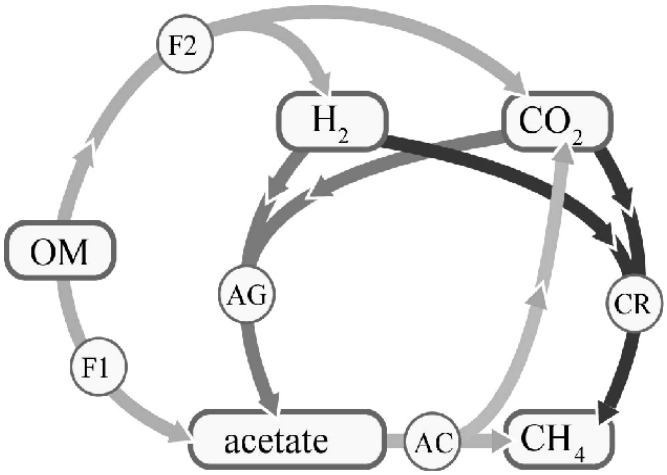

Fig. 6-1: Cartoon-like illustration of the major microbial acetogenic and methanogenic reactions in wetlands. High molecular weight organic matter (OM) is decomposed by two different fermentation reactions (F1; F2) into acetate ($2(CH_2O)_n => (CH_3COO^-)_n + (H^+)_n$), hydrogen and carbon dioxide ($CH_2O + H_2O => CO_2 + 2H_2$). Acetoclastic reactions (AC) allow further splitting of acetate to produce methane and carbon dioxide ($CH_3COO^- + H^+ => CH_4 + CO_2$). Hydrogen and carbon dioxide can recombine to form methane by CO_2 reduction (CR: $CO_2 + 4\ H_2 => CH_4 + 2H_2O$) or again form acetate by acetogenesis (AG: $2CO_2 + 4\ H_2 => CH_3COOH + 2H_2O$).

In terms of consistency and hydrological properties, peat bogs are conveniently divided into two zones: i) The acrotelm at the top is not always water-saturated and has a relatively high vertical hydraulic conductivity. It is therefore particularly sensitive to seasonal temperature change. ii) The catotelm, by contrast, represents the layer of permanently water-saturated (and hence entirely anaerobic) peat underlying the acrotelm. - In the Etang de la Gruère (EGr), the acrotelm corresponds to a zone of about the upper 50 cm of the bog. Geochemical processes in this zone are largely dependent on temperature changes and variations in the height of the water table (cf. Hornibrook, 1997; Hornibrook et al., 1997; Waldron et al., 1998; Avery Jr. et al., 1999; Weyhenmeyer, 1999).

Despite their generally much larger volumes, deeper bog parts have only attracted little scientific attention with respect to acetate concentration patterns and their implications for methanogenic activity (e.g. Charman et al., 1999; Steinmann et al., 1998). The focus of this paper is on acetoclastic methanogenesis in the catotelm (i.e. deeper than ca. 50 cm below ground surface) of the EGr bog using concentrations of pore water acetate and dissolved methane.

6.1.3 The Site

The EGr bog is situated in Franches Montagnes, a carstic plateau within the Jura Mountains, NW Switzerland (cf. Fig. 3-2). The average elevation above sea level is about 1000 m. Temperature variation (annual mean 5.4 °C, MeteoSwiss Station Saignelégier; ca. 4 km WNW of EGr) shows continental influence. Precipitation, however, is high due to elevation and the exposition of the Franches Montagnes in the luff of predominantly westerly winds. The average annual precipitation measured at the Saignelégier meteorological station for the

time period from 1961 to 1990 is 1511 mm (MeteoSwiss). The water table at the EGr field site was relatively constant at 4 to 17 cm below ground surface throughout the study period.

The well-studied EGr site (e.g. Joray, 1942; Steinmann and Shotyk, 1997a&b; Shotyk et al. 1998, Shotyk et al., 2001) is exemplary in terms of its ombrotrophic peat formation. Peat covers a total area of 22.5 ha (Grünig et al., 1984): on the remarkably domed peninsula, below an artificial lake, and on its margins (cf. Fig. 3-4). Up to 8 m of peat (ca. 6.5 m at the sampling site) have accumulated more or less continuously over the last ca. 14,500 calendar years (Shotyk et al., 1998). The peat at the sampling site is dominated by *Sphagnum* in the uppermost part, *Sphagnum-Eriophorum* from 60 - 250 cm, *Eriophorum* from 250 - 370 cm and by *Carex* below. A zone of more decomposed peat (H8, according to the von Post humification scale; cf. e.g. Shotyk, 1988) is situated between 130 and 370 cm (Steinmann, 1995). Accordingly, the vertical hydraulic conductivity of this zone is much lower than above and below (10^{-6} m/s; McKenzie et al., 2002).

6.1.4 Methods

Pore water samples were obtained in situ using plexiglass diffusion chambers ("peepers"; cf. Steinmann and Shotyk, 1996). The sampling volume of the peepers was ca. 30 ml. A 0.2 µm polysulfone membrane (total surface ca. 25 cm^2) at two sides of each chamber allowed diffusion between the bog pore water and the chamber liquid. The peepers were installed at different depths from ca. 50 to almost 590 cm. The depth resolution varied between 14 and 60 cm (see sampling points shown in Figs. 6-2, 6-3, and 6-4).

Prior to installation in the peat, all peepers had been filled with deionised and degassed water. The peepers remained 5 to 7 weeks in the bog, what is largely sufficient for the chamber liquid to equilibrate with the pore water in the peat (Steinmann and Shotyk, 1996). After removing the peepers from the bog, pore water samples were carefully drawn up into 20 ml plastic syringes. For the methane analyses, two times 5 ml of pore water were immediately injected into evacuated standard rubber-sealed tubes ("vacutainers") in the field (for the sample and a duplicate). The syringes were subsequently plugged to prevent degassing and kept in a cold box for transport. Chemical analysis of the samples was carried out on the same day upon arrival at the laboratory in Neuchâtel. Dissolved anions were determined using a Dionex DX-500 ion chromatograph equipped with an IonPak AS/AG 11-HC column and an EG 40 eluent generator. Organic acid anions (acetate, lactate and propionate) were separated from inorganic anions (chloride, carbonate corresponding to total DIC, sulphate and nitrate) using a gradient method similar to the one used by Steinmann and Shotyk (1995). In this method, the initial eluent concentration of 2 mM KOH is increased to 25 mM between 8 to 10 minutes after the start of the analysis and the chromatography stops after 20 minutes.

Methane concentration values for the bog pore water were obtained indirectly by measuring the methane concentrations in the headspace (Voice and Kolb, 1993; Sims et al., 1991). Methane was detected using a Perkin-Elmer 8500 gas chromatograph equipped with a flame ionisation detector (FID). The time interval between sample taking and analysis was less than 24 hours during which the vacutainers were kept refrigerated in a cold room and in dark. Tests had shown no measurable gas loss from the vacutainers during this time interval. Headspace gas was drawn up to the mark of 1 ml into a gas-tight syringe (to be used for gas injection into the GC). Then, the piston was moved to the mark of 2 ml on the syringe scale, while the syringe remained locked. Reopening of the syringe lock allowed subsequent pressure equilibration with ambient air. This was done to account for low pressure as well as for overpressure of up to 2 bars of the headspace. The sample temperature at injection was 22 °C

and heating of the column was isothermal at 80 °C. The methane concentration in the pore water was calculated from the measured headspace concentrations (the volume of gas injected was 0.5 ml), correcting for the unequal volumes of liquid and headspace in the vacutainer and for the above-mentioned two-fold dilution. It should be noted that in the early phase of this study (until March 2000) the methane concentration of the pore water samples was measured in Finland applying a method different from the one described above. The transfer of samples into special vacutainers for shipping and prolonged storage sometimes resulted in poor reproducibility. Nevertheless, the data have been included since the general trends are not affected by this.

The dissolved organic carbon (DOC) content of the peeper liquid was determined with a Dohrmann TOC DC - 190 modular organic carbon analyser operated by the "Service cantonal de la protection de l'environnement" in Neuchâtel. Due to the high DOC concentration in the bog pore water, the samples were 10-fold diluted with deionised water before being analysed. Pore water temperature at the EGr sampling site was measured using an electronic temperature probe mounted on extendible rods (total length 6.2 m).

6.1.5 Results

The acetate concentrations measured in the catotelm of the EGr bog from October 1999 to August 2001 generally increase with depth (Fig. 6-2), with highest concentrations around or below a depth of 5 m. The maximum acetate concentrations are typically around 100 µM (with exceptional observations of 181 and 184 µM in June 00 and 01, respectively). The 5 m - maximum at EGr was not observed early winter 1999, when absolute concentrations in the deeper parts of the bog had been anomalously low. A second, less pronounced acetate maximum is often observed at about 3.2 m depth, with acetate concentrations increasing from well below 5 µM in the upper catotelm towards values as high as 42 µM (April 2000). The maximum at 3.2 m depth could not be observed in autumn/early winter 2000. A third maximum at only 1.8 m occurs in early June 2000, and again in late May 2001. Below ca. 5.5 m depth, acetate concentrations declined rapidly towards the ground of the bog (at approximately 6.5 m) in summer and autumn 2000. In 2001, this decline was less noticeable and in May 01 acetate concentrations even increased slightly down to a depth of 5.9 m. The observed acetate values are relatively low, when compared to other methanogenic environments: For example, the near surface (acrotelm) peat pore water of a nearby bog in the Jura Mountains contains up to 450 µM (Steinmann et al., 1998); Michigan peatlands show acetate concentrations close to 1 mM (Shannon and White, 1996). Marine sediments are characterized by considerably higher acetate concentrations, e.g. up to 2.3 mM (Hoehler et al., 1999) or up to 15 mM (Wellsbury et al., 2000).

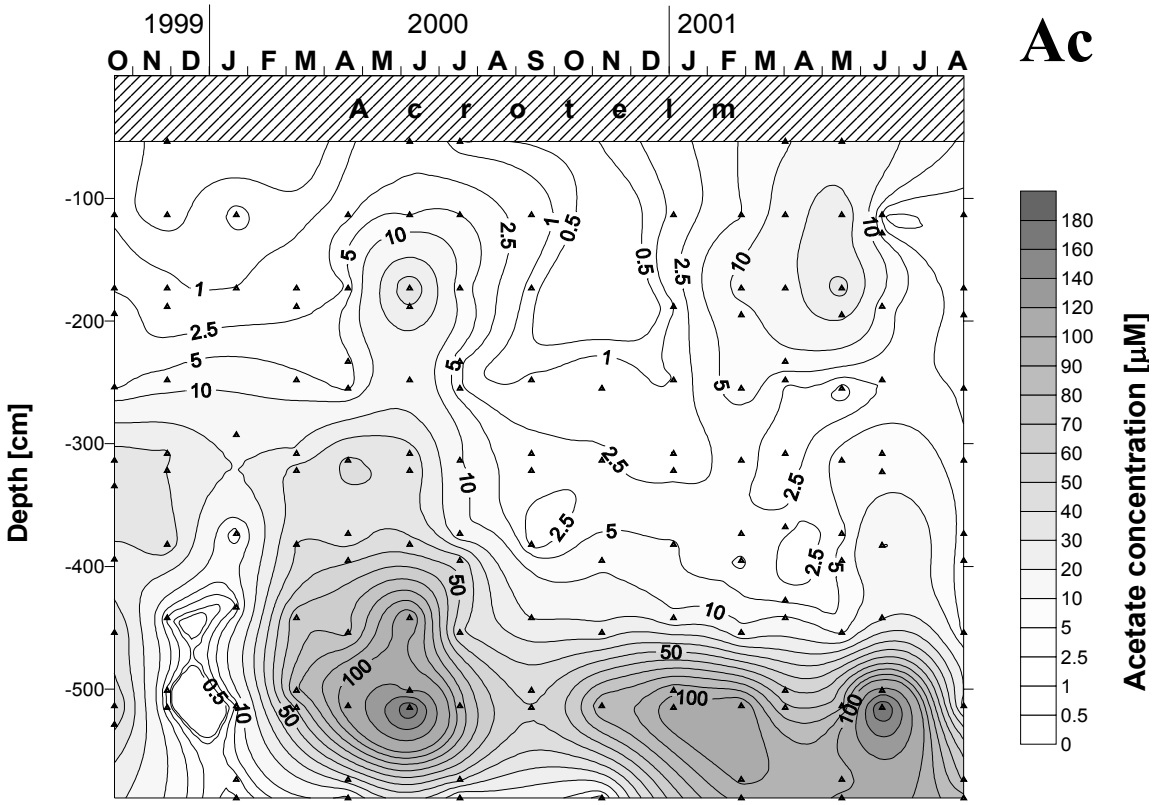

Fig. 6-2: Pore water acetate concentration patterns in the catotelm (below 50 cm) of the Etang de la Gruère bog as measured in the period from October 1999 to August 2001 using peepers for in situ filtration. The triangles represent the data points.

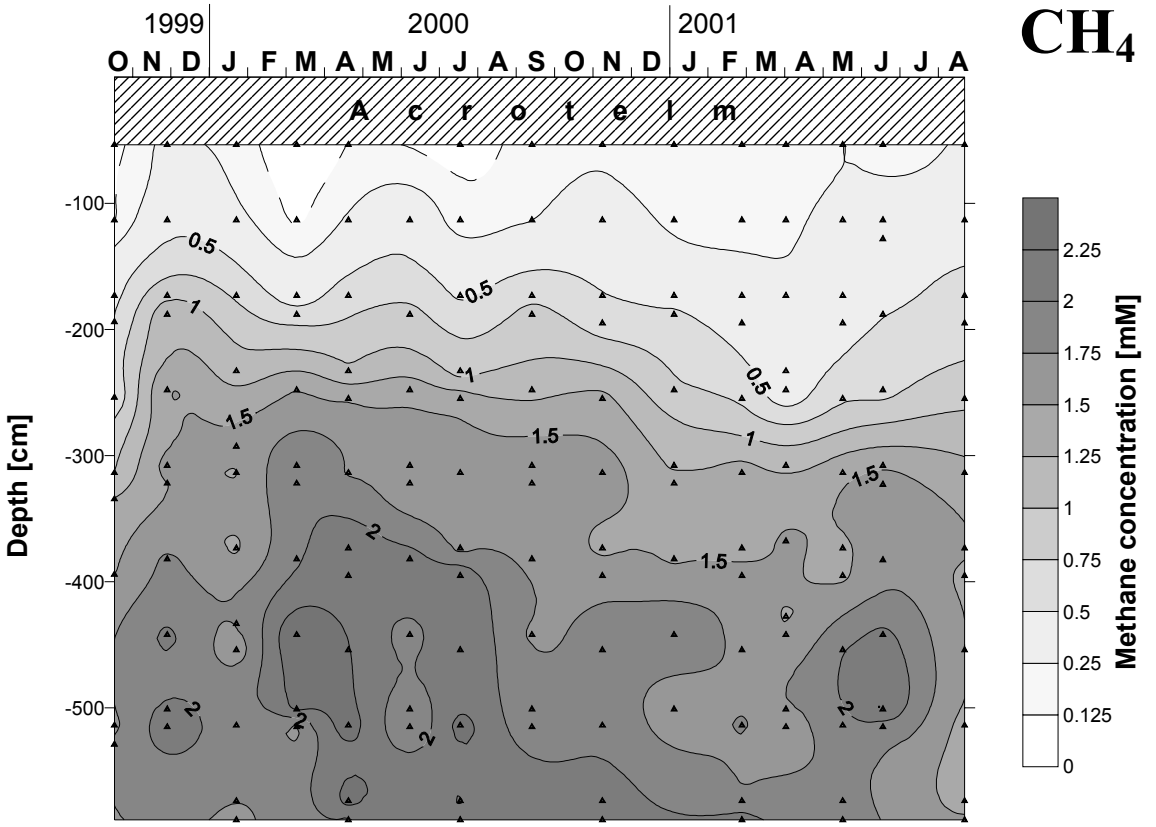

Fig. 6-3: Methane concentration from Etang de la Gruère catotelm (below 50 cm) pore water samples for the study period from October 1999 to August 2001. The triangles represent the data points.

Alike acetate, methane concentrations are also increasing with depth (Fig. 6-3). While the absolute concentrations are up to three orders of magnitude higher than those of acetate, the concentration gradient from shallow to deep peat layers is significantly (approximately 50 times) lower than that of acetate. Methane concentration values in the upper catotelm (up to ca. 0.5 mM) are comparable to those reported from shallow peat at other locations (Hornibrook et al., 1997; Shannon and White, 1996; Lansdown et al., 1992; Crill et al., 1988). At EGr, methane concentrations in 3 m depth are above 1 mM. Values continue to increase to almost 2.4 mM in the deep layers (5.15 m; April 2000). Higher methane concentrations in peatland pore waters have been reported by Siegel et al. (2001). Still higher values occur in marine sediments, e.g. 19 mM were measured in anoxic sediments from an upwelling area at a depth of ca. 14 m (Niewöhner et al., 1998).

The DOC content in the EGr bog also increases with depth. The DOC maximum concentrations (up to 140 mg C/l) are almost independent of seasonal influences and are well defined at about 3.8 m (cf. Fig. 6-4). This depth coincides with a relative minimum in acetate concentrations and corresponds to the lower limit of the more decomposed peat.

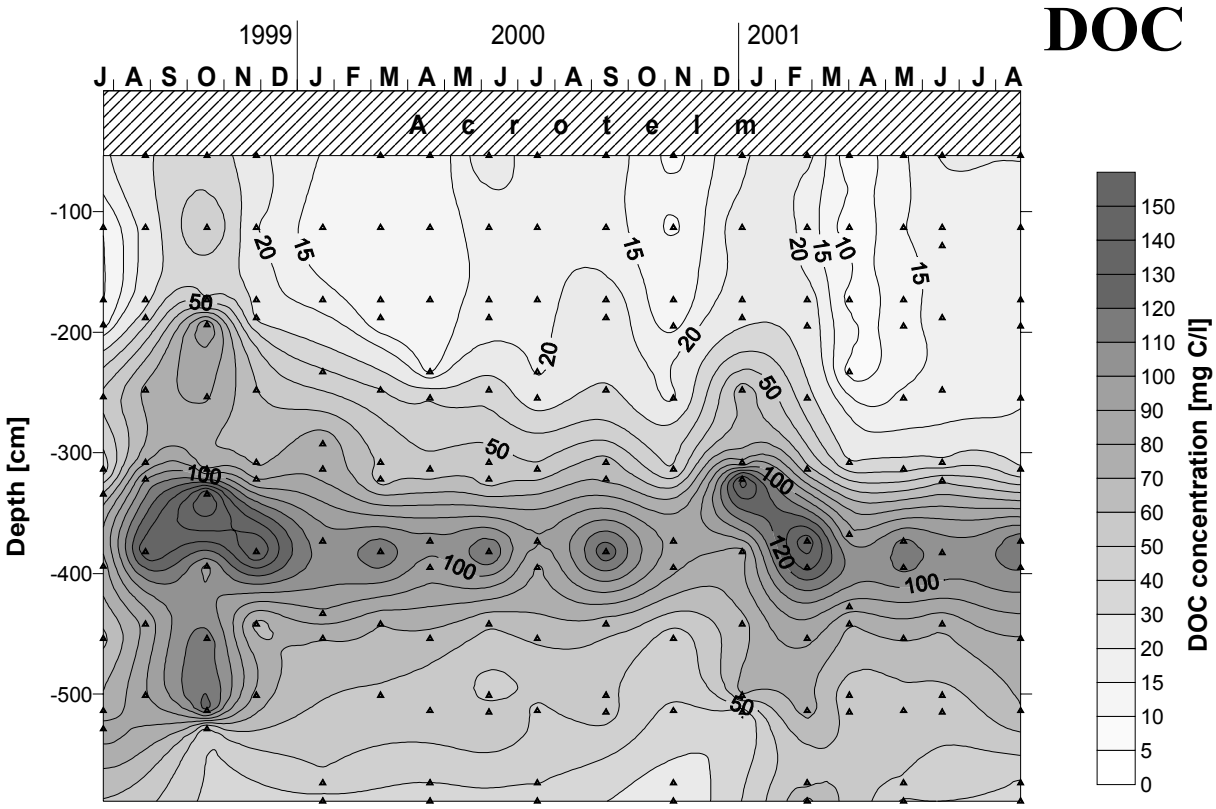

Fig. 6-4: Pore water dissolved organic carbon (DOC) concentration in the catotelm (below 50 cm) of the Etang de la Gruère bog as measured in the study period from July 1999 to August 2001 using peepers for in situ filtration. The triangles represent the data points.

6.1.6 Discussion

Both, temporal (seasonal) and spatial (vertical) successions of the methanogenic reactions are reported in the literature. According to Shannon and White (1996) and Avery Jr. et al. (1999), who studied two Michigan peatlands, acetate accumulates during winter and spring, when low temperatures favour the activity of acetogenic bacteria. Above a peat temperature of ca. 15 °C, the pool of acetate decreased, whereas the concentration and flux of methane increased,

most likely due to acetoclastic methanogenesis. In one of their sites, higher sulphate concentration delayed the onset of acetate accumulation.

As for the EGr bog, temperature effects might be important for the 1.8 m maximum observed in early June, but are certainly unimportant for the 3.2 and 5 m maxima, where the temperature changes are small (<1 °C) and do only occur with a delay of several months with respect to the upper acrotelm (cf. Fig. 5-17). At 1.8 m depth, the temperature varies between 6 and 10 °C. Acetate starts to accumulate in April when pore water temperatures are lowest. The onset of acetogenic activity in the EGr bog is not influenced by sulphate reducers, as sulphate concentrations are below 1 µM throughout the whole profile (Steinmann and Shotyk, 1997a). Acetate concentrations at 1.8 m decline as temperature rises markedly in late spring. This, however, is not accompanied by a distinct increase in pore water methane concentrations. If our assumption is correct that the relatively small annual temperature variations at this depth play a role, this would mean that the natural consortium of microbes may be more sensible to temperature changes than generally thought (e.g. Avery et al., 1999, and references therein). Another possible explanation for the acetate maximum at 1.8 m is downward advection of acetate from the upper part of the bog (including the acrotelm). Advection is a probable source for many dissolved species especially because in the upper part of the bog, the vertical hydraulic conductivity is higher than in its middle part. Acetate formed in spring (Shannon and White, 1996) may have been transported downward by early summer. Yet, the direct import from the above layers is contradicted by a minimum between the relative high acrotelm concentrations (Steinmann et al., 1998) and the 1.8 m maximum. More likely, downward advection of labile DOC is responsible for acetate fermentation at 1.8 m. The breakdown of DOC, however, is not reflected in the variations of total DOC concentrations (cf. Fig. 6-4). This indicates that labile DOC represents only a minor fraction of total DOC.

The annual variations of the pooled (i.e. the quantity of species in the pore water column beneath a defined area of the bog) acetate and methane at EGr are shown in Fig. 6-5. In general, the pooled acetate and methane concentrations followed similar trends throughout the period of measurement. It has been found - not only in the Michigan peatlands cited above, but also in paddy soils (Sigren et al., 1997) - that a maximum in pore water acetate is preceding a maximum in the pool of pore water methane by several weeks. At EGr, the maximum of pooled pore water methane concentrations occurs simultaneously (summer 2001) or even before (spring/summer 2000) the acetate maximum. Perhaps, the accumulation of both CH_4 and acetate is triggered by a common factor. The small seasonal temperatures differences in the lower catotelm (+/- ca. 1 °C) certainly cannot explain the sharp decrease in acetate concentration observed in autumn 1999 and summer 2000/2001. The cause for this might be a rather abrupt change of the pore water advection rate (flushing or interrupted flow) along with fluctuation of the microbial acetate producing communities. This, however, is not confirmed by precipitation data that do neither show substantial increase nor decrease in the time-span of concern. Since the CH_4 concentrations diminish much more slowly than the acetate concentrations (June 2000 - November 2000; June 2001 - August 2001), acetoclastic methanogenesis is possibly responsible for the fast decline of the acetate pool at EGr.

With respect to the vertical succession of methane-related microbial reactions, it has been suggested that some peatlands are structured in a way that acetoclastic methanogenesis dominates in the upper part of the bog, while CO_2 reduction is more important in the deeper peat layers (Hornibrook et al. 1997; cf. also discussion and reply by Waldron et al, 1998 and Hornibrook et al. 1998). As a likely cause these authors put forward the lack of fermentable

substrate in the deeper layer preventing the formation of sufficient acetate. In this study, we found relatively high acetate concentrations in deep peat at EGr. Thus, the availability of acetate seems not to be a factor that limits acetoclastic methanogenesis in the deep layers. The relative importance and the turnover rates of the various methanogenic reactions at different depths, however, cannot be directly estimated from the concentration profiles alone.

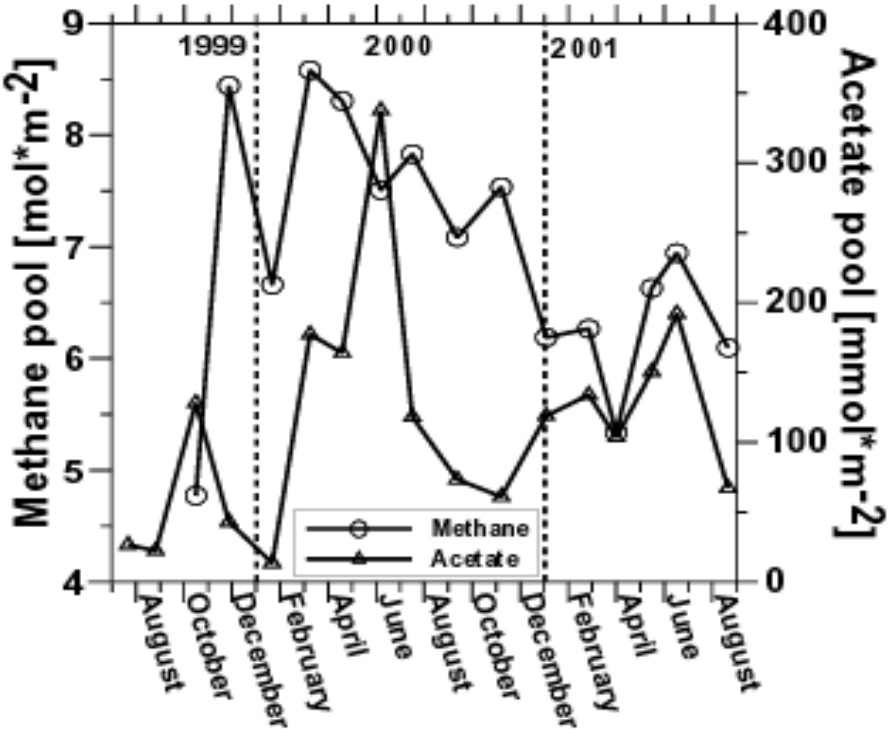

Fig. 6-5: Pooled acetate and methane in the pore water of the Etang de la Gruère Bog. The concentration values were averaged for each meter of the profile.

Nevertheless, these data give some insight in the acetate dynamics in the catotelm of this bog. The observed increase of acetate with depth below 4 m clearly indicates active formation of acetate by fermentation and/or acetogenesis. Declining concentrations of acetate (but also of methane and DOC) near the ground of the bog are probably a consequence of lateral flow of water. The strong temporal variation in deep acetate concentrations - e.g. the marked increases from January to March 2000 and from April to June 2000, or the decrease from June - July 2000, which is not accompanied by a decrease in CH_4 - again confirm the hypothesis of dynamic *in situ* production and consumption of acetate at these depths. A seasonality of catotelm acetate is possibly induced, when advection comes to a halt in winter (due to the snow cover). This may also result in a shortage of labile DOC and hence decreased fermentative acetate production as observed in December 1999. If the subsequent minimum in methane concentration (January 2000) is indeed a consequence of low acetate, this would imply that acetoclastic methanogenesis is an important process in the catotelm.

Is the observed size of the acetate reservoir relevant with respect to methane emission to the atmosphere? If we assume, arbitrarily, an acetate turnover time of one year, then acetate dissimilation could account for methane emission in the order of 10 mg m^{-2} d^{-1}. This rate is comparable to typical peatland values (e.g., Alm et al., 1999). By pointing out the evidence for acetoclastic methanogenesis in the deep bog, we do not question an important role of CO_2 reduction. Indeed, CO_2 reduction is considered to be the major microbial methane-producing pathway at low temperatures, i.e. below 15 °C (cf. Lansdown et al., 1992; Shannon and

White, 1996; Avery Jr. et al., 1998). Moreover, organic matter becomes less labile with increasing depth in wetland soils (e.g. Clymo, 1983; Farrish and Grigal, 1988). A decrease in degradability of organic matter will result in an enhanced contribution of CH_4 from CO_2 reduction (Westerhoff et al., 1984), Miyajima et al. (1997). A depth dependent shift from an acetate splitting towards a CO_2 reducing methanogenic pathway is therefore possible within one and the same bog and has been stated for various examples (e.g. Hornibrook et al., 1997).

6.1.7 Conclusions

The Etang de la Gruère bog's acetate concentration increases with depth along a steep chemical gradient up to 200-fold from the upper to the lower catotelm, where highest concentration are observed throughout the whole year. A potential for acetoclastic methanogenesis is hence given in deep bog environments. Two persistent levels of maximum acetate concentration (at ca. 3.2 and at 5 m depth) are present in the Etang de la Gruère bog. They are relatively stable throughout the year and probably to be linked to the peat stratigraphy, which controls both, the pore water flow patterns and the type of substrate available.

Another acetate concentration maximum in the upper catotelm (at about 1.8 m depth) has been observed in late spring 2000 and 2001. The seasonal variation of the acetate concentration in the upper catotelm is characterized by relatively high values in the early summer season and low values in late autumn and winter. These concentration patterns are likely due to the combined effect of a) a downward advective transport of acetate and labile DOC produced in the acrotelm in spring, and, b) a seasonal delay of acetoclastic methanogenesis in deeper bog parts corresponding to higher relative pore water temperatures in the deep bog in autumn and early winter.

Higher ambient pore water temperatures in the upper catotelm in summer and autumn seem to facilitate acetate consumption (by acetoclastic methanogenesis) but not acetate production. The thereby formed gases may dissolve and biochemically recycle or, in case of low solubility (CH_4), preferentially escape from the system by bubble formation. Accordingly, the methane concentration in the pore water shows only a slight increase. The repeatedly observed acetate deficiency in the deep catotelm in autumn/early winter is nevertheless reflected by a subsequent significant decline in methane concentration with a maximum effect about 2 to 3 months later, thus highlighting the significance of acetate as a key-metabolite for methanogenesis.

6.2 Pathways of methanogenesis in peatlands: Acetate splitting vs. CO_2 reduction - Implications from carbon stable isotope data (paper in preparation)

6.2.1 Abstract

Wetlands are significant sources of methane to the atmosphere. With ca. 115 Tg/a, peatlands contribute to more than 70 % of the natural methane sources and to about one fifth of the total sources. Two major metabolic pathways are known to be responsible for microbial methanogenesis in peatlands: acetate splitting and CO_2 reduction. The two pathways can be distinguished with respect to the carbon stable isotope composition of the methane produced.
This study reports the results of field research from October 1999 to August 2001 at the Etang de la Gruère (EGr) Bog in the Swiss Jura Mountains. Pore water samples were obtained in situ using diffusion chambers ("peepers") to a depth of almost 6 m. The relatively low CH_4 – DIC carbon stable isotope fractionation in the upper catotelm indicates acetate splitting as the dominant methanogenic pathway. Below a depth of ca. 1.5 m, increasing isotope fractionation values (55 to up to 71 ‰) point to a predominant methane production via the CO_2 reduction pathway. While $\delta\ ^{13}C\text{-}CH_4$ values of EGr pore water methane showed no straight trend with depth, DIC became less depleted in ^{13}C with depth. The $\delta\ ^{13}C$-DIC values ranged from -22 ‰ vs. VPDB in the upper to +9 ‰ in the lower catotelm. 'Static', depth-dependent and 'dynamic' seasonal isotope patterns indicate that CO_2 reduction acts as a "background" microbial process, while the occurrence of acetate splitting is directly dependent on the availability of this methanogenic metabolite and on temperature.

6.2.2 Introduction

Due to its role as a potent greenhouse gas, methane has become a premier topic of environmental research. Over the last decade, the scientific community has worked out detailed quantitative emission estimates for the different anthropogenic and natural sources. Wetlands represent by far the largest single natural source of methane to the atmosphere. Recent estimates range from 145 Tg/a (Houwelling et al., 1999) to 237 Tg/a (Hein et al., 1997). According to Houwelling et al. (1999), this constitutes more than 80 % of all natural and about 25 to 40 % of the total, i.e. natural and anthropogenic, emissions (IPCC, 2001). With ca. 115 Tg/a, peatlands (thickness of peat layer >30 cm) contribute to more than 70 % of the natural methane sources and to about one fifth of the total sources (Houghton et al., 1995; cf. Fig. 2-4). While the actual emission calculations are widely acknowledged, the occurrence and relative importance of biochemical pathways that lead to methane formation ("methanogenesis") in wetlands are still subject of vivid debate (e.g. Chanton et al., 1989a; Hornibrook et al., 1997; Waldron et al., 1998; Hornibrook et al., 2000).

CO_2 reduction and methylotrophism represent the two major metabolic pathways known to be responsible for microbial methanogenesis (Lovley and Klug, 1986; Boone et al., 1993). CO_2 reduction denotes a microbial metabolic process, where CO_2 (or other dissolved inorganic carbon species such as HCO_3^-) is reduced and converted into methane. The necessary electrons derive primarily from oxidation of H_2. Hydrogen, in turn, derives from fermentation of organic matter (cf. Fig. 6-1). Methylotrophic bacteria, by contrast, catabolise organic compounds that contain methyl groups (e.g. methanol, ethanol, dimethyl sulphide, methylated amines). The methyl group is reduced to CH_4 using electrons from oxidation of other methyl groups or from hydrogen. Acetoclastic methanogenesis is a special case of methylotrophism, as the electrons used for reduction of the acetate's methyl group derive from its carboxyl

group, which is oxidised to CO_2 (Boone et al., 1993). Alike hydrogen, the key-metabolite acetate is a product of organic matter fermentation (cf. Fig. 6-1).

The carbon stable isotope composition of atmospheric CH_4 (and co-existing CO_2) has been widely used to identify and to evaluate the various sources of methane in the environment (e.g. Cicerone and Oremland, 1988; Fung et al., 1991) and in particular in fossil fuel-related sources (e.g. Schoell, 1988; Tang et al., 2000). It is however also a powerful tool to characterise microbial methanogenic processes in sediments. In the absence of oxidation effects (cf. Bergamaschi, 1997), changes in pathways of methane production occurring in wetland soils and sediments have been suggested as a mechanism for the isotopic shifts (e.g. Martens et al., 1986, Shannon and White, 1996). Both, acetate splitting and CO_2 reduction, produce isotopically light methane, the fractionation is however stronger for CO_2 reduction. Whiticar et al. (1986) postulated that methane produced by CO_2 reduction in marine environments had significantly lighter carbon stable isotope signatures (ranging from ca. -110 to -60 ‰) than methane produced by acetate splitting in freshwater settings (ca. -65 to -50 ‰). What determines the methanogenic pathways, however, is not the depositional environment (Schoell, 1988), but chemical (e.g. the pore water sulphate and labile organic matter concentrations; Capone and Kiene, 1988) and physical (e.g. temperature; Avery et al., 1999) constraints. CO_2 reduction is thought to be predominant in marine sediments because the depletion of labile substrates occurs within the overlying sulphate reduction zone, whereas acetate splitting seems to be the main methanogenic pathway in freshwater environments due to typically low sulphate concentrations and abundant labile organic matter (Hornibrook et al., 2000). Hornibrook et al. (2000) state further, that in freshwater environments, the ratio of methane produced by the acetoclastic and the CO_2 reduction pathway is ca. 70 : 30, respectively. Incubation experiments indicate that higher temperatures result not only in an increase of methane production, but seem to favour the acetate splitting methanogens (Avery et al., 1999).

The carbon stable isotope compositions of methane may vary considerably for different peat bogs. Published values for $\delta\ ^{13}C\text{-}CH_4$ range from -46 ‰ (predominant methylotrophism; Martens, et al. 1992; Hornibrook at al., 2000) to -82 ‰ (predominant CO_2 reduction; Lansdown et al., 1992). Assuming $(CH_2O)_n$ composition for organic matter composition, a 1 : 1 production ratio of CH_4 and CO_2 should be expected from the principal microbial reactions in wetlands (cf. Fig. 6-1). An organic matter substrate richer in hydrocarbon units would, however, lead to more CH_4 production, e.g. "propionate-type" $4C_3H_6O_2 + 2H_2O \Rightarrow 7CH_4 + 5CO_2$ or "ethanol-type" substrate: $2C_2H_6O \Rightarrow 3CH_4 + CO_2$. Given the same isotope composition of the "raw material" (organic matter) for the microbial reactions, the $\delta\ ^{13}C$ value of dissolved inorganic carbon (DIC) should increase as $\delta\ ^{13}C\text{-}CH_4$ decreases. This correlation is a consequence of the kinetic isotope effect: ^{12}C goes preferably into CH_4, whereas the produced CO_2 (and hence DIC) becomes more enriched in the heavy isotope. In case of CO_2 reduction, this is due to the necessary cleavage of the C-O bond. In case of acetate splitting, this is an inherited signature, as the acetate's methyl group has already been depleted in ^{13}C, when the acetate formed. The carbon stable isotope composition of DIC can therefore be regarded as a linked parameter to $\delta\ ^{13}C\text{-}CH_4$. The $\delta\ ^{13}C$-DIC values in peat pore water typically range between -25 and +10 ‰ (e.g. Whiticar et al., 1986; Hornibrook et al., 1997, 2000; Steinmann et al., 2000). It seems that $\delta\ ^{13}C$-DIC values increase as $\delta\ ^{13}C\text{-}CH_4$ values decrease with depth. (Avery et al. 1999; Waldron et al., 1999; Hornibrook et al., 2000). The published information about isotope trends in the upper part of peatlands is ambiguous (Reeburgh et al., 1997). Research on carbon stable isotope trends for CH_4 and DIC in deep bog environments has rarely been endeavoured. This is despite the fact that both, methane and

DIC concentrations are much higher in the catotelm (i.e. in the permanently water-saturated deep layers of the bog, generally below 50 cm depth) than in the acrotelm (i.e. in the upper part of a bog; cf. chapter 2.3).

In the following, the results of a long-term investigation on methane, DIC and DOC carbon stable isotope composition in the catotelm of an almost 6 m deep peat bog profile in the Etang de la Gruère, Switzerland, are presented. Seasonal as well as depth-related variations in the isotope signature are correlated to the concentration patterns of the respective chemical species and implications for the potential methanogenic pathways are discussed.

6.2.3 Methods

6.2.3.1 Pore water sampling

Pore water samples were obtained in situ using plexiglass diffusion chambers ("peepers"; cf. Steinmann and Shotyk, 1996). The method of pore water sampling is described in chapter 4.1.

6.2.3.2 Methane carbon stable isotope analysis

Markus Leuenberger from the Department of Climate and Environmental Physics at the Physics Institute of Bern University carried out the isotope analysis of the samples. - The method of methane carbon stable isotope analysis is described in chapter 4.4.2.

6.2.3.3 DIC carbon stable isotope analysis

C. Weyhenmeyer at the Isotope Laboratory of the Geological Institute of Bern University carried out the DIC carbon stable isotope analysis. The method applied and the technical details are similar to those described by Krishnamurthy et al. (1997) and Atekwana and Krishnamurthy (1998). Confer chapter 4.4.3.

6.2.3.4 Methane concentration analysis

Methane concentration values for the bog pore water were obtained indirectly by measuring the methane concentrations in the headspace of the vacutainers. Methane was detected using a gas chromatograph equipped with a flame ionisation detector (FID), as described by Eilrich and Steinmann (submitted). Confer chapter 4.4.3.

6.2.4 Results

6.2.4.1 $\delta^{13}C$-CH_4

During the period of study from July 1999 to August 2001, the $\delta\ ^{13}C$ values for pore water methane at EGr ranged from ca. -71 to -58 ‰ vs. the VPDB standard (Fig. 6-6). Lowest values (between ca. -71 and -65 ‰) occurred in a zone from ca. 0.8 to 1.7 m below ground surface. Below this zone, the pore water methane became gradually less depleted in ^{13}C to a depth of approximately 4.5 m, where the $\delta\ ^{13}C$-CH_4 values (-61 to -58 ‰) were highest. The near-bottom peat pore waters as measured down to a depth of 5.9 m showed slightly (by 1 - 2 ‰) decreasing $\delta\ ^{13}C$-CH_4 values.

Seasonally, the methane isotope composition was much more variable in the upper (<3 m depth) than in the lower (>3 m depth) catotelm, where only in winter a minor shift towards isotopically lighter compositions was observed. This shift was well noticeable in 1999/2000 with more than 2 ‰ lower $\delta\ ^{13}C$-CH_4 values in January 2000 than during the year's average. It was however not repeated in winter 2000/2001, when only the pore water methane in depths below 5 m showed lighter compositions than those of the rest of the year. In contrast to this, a clear and seasonally repeated variation could be observed in the upper catotelm: In late

spring, summer, and, less consistently, also in autumn, the shallow (to a depth of approximately 2 m) EGr pore water methane was much more depleted in ^{13}C than in winter. The differences were usually between 1 and 3 ‰, but could be as high as 7 ‰ (winter 1999/2000).

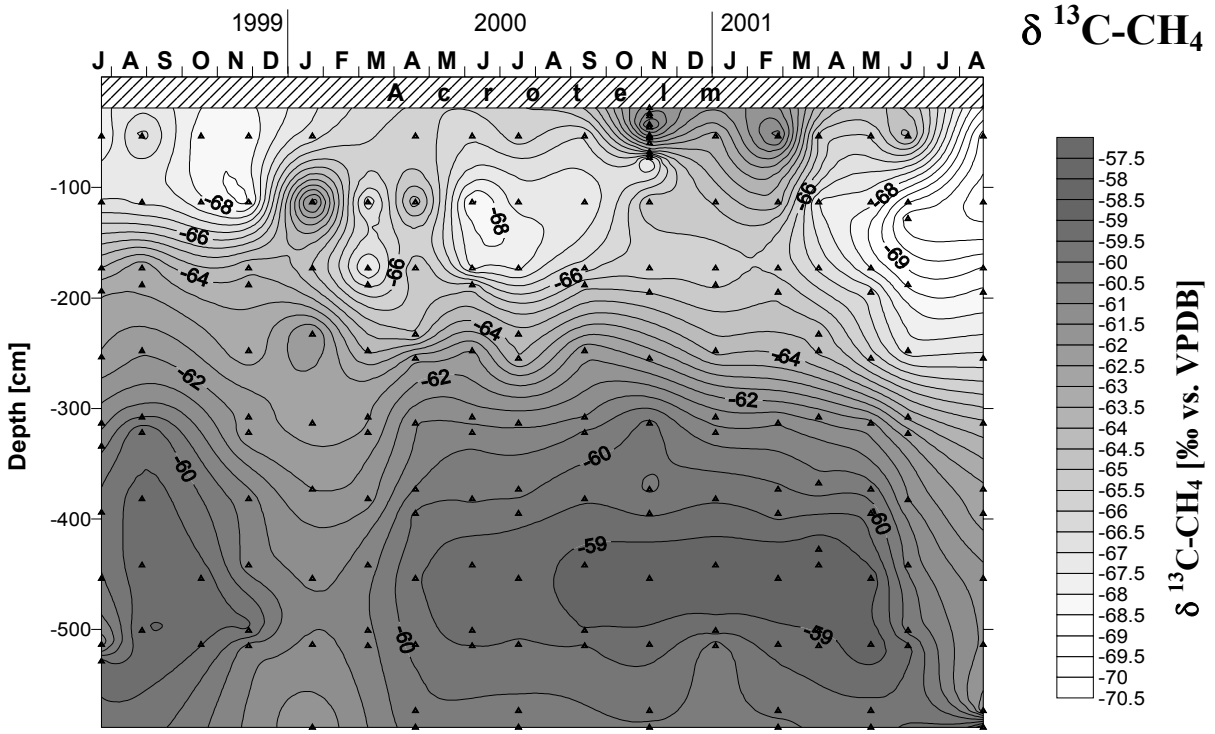

Fig. 6-6: Isopleth diagram showing the $\delta^{13}C$ values for methane in the pore water of EGr during the period of measurement from July 1999 to August 2001. The triangles represent the data points.

Isotope analysis of pore water sampled near the bog's surface at a different site (ca. 3.5 m SW of the main sampling hole) in November 2000, yielded downward decreasing $\delta^{13}C$-CH_4 values from ca. -61.6 (at 28 cm depth) to -67.8 ‰ (at 73 cm depth). These values confirm the observation made by Waldron et al. (1999) that the bog's pore water methane is most depleted in ^{13}C in the shallow catotelm and not in the acrotelm. The data provided by Hornibrook et al. (2000) indicate a similar trend. However, they are confined to a maximum depth of 1.8 m.

6.2.4.2 $\delta^{13}C$-DIC

The $\delta^{13}C$-DIC values determined for the study period from July 1999 to August 2001 are shown in Fig. 6-7. They ranged from -21.7 ‰ in a depth of ca. 0.5 m (March 2000) to +8.8 ‰ vs. VPDB in almost 6 m depth (May and August 2001). While, for methane, $\delta^{13}C$ values were generally downward decreasing, $\delta^{13}C$-DIC were in most cases increasing with depth. This trend was observed for the entire profile to the bottom of the bog and for almost the entire period of study. The only major exception to this trend occurred in the August 1999 series, when a sample in 4.42 m depth showed a remarkably high $\delta^{13}C$-DIC value (8.3 ‰), which was followed by decreasing values in the samples beneath. The downward increase in $\delta^{13}C$-DIC was particularly pronounced in the upper catotelm (<3 m depth), whereas in the lower catotelm, it was more sluggish.

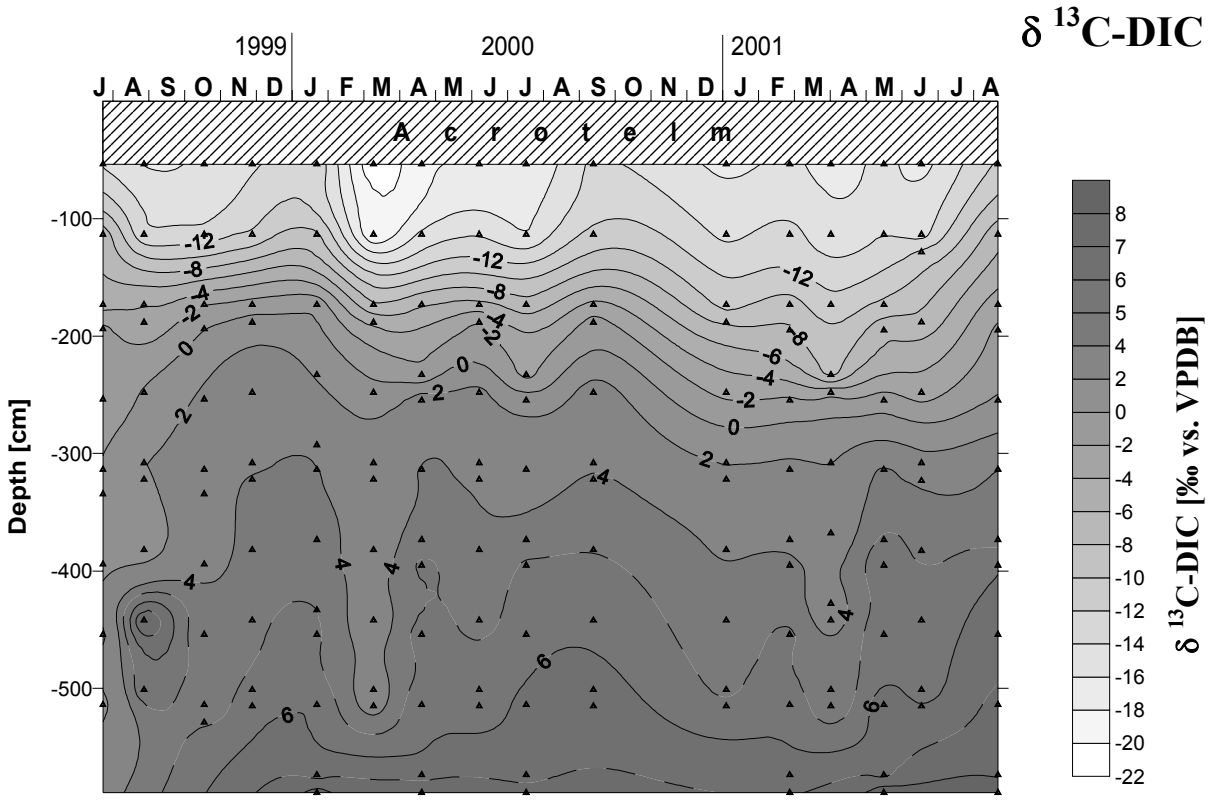

Fig. 6-7: Isopleth diagram showing the δ ^{13}C values for dissolved inorganic carbon (DIC) in the pore water of EGr during the period of measurement from July 1999 to August 2001. The triangles represent the data points.

The seasonal variations of the carbon stable isotope signature are less evident for DIC than for methane. DIC nevertheless exhibits a marked excursion towards lower δ ^{13}C values in late winter / early spring, which is relatively pronounced in the upper catotelm with values up to ca. 6 ‰ below the year's average, and still noticeable in the lower catotelm with values up to ca. 2.5 ‰ below the year's average. By and large, the DIC in the upper catotelm seems to be less depleted in ^{13}C in late autumn and winter than in spring and summer.

6.2.4.3 δ^{13}C-DOC

δ ^{13}C-DOC values were only determined for selected sample series (July 1999; August 1999). The values ranged from -27.9 ‰ to -24.7 ‰ and generally increased with depth (Fig. 6-8a). The increase, however, is not as steady as was observed for δ ^{13}C-DIC. For all series measured, the δ ^{13}C-DOC values were considerably higher in a zone from 4 to 5 m depth than above and beneath.

6.2.4.4 δ^{13}C of humic and fulvic acids

For the April 2000 samples series, δ ^{13}C values were determined on separated humic and fulvic acids (Fig. 6-8b). The δ ^{13}C values ranged from -26.7 to -24.8 ‰ for the humic acid samples and from -25.8 to -25.0 ‰ vs. VPDB for the fulvic acid samples. Isotopically, the humic acids followed a similar trend to what was observed for total DOC with downward increasing values to a depth of about 4 m. Beneath this depth, the values slightly decreased, but do not reveal a particular trend. Qualitatively, the fulvic acids show a similar pattern, albeit the range of isotope compositions is much more narrow.

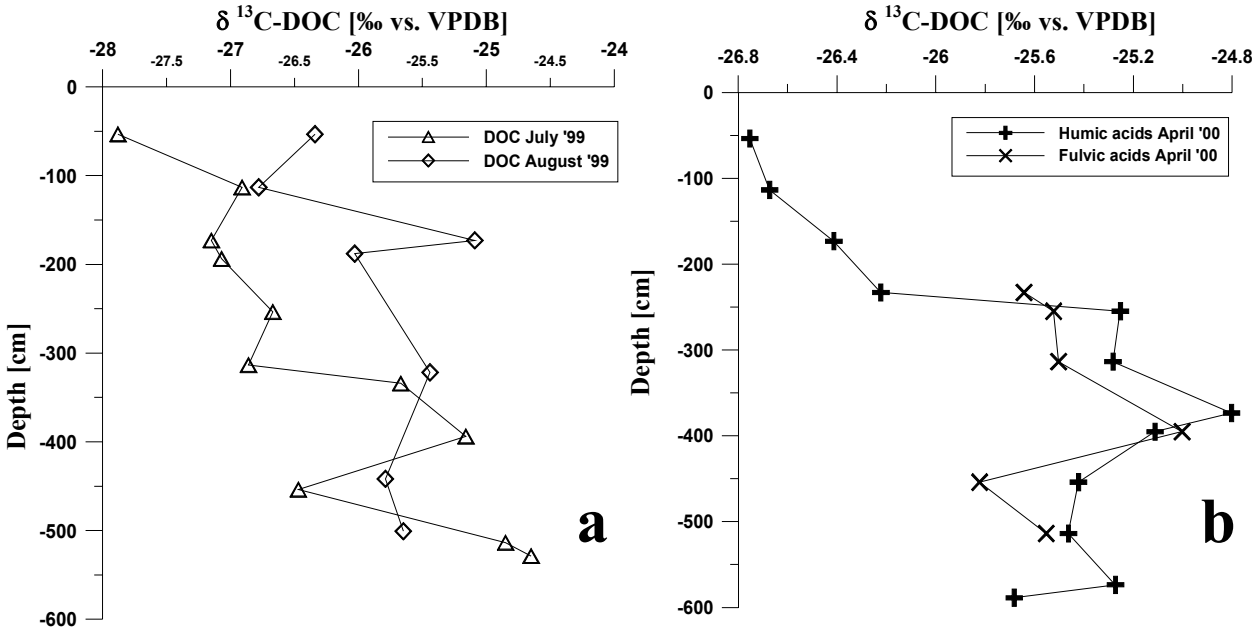

Fig. 6-8a&b: δ ^{13}C values for dissolved organic carbon (DOC) in the pore water of EGr **a)** for the July 1999 and the August 1999 sampling series; **b)** for the April 2000 sampling series, when humic and fulvic acids had been separated.

6.2.5 Discussion

In the upper catotelm of EGr, δ ^{13}C-CH_4 values were decreasing to depths of 1 to 2 m, depending on season. Similar trends of downward decreasing δ ^{13}C-CH_4 values from ca. -50 near the surface to as low as -75 ‰ vs. VPDB at a depth of about 2 m have been observed in several other northern hemisphere peat bogs, as for example in the Sifton Bog or the Point Pelee Marsh in SW Ontario (Hornibrook et al., 1997; Hornibrook et al., 2000). Studies of δ ^{13}C in methane from deeper bog layers, however, are rare. To our knowledge, the investigation of Waldron et al. (1999) is the only study that provided isotope data from deep peat gas: Waldron et al. (1999) measured in situ the catotelm methane and CO_2 carbon stable isotope signatures down to a depth of 5 m at the Ellergower Moss in SW Scotland. According to that study, the δ ^{13}C-CH_4 values range from -83 to -70 ‰ vs. the PDB standard and are hence significantly lower than the values observed at EGr. They confirm, however, downward decreasing values in the upper catotelm and generally increasing values in the lower catotelm, which have also been observed at EGr. Lansdown et al. (1992) report lower δ ^{13}C-CH_4 values from the King's Bog in the NW of the US than were observed at EGr. In this investigation, however, only single near surface values are stated, so that no trend with depth can be deduced. Subtropical and tropical wetlands are characterised by generally higher δ ^{13}C-CH_4 values; e.g. up to -45 ‰ at an Amazon floodplain site (Chanton et al., 1989b) or -48 ‰ at Baringo Lake, Kenya (Tyler et al., 1988). For an overview of δ ^{13}C-CH_4 measured at different natural wetland and bog sites worldwide, confer Lansdown et al. (1992).

The δ ^{13}C values of methane observed at EGr during the period of study do not allow an unambiguous determination of the CH_4-producing pathway. According to Whiticar et al. (1986), typical isotope signatures for methane produced by CO_2 reduction average at about -70 ‰. (Such values occur mainly in marine systems and range from ca. -110 to -60 ‰ vs. PDB). Acetate splitting yields δ ^{13}C-CH_4 values in the range of -65 to -50 ‰ vs. PDB. Further more, Whiticar et al. (1986) state that acetate splitting accounts for about 70 % of the methane

production in freshwater systems. The EGr data do not confirm this interpretation (cf. discussion below).

For a correct carbon stable isotope-based evaluation of the microbial methanogenic pathway, it is important to consider not only the carbon stable isotope composition of methane but also the carbon stable isotope composition of the inorganic carbon dissolved in the pore water (δ ^{13}C-DIC). As can be inferred from Fig. 6-1, methanogenic breakdown of organic matter leads to a 1 : 1 production of these two species. The isotope fractionation between methane and DIC is related to the microbial methanogenic pathway. According to Whiticar et al. (1986), an isotope fractionation of about 50 ‰ indicates acetate splitting, whereas an isotope fractionation of 60 to 70 ‰ is indicative of CO_2 reduction. Fig. 6-9 shows the CH_4-DIC carbon stable isotope fractionation in the pore water of the EGr Bog during the study period.

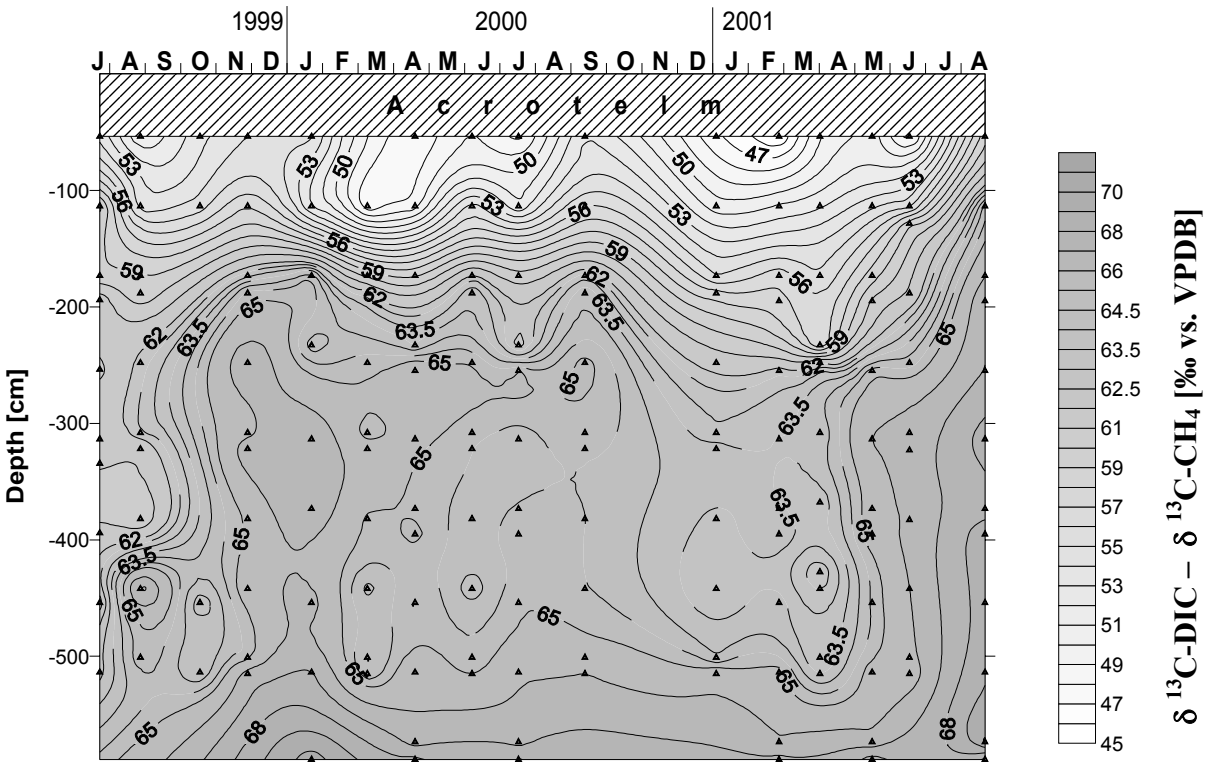

Fig. 6-9: Isopleth diagram showing the carbon stable isotope fractionation in the pore water of the EGr during the period of measurement from July 1999 to August 2001. The triangles represent the data points.

It shows relatively low CH_4 – DIC carbon stable isotope fractionation in the upper catotelm and hence indicates acetate splitting as the dominant methanogenic pathway. Below a depth of ca. 1.5 m, increasing isotope fractionation values (55 to up to 71 ‰) point to a predominant methane production via the CO_2 reduction pathway. While the increase in carbon stable isotope fractionation is pronounced in the uppermost ca. 2 m of the EGr, isotope fractionation values are almost depth-invariant between 2 and 5 m. Below ca. 5 m depth they increase again. Together with the absolute δ ^{13}C-CH_4 values, the observed fractionation pattern indicates that the methane produced in the upper catotelm is not effectively transported down into deeper parts of the bog (below ca. 2 m depth). Upward directed gas transport by bubble formation and ebullition therefore outweighs downward directed methane transport by pore water advection. In final consequence, this relationship causes methane emissions at the bog's

surface. Compared to ebullition and advection, molecular diffusion represents a relatively inefficient process for species transport (cf. chapter 6.4.3.2). Bubble formation, by contrast, is high in the upper catotelm due to a high gas production (higher temperature and turnover; cf. below) and a yet low confining hydrostatic pressure. Below approximately 2 m depth, increased decomposition (cf. Fig. 3-6) and hence a more compact peat structure seems to effectively hamper downward advection.

It is also very likely that the relatively high $\delta\ ^{13}C\text{-}CH_4$ values in the pore water between 3 and 5 m correspond to methane, which was produced in situ and had not been transported to this depth from above due to pore water advection: One reason for this assumption is that in peat bogs, the ebullitive flux, i.e. by bubble formation is most important for transport of poorly water-soluble species, such as methane. Model results (cf. chapter 6.4.3.2) indicate that ebullition removes more than 10 times as much methane from the pore water system as is produced in the respective depth. Other authors, e.g. Engle and Melack (2000) attribute almost 70 % of the total methane flux to ebullition. Predominant upward transport of methane should therefore be expected. It should however be noted, that according to the model assumptions, the role of advection may also be pronounced with up to 2 orders of magnitude more methane being advectively transported than produced at the corresponding depth. Peat permeability and downward advective flow is however not (as it is simplistically assumed in the model) constant over the entire depth of the peat profile, but decreases from the upper to the lower catotelm.

The low variation of the isotope fractionation values between 2 and 5 m depth seems to reflect the lower turnover rates of organic matter at low (7 – 8 °C) and also almost invariant pore water temperatures. Further more, the plant material in the peat is several thousands years old and labile organic precursors are therefore rare. A low methane production can hence be assumed, despite of the high methane concentrations measured in this depth range, which are due to higher hydrostatic pressure and very likely also due to the more compact and therefore less permeable structure of the peat in the lower catotelm.

The strong carbon stable isotope fractionation in the deep catotelm of the EGr may not only be the result of exclusive CO_2 reduction. Acetogenic production of acetate is characterised by a higher carbon stable isotope fractionation fermentative acetate production (cf. Fig. 6-1). Acetogenically produced acetate therefore shows a more ^{13}C-depleted isotope composition (with a mean value of -58.6 ‰ vs. PDB according to Gelwicks et al., 1989) than the acetate produced by fermentation. The isotope signature is then inherited when methane is produced via the acetate splitting. The low $\delta\ ^{13}C\text{-}CH_4$ observed in the deep catotelm may hence also bear a signal from the acetoclastic pathway, which – on the basis of the present data set – can not be distinguished from the CO_2 reduction signal.

The observed increase of the carbon stable isotope fractionation values below ca. 5 m depth can be attributed to the strong increase of the $\delta\ ^{13}C$-DIC values in this depth, which is probably a consequence of ground water mixing near the bottom of the bog. The observed signal is therefore not characteristic for the peatland methanogenic processes.

Kinetic isotope effects (KIEs) need to be taken into account, especially, when considering the vertical carbon stable isotope patterns for methane in the bog pore water. $^{12}C\text{-}CH_4$ is more mobile than $^{13}C\text{-}CH_4$. Methane containing the lighter isotope hence will go preferentially in the gas phase (e.g. Sugimoto and Wada, 1993) and is also transported more easily by molecular diffusion (e.g. Bondar, 1987; Pernaton et al., 1996). We can therefore expect that

an upward directed gas transport would increase ^{12}C-CH_4 share in the upper catotelm pore water and in the methane emissions. 6 gas emission samples were obtained at EGr in September and October 2001 (cf. chapter 4.5.2). The ^{13}C-CH_4 values of these samples ranged from -68.5 to -64.7 vs. VPDB. These values indicate predominant degassing of methane containing the lighter carbon isotope. If this observation is indicative of a fractionation process for methane moving up the pore water column, the remaining methane in the lower catotelm would get enriched in the heavy isotope. This contributes to the carbon stable isotope patterns of pore water methane observed at EGr without assuming different methanogenic production pathways. KIEs due to CH_4 oxidation in the gas samples need however also to be taken into account.

The effect of solely transport-related KIEs based on different diffusivities for ^{12}C-CH_4 and ^{13}C-CH_4 has been simulated for an EGr bog pore water model (cf. chapter 6.4). In accordance with other studies (e.g. Schoell, 1980), the modelling results indicate clearly that the observed isotope patterns cannot be explained by fractionation due to transport only. While over long distances (e.g. in natural gas systems) migration-related isotope fractionation may play an important role (Syngayevsky et al., 1978; Prinzhofer and Pernaton, 1997), its influence is minor in peat systems. The different methane production pathways and pore water transport processes can therefore be regarded as predominant for the observed $\delta\ ^{13}C$-CH_4 patterns.

6.2.5.1 Depth dependent "static" patterns

For the upper bog (above ca. 1 m depth), the published carbon stable isotope trends for methane are ambiguous. While some studies show clear downward decreasing $\delta\ ^{13}C$-CH_4 values (e.g. Hornibrook et al., 1997, Avery et al., 1999; Hornibrook et al., 2000), others show a trend towards less ^{13}C-depleted methane compositions (e.g. Lansdown et al., 1992; Reeburgh et al., 1997). According to the consideration made in the previous paragraph, such trends should also be explained primarily by different methanogenic pathways and pore water transport, yet only to a smaller degree by transport-related fractionation.

The lowest $\delta\ ^{13}C$-CH_4 values in the zone of 1 - 2 m depth are probably due to the generally very low concentrations of organic precursors for methylotrophy, in particular of acetate in this depth. At EGr, acetate concentrations in this zone are below 2.5 µM for most of the sample series (Fig. 6-2; cf. also Figs. 6-10 and 6-11). The acrotelm and upper catotelm pore water sampled with a separate peeper in November 2000 show considerably higher acetate concentration (up to 16 µM at 28 cm depth) than in the zone between 1 and 2 m depth, where acetate concentration levels were below the detection limit (cf. Eilrich and Steinmann, in prep.; chapter 6.1). A similar acetate concentration maximum in ca. 60 cm depth (June 1993 series) can also be inferred for a different bog in the Franches Montagnes Region, the Tourbière de Genevez (cf. chapter 3.2; Steinmann et al. 1998, Steinmann, 1995). – Concerning the seasonal variations (spring and early summer), when higher concentrations were measured, a possible explanation will be given in the following paragraph. – It seems likely that CO_2 reduction only becomes the dominant methanogenic pathway, when organic precursors (and acetate in particular) for methylotrophism are missing or when the temperature is too low acetoclastic methanogenesis. This view is supported by the $\delta\ ^{13}C$ isotope signature of methane and has already been suggested by other authors (e.g. Shannon and White, 1994; Hornibrook et al., 2000). It is interesting to note, that investigators tried to quantify the relative importance of one methanogenic pathway with respect to another. Lansdown et al. (1992), for instance, postulated that more than 99 % of the methane produced in King's Lake Bog could have derived from CO_2 reduction as the average $\delta^{13}C$-CH_4 value of the chamber flux samples was -74 +/- 5 ‰. This statement is based on laboratory experiments

for which the rate of produced ^{13}C-CH_4 was determined after incubation with sodium bicarbonate and ^{14}C-labelled acetate. Acetate concentrations in the bog were not measured. Based on laboratory experiments, acetate was considered "not an important precursor for methanogenesis". Obviously such interpretations cannot be generalised for all bogs. Apart from that, laboratory experiments may perhaps not truly reflect the microbial processes that occur in nature, for example due to the limit in size and the inevitable changes in the peat structure and its microbial communities on extraction of the peat (cf. Moore and Dalva, 1997). Incubation experiments carried out by Avery et al. (1999) showed that acetate splitting may well be an important methanogenic pathway and that at higher temperatures (>15 °C), acetate splitting would even be the dominant pathway. The published $\delta\ ^{13}C$ values for peatland pore water methane in the range of -60 to -48 ‰ vs. VPDB, are nevertheless usually interpreted as of acetoclastic origin (Whiticar et al., 1986; Hornibrook et al., 2000).

At EGr, the highest methane carbon stable isotope values were consistently observed in a zone between ca. 4 and 5.2 m below ground surface independent of the season. Below ca. 5.2 m depth, the $\delta\ ^{13}C$-CH_4 values slightly decreased again by 1 to 2 ‰ towards the ground of the bog (The lowermost samples were obtained from 5.9 m depth.). This observation correlates well with the acetate concentrations for the deep catotelm, which increase significantly below ca. 4 m depth and show in most cases a distinct maximum at about 5 m depth (cf. Fig. 6-2). Parallel to the $\delta\ ^{13}C$-CH_4 values, which decreased, the acetate concentrations decreased in the lowermost samples. This is in harmony with the interpretation given above according to which methanogenesis primarily relies on acetate, if this precursor is available and can be metabolised (temperature!). To our knowledge, peat bog acetate concentrations have not been measured to such depths before. It is therefore impossible to provide supportive evidence for this interpretation from other sources. Carbon stable isotope composition data for methane samples from the lower part of Ellergower Moss in SW Scotland published by Waldron et al. (1999) range from -83 to -70 ‰ and imply CO_2 reduction as the dominant methanogenic pathway for that site. The $\delta\ ^{13}C$-CO_2 values in the lower catotelm range from ca. 5 to 10 ‰ and hence indicate CO_2 reduction-type isotope fractionation (Whiticar et al., 1986). Nevertheless, the data from Waldron et al. (1999) point to a change towards the ground of the bog with generally increasing $\delta\ ^{13}C$-CH_4 values (and slightly decreasing $\delta\ ^{13}C$-CO_2 values) as had been observed for the EGr.

6.2.5.2 Seasonal "dynamic" patterns

The seasonal variations in $\delta\ ^{13}C$-CH_4 observed at the EGr are particularly interesting with respect to their implications for methanogenic pathways.

Upper catotelm

In late autumn and winter, relatively high $\delta\ ^{13}C$-CH_4 values (-67 to -64 ‰) occur in the upper catotelm from 0.5 to 1 m depth. This points to an increased share of ^{13}C-enriched methane produced by acetate splitting. Absolute methane concentrations are very low in this depth (<0.5 μM). The acetate concentrations, which remain also low in winter (<2.5 μM for most of January and February), could therefore reflect a low production of precursors and a low overall methanogenic turnover due to low pore water temperature. In spring, the EGr pore water methane shows a considerable depletion in ^{13}C-CH_4 with $\delta\ ^{13}C$-CH_4 values as low as -68 ‰ (June 2000; Mai, June 2001). This indicates a decreasing relative importance of the acetoclastic vs. the CO_2 reduction pathway. Acetate concentrations, however, increase considerably in spring and early summer with values up to 5 times as high as average pore water values at comparable depths. This is probably due to the pathway change as well as to then potentially higher degradation rates of labile organic matter in the acrotelm. The

concentration changes are thereby regarded as proxies for microbial methanogenic turnover rates neglecting the influence of transport processes for the chemical species. There seems to be a time lag of ca. 2 months between the increase of shallow acetate concentrations at EGr and the maximum isotopic effect marked by $\delta\ ^{13}C\text{-}CH_4$ values (cf. Fig. 6.2 and 6-3). On the other hand, the low acetate concentrations measured in November / December 1999 in the lower catotelm are not followed by decreasing $\delta\ ^{13}C\text{-}CH_4$ values until January / February 2002, the role of acetate splitting in the uppermost catotelm (above 1 m depth). It should however be noted that acetate produced by acetogenesis (cf. Fig. 6-1) is characterised by more negative $\delta\ ^{13}C\text{-}CH_4$ values than acetate produced by fermentation reactions (Gelwicks et al., 1989). This could, for the uppermost catotelm, explain the relative low $\delta\ ^{13}C\text{-}CH_4$ values in presence of acetate without assuming a time lag. The observations made for the EGr in spring seem to contrast sharply with the results of a study by Shannon and White (1996) for the upper 40 cm of a Michigan bog, where a drastic decrease in acetate concentration in late spring had been observed and explained by the onset of acetoclastic methanogenesis at higher pore water temperatures (cf. Avery et al., 1999). As is pointed out in the introduction, isotope and concentration patterns are subject to important changes in the upper layers of a bog. Observations made in the acrotelm may well be different from the observations made in the catotelm, which are discussed here, as important parameters (pore water temperature and availability of a labile organic substrate) are also very different. Mere temperature boundaries deduced from laboratory experiments are probably insufficient for pinpointing microbial pathways in nature.

Lower catotelm

In the lower catotelm (below ca. 2 m depth) the seasonal variations are much less pronounced than in the upper catotelm (cf. Fig. 6-6). This can be explained by the influence of temperature on microbial geochemical reactions and by the distance from the acrotelm, which represents the predominant source for labile organic precursors.

In late autumn 1999 and early winter 1999/2000, acetate concentrations in the lower catotelm are unusually low (Fig. 6-2). Such acetate concentration deficiencies are probably responsible for the marked depletion in $^{13}C\text{-}CH_4$ observed in the lower catotelm in early 2000 (Fig. 6-6), as less methane could then be produced by the acetate splitting pathway. The cause for these low acetate concentrations remains unclear. The potential influence of increased methanogenic turnover and the influence of surface ice-cover for pore water advection and the supply of labile organic matter are being discussed (cf. Eilrich and Steinmann, in prep.; cf. chapter 6.1). Relatively low acetate concentrations in the deep catotelm were also detected in September and October 2000. These concentrations were however considerably higher than those of late autumn 1999.

6.2.5.3 $\delta^{13}C$-DIC

Depth-dependent "static" patterns

The observed range of $\delta\ ^{13}C$-DIC values at EGr (-21.7 ‰ in a depth of ca. 0.5 m; +8.8 ‰ at 5.9 m depth; cf. Fig. 6-7) correspond very well to $\delta\ ^{13}C$-DIC values reported for similar depths at other sites (e.g. Hornibrook, 2000; Waldron et al., 1999). They are however significantly higher than those observed in shallow non-peat soil environments (e.g. -34 to -24 ‰ vs. PDB; Telmer and Veizer, 1999).

As was the case with CH_4, the carbon stable isotope composition of DIC showed a clear trend towards higher $\delta\ ^{13}C$-DIC values with depth. As the isotope composition of CH_4 varies in function of the isotope composition of the CO_2 pool, this is an indication that also at EGr, CO_2 reduction is a major microbial pathway for methane production. Other authors, e.g. Crill

et al. (1988), Lansdown et al. (1992), Waldron et al. (1999), and Hornibrook et al. (2000) reported downward increasing δ ^{13}C-DIC values. It is remarkable that the increase in δ ^{13}C-DIC is most pronounced between 1 and 2 m depth. With respect to CH_4 carbon stable isotopes, this zone is characterised by generally relatively stable and low δ ^{13}C-CH_4 values. It may therefore be inferred that the zone between 1 and 2 m depth and, to a smaller degree also the peat layers below and above, are marked by a mixture of CH_4 produced via both pathways, CO_2 reduction and more pronounced acetate splitting at depth. The influx of methane from below, which is less depleted in ^{13}C probably causes the low vertical variation of the CH_4 carbon stable isotope composition. The corresponding methane source is predominantly fed via the acetate splitting pathway.

Methane is transported to the upper catotelm by molecular diffusion (cf. chapter 2.5.2) and, notably, ebullition (cf. chapter 2.5.3). The carbon isotope signature of methane and DIC in the incoming pore water seems to be mainly influenced by acetate splitting, methane oxidation and respiration effects. In the upper catotelm above 1 to 2 m depth, probably, mixing occurs of the acrotelm signal and the major background catotelm signal. The latter shows a strong influence of CO_2 reduction and, more importantly in the deeper catotelm, acetogenesis with an inherited markedly negative carbon stable isotope composition.

Seasonal "dynamic" patterns

The seasonal fluctuations in the DIC carbon stable isotope composition were minor (cf. Fig. 6-7). Slightly (by ca. 2 ‰) lower values than in the year's average were observed for most depths in late winter / early spring and are probably related to melting of the ice cover at the surface of the bog and recommencing pore water advection, which takes isotopically lighter DIC into greater depths. Due to the lack of continued measurements at such depths, it is impossible to confirm this observation using data from literature. The data sets published by Lansdown et al. (1992) and Hornibrook et al. (2000), for instance, cover only depths of up to 0.7 and 1.8 m respectively.

Isotopically light DIC from the acrotelm and the upper catotelm, temporarily seems to decrease the δ ^{13}C-DIC values before a new equilibrium is attained. The δ ^{13}C-DIC stratification is largely depth-dependent and there are only minor seasonal changes. This supports the interpretation of CO_2 reduction as the important uninterrupted "background" microbial process, while the influence of acetate splitting is generally less pronounced and depends on a sufficiently large acetate reservoir (and possibly temperature). If this view is correct, the remarkably low δ ^{13}C-CH_4 values in the lower catotelm (>3 m depth) in winter 1999/2000 represent a change towards exclusive CO_2 reduction as the acetate concentrations had become anomalously low ca. one to two months before (cf. Fig. 6-2). An impeded methane production due to the shortfall of acetate splitting and a more depleted DIC pool due to the increased importance of the CO_2 reducing microbes should therefore be expected. This is exactly what was observed in January 2000, when anomalously low pore water methane and DIC concentrations have been measured. The reduced role of species transport, mainly with respect to advection and ebullition, probably contributed to the anomalous concentration and carbon stable isotope patterns during the relatively harsh winter 1999/2000.

6.2.5.4 Isotope fractionation and organic matter

If the observed average carbon stable isotope fractionation of 65 ‰ as well as average δ ^{13}C values of -60 and +5 ‰ vs. VPDB are considered for microbially produced CH_4 and CO_2, respectively, the δ ^{13}C value for degradable organic matter will yield a δ ^{13}C of -27.5 ‰. This is in tune with the results of carbon stable isotope measurements of humic and fulvic acids (-27 to -24 ‰) of the Etang de la Gruère Bog. The light δ ^{13}C values of around -16 ‰ for the

DIC in shallow depths can be explained by ^{13}C-depleted CO_2 from oxidation of organic matter in the acrotelm and respiration. The $\delta\ ^{13}C$ values of the EGr peat matrix decreased with depth from ca. -25.5 ‰ in the acrotelm (at 20 cm below ground surface) to -28.5 ‰ in the deep catotelm (at 5.8 m below ground surface; S. Huon - pers. comm.).

6.2.6 Conclusions

Over the period of study, the carbon stable isotope composition of EGr pore water methane revealed characteristic patterns - "static", i.e. depending on depth as well as "dynamic" with respect to seasonal variations. Both, static and dynamic patterns can be mainly explained by the corresponding influences of two major microbial pathways, acetate splitting and CO_2 reduction. The observed isotope fractionation of about 65 ‰, however, does not allow an unambiguous determination of the methane producing biochemical pathway.

The fact that the isotopic trend of CH_4 follows CO_2 for most of the catotelm (from ca. 1 to ca. 5 m depth) underlines the role of CO_2 reduction as the major microbial pathway for methane production in the bog. The relatively low CH_4 – DIC carbon stable isotope fractionation in the upper catotelm indicates acetate splitting as the dominant methanogenic pathway. Below a depth of ca. 1.5 m, increasing isotope fractionation values (55 to up to 71 ‰) point to a predominant methane production via the CO_2 reduction pathway. The observed isotope and fractionation pattern indicate that the methane produced in the upper catotelm is not effectively transported down into deeper parts of the bog (below ca. 2 m depth).

The largely depth-dependent $\delta\ ^{13}C$-DIC stratification of the bog and only minor seasonal changes support a view according to which CO_2 reduction represents the uninterrupted "background" microbial process, while the intensity of acetate splitting is much more variable depending on the availability of acetate as methanogenic precursor and temperature. A time lag for the onset of acetate splitting after filling of the acetate reservoir seems to be likely. Comparison of concentration and isotope data from EGr shows that the occurrence and the relative importance of these two pathways are probably very much more dependent on the availability and degradability of organic precursors, in particular acetate.

Transport processes, in particular ebullition and pore water advection, yet to a smaller degree also molecular diffusion, certainly influence the distribution of chemical species and their isotope compositions. It is however difficult to quantify this influence. The observed CH_4 and DIC concentration and isotope composition anomalies in winter 1999/2000 are probably caused by increased advective flow and species transport after melting of the ice cover at the bog's surface.

6.3 Observations on the influence of other species

Methylotrophic methanogenesis may not only be based on acetate as metabolic precursor, but also on the anions of other volatile fatty acids such as formate, propionate and lactate.

The concentration of formate in the pore water of EGr has only been measured for the January and the March 2000 series. The January 2000 formate concentrations were below 20 ppb at all depths except for the uppermost peeper at ca. 50 cm depth, where exceptionally 113 ppb were measured. In March 2000, the formate concentrations were below the detection limit of ca. 5 ppb. Propionate has been measured regularly for all series from January 2000 to August 2001, but only detected in about 50 % of the samples (Fig. 6-10). During the period of study, propionate showed rather abrupt concentration changes in different depths, yet high levels (up

to almost 3500 ppb) were generally reached in the lower catotelm (cf. Fig. 6-10). Qualitatively however, the propionate concentration patterns were similar to those of acetate. An even higher degree of similarity was observed for another species, which could not be exactly determined but is probably a lactate isomer (Fig. 6-11). Despite of generally lower concentrations, this species could be detected much more often in EGr pore water than propionate.

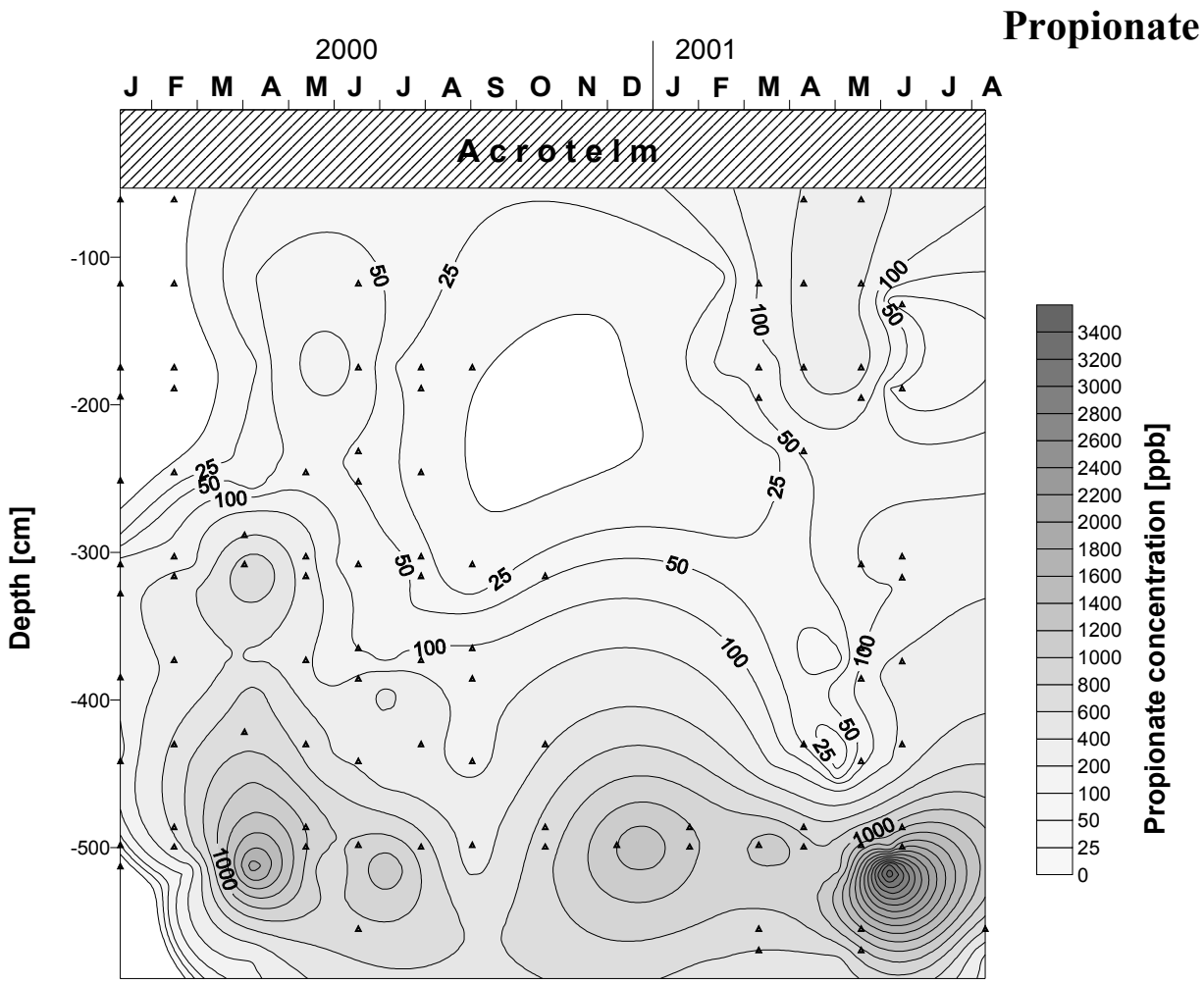

Fig. 6-10: Isopleth diagram showing the propionate concentration in the pore water of EGr during the period of measurement from July 2000 to August 2001. The triangles represent the data points. Propionate was only detected in about half the samples and that large areas in the time/depth space of the isopleth diagram are extrapolated without a sufficient database.

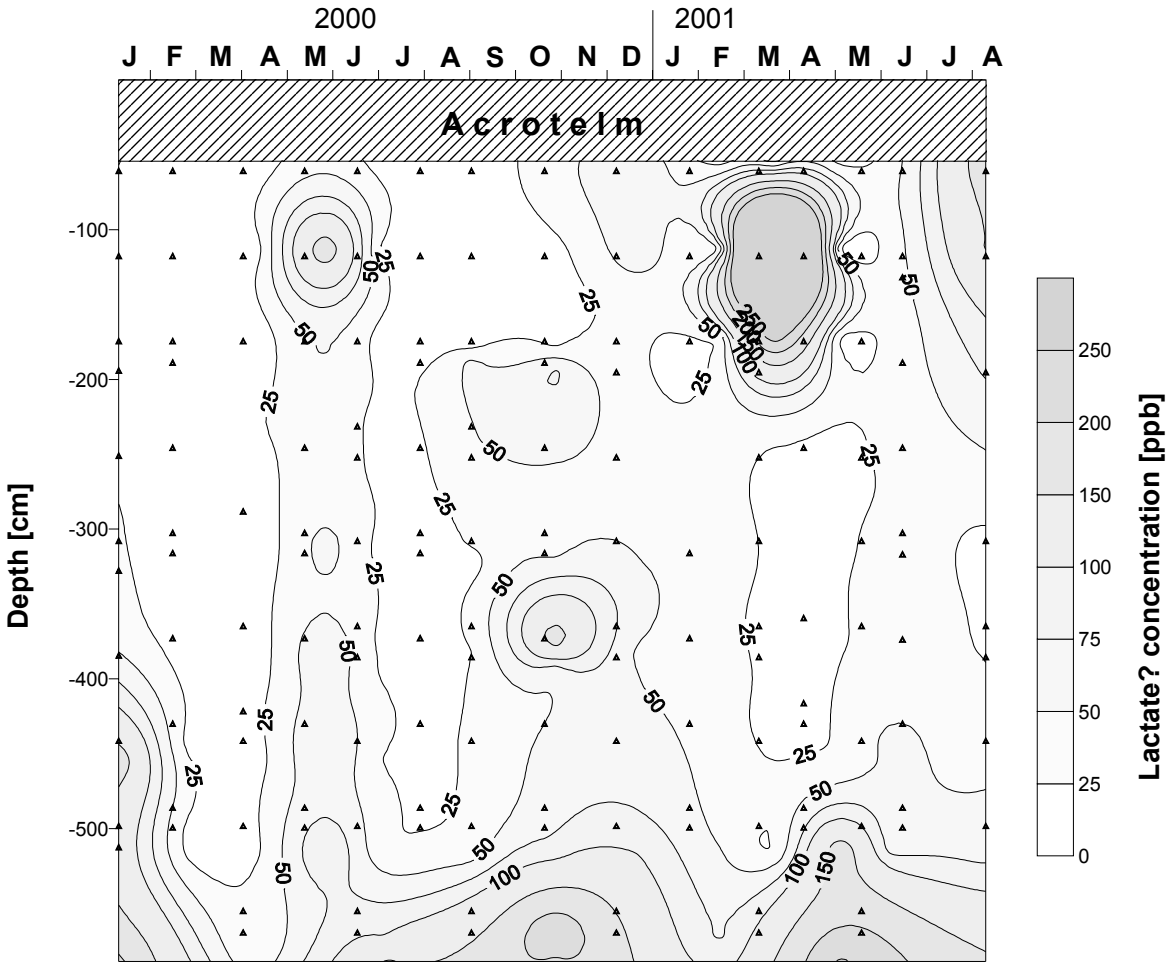

Fig. 6-11: Isopleth diagram showing the concentration of a fatty acid (lactate? - cf. chapter 4.3.2.1) in the pore water of EGr during the period of measurement from July 2000 to August 2001. The triangles represent the data points.

The observed similarity with acetate supports the interpretation of a prevailing dissociative methanogenesis ("acetate splitting") in the lower catotelm, while, in the upper catotelm (in particular between 1 and 2 m depth), methane production is predominantly assimilative ("CO_2 reduction"). Furthermore, it should be noticed that the term "acetate splitting" as it is used here for distinction from CO_2 reduction, probably implies a range of methylotrophic processes and not only dissociation of acetate itself.

6.4 A model of methane and CO_2 production and transport in deep peatlands - Implications for greenhouse gas emissions **(paper in preparation)**

6.4.1 Abstract

Methane is an efficient greenhouse gas and wetlands are significant sources of methane to the atmosphere. In wetlands, methane and CO_2 are produced in all depths by microbial communities, which decompose organic matter in the anaerobic environment. Gas transport processes such as pore water advection, molecular diffusion, and ebullition have a major impact on the concentration distribution of the chemical species in the pore water and on the quantity of gas emitted via the acrotelm.

A numerical model has been developed to simulate the effect of methane and CO_2 production and transport processes on pore water concentrations and carbon stable isotope patterns in the catotelm of a peat bog. The model is based on field and analytical data from the Etang de la Gruère Bog (EGr) in the Swiss Jura Mountains, where hydrological and pore water chemical parameters had been investigated to up to 6 m depth from October 1999 to August 2001. The model was fitted to these data. The model results show a concentration increase with depth (about 10-fold for dissolved inorganic carbon and more than 20-fold for methane), which is almost as high for the measured concentrations, whereas other gases such as nitrogen are rapidly, almost completely within the first meter, removed from the pore water. Discrepancies between model and field results underline the influence of the heterogeneous peat structure and different vertical conductivities, labile organic precursors, over-saturation and ground water mixing near the base of the bog, which are not or not sufficiently taken into account in the model. The simulation further indicates that gas loss by bubble formation is by far (maybe over 70 times) more efficient than by diffusion. In the upper catotelm (above ca. 0.8 m depth), bubbles are mainly composed of nitrogen, which enters the catotelm by pore water advection from the acrotelm. Below ca. 0.8 m depth, according to the model, methane is the constituent of the gas bubbles and contributes to up to 90 % of the bubble volume. In the deep catotelm below ca. 4 m depth, CO_2 takes a slightly higher share in the gas bubbles, while the total bubble volume is declining to virtually zero in 5 m depth.

The range of the modelled $\delta\ ^{13}C\text{-}CH_4$ values reflects well in absolute numbers the measured range. The relative variations in the carbon stable isotope composition for the different depths, however, could not be reproduced in the model.

6.4.2 Introduction

Natural wetlands represent the largest single source of methane to the atmosphere. Recent estimates range from 145 Tg/a (Houwelling et al., 1999) to 237 Tg/a (Hein et al., 1997). According to Houwelling et al., 1999, this constitutes more than 80 % of all natural and about 25 to 40 % of the total, i.e. natural and anthropogenic, emissions (IPCC, 2001). With ca. 115 Tg/a, peatlands (i.e. natural wetlands with a thickness of the peat layer of more than 30 cm) contribute to more than 70 % of the natural methane sources and to about one fifth of the total sources (Houghton et al., 1995; cf. Fig. 2-4).

This study refers to field research carried out from October 1999 to August 2001 at the Etang de la Gruère Bog (EGr) in the Swiss Jura Mountains. Pore water samples were obtained in situ from the catotelm using diffusion chambers ("peepers") to a depth of 5.9 m. The term catotelm represents the zone of permanently water-saturated and often significantly decomposed peat underlying a less decomposed and only partly water-saturated “root zone”

(acrotelm) at the top of the bog (cf. chapter 2.3). The samples were analysed for their major ion content including the volatile fatty acid (acetate, propionate, formate), dissolved methane, inorganic and organic carbon (DIC and DOC, respectively) as well as the carbon stable isotope composition of methane, DIC, and DOC. The pH and additional physical parameters such as pore water temperature, water level, and water flow direction were measured as well.

6.4.2.1 The model: Purpose and concept

In an attempt to gain more insight, a computer model has been developed to simulate gas production and transport processes and their effects on the distribution of methane and inorganic carbon in the catotelm, i.e. the deeper parts of a peatland. The model is based on and adapted to the analytical data described above and additional hydrological information from earlier investigations at EGr. The species considered were basically methane and CO_2. These two gases are produced by microbial degradation of organic matter in anaerobic environments such as wetland soils. The modelled processes are microbial gas production, pore water advection, molecular diffusion and gas loss by bubble formation (ebullition). They are schematically illustrated in Fig. 6-12. In case of methane for example, the concentration change due to these processes can be summarised as

$$[CH_4]_i\ (t+\Delta t) = [CH_4]_i\ (t) + \Delta t * (CH_4\_prod_i + CH_4\_adv\_in_i + CH_4\_diff\_in_i - CH_4\_ebul\_out_i - CH_4\_diff\_out_i - CH_4\_adv\_out_i)$$

, where

Δt	= finite time interval ("step") of each single calculation
$[CH_4]_i\ (t+\Delta t)$	= newly calculated methane concentration at depth-level i after the time interval Δt
$[CH_4]_i\ (t)$	= methane concentration at depth-level i before the calculation
$CH_4\_prod_i$	= methane flux into the cell due to microbiological production at depth-level i
$CH_4\_adv\_in_i$	= methane flux into the cell due to advection at depth-level i
$CH_4\_adv\_out_i$	= methane flux out of the cell due to advection at depth-level i
$CH_4\_ebul\_out_i$	= methane flux out of the cell due to ebullition at depth-level i
$CH_4\_diff\_in_i$	= methane flux into the cell due to diffusion at depth-level i
$CH_4\_diff\_out_i$	= methane flux out of the cell due to diffusion at depth-level i

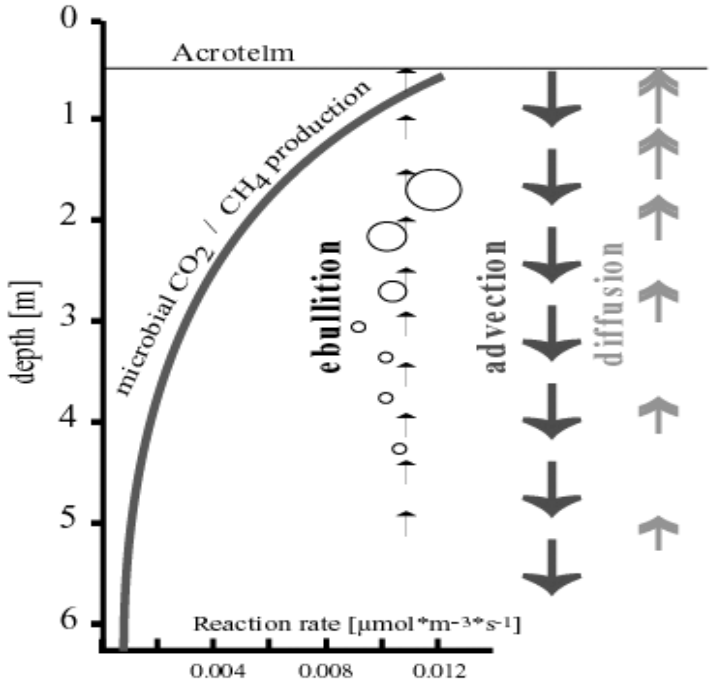

Fig. 6-12: Graphical illustration of the processes of gas production and transport referred to in the model. In peatlands, advective species transport is usually downward directed, whereas species transport by diffusion is generally upward directed due to the prevailing concentration gradients (cf. chapter 6.2 and Figs. 5-7 & 6-3).

The so obtained model is relatively simple in the number of variables and reactions used, but considerably complicated by adding gas loss due to bubble formation. While, primarily, the model results concern the concentration patterns of methane and CO_2, further implications may include a large variety of issues such as the carbon stable isotope composition patterns of methane, principal zones of bubble formation and bubble composition, the influence of the pH gradient for CO_2 in the bubbles, the role of diffusive versus ebullitive and advective gas transport within the pore water column as well as the effect of interrupted pore water advection over a longer time-span.

6.4.2.2 Realisation

Computational platform: The available geochemical codes such as PhreeqC or Crunch, proved to be difficult to adapt for solving the given problem. For example, a pH gradient or vertically changing production parameters are not foreseen. Therefore, a simple, explicit, forward ("upwind") formulation was developed, which can be calculated using spreadsheets (e.g. Microsoft Excel). Commercial spreadsheet calculation programs do not warrant convergent, stable and consistent model calculation. AQUASIM, which has been developed by P. Reichert at the Swiss Federal Institute for Environmental Science and Technology (EAWAG), has therefore been chosen for control over the model results and for another numerical calculation (cf. chapter 6.4.4.6).

Model dimensions: The model is one-dimensional. It can be described as a box model with a vertical extension dx (e.g. 10 cm) of each box.

General model assumptions: The hydraulic conductivity is assumed to be homogeneous over the entire length of the modelled profile. The principal transport processes integrated in the model are molecular diffusion and pore-water advection. A sink term has however been introduced representing the hypothetical gas bubble formation and specific gas loss due to ebullition. The integration of these parameters into the model is described below. In accordance with the measured advective flow, the species transport at the upper and lower model boundaries, i.e. from the acrotelm through the modelled depth range into an undefined substratum, is always downward directed (cf. Fig. 6-12). Diffusive species transport may be upward and downward depending on the respective concentration patterns. Ebullition was not modelled as a transport process for chemical species, but as a process that instantaneously removes species from the system according to the definition set. In addition to advective and diffusive transport as well as species loss due to bubble formation, CH_4 and CO_2 were allowed to form in all depths of the bog. The basis for methane and CO_2 production in wetlands is biological (microbial) degradation of organic matter, e.g. by fermentation (Boone et al., 1993). The production rate was assumed to decline exponentially with depth (Fig. 6-12). Absorptive processes such as the Freundlich and the Langmuir adsorption were assumed to have a neutral effect under steady state conditions and are therefore not considered in the model. The model has been adapted to the situation and conditions at the EGr peat bog. The modelled depth range can be varied using different values for the vertical extension of the box (dx) or a different number of boxes. It roughly corresponds to the catotelm at the study site at EGr (ca. 0.5 - 6 m below ground surface), but can be much longer in order to avoid boundary condition effects ("open" lower boundary). Microbial processes in the catotelm are entirely anaerobic. Molecular oxygen or electron acceptors (e.g. by NO_3^-; or SO_4^{2-}) for chemoautotrophically mediated oxidation can be assumed absent in the catotelm (Steinmann and Shotyk, 1997b).

Boundary conditions: The model has a definite upper boundary with a fixed concentration in an upper ghost-cell in the acrotelm. The lower end is "open" and has no fixed boundary, i.e. diffusion from below is included by means of an extrapolated diffusion gradient.

6.4.2.3 Model parameters

An overview of the parameters and the constants used in the model is given in chapter 11.AIV.

Pore water advection and advective species transport

In a hydrological study conducted by McKenzie et al. (2002) from July 1st, 1997 to August 31st, 1998, piezometer measurements showed a positive vertical hydraulic gradient and hence downward flow of pore water (cf. chapter 5.2.5). Recent piezometer data, obtained during the study at EGr presented here, confirm almost invariably downward directed pore water advection in all parts of the catotelm (cf. chapter 5.2.4), in all seasons and during the entire period of measurement. In the model, advection is simulated quantitatively as an advective flow rate (Microsoft Excel) or 'inlet input' (AQUASIM), respectively. The flow is loaded with initial species concentrations for methane, DIC and N_2 (as derived from the overlying acrotelm). The flow rate is $3.125*10^{-7}$ $m*s^{-1}$ (≈ 0.03 $m*d^{-1}$), which corresponds to the average calibrated bulk vertical hydraulic conductivity determined at the EGr (McKenzie et al, 2002). The flow rate is high, when compared the annual average precipitation (cf. chapter 3.1.3) but representative for periods of high precipitation.

For CH_4 and DIC, the flux derived from the acrotelm was assumed to correspond to the respective average concentrations of two sample series (July 2000 and November 2000) measured at ca. 50 cm depth, i.e. 0.17 mM for CH_4 and 1.6 mM for DIC. The depth of ca. 50 cm corresponds to the uppermost pore water sample that has regularly been obtained using diffusion chambers) for in situ filtration (peeper Type B; cf. chapter 4.1; Steinmann and Shotyk, 1995; Eilrich and Steinmann, in prep.). The July and November 2000 EGr pore water methane and DIC concentrations are typical. During the period of field research from June 1999 to August 2001, the methane and DIC concentrations ranged from 0.026 to 0.3 mM and from 0.98 to 3.43 mM, respectively. N_2 was considered to be the only other gas species in the pore water of EGr. The partial pressure of N_2 (pN_2) was taken to correspond to the difference of the hydrostatic pressure (1.054 bar) and the sum of the CH_4 and CO_2 partial pressures (0.163 bar) at ca. 50 cm depth. A theoretical N_2 concentration (0.607 mM) in the acrotelm and hence the N_2 flux from the ghost-cell across the upper model boundary could therefore be determined using Henry's law constant for an assumed pore water temperature of 8 °C (cf. chapter 11.AIV). It should be noted that the pN_2 used in the model (0.891 bar) is higher than the pN_2 in the atmosphere (0.79 bar). This is however not surprising and can be explained by the fact that in the model, pN_2 also includes the partial pressures of other gases, which are not considered for the calculation yet potentially also present in peat bog water, e.g. N_2O, CO, H_2, C_2H_2. In addition, the N_2 concentration may increase in the acrotelm as it may also be produced by microbial activity.

6.4.2.4 Diffusive species transport

Diffusion was integrated in the model according to Fick's first law (cf. chapter 2.5.2 and the mathematical approach for saturated soil layers by Makhov and Bazhin, 1999). The diffusion coefficients were taken from the literature (Stein and Lieb, 1986; Lide, 1996) and decreased by about 40 % to account for the specific conditions of diffusive transport in a pore water environment, in particular with respect to tortuosity (P. Steinmann, S. Burns, pers. comm.). For CH_4 and DIC in aqueous environment, molecular diffusion constants of $1.10*10^{-9}$ and

$1.25*10^{-9}$ m^2*s^{-1}, respectively, were thus inferred. N_2, as such, is not of primary concern for the endeavoured simulation. The N_2 concentration in the bog pore water column, however, exercises a partial pressure, which needs to be taken into account in the model, as it plays a role for the formation of bubbles (cf. chapter 6.4.2.5 below). The molecular diffusion constant used for N_2 is $1.38*10^{-9}$ m^2*s^{-1}.

6.4.2.5 Bubble formation and ebullition

In principle, bubble formation can be assumed, when the gas pressure in the liquid phase ($pCH_4 + pCO_2 + pN_2$) exceeds the confining hydrostatic pressure. Bubbles are thought to be composed proportional to the relative partial pressures of the three gas species considered, i.e. CH_4, CO_2 and N_2. Once formed, the hypothetical bubbles are considered 'out of the system', i.e. they are thought to have moved up the pore-water column into the acrotelm, where they might oxidise, escape to the atmosphere, or re-dissolve.

6.4.2.6 Gas over-saturation of the pore water

It can be inferred from several field studies (e.g. Siegel et al., 1997; Reeve et al., 2001; Siegel et al., 2001) that the deeper parts of the peat pore water are over-saturated with dissolved gases. In case of over-saturation, the total partial pressure (i.e. the sum of the partial pressures of all gas species dissolved in the pore water) is higher than the confining hydrostatic pressure for the respective depth level. For EGr, the calculation of the combined partial pressure of CH_4 and CO_2 on the basis of the observed concentrations of these species in the pore water shows that there is a significant over-saturation in depths below ca. 2.5 m, while above this depth, the combined partial pressures of CH_4 and CO_2 are inferior to the confining hydrostatic pressures (cf. chapter 11.AIII-Goldschmidt'00-Fig.2a). This is mainly a consequence of ignoring nitrogen. Nitrogen gas is poorly soluble in water and hence may contribute to the total partial pressure in the upper catotelm, where it should be still present due to pore water advection from the acrotelm. Nitrogen concentrations, however, have not been measured at EGr. The whole N-cycle (including N_2O gas) is not considered due to its lower magnitude. The calculated over-saturation of the gases dissolved in the EGr pore water below ca. 2.5 m depth can be expressed in terms of the total partial pressure of the dissolved gas species (CH_4 and CO_2). In a first approach, over-saturation was not permitted in the model. In a modified approach, pore water gas saturation was set between 100 % (at 2 m depth) and 180 % (at 5 m depth). This range represents the typical actual over-saturation of the pore water with CH_4 and CO_2 observed at EGr during the period of field research.

6.4.2.7 Methane and CO_2 production in the catotelm

In the absence of molecular oxygen and other electron acceptors such as NO_3^- or SO_4^{2-}, microbial degradation of organic matter ultimately leads to the formation of methane and CO_2 (cf. Fig. 2-5). A schematic illustration of methanogenic and CO_2 producing processes is given in Fig. 6-1. The overall effect of the two major microbial processes (acetate splitting and CO_2 reduction) for $(CH_2O)_n$ organic matter is a 1 : 1 stochiometric production of CH_4 and CO_2. In the model, the production rates of CH_4 and CO_2 are therefore also considered equal. Identical microbial processes are assumed for all depths. The initial production rate, i.e. the production at the upper boundary of the model at 53.6 cm depth, was in a first approach set as 0.012 $\mu M*s^{-1}$, which is comparable to experimental data (e.g. Avery et al., 1999). The value for the initial CH_4 and CO_2 production rate was later varied.

The gas production in the bog pore water is thought to decrease with depth, as temperatures generally also decrease with depth and due to the aging of the peat layers, that probably yield less labile organic substrate. In the model, the decrease in gas production was described

mathematically using an exponential decay function (e^{-x*a}, where x represents the depth in metres. The constant *a* determines the microbial CH_4 and CO_2 production. The CH_4 and CO_2 production parameter *a* represents a purely mathematic approximation to adapt the modelled concentrations to the measured concentrations. It has a positive value and appears in the exponent of a natural decay function. The mathematical expression

$e^{-a*depth}$ * *iniprod*, where *iniprod* stands for the initial CH_4 and CO_2 production rate,

hence describes the assumed decrease in CH_4 and CO_2 production with depth due to the declining metabolic potential of the older organic matter in the deep layers (cf. Fig. 6-12). A higher value for *a* therefore characterises a bog with more rapidly downward declining CH_4 and CO_2 production rates, whereas a lower value of *a* means more homogeneous geochemical and physicochemical conditions throughout the bog profile and slower decline of the initial CH_4 and CO_2 production rates. In a first approach for the model presented here, *a* has been chosen arbitrarily to fit the measured July 2000 and November 2000 DIC concentrations in the upper catotelm. The numerical value of *a* thus derived is 0.7. The influence of changing the value for *a* will be described below.

6.4.2.8 DIC vs. CO_2

When carbon dioxide is dissolved in water the thereby formed theoretic carbonic acid H_2CO_3* partly dissociates to form HCO_3^- and CO_3^{2-}. The equilibrium among these species ("carbonate equilibrium") is described by two equilibrium constants (pK_1 = 6.35 and pK_2 = 10.33 at 25 °C). The equilibrium concentrations strongly depend on pH. Under acid conditions (pH <6.35), H_2CO_3* is the predominant species, while CO_3^{2-} is virtually inexistent. At high pH (>10.33), CO_3^{2-} is prevailing. The partial pressure of dissolved CO_2 needs to be known in the model for the calculation of the total partial pressure. It is proportional to the H_2CO_3* concentration only. The relationship follows Henry's Law. When considering the overall dissolved inorganic carbon (DIC) content in the bog pore water and the flux of carbonate species (e.g. by advection), all carbonate species (i.e. H_2CO_3*, HCO_3^-, and CO_3^{2-}) need to be taken into account.

For the sake of simplicity, identical diffusion coefficients have been assumed for all carbon species. Effects of charge imbalance due to the diffusion of negatively charged species have been neglected.

6.4.2.9 pH gradient

Based on the averaged pH values measured at EGr during the period of fieldwork (cf. Fig. 5-10), a linear, depth-dependent pH gradient has been integrated in model.

6.4.2.10 Calculation time interval

For simulation, a calculation routine is repeated until a steady state, i.e. constant concentrations can be assumed. The so-obtained steady state solution correspond to an analytical steady state solution for CO_2 production, pore water advection and molecular diffusion (S. Burns, pers. comm.).

A finite simulation time step (Δt) needs to be determined for which the computer calculates the numeric values of the different parameters (e.g. concentrations of methane, DIC, N_2) for the nodes (i.e. the "boxes" representing grid points in the one-dimensional grid with a distance of Δx between each other) in the modelled depth range. The single time intervals ("steps") should be long enough to keep the overall calculation time short, but short enough to ensure stability in the model cycles and convergence. A general criterion with respect to advection is the Courant number ($C_{FL} = \nu*\Delta t*\Delta x^{-1}$, where ν stands for the rate of advection).

If $C_{FL} > 1$, cells might be skipped. In the spreadsheet model, the step size was set either as 0.05 days (1 h 12 min) or 0.005 days (7.2 min). For $\nu = 3.125*10^{-7}$ m*s^{-1} and $\Delta x = 0.1$ m, the values for C_{FL} are hence 0.0135 and 0.00135, respectively, i.e. <<1. A significantly higher value for Δt (e.g. 1 day) could not be chosen, as the model showed increasingly unstable behaviour for steps over 0.05 days. Unstable model behaviour is mainly introduced by abrupt species removal due to the modelled bubble formation. The theoretical depth of the advection front can be calculated by multiplication of ν with Δt and the number of steps, which is the number of calculation routines.
The calculation routine for the 0.05 and 0.005 day steps was repeated 100,000 or 1,000,000 times, respectively, corresponding to an overall simulation time of ca. 14 years. Steady state conditions could be expected after ca. 2 years of simulation time. After that, no other noticeable changes were observed for the modelled concentration and isotope patterns.

6.4.2.11 Methane carbon stable isotopes

In an extension of the model, the production and transport of methane has been simulated separately for ^{12}C-CH_4 and ^{13}C-CH_4. For the incoming methane from the acrotelm, a carbon stable isotope composition was assumed, which corresponds to average $\delta\ ^{13}C$ values determined for the DOC concentrations in ca. 50 cm depth (-27.0 ‰ vs. VPDB). This carbon stable isotope composition is assumed for the peat matrix and hence for the other potential substrate of microbial CH_4 and CO_2 production. It corresponds to the $\delta\ ^{13}C$ values determined for peat matrix samples (cf. chapter 11.AII-15). The modelled methane production was assumed to show isotope fractionation with a fractionation factor of 1.022 for ^{12}C-CH_4/^{13}C-CH_4 (Reeburgh et al., 1997). Correspondingly, also a slightly smaller molecular diffusion constant for ^{13}C-CH_4 ($1.08*10^{-9}$ m^2*s^{-1}) than for ^{12}C-CH_4 ($1.10 * 10^{-9}$ m^2*s^{-1}) was used (Reeburgh et al., 1997). Processes and dependent parameters for the other chemical species have not been changed. Fractionation into the gas phase has been neglected.

6.4.3 Results

6.4.3.1 Modelled methane, DIC, and N_2 concentrations

Modelled concentrations of methane and DIC are increasing with depth (Fig. 6-13). Although production rates are equal, the modelled DIC concentrations are considerably (ca. 3 to 10 times) higher than the modelled methane concentrations. The methane concentration increase is particularly pronounced in the upper part of the bog to a depth of ca. 2 m. In the lower catotelm (below ca. 2 m depth), modelled pore water methane concentrations are still increasing with depth, but at much slower rates than above, reflecting the much lower production rate in the deep catotelm. As for the DIC, a relative rapid concentration increase is noticeable to deeper levels in the upper catotelm (to a depth of ca. 3 m) before the curve starts to trend parallel to the methane concentration curve (Fig. 6-13). Nitrogen is very rapidly removed from the pore water. In 1 m depth already, modelled pore water N_2 concentrations are less than 10 % of the original concentration value at the upper boundary of the model.

To a depth of ca. 2.3 m, the modelled methane concentrations are generally higher than typical methane concentrations measured at the EGr. Between 2.3 and 5.5 m depth, modelled methane concentration values tend to be progressively lower than observed concentrations. Due to adaptation the production parameter *a*, the modelled DIC concentrations reflect well typical observed concentrations at EGr in the upper catotelm to a depth of ca. 1.8 m. Alike methane, in the central and lower catotelm, modelled DIC concentrations tend to be progressively lower than the observed concentrations. In contrast to methane, the difference

between modelled and observed concentrations is even increasing below 5.5 m depth, where the observed concentrations are almost 3 times higher than those modelled.

6.4.3.2 Diffusion vs. bubble formation

The model results show that the total gas loss of the system by bubble formation is much higher than the loss by diffusion. For CO_2 (DIC), ebullition represents a ca. 5000 times and for methane, ebullition represents an almost 100,000 times more effective process to remove gas species from the system. To a lesser degree, this is also the case, when overpressure is permitted in the model.

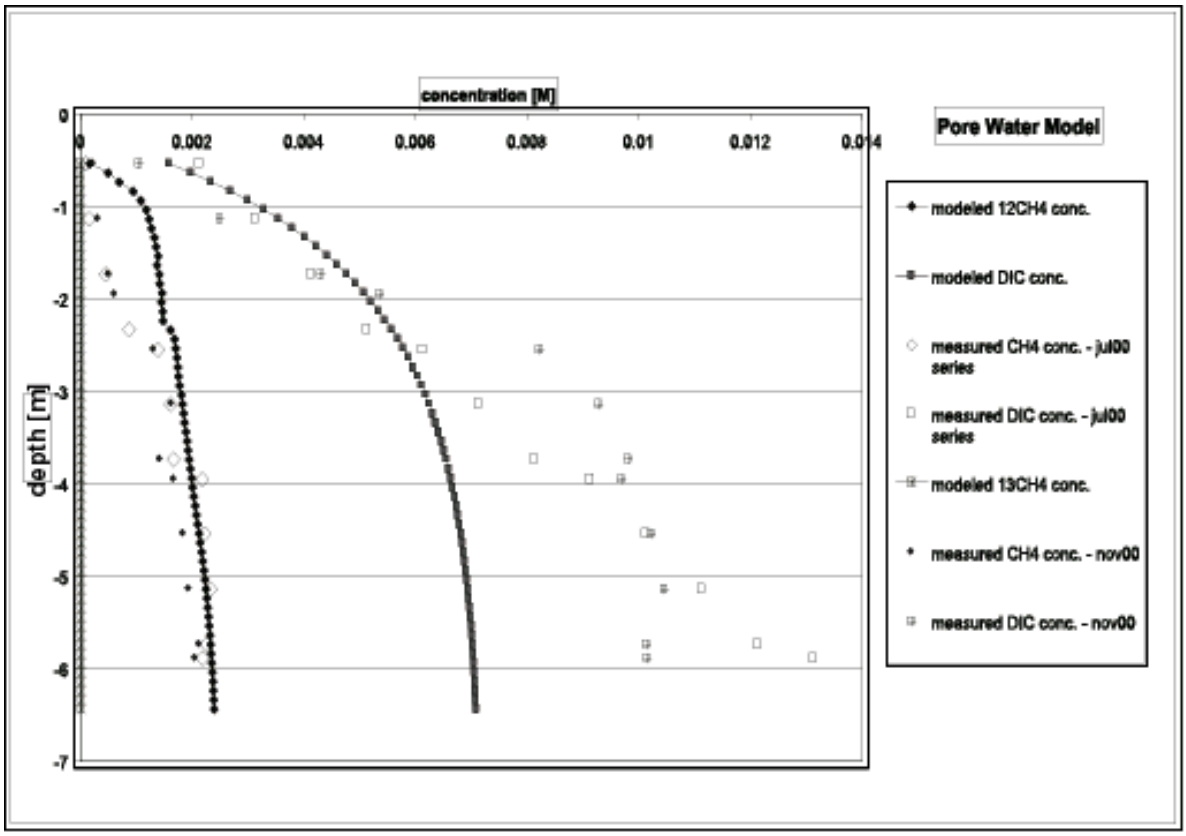

Fig. 6-13: Measured (July 2000 and November 2000 series) and modelled methane and DIC concentrations. Modelling is based on EGr data. The kink in the modelled methane concentration curve at ca. 2.2 m depth is an artefact.

6.4.3.3 Diffusion vs. advection

According to the model, molecular diffusion is even more negligible with respect to pore water advection than it is with respect to ebullition. Species transport by pore water advection is about 5 to 7 orders of magnitude more effective than diffusive species transport. The high value of the Peclet number (ca. 28 for CH_4 and ca. 25 for CO_2) confirms this finding. The Peclet number (Pe_{grid}) is defined as the product of $\nu*\Delta x*D^{-1}$, where n represents the advection rate, D diffusion, and Δx the distance between single grid points (nodes).

6.4.3.4 Bubble composition

The composition of the gas in the bubbles varies significantly in the upper catotelm (Fig. 6-14). According to the model results, N_2 is probably the most important constituent of the bubbles that form in the uppermost catotelm (to a depth of ca. 80 cm) and is followed by

methane and CO_2. The importance of N_2 for the bubble composition is decreasing with depth. In bubbles that form in the central catotelm to a depth of ca. 4.5 m, methane is by far the most important constituent with a share of up to 90 % of the volume. The rest volume is mainly composed of CO_2. N_2 is practically absent below ca. 2 m depth. As confirmed by the model results, the role of bubble formation and ebullitive transport decreases dramatically in the deep catotelm. Below ca. 4.5 m, species loss due to bubble formation is virtually zero. (cf. Fig. 6-15). This is due to higher hydrostatic pressures and decreased microbial gas production.

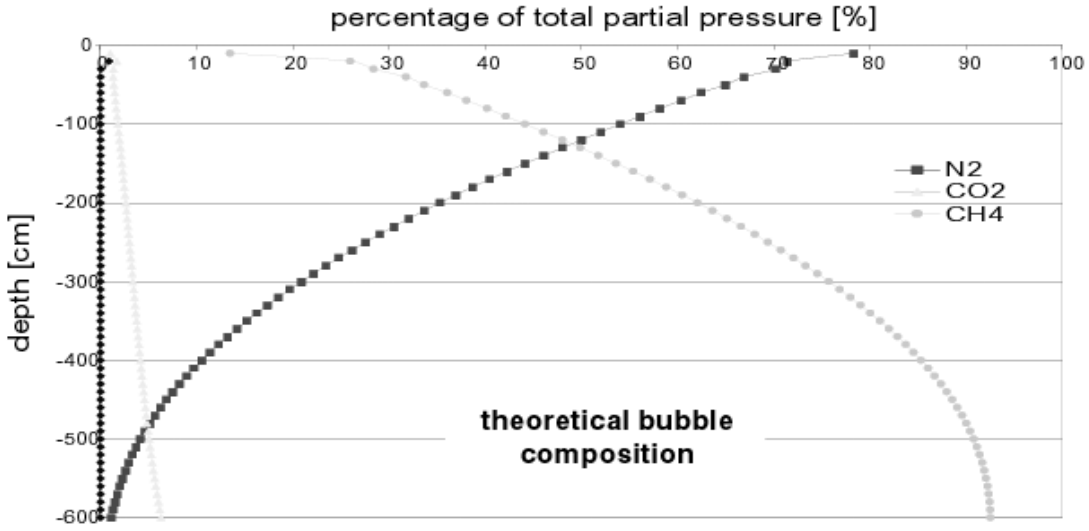

Fig. 6-14: Modelled composition of the gas bubbles at the moment of formation as expressed by the gases' respective share of the total partial pressure.

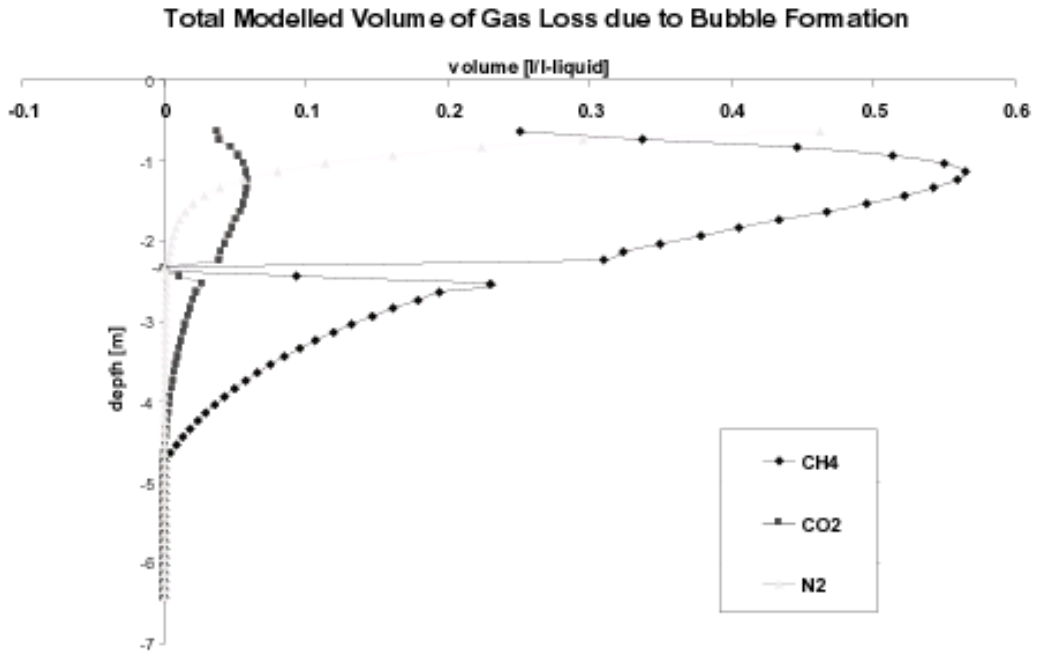

Fig. 6-15: Total modelled volume of gas loss per litre of pore water due to bubble formation and ebullitive species transport after ca. 15 months of simulation time. The anomalously low values at ca. 2.3 m depth are an artefact due to a model instability.

6.4.3.5 Carbon stable isotope characteristics for pore water methane

Simulation of separate ^{12}C-CH_4 and ^{13}C-CH_4 production and transport processes for the EGr bog pore water yields δ ^{13}C-CH_4 values of around -40 ‰ vs. VPDB. The carbon stable isotope composition of methane in the pore water of EGr shows however more negative δ ^{13}C-CH_4 values between -69 and -58 ‰ vs. VPDB (cf. chapter 6.2; Fig. 6-6). The modelled values show a slight decrease in the range of 4 ‰ from 0.5 to ca. 1.5 m depth, which coincides with the results obtained at EGr. Below that depth, the measured δ ^{13}C-CH_4 values are generally downwards increasing (by up to 10 ‰), while the modelled values remain virtually unchanged. The difference between the modelled and the measured δ ^{13}C-CH_4 values shows that the true carbon stable isotope composition value for the organic substrate (ca. -26 ‰ vs. VPDB; cf. chapter 11.AII-15) needs to be used in the model, what has not yet been done. The resulting δ ^{13}C-CH_4 value (-66 ‰) of simple addition of the negative δ ^{13}C-CH_4 values, -40 ‰+ (-26 ‰), would well be in the range of the measured values (-69 and -58 ‰ vs. VPDB).

6.4.4 Discussion

6.4.4.1 Methane and DIC concentrations

The modelled DIC concentrations are significantly higher than the methane concentrations despite the assumed equal rate formation of CH_4 and CO_2. This can be attributed to a) an almost 10-fold higher advective input of carbonate species (H_2CO_3*; HCO_3^-, CO_3^{2-}) from the acrotelm and b) reduced removal of CO_2 by bubble formation with respect to CH_4, as a consequence of the high solubility of CO_2 in water. The Henry constant for CO_2 is about 25 times higher than the Henry constant for CH_4 (cf. chapter 11.AIV). In addition, as CO_2 is dissolved as HCO_3^- and CO_3^{2-}, the pH increase with depth further reinforces the solubility of CO_2.

For the upper catotelm (above ca. 2.5 m depth), the model predicts significantly higher methane concentrations than those measured at EGr. In particular, the strong concentration increase between 2 and 2.5 m depth is not reflected in the model (cf. Fig. 6-13). A changing peat structure with decreasing permeability, and hence decreased degassing from the pores, is probably responsible for the observed pronounced concentration increase. It is however not possible to provide supporting information for this interpretation directly from the degree of peat decomposition in the zone of concern: The degree of peat decomposition is described as ‘H8’ according to the Von Post scale (Von Post, 1925) and is virtually invariable from 1.25 m to 3.7 m (Steinmann, 1995). According to Steinmann (1995) and P. Steinmann (pers. comm.) however, the peat above 2.5 m depth is less decomposed resulting in more vertical plant fibres (e.g. of *Eriophorum*) present. This could facilitate vertical gas transport with respect to the much more *Sphagnum*-dominated peat matrix below. The lower methane concentrations in the upper catotelm are probably for this reason not reflected in the model.

For DIC, the model results qualitatively and quantitatively reflect typical measured concentrations in the upper catotelm (above ca. 2 m depth). Below ca. 2 m depth, the modelled DIC concentrations are considerably (up to 60 %) lower than the observed concentrations, but still follow the same trend (cf. Fig. 6-13). Although, it is possible to adapt the model to the measured lower catotelm concentrations by decreasing the gas production constant *a* (cf. chapter 6.4.4.2 below), this has not been done in the main model, as otherwise the methane and the DIC concentrations in the upper catotelm could not be well reflected anymore. The discrepancy between the model results and the DIC concentrations in the lower catotelm is probably due to discrepancies on the boundary conditions considered for diffusion

from the substratum. A flux of bicarbonate and carbonate ions from the substratum should also be expected. These ions may derive from the marly substratum of the EGr Bog due to flow reversal and mixing of pore and ground waters there and by dissolution of inorganic carbon from earlier formed (fen) peat layers with a higher ash content. This flux may lead to high DIC concentrations in the lower catotelm, which are not due to microbial CO_2 production and advective transport. They are therefore not represented in the model results. The flux of carbonate and bicarbonate ions from the ground is also indicated by a strong Ca^{2+} and Mg^{2+} concentration increase observed near the bottom of the bog.

The above results are described for a value for *a* equal to 0.7. Qualitatively, the results do not significantly change for different values of *a*, quantitatively and in particular for the DIC concentration, such a change is observed: A smaller value for *a* ($0 \leq a \leq 0.7$) evokes an increase in the CH_4 and CO_2 production in the bog as the production rate is more gently declining with depth. While most of the additional CH_4 produced leaves the bog system via bubble formation resulting in only a slight increase in the pore water CH_4 concentration, the modelled DIC concentration is considerably increasing and exceeds for a value of $a = 0.25$ the typical measured concentrations at all depths. A higher value for *a* (>0.7) evokes a decreased CH_4 and CO_2 production in the bog as the production rate is more rapidly declining with depth. Again, the impact on the modelled CH_4 concentration is small, whereas for a value of $a = 1.5$, the modelled DIC concentration is clearly below typical measured concentrations for depths below 1 m already.

6.4.4.2 Influence of species loss due to bubble formation and ebullition

The modelled bubble formation and gas loss lead to weaker depth-dependent concentration gradients for CH_4 and CO_2 below ca. 2.5 m depth. The almost vertical graphs representing concentration in Fig. 6-13 illustrate this model result. When over-saturation is permitted, the concentration gradients in this region are stronger and do better reflect the measured concentrations (cf. chapter 6.4.4.3). Ebullition is hence a very effective transport process for chemical species in peatlands. The underlying physical processes of bubble formation (cf. chapter 2.5.3) and bubble transport (e.g. surface tension, maximum possible size of bubbles, edging out of water volume, re-equilibration of the bubble composition) are ignored in the model. Ebullitive transport is therefore more likely over- than underestimated. Re-equilibration of the bubble composition probably results in a higher share of N_2 in the bubbles due to high N_2 pore water concentration in the upper part of the bog, and, hence, in even more effective removal of this species in the upper bog. At the same time, re-equilibration of the bubble composition, leads to a lower share of CH_4 and CO_2 and hence - in tune with the measurements - to higher pore water concentration of these species than those modelled for the upper catotelm. Significant re-dissolution in the catotelm, however, is probably not realistic, as no substantial low-pressure was observed. By contrast, re-dissolution of gas trapped in the bubbles is likely near the surface due to temporary (e.g. atmospheric) pressure changes. In summary, it can be said that ebullition clearly outweighs diffusion in the catotelm, although diffusive species transport may still be significant in the upper part of peatlands. This view is also supported by laboratory experiments. According to Fechner and Hemond (1992), ebullition dominates in the saturated zone of a *Sphagnum* bog, but diffusion and oxidation in the unsaturated zone control the CH_4 escape to the atmosphere.

6.4.4.3 Influence of pore water over-saturation

When over-saturation is taken into account, the model is well capable of approaching the measured methane concentrations in the central and deep catotelm. Applying the same peat constant *a*, it is however not possible to quantitatively reflect both, the measured CH_4 and the

measured DIC concentrations at the same time. In the lower catotelm, the latter are about 2 times higher than those predicted by the model. An explanation for the measured high DIC concentrations is given in chapter 6.4.4.1.

6.4.4.4 Influence of pH

The DIC concentration change caused when, for instance, using a depth-invariant pH of 5 instead of a pH that increases from 5 (at 0.5 m depth) to 6.7 (at 6.5 m depth), is less than 3 %. The influence, that the typical pH range of catotelm peat bog pore waters (ca. 4 - 7; cf. chapter 2.4) can have on DIC concentrations and CO_2 degassing, hence seems to be minor.

6.4.4.5 Calculated methane emissions

Calculation of the methane emissions from the bog using the data the model suggests, yields about 1500 to 1800 ml CH_4 m^{-2} d^{-1}. The methane emissions are mainly a consequence of gas transport by bubble formation (cf. Fig. 6-15). These numbers given above are however only of theoretical nature. The real methane emissions to the atmosphere are probably much lower, as most of the methane is oxidised in the acrotelm before reaching the bog's surface (cf. chapter 2.7). Furthermore, the model data for example do not take the chemical equilibration of the gas bubbles on their way up into account. The composition of the bubbles in the upper catotelm and in the acrotelm probably shows a shift towards higher N_2 concentrations, as the partial pressure of N_2 is much higher near the top of the bog (cf. chapter 6.4.4.4). This will also result in less methane emission than suggested by the model data.

6.4.4.6 Agreement of the model results

The model results correspond to the results obtained using a different computational platform, AQUASIM. AQUASIM has been developed by P. Reichert at the Swiss Federal Institute for Environmental Science and Technology (EAWAG). It provides another numerical solution for the problem.

AQUASIM is a computer program for the identification and simulation of aquatic systems. In this study, it was used for modelling the concentrations of chemical species in bog pore water. AQUASIM allows the user to define the spatial configuration of the system to be investigated as a set of compartments, which can be connected to each other by links. 6 different predefined model compartments for various aqueous systems such as lakes, rivers, soils, and sewage systems are currently available. These compartments include, mixed reactors, biofilm reactors, advective-diffusive reactors, river sections, lake sections and saturated soil columns. For this study, the saturated soil column compartment was used for modelling, as it corresponds best to the chemical and physical processes, which need to be considered in wetland soils. For instance, bubble formation, a major transport process could be simulated using the built-in logarithms for species sorption. Advection and diffusion could nevertheless be integrated in the saturated soil compartment. In the AQUASIM model, a step size of 0.1 days (2 h 24 min) was chosen and the calculation was repeated 10,000 times corresponding to an overall simulation time of ca. 3 years. A steady state in the processes could be inferred after less than 100 days of simulation time. Given the fact that concentrations of the respective chemical species are generally increasing with depth, diffusion in AQUASIM was regarded to cause only upward transport of chemical species. This simplification was necessary since the number of independent parameters was already relatively high (75). A higher number and the multitude of interdependent calculations would have rendered model simulation impracticable. Two-way, i.e. upward and downward directed transport by molecular diffusion was however permitted in the spreadsheet model, which showed only marginally differing results. A separate, yet simplified AQUASIM model with upward and

downward directed diffusive species transport confirmed the results of the spreadsheet model. This again indicates that species transport by downward diffusion is minor.

6.4.5 Conclusions

Numeric modelling of CH_4 and DIC pore water concentrations generally yields good agreement with typical measured concentrations at EGr. The modelling is based on assumptions for microbial production of methane and CO_2, pore water advection, molecular diffusion, and gas loss due to bubble formation.
The divergences between modelled and measured concentrations can largely be explained by the inhomogeneous peat structure and the presumed mixture of pore water with ground water near the base of the bog due to flow reversal. Changes in the peat stratigraphy and the peat's higher content of *Eriophorum* stems above ca. 2.5 m depth seem to facilitate the degassing of the pore water in this part of the bog. More decomposed and probably less permeable peat layers in the lower part, by contrast, cause considerable over-saturation and, hence, contribute to the high concentrations measured.

The model results further indicate that advection and ebullition are by far the most efficient processes for species transport in peat bog waters and that the role of molecular diffusion is minor. This is even the case, when low rates of advection (<1 cm per day) and a high (150 % or more) over-saturation of the pore waters with methane and DIC are assumed in the model.

The total volume of gas bubble formation decreases with depth due to higher hydrostatic pressure, more pronounced over-saturation, as well as downward decreasing methane and CO_2 production rates. While, according to the model, in the upper catotelm to a depth of ca. 0.8 m, the bubbles are mainly composed of nitrogen and other potential peatland gases such nitrous oxide, carbon monoxide, or hydrogen, methane clearly represents the dominant constituent for the central and lower catotelm with a share of up to 90 % by volume. The share of CO_2 in the newly formed bubbles is increasing with depth, but barely reaches 10 % in the deepest layers modelled.

The pH gradient has only a minor influence on the DIC concentrations in the lower catotelm and, hence, on share of CO_2 in the bubbles.

The range of the carbon stable isotope composition values of methane predicted in the model (ca. -40 ‰ vs. VPDB) may correspond to the range of measured values (-70 to -60 ‰ vs. VPDB), if the true value for the $\delta\ ^{13}C$ in the organic matter (ca. -26 ‰) is considered and not a composition of +/- 0 ‰. The observed relative variations for $\delta\ ^{13}C\text{-}CH_4$ values for different depths and general trends such as the observed decreasing $\delta\ ^{13}C\text{-}CH_4$ values in the upper catotelm and substantially increasing $\delta\ ^{13}C\text{-}CH_4$ values in the lower catotelm, nevertheless are only poorly reflected in the model. This is the result of the false (see above) or too rigorous model assumptions that do not account for differences in the carbon stable isotope compositions of the methane produced due to the prevailing methanogenic pathways and kinetic isotope effects such as isotope fractionation during the production of methanogenic precursors and while bubble formation and gas emission.

Comparison of the explicit, forward formulation using spreadsheet calculation with an analytical solution obtained by an independent computational platform (AQUASIM) shows no noticeable disparities.

7 GENERAL CONCLUSIONS

The pore water in the catotelm of the Etang de la Gruère Bog (EGr) shows distinct seasonal and depth-dependent variations with respect to most of the species concentrations and the carbon stable isotope patterns of methane and DIC. These variations represent the combined effect of changes in the microbial gas-producing activity as well as physico-chemical transport processes, such as pore water advection, ebullition and diffusion. Similar variations have also been reported for the upper catotelm parts of other peatlands. With respect to the deeper catotelm (below ca. 2 m depth), the here provided results help to fill a gap, as published data are scarce, especially for methane and volatile fatty acids.

As could be shown for the entire period of study, the pore water methane and DIC concentrations at EGr increase significantly from the upper to the lower catotelm, i.e. from 0.5 to ca. 6 m depth. For methane, this increase was more than 20-fold with maximum concentrations of 2 - 2.5 mM at ca. 5 m depth. For DIC, the increase was about 10-fold with maximum concentrations of 10 to 12 mM between ca. 5 and 6 m depth.

Carbon stable isotope composition data of methane and DIC indicate that both, the CO_2 reducing and the acetate splitting pathway contribute to methanogenesis in the catotelm of EGr. The here presented results confirm earlier studies according to which acetate splitting is important in the upper layers (acrotelm and upper catotelm), and that methanogenesis via the CO_2 reduction pathway becomes more noticeable or even dominant at greater depths. CO_2 reduction can be described as the "background methanogenic process", while the efficiency of the acetate splitting depends primarily on the availability of acetate as a methanogenic precursor and temperature.

A numerical model has been developed to simulate gas production and transport processes in peat bog waters. It takes microbial CH_4 and CO_2 production, pore water advection, molecular diffusion, and bubble formation into account. Using uniform downward advection with a plausible Darcy velocity, and exponentially decreasing methanogenic activity, the observed concentrations and isotope patterns can be reasonably well reproduced. The model also yields methane carbon stable isotope patterns, which are comparable to those observed at EGr. Differences between modelled and measured concentrations can largely be explained by the effects of an inhomogeneous peat profile and ground water mixing near the base of the bog, which are not taken into account in the model. Primarily, the inhomogeneities of the peat profile concern the (vertical) hydraulic conductivity, the distribution of the different microbial communities, and the availability of labile organic matter as a substrate for microbial metabolism.

The model further indicates that pore water advection and ebullition are the dominant transport processes for dissolved methane and carbonate species in the bog pore water, and that the role of molecular diffusion is minor. According to the model, the bubble composition changes significantly in the first two metres below ground surface, but for most of the catotelm, methane is the primary constituent of the bubbles. Only in the deep catotelm, CO_2 takes a slightly larger share in the bubble composition, while the total bubble volume decreases to virtually zero.

8 SUMMARY

8.1 English version

This thesis investigates the formation of methane and CO_2 in deep peatlands, the role of different gas transport processes (advection, diffusion, ebullition) and their implications for seasonal geochemical and hydrological variations.
The study is based on field research at the Etang de la Gruère Bog (EGr) located in the Swiss Jura Mountains, a typical northern hemisphere peatland, where peat has accumulated continuously over the last ca. 14,500 years. Pore water chemical parameters, such as major ion, organic acid, methane, and dissolved organic carbon concentrations were measured on a monthly basis using diffusion chambers for in situ filtration ("peepers"), which were installed up to a depth of 6 m below ground surface. The carbon stable isotope composition for the dissolved methane, for the organic and the inorganic carbon in the pore water, for the peat matrix as well as for the methane and CO_2 emissions at the bog's surface was determined by isotope ratio mass spectrometry. Major physical parameters investigated included pore water temperature, depth of the water table, and groundwater flow direction. Field research at EGr included 22 campaigns during the period from June 1999 to October 2001.
The methane concentrations measured in the EGr pore water ranged from below 0.1 mM, in the upper catotelm, to almost 2.5 mM at 5 m depth. These levels show seasonal variations of ca. 20 to 30 %. The lower concentrations, particularly in the deep catotelm (>3 m depth) in winter, can be explained by declining turnover in that season. This is probably a consequence of a depleted acetate pool and hence reduced acetoclastic methanogenesis. Carbon stable isotope composition data support this interpretation. The $\delta\ ^{13}C\text{-}CH_4$ values mark a gas mixture produced by two pathways, acetate splitting and CO_2 reduction. In the lower catotelm, $\delta\ ^{13}C\text{-}CH_4$ ranged from ca. -69 to -63 ‰ and showed a distinct trend towards more negative values in early 2000, indicating the influence of the acetate splitting pathway is less in winter. Acetoclastic methanogenesis is the predominant methanogenic pathway in the upper catotelm (<1.5 m depth) in all seasons, yet particularly in winter and spring. CO_2 reduction is important in the lower catotelm. In more general terms, CO_2 reduction seems to represent the "background" methanogenic process, whereas acetate splitting occurs predominantly a function of the availability of acetate as a precursor and temperature. However, a direct dependence upon temperature thresholds for the onset of methanogenic mechanisms, as postulated by some authors, has not been observed at EGr.
Pore water advection, molecular diffusion and gas transport by ebullition may considerably affect concentration and isotope patterns. A numerical model developed to simulate gas production and transport processes for the EGr peat bog provides good fit for the measured concentrations. Moreover, hydrological data indicate that pore water advection is sluggish with rates of less than 2 cm per day. The model results are coherent with laboratory experiments and clearly show the predominance of two-phase transport by ebullition over molecular diffusion. In the catotelm below ca. 1 m depth, i.e. in the bulk of the bog, ebullition is a particularly efficient means of transport for methane, which, according to the model, constitutes 70 to 90 % of the bubble volume.

8.2 *Résumé en français (French version)*

Le but de cette thèse est d'examiner la production de méthane et de CO_2 dans les sols marécageux profonds, autant que d'évaluer le rôle des différents processus de transport de gaz (advection, diffusion, ébullition). Les implications de ceux-ci pour les variations saisonnières et hydrologiques seront discutées.

Cette recherche est basée sur des études de terrain dans une tourbière typique de l'hémisphère nord, le haut marais de l'Etang de la Gruère (EGr) dans le Jura Suisse. La tourbe s'y est accumulée sans interruption pendant les dernières 14500 années environ. Des paramètres chimiques de l'eau interstitielle, comme les concentrations en ions principaux, acide organique, méthane et carbone organique dissous ont été mesurés mensuellement en utilisant des alvéoles de diffusion pour filtration in situ (« peepers »), qui ont été installés jusqu'à une profondeur de presque 6 m. La composition des isotopes stables du carbone a été déterminée pour le méthane dissous, pour le carbone organique et inorganique, pour la tourbe ainsi que pour le méthane et le CO_2 des émissions superficielles de la tourbière. La température, la hauteur et la direction d'écoulement de l'eau interstitielle constituent les principaux paramètres physiques examinés. Le travail de terrain à EGr inclut 22 campagnes durant la période de juin 1999 à octobre 2001.

Les concentrations en méthane mesurées dans l'eau interstitielle d'EGr étaient élevées. Elles s'échelonnaient de moins de 0.1 mM dans le catotelm supérieur à presque 2.5 mM à une profondeur de 5 m. D'importantes variations saisonnières, par exemple une diminution hivernale de la concentration de 20 à 30 %, surtout dans le catotelm profond (>3 m de profondeur), peuvent être expliquées par des taux de transformation en baisse : Une transformation biochimique réduite en hiver est probablement la conséquence d'un réservoir d'acétate qui s'épuise et provoque ainsi une réduction de la quantité de méthane produit par dissociation d'acétate. La composition des isotopes stables du carbone appuie cette interprétation. Les valeurs $\delta\ ^{13}C\text{-}CH_4$ sont caractéristiques pour une mélange de méthane produit par deux mécanismes microbiens différents, la dissociation d'acétate et la réduction de CO_2. Dans le catotelm inférieur, le $\delta\ ^{13}C\text{-}CH_4$ s'étage d'environ -69 à -63 ‰. Au début de l'année 2001, il a montré une tendance vers des valeurs encore plus négatives, ce qui indique une influence affaiblie de la dissociation d'acétate durant cette période-là. Dans le catotelm au-dessus de 1,5 m de profondeur, la dissociation d'acétate prédomine, pendant toute l'année, mais surtout en hiver et en printemps. La réduction de CO_2 est plus importante dans le catotelm inférieur. Plus généralement, la réduction de CO_2 semble représenter un processus méthanogène toujours actif à l'arrière-plan, tandis que la dissociation d'acétate se produit principalement en fonction de la disponibilité de l'acétate comme précurseur et de la température. Une dépendance directe des seuils de température pour le commencement des mécanismes méthanogènes, comme cela a été postulé par un certain nombre d'auteurs, n'a pas été observée à EGr.

L'advection de l'eau interstitielle, la diffusion moléculaire et le transport de gaz par ébullition peuvent affecter sensiblement les concentrations et les compositions isotopiques du carbone. On présente un modèle numérique, qui simule la production et les mécanismes de transport de gaz au sein de la tourbière EGr. Les concentrations obtenues par la simulation correspondent à celles de l'analyse. En outre, les données hydrologiques indiquent que l'advection de l'eau interstitielle constitue un processus lent avec des taux de mouvement inférieurs à 2 cm par jour. En concordance avec des résultats d'expériences de laboratoire, le modèle montre clairement que le transport en deux phases par ébullition est plus important que la diffusion moléculaire. L'ébullition est particulièrement efficace pour le transport de méthane dans le catotelm au-dessous d'un mètre de profondeur, c'est-à-dire dans la partie la plus volumineuse de la tourbière. Selon le modèle, le méthane y occupe entre 70 et 90 % du volume des bulles.

8.3 Zusammenfassung auf Deutsch (German version)

In dieser Arbeit soll die Bildung von Methan und CO_2 in tiefen Mooren untersucht, sowie die Rolle verschiedener Gastransportprozesse (Advektion, Diffusion, Blasenbildung) und deren Verflechtung mit den beobachteten jahreszeitlichen und hydrologischen Veränderungen erörtert werden.

Die Studie fusst auf Feldforschung in einem typischen Moorgebiet nördlicher Breiten, dem Etang de la Gruère Hochmoor (EGr) im Schweizer Jura, wo es während der letzten ca. 14500 Jahren zu kontinuierlicher Torfakkumulation kam. Im Monatsabstand wurden chemische Porenwasserparameter wie etwa die Konzentration wichtiger Ionen, organischer Säuren, Methan und gelösten organischen Kohlenstoffs mittels Diffusionskammern zur Insitufiltration („Peeper“) gemessen. Die Kammern wurden bis in eine Tiefe von fast 6 m installiert. Die Zusammensetzung der stabilen Kohlenstoffisotope wurde für gelöstes Methan, organischen und anorganischen Kohlenstoff, Torf, sowie auch für Methan und CO_2 aus Entgasungen an der Mooroberfläche bestimmt. Zu den wesentlichen physikalischen Parametern, die untersucht wurden, gehören Temperatur, Oberflächenabstand und hydrologisches Fliessverhalten des Porenwassers. Die Arbeit im Gelände umfasste 22 Messkampagnen zwischen Juni 1999 und Oktober 2001.

Das EGr Porenwasser wies eine hohe Methankonzentration auf. Sie bewegte sich von weniger als 0.1 mM im oberen Katotelm bis fast 2.5 mM in 5 m Tiefe. Erhebliche jahreszeitliche Unterschiede z.B. mit ca. 20 bis 30 % niedrigeren Konzentrationen vor allem im Winter und im Katotelm unterhalb 3 m Tiefe lassen sich durch zurückgehenden Stoffumsatz erklären: Geringerer Stoffumsatz im Winter ist wahrscheinlich Folge zurückgehender Acetatkonzentrationen und dementsprechend verminderter Methanbildung durch Acetatspaltung. Für diese Deutung spricht auch die Zusammensetzung stabiler Kohlenstoffisotope. Die $\delta\ ^{13}C\text{-}CH_4$ Werte kennzeichnen eine Mischung von Methangas, das auf zweierlei Weise, nämlich durch Acetatspaltung und CO_2-Reduktion, gebildet wurde. Im unteren Katotelm lagen die $\delta\ ^{13}C\text{-}CH_4$ Werte zwischen ca. -69 und -63 ‰ und zeigten Anfang 2000 einen ausgeprägten Trend zu noch negativeren Werten, was auf einen geringeren Einfluss der Acetatspaltung hinweist. Im Katotelm oberhalb von 1,5 m Tiefe überwiegt die Acetatspaltung zu allen Jahreszeiten, insbesondere aber im Winter und im Frühling. Die CO_2-reduzierende Methanbildung ist im unteren Katotelm bedeutender. Verallgemeinert lässt sich CO_2-Reduktion als ein im Hintergrund wirkender methanbildender Prozess beschreiben, wohingegen Acetatspaltung hauptsächlich bei höheren Temperaturen auftritt, und wenn genügend Acetat als Ausgangsstoff zur Verfügung steht. Eine direkte Temperaturabhängigkeit des Einsetzens methanbildender Prozesse, wie sie von manchen Autoren postuliert wurde, ist in der EGr Studie nicht beobachtet worden.

Porenwasseradvektion, molekulare Diffusion und Gastransport infolge Blasenbildung können die Konzentrations- und Isotopenverteilung stark beeinflussen. In einem numerischen Model wurden Gasbildung und Transportprozesse für das EGr Hochmoor simuliert. Modellierte und gemessene Konzentrationen stimmen gut miteinander überein. Des weiteren deuten die hydrologischen Daten darauf hin, dass das Porenwasser träge mit weniger als 2 cm pro Tag nach unten fliesst. Die Ergebnisse der Modellierung zeigen deutlich und im Einklang mit Laborexperimenten das Überwiegen von zweiphasigen Blasentransport gegenüber molekularer Diffusion. Einen besonders effizienten Transport von Methan bewirkt Blasenbildung im Katotelm unterhalb 1 m Tiefe, dem volumenmässig grössten Teil des Moores. Gemäss dem Modell macht Methan dort 70 bis 90 % des Blasenvolumens aus.

9 ACKNOWLEDGEMENTS

Dr. STEPHEN J. BURNS, Prof. KARL B. FÖLLMI, Prof. JEAN-MICHEL GOBAT, Dr. MARKUS LEUENBERGER, and Dr. PHILIPP STEINMANN are the members of the jury. I wish to thank them for having accepted adjudicating and for reading my thesis.

Dr. **PHILIPP STEINMANN** played the essential role in my PhD, as he initiated the project and tutored my thesis. I am very much indebted to him, and it is a pleasure to thank him for the three years, when I could work under his supervision. His ideas, foresight and thorough consideration made this work possible. His well-founded advice was very valuable in all phases of my thesis. His guidance was deliberate and focussed. On a personal basis, I would like to express my appreciation of Dr. Steinmann's kind, thoughtful attitude and his fine sense of humour.

I thank Prof. KARL B. FÖLLMI for reception into the Geochemical and Environmental Analyses Group and for granting me a 12.5 % position as a teaching and laboratory assistant. Although my subject was not part of his research, he has shown interest in the course of my studies. I am appreciative of his open-mindedness towards the suggestions and ideas I have had. In November 2000, Prof. Föllmi sent me as a technical research assistant "out of area" to Venezuela, which has been one of the most interesting missions I have had in my life.

I thank all the members of the Geological Institute who have supported me during my thesis work. In particular…

- Prof. JEAN-PAUL SCHAER for the words he wrote down for me, when I started my thesis.
- my former office colleague, Dr. MARCUS GURK for helping me to make my first steps in Neuchâtel easier and his expertise, whenever there was a computer problem.
- my present office colleague, MAHMOUD MEKKAWI for his helpfulness and the friendly, accommodating atmosphere in our office, which was necessary for efficient work and timely completion of this dissertation.
- the "Groupe de Géomagnetism" for its continued and unconditional support. Dr. PIERRE SCHNEGG gave me free access to the group's local computing infrastructure and to its well-serviced car, when - as it happened several times on the morning of fieldwork - the reserved car had mysteriously disappeared. ROBERTO COSTA engineered the specialised temperature probe for in-depth measurements described in chapter 4.2.1.1. Beyond that, he would provide well-founded technical advice on data-loggers, rechargeable batteries, and other technical instrumentation.
- ANDRÉ VILLARD who has ingeniously manufactured the tubes for gas sampling and flux measurements.
- KHAOULA HAMILA, TONG ETTLIN, SÉBASTIEN RYSER, and JOSÉ RICHARD for their help in the laboratory and with sample preparation and analysis.
- Claire M. C. Rambeau for correction of the French version of the summary
- Raymond M. Flynn for correction on the English version of the summary
- Prof. ERIC VERRECCHIA for his help with statistics.
- our secretaries, especially SABINE ERB, truly omniscient: she would always bring quick and efficient relief to any kind of problem. I will not forget her lovely smile and the humble words "…mais de rien."
- MANUEL DA SILVA for much more than keeping every clean and tidy.

-, and, albeit this is not directly related to my work in Neuchâtel, I would like to mention that I feel deeply obliged to my fellow PhD student ALEXEI ULJANOV, who very patiently and without demanding anything in return, taught me Russian during the last year of my thesis.

I thank FRANK P. BOSCH from the Hydrogeology Centre for his committed and very vivid assistance concerning hard- and software.

I thank the Microbiology Laboratory of the Institute of Botany at Neuchâtel University for cooperation in my PhD project and in particular Dr. PIERRE ROSSI and SIMONA CASATI for the detailed microbiological examination of a more than 5 m long peat core, which had been taken on July 17th, 2000. The preceding and subsequent discussions of major biological aspects of my work fostered further insight and cleared some over-simplistic views.

I thank the Isotope Laboratory of the Geological Institute at Bern University for cooperation and in particular Dr. CONSTANZE E. WEYHENMEYER and Dr. STEPHEN J. BURNS. Dr. Burns, who has been a co-applicant of the project, introduced me to his earlier geochemical peat pore water modelling. Before leaving Bern, he (and his PhD student, GUILLEMETTE MÉNOT) measured the carbon stable isotope composition of dissolved inorganic carbon as well as humic and fulvic acids for several sample series and provided very knowledgeable help for data interpretation. I thank especially Dr. Weyhenmeyer, who readily continued Dr. Burns' work in Bern and measured numerous pore water samples for the carbon stable isotope compositions of their dissolved inorganic carbon. It was noticed that Dr. Weyhenmeyer would spend several nights on the measurements and on the perfection of the method. Her comments and contributions to the interpretation were highly appreciated.

I thank the Climate and Environmental Physics Division of the Physics Institute at Bern University for cooperation and in particular DR. MARKUS LEUENBERGER for determining the methane and CO_2 carbon stable isotope compositions of numerous pore water and gas samples. Dr. Leuenberger elaborated a special method to cope with the relatively high methane concentrations of bog pore waters while keeping the analytical precision at world-class standards. His participation in the discussions and contributions were essential to this project.

I thank Dr. JUKKA ALM from the Department of Biology at Joensuu University, Finland, for pore water methane concentration analysis of several sample series in 1999 and early 2000, when the gas chromatograph at Neuchâtel University had not been ready. The investigation on methane could have seriously been jeopardised without Dr. Alm's timely warning about a potential contamination of the vacutainers used in July 1999.

I thank the RAAS Institute of Peat in Tomsk, Russia, for its cooperation and in particular Prof. LIDIA I. INISHEVA for her kind invitation to Siberia. Prof. Inisheva and especially Dr. TATJANA V. DEMENTJEVA among many other members of the Institute provided great help for organising my stay in Tomsk and our joint fieldwork in the Vasjugan Bog in June and July 2001. Without the efficient advice on protection and their deterrents against mosquitoes and horseflies, I certainly would not have survived one single day in the Vasjugan Bog.

I thank the "Service cantonal pour la protection de l'environnement" in Neuchâtel, and in particular Dr. JIRI ONDRUZ, for cooperation. BERNADETTE CALAME, CATHÉRINE CSESALVAY, MARIE FARINE, and SYLVIANE PIERREHUMBERT have been charming and in such an

uncomplicated way helpful that, for a long time, I did not even know their family names. They are thanked for always reliably running the dissolved organic carbon measurements. MICHEL DEVAUD is thanked for having me repeatedly brought back safe and sound to Neuchâtel Nid-du-Crô Harbour after our adventurous trips on the "Do-Re-Mi", a research vessel, which was at least as charming as wrecked.

I thank Dr. SYLVAIN HUON from the "Laboratoire de Biogéochimie Isotopique" at the UPMC in Paris, France, for analysing several peat and dissolved organic carbon samples for their carbon stable isotope signature free of charge.

I thank Prof. NIKOLAI M. BAZHIN from the Institute of Chemical Catalysis in Novosibirsk-Akademgorodok for many fruitful discussions on methane emission from peatlands. I am also grateful to him for the effort and time he provided to make my stays in Akademgorodok as comfortable as possible.

I thank the "Service informatique et télématique" at Neuchâtel University for providing and maintaining excellent computational and network services.

I thank the "Service de l'eau et du gaz" of the Canton Neuchâtel and in particular FRANCIS GUENOT for the kind help and understanding, when a poster had again to be very quickly printed out after a sudden deadline arose.

I thank Dr. BERNARD JACQUAT from the "Office des eaux et de la protection de la nature" of the Canton of Jura for giving access to the protected Etang de la Gruère site.

The Geological Institute at Bern University is acknowledged for ceding me for my research diffusion chambers for in situ pore water sampling ("peepers"). The use of peepers was fundamental to my research. I would like to thank ANTON STEINMANN from Schötz and technicians from the University of Bern who had then designed and manufactured the peeper sets.

The Institute of Geology and the Hydrogeology Centre at Neuchâtel University are acknowledged for having entrusted me various motor vehicles for fieldwork.

The Institute of Botany at Neuchâtel University is acknowledged for providing me with field equipment from the BERI project, including an infrared gas analyser for CO_2 detection, an automatic data logger and the plexiglass chambers for gas flux measurements. I thank Dr. EDWARD A. D. MITCHELL, Dr. GAËLLE J. VADI, and Prof. ALEXANDRE BUTTLER for their explanations how to best use the instruments. I thank Prof. JEAN-MICHEL GOBAT for his support of the project as a co-applicant. The temperature probe, which had been in use until mid 2000, for instance, was manufactured in the Institute's workshop under the skilful supervision of Mr. LAURENT NEMITZ, whose advice was highly appreciated.

I thank all those who assisted me in the field: KASPAR S. ARN, Dr. EKATARINA V. BELOVA, SIMONA CASATI, Dr. TATJANA V. DEMENTJEVA, Dr. URS EICHENBERGER, WALTRAUD EILRICH, RAYMOND M. FLYNN, Dr. YEVGENIJA A. GOLOVATSKAJA, Dr. YURI GOLOVATSKY, AXEL GROßMANN, KRISTIN GROßMANN, Dr. MARCUS GURK, URS HELG, RACHEL HOSEIN-NISBET, Dr. MING-TAK HUE, ATTILA KOVACS, FRANÇOISE MAEDER, CAROLIN F. RICHTER-BANAŠEK, FIONA ROOS, Dr. PIERRE ROSSI, IRINA A. RUIBAKOVA, JULIA V. SANNIKOVA,

JULIEN SCHOCH, Prof. WILLIAM SHOTYK, Dr. PHILIPP STEINMANN, ALEXEI ULJANOV, and Dr. CONSTANZE E.WEYHENMEYER.

Many people have probably been omitted in this list. I thank them for not taking it personally.

I thank the Swiss National Science Foundation for funding this project (Grant Nos. 55630.98 21-55558.98 and 20-63841.0021-55558.00). Without this, all would not have been possible.

I thank the International Geosphere Biosphere Programme for a poster award on the occasion of the "First Swiss Global Change Day" held on April 6th, 2000 in Bern.

I thank the IIIe Cycle Programme for a travel bursary that allowed me to participate at the "International Conference Geology of Oman" held in Muscat from January 12 - 16th, 2001.

My friends and family, thank you for the many moments you gave me to think about other things than this work.

10 REFERENCES

Abegg F. and Anderson A. L. (1997) The acoustic turbid layer in muddy sediments of Eckernfoerde Bay, western Baltic; methane concentration, saturation and bubble characteristics. *Marine Geology* **137**(1-2), 137-147.

Aerts R., Wallén B., and Malmer N. (1992) Growth-limiting nutrients in *Sphagnum*-dominated bogs subject to low and high atmospheric nutrient supply. *J. of Ecology* **80**, 131-140.

Alm J., Saarnio S., Nykänen H., Silvola J., and Martikainen P. J. (1999) Winter CO_2, CH_4 and N_2O fluxes on some natural and drained boreal peatlands. *Biogeochemistry* **44**, 163-186.

Armstrong W. and Boatman W. J. (1967) Some field observations relating the growth of bog plants to conditions of soil aeration. *J. Ecol.* **55**, 101-110.

Atekwana E. A. and Krishnamurthy R. V. (1998) Seasonal variations of dissolved inorganic carbon and $\delta\ ^{13}C$ of surface waters: application of a modified gas evolution technique. *J. Hydrology* **205**, 265-278.

Avery Jr. G. B., Shannon R. D., White J. R., Martens C. S., and Alperin M. J. (1999) Effect of seasonal changes in the pathways of methanogenesis on the $\delta\ ^{13}C$ values of pore water methane in a Michigan peatland. *Global Biogeochem. Cycles* **13**(2), 475-484.

Bartlett K. R. and Harriss R. C. (1993) Review and assessment of methane emissions from wetlands. *Chemosphere* **26**, 261-320.

Bergamaschi P. (1997) Seasonal variations of stable hydrogen and carbon isotope ratios in methane from a Chinese rice paddy. *J. Geophys. Res.* **102**, 25,383-25,393.

Berner E. K. and Berner R. A. (1987) *The Global Water Cycle: Geochemistry and Environment*. Prentice-Hall, 397 pages

Bondar A. D. (1987) Role of diffusion in differentiation of carbon isotopes of methane of the earth's crust (in Russian). *Geokhimiya* **9**, 1274-1283.

Boone D. R., Whitman W. B., and Rouvière P. (1993) Diversity and taxonomy of methanogens. In *Methanogenesis: Ecology, Physiology, Biochemistry and Genetics* (ed. F. G. Ferry), 35-82, Chapman & Hall.

Brand W. A. (1995) Precon: A fully automated interface for the pre-GC concentration of trace gases in air for isotopic analysis. *Isotopes Environ. Health Studies* **31**, 277-284.

Brown K. A. (1985) Sulphur distribution and metabolism in waterlogged peat. *Soil Biol. and Biochem.* **17**, 39-45.

Bubier J. L., Moore T. R., and Roulet N. T. (1993) Methane emissions from wetlands in the midboreal region of northern Ontario, Canada. *Ecology* **74**, 2240-2254.

Bülow K. (1929) *Allgemeine Moorgeologie - Handbuch der Moorkunde (German)*. 308 pages

Büttikofer J. (1942) Hochmoor Etang de la Gruère (German). *Naturschutz* **8**(5/6), 122-123.

Capone D. G. and Kiene R. P. (1988) Comparison of microbial dynamics in marine and freshwater sediments: Contrasts in anaerobic carbon catabolism. *Limnol. Oceanogr.* **33**, 725-749.

Chanton J. P., Crill P. M., Bartlett K. B., and Martens C. S. (1989a) Amazon capims (floating grassmats): A source of ^{13}C-enriched methane to the troposphere. *Geophys. Res. Lett.* **16**, 799-802.

Chanton J. P., Martens C. S., and Kelley C. A. (1989b) Gas transport from methane-saturated, tidal freshwater and wetland sediments. *Limnol. Oceanogr.* **34**(5), 807-819.

Charman D. J., Aravena R., Bryant C. L., and Harkness D. D. (1999) Carbon isotopes in peat, DOC, CO_2 and CH_4 in a Holocene peatland on Dartmoor, southwest England. *Geology* **27**(6), 539-542.

Chason D. B. and Siegel D. I. (1986) Hydraulic conductivity and related physical properties of peat, Lost River Peatland, Northern Minnesota. *Soil Science* **142**, 91-99.

Chodat F. (1924) La concentration en ions hydrogène du sol et son importance pour la constitution des formations végétales (French). PhD, Genève, 115 pages

Cicerone R. J. and Oremland R. S. (1988) Biogeochemical aspects of atmospheric methane. *Global Biogeochem. Cycles* **2**, 299-327.

Clymo R. S. (1983) Peat. In *Mires: Swamp, Bog, Fen, and Moor* (ed. A. J. P. Gore), 159-224, Elsevier.

Crill P. M., Bartlett K. B., Sebacher D. I., Harriss R. C., E.S. V., Gorham E., Madzar L., and Sanner J. (1988) Methane flux from Minnesota peatlands. *Global Biogeochem. Cycles* **2**, 371-384.

Crill P. M., Martikainen P. J., Nykanen H., and Silvola J. (1994) Temperature and N fertilization effects on methane oxidation in a drained peatland soil. *Soil. Biol. Biochem.* **26**, 1331-1339.

Crum H. A. (1984) *Sphagnopsida, Sphagnaceae*. 180 pages

Dachnowski A. (1912) Peat deposits of Ohio. Their origin, formation and uses. *Geol. Survey Ohio Bull.* **16**, 424.

Dahlman O., Mörck R., Ljungquist P., Reimann A., Johansson C., Borén H., and Grimvall A. (1993) Chlorinated structural elements in high molecular weight organic matter from unpolluted waters and bleached-kraft mill effluents. *Environ. Science and Techn.* **27**, 1616-1620.

Davidson E. A. (1991) Fluxes of nitrous oxide and nitric oxide from terrestrial ecosystems. In *Microbial Production and Consumption of Greenhouse Gases: Methane, Nitrogen Oxides and Halomethanes* (ed. J. E. Rogers and W. B. Whitman), 219-235, American Soc. for Microbiol.

Dedysh S. N., Panikov N. S., Liesack W., Grosskopf R., Zhou J., and Tiedje J. M. (1998) Isolation of acidophilic methane-oxidising bacteria from northern peat wetlands. *Science* **282**, 281-284.

Dise N. B. and Verry E. S. (2001) Suppression of peatland methane emission by cumulative sulfate deposition in simulated acid rain. *Biogeochemistry* **53**(2), 143-160.

Dobson A. T. (1979) Mire types of New Zealand. *International Symposium on Classification of Peat and Peatlands*, 82-95.

Drever J. I. (1982) *The Geochemistry of Natural Waters*. Prentice-Hall, 388 pages

Drever J. I. (1997) *The Geochemistry of Natural Waters: Surface and Ground Water Environment*. Prentice-Hall, 436 pages

Dungan P. (1990) Wetland conservation: A review of current issues and required action, page 99, IUCN-The World Conservation Union.

ECPA. **(2000)** *Position Paper on Soil Non-Extractable Residues*. European Crop Protection Association.

Eilrich B. and Steinmann P. (in prep.) Acetate in deep peat bog environments - Seasonal variation and implications for methanogenesis: Investigation of an ombrotrophic peat bog in the Jura Mountains, Switzerland.

EMPA. **(1985-1991)** *Nabel 1985-1991*. (Swiss Federal Laboratory for Materials Testing and Research); BUWAL (Bundesamt für Umwelt, Wald und Landschaft).

Engle D. and Melack J. M. (2000) Methane emissions from an Amazon floodplain lake: Enhanced release during episodic mixing and during falling water. *Biogeochemistry* **51**(1), 71-90.

Farrish K. W. and Grigal D. F. (1988) Decomposition in an ombrotrophic bog and a minerotrophic fen in Minnesota. *Soil Sci.* **145**, 353-358.

Fechner E. J. and Hemond H. F. (1992) Methane transport and oxidation in the unsaturated zone of a *Sphagnum* peatland. *Global Biogeochem. Cycles* **6**(1), 33-44.

Feldmeyer-Christe E. (1990) Etude pyto-écologique des tourbières des Franches-Montagnes (canton du Jura et de Berne, Suisse) (French). *Mat. levé géobot. de la Suisse* **66**, 1-163.

Forkert E. (1932) Geologische Beschreibung des Kartengebietes Tramelan im Berner Jura (German). *Eclogae Geol. Helv.* **26**, 1-41.

Freeman C., Lock M. A., and Reynolds B. (1993) Fluxes of CO_2, CH_4, and N_2O from a Welsh peatland following simulation of water table draw-down. Potential feedback to climate change. *Biogeochemistry* **19**, 51-60.

Freeze R. A. and Cherry J. A. (1979) *Groundwater*. Prentice Hall, 604 pages

Frenzel P. and Karofeld E. (2000) CH_4 emission from a hollow-ridge complex in a raised bog: The role of CH_4 production and oxidation. *Biogeochemistry* **51**(1), 91-112.

Frenzel P. and Rudolph J. (1998) Methane emission from a wetland plant - the role of CH_4 oxidation in *Eriophorum*. *Plant & Soil* **202**(1), 27-32.

Früh J. and Schröter C. (1904) *Die Moore der Schweiz, mit Berücksichtigung der gesamten Moorfrage (German)*. A. Francke, 750 pages

Fung I., John J., Lerner J., Matthews E., Prather M., Steele L. P., and Fraser P. J. (1991) Three-dimensional model synthesis of the global methane cycle. *J. Geophys. Res.* **96**, 13,033-13,065.

Gelwicks J. T., Risatti J. B., and Hayes J. M. (1989) Carbon isotope effects associated with autotrophic acetogenesis. *Org. Geochem.* **14**(4), 441-446.

Glenn S., Heyes A., and Moore T. R. (1993) Carbon dioxide and methane fluxes from drained peat soils, southern Quebec. *Global Biogeochem. Cycles* **7**, 247-257.

Gobat J.-M., Aragno M., and Matthey W. (1998) *Le sol vivant : bases de pédologie, biologie des sols (French)*. Presses polytechniques et universitaires romandes, 519 pages

Gore A. J. P. (1983) Ecosystems of the World, Vol. 4a - Mires: Swamp, bog, fen and moor. Elsevier.

Gorham E. (1991) Northern peatlands, role in the carbon cycle and probable responses to climate warming. *Acol. Appl.* **1**, 182-195.

Gorham E., Eisenreich S. J., Ford J., and Santelmann M. V. (1985) The chemistry of bog waters. In *Chemical Processes in Lakes* (ed. W. Stumm), 339-363, John Wiley & Sons.

Grünig A., Vetterli L., and Wildi O. (1984) *Inventaire des hauts-marais et marais de transition de Suisse (French/German)*. Swiss Fed. Inst. For. Res., 2100 pages

Harcourt. **(2002)** *Dictionary of Science and Technology*. Reed Elsevier.

Haworth R. D. (1971) The chemical nature of humic acid. *Soil Science* **111**(1), 71-79.

Hein R., Crutzen P. J., and Heimann M. (1997) An inverse modeling approach to investigate the global atmospheric methane cycle. *Global Biogeochem. Cycles* **11**, 43-76.

Hoehler T. M., Albert D. B., Alperin M. J., and Martens C. S. (1999) Acetogenesis from CO_2 in an anoxic marine sediment. *Limnol. Oceanogr.* **44**, 662-667.

Holdgate M. W. (1990) Wetlands in a changing world. In *4th Meeting of the Conference of the Contracting Parties*, page 8.

Holleman A. F. and Wiberg N. (1985) *Lehrbuch der Anorganischen Chemie (German)*. De Gruyter, 1456 pages

Hornibrook E. R. C. (1997) Aspects of carbon mineralization in temperate zone freshwater wetlands. PhD, University of Western Ontario, 295 pages

Hornibrook E. R. C., Longstaffe F. J., and Fyfe W. S. (1997) Spatial distribution of microbial methane production pathways in temperate zone wetland soils: Stable carbon and hydrogen isotope evidence. *Geochim. Cosmochim. Acta* **61**(4), 745-753.

Hornibrook E. R. C., Longstaffe F. J., and Fyfe W. S. (1998) Reply to Comment by S. Waldron, A. Fallick, and A. Hall on "Spatial distribution of microbial methane production pathways in temperate zone wetland soils; stable carbon and hydrogen isotope evidence." *Geochim. Cosmochim. Acta* **62**, 373-375.

Hornibrook E. R. C., Longstaffe F. J., and Fyfe W. S. (2000) Evolution of stable carbon isotope compositions for methane and carbon dioxide in freshwater wetlands and other anaerobic environments. *Geochim. Cosmochim. Acta* **64**(6), 1013-1027.

Houghton J. T., Meira Filho L. G., Callandar B. A., Haites E., Harriss N., and Maskell K. (1995) *Climate change 1994. Radiative forcing of climate change and an evaluation of the IPCC IS92 emission scenarios*. Cambridge University Press.

Houvelling S., Kaminski T., Dentener F., Lelieveld J., and Heimann M. (1999) Inverse modeling of methane sources and sinks using the adjoint of a global transport model. *J. Geophys. Res.* **104**, 26,137-26,160.

Hvorslev M. J. (1951) Time lag and soil permeability in ground-water observations. *U.S. Army Corps of Engineers' Bulletin* **36**, 50.

Inisheva L. I., Semtshov A. A., Liss O. L., Novikov C. M., and Inishev N. G. (2000) *Vasjugan Bog - Nature Conditions, Structure and Functioning*. Institute for Peat Research.

IPCC (1996) *How do bogs form?* Irish Peatland Conservation Council.

IPCC (2001) *Third Assessment Report - Climate Change 2001; The Scientific Basis & Summary for Policy Makers*. Intergovernmental Panel on Climate Change. pages

IPS (2002) http://www.peatsociety.fi/

Jasper J. P. (2001) Quantitative estimates of precision for molecular isotopic measurements. *Rap. Comm. Mass Spectrom* **15**, 1554-1557.

Jasper J. P., Edwards J. S., and Ford L. C. (2002) A novel method for Arson accelerant analysis: Gas chromatography/isotope ratio mass spectrometry. In *Arson Stable Isotope Analysis*, 11 pages.

Joray M. (1942) L'Etang de la Gruère. Etude pollenanalytique et stratigraphique de la tourbière (French). *Mat. levé géobot. de la Suisse* **25**, 1-117.

Kendall C. and Caldwell E. A. (1998) Isotope tracers in catchment hydrology (ed. C. Kendall and J. J. McDonnell), 51-86. Elsevier Science B.V.

Kettunen A., Kaitala V., Alm J., Silvola J., Nykanen H., and Martikainen P. J. (1996) Cross-correlation analysis of the dynamics of methane emissions from a boreal peatland. *Global Biogeochem. Cycles* **10**(3), 457-471.

Kivinen E. and Pakarinen P. (1981) Geographical distribution of peat resources and major peatland complex types in the world. *Ann. Acad. Sci. Fennicae* **AIII**(132), 28 pages.

Kotilainen M. J. (1927) *Untersuchungen über die Beziehungen zwischen der Pflanzendecke der Moore und der Beschaffenheit, besonders der Reaktion des Torfbodens (German).* 229 pages

Krauskopf K. B. and Bird D. (1995) *Introduction to Geochemistry*. Mc Graw-Hill, 647 pages

Krishnamurthy R. V., Atekwana E. A., and Guha H. (1997) A simple inexpensive carbonate-phosphoric acid reaction method for analysis of carbon and oxygen isotopes of carbonate. *Anal. Chem.* **69**, 4256-4258.

Kurz H. (1928) Influence of *Sphagnum* and other mosses on bog reactions. *Ecology* **9**, 56-69.

Küttel M. (1997) Mapping of mires in Switzerland - starting point and results. In *Global Peat Resources* (ed. E. Lappalainen), 145-148, International Peat Society.

Lang C., Leuenberger M., Schwander J., and Johnsen S. (1999) 16 °C Rapid temperature variation in Central Greenland 70,000 years ago. *Science* **286**, 934-937.

Lansdown J. M., Quay P. D., and King S. L. (1992) CH_4 production via CO_2 reduction in a temperate bog: A source of ^{13}C-depleted CH_4. *Geochim. Cosmochim. Acta* **56**, 3493-3503.

Lappalainen E. (1997) General review on World peatland and peat resources. In *Global Peat Resources* (ed. E. Lappalainen), 53-56, International Peat Society.

Lelieveld J., Crutzen P., and Dentener F. J. (1998) Changing concentration, lifetime and climate forcing of atmospheric methane. *Tellus* **50B**, 128-150.

Leuenberger M., Lang C., and Schwander J. (1999) Delta 15N measurementsas a calibration tool for the paleothermometer and gas-ice age differences: A case study for the 8200 B.P. event on GRIP ice. *J. Geophys. Res.* **104**(D18), 22,163-22,170.

Leuenberger M., Nyfeler P., Moret H. P., Sturm P., and Huber C. (2000a) A new gas inlet system for isotope ratio mass spectrometer improves reproducibility. *Rapid Communications in Mass Spectrometry* **14**(16), 1543-1551.

Leuenberger M., Nyfeler P., Moret H. P., Sturm P., Indermühle A., and Schwander J. (2000b) CO_2-concentration measurements on air samples by mass spectrometry. *Rapid Communications in Mass Spectrometry* **14**(16), 1552-1557.

Leuenberger M. and Siegenthaler U. (1992) Ice-age atmospheric concentration of nitrous oxide from an Antarctic ice core. *Nature* **360**(6403), 449-451.

Lide D. R. (1996) CRC Handbook of Chemistry and Physics. CRC Press.

Likens G. E., Bormann F. H., Pierce R. S., Eaton J. S., and Johnson N. M. (1977) *Biogeochemistry of a forested ecosystem*. Springer, 135 pages

Lovley D. R. and Klug M. J. (1986) Model for the distribution of sulfate reduction and methanogenesis in freshwater sediments. *Geochim. Cosmochim. Acta* **50**, 11-18.

Maeder F. (2000) Influence d'enrichissement en CO_2 et en azote sur les communautés *bacteria* et *archaea* d'une tourbière à sphaignes du Jura (Projet BERI) (French). PhD, Université de Neuchâtel, 108 pages

Makhov G. A. and Bazhin N. M. (1999) Methane emission from lakes. *Chemosphere* **38**(6), 1453-1459.

Maltby E. (1988) Properties, geomorphology and classification of peatlands. - Symposium on the hydrology of wetlands in temperate and cold regions. *The Publications of the Academy of Finland* **2**(5), 5-13.

Maltby E. and Proctor M. C. F. (1997) Peatlands: Their nature and role in the biosphere. In *Global Peat Resources* (ed. E. Lappalainen), pp. 11-19. International Peat Society.

Malterer T. J. (1997) Peat resources of the United States. In *Global Peat Resources* (ed. E. Lappalainen), pp. 253-260. International Peat Society.

Martens C. S., Blair N. E., Green C. D., and Des Marais D. J. (1986) Seasonal variation in the stable carbon isotope signature of biogenic methane in coastal sediment. *Science* **233**, 1300-1303.

Martens C. S., Kelley C. A., Chanton P. J., and Showers W. J. (1992) Carbon and hydrogen isotopic characterization of methane from wetlands and lakes of the Yukon-Kuskokwim Delta, western Alaska. *J. Geophys. Res.* **97**, 16,689-16,701.

Martikainen P. J. (1997) The fluxes of greenhouse gases CO_2, CH_4 and N_2O in northern peatlands. In *Global Peat Resources* (ed. E. Lappalainen), 29-36, International Peat Society.

Martikainen P. J., Nykanen H., Alm J., and Silvola J. (1995) Change in fluxes of carbon dioxide, methane and nitrous oxide due to forest drainage of mire sites of different trophy. *Plant and Soil* **168/169**, 571-577.

Martikainen P. J., Nykanen H., Crill P. M., and Silvola J. (1993) Effect of lowered water table on nitrous oxide fluxes from northern peatlands. *Nature* **366**, 51-53.

McKenzie J. M., Siegel D. I., Shotyk W., Steinmann P., and Pfunder G. (2002) Heuristic numerical and analytical models of the hydrologic controls over vertical solute transport in a domed peat bog, Jura Mountains, Switzerland. *Hydrol. Process.* **16**, 1047-1064.

Ménot G. and Burns S. J. (2001) Carbon isotopes in plants as climatic indicators: Calibration from an altitudinal transect of ombrotrophic peat bogs in Switzerland. *Org. Geochem.* **32**(233-245).

Miyajima T., Wada E., Hanba Y. T., and Vijarnsorn P. (1997) Anaerobic mineralisation of indigenous organic matters and methanogenesis in tropical wetland soils. *Geochim. Cosmochim. Acta* **61**, 3739-3751.

Moore T. R. and Dalva M. (1997) Methane and carbon dioxide exchange potentials of peat soils in aerobic and anaerobic laboratory incubations. *Soil Biol. Biochem.* **29**(8), 1157-1164.

Moore T. R. and Knowles R. (1989) The influence of water table levels on carbon dioxide emissions from peatland soils. *Canadian J. Soil Sci.* **69**, 33-38.

Moore T. R. and Knowles R. (1990) Methane emissions from fen, bog and swamp peatlands in Quebec. *Biogeochemistry* **11**, 45-61.

Moore T. R. and Roulet N. T. (1991) A comparison of dynamic and static chambers for methane emission measurements from subarctic fens. *Atmos. Ocean.* **29**(1), 102-109.

Mulhauser B. (1996) *La Gruère - Pays d'etangs et de marais noirs (French)*. Fondation Les Cerlatez. 39 pages

Niewöhner C., Hensen C., Kasten S., Zabel M., and Schulz H. D. (1998) Deep sulfate reduction completely mediated by anaerobic methane oxidation in sediments of the upwelling area off Namibia. *Geochim. Cosmochim. Acta* **62**, 455-464.

Nikonov M. N. and Sluka V. K. (1964) Distribution of peatlands (in Russian). *Pocvovedenie* **10**, 44-50.

Nykanen H., Alm J., Silvola J., Tolonen K., and Martikainen P. J. (1998) Methane fluxes on boreal peatlands of different fertility and the effect of long-term experimental lowering of the water table on flux rates. *Global Biogeochem. Cycles* **12**(1), 53-69.

Nykanen H., Silvola J., Alm J., and Martikainen P. J. (1997) The effect of peatland forestry on fluxes of carbon dioxide, methane, and nitrous oxide. In *Northern Forested Wetlands; Ecology and Management* (ed. C. C. Trettin, M. F. Jurgensen, D. F. Grigal, M. R. Gale, and J. K. Jeglum), 325-339, Lewis Publishers.

Panikov N. S., Semenov A. M., Tarasov A. A., Belyaev A. S., Kravchenko L. K., Smagina M. V., Palejeva M. V., Zelenev V. V., and Skupchenko K. V. (1993) Methane production and uptake in soils of the European part of the USSR. *J. Ecol. Chem.* **1**, 7-18.

Pernaton E., Prinzhofer A., and Schneider F. (1996) Reconsideration of methane signature as a criterion for the genesis of natural gas: influence of migration on isotopic signature. *Rev. IFP* **51**(5), 635-651.

Piteau A. (1993) *Groundwater Mapping and Assessment in British Columbia*. Piteau Associates - Resources Inventory Committee.

Prinzhofer A. and Pernaton E. (1997) Isotopically light methane in natural gas: bacterial imprint or diffusive fractionation? *Chem. Geol.* **142**, 193-200.

Puustjärvi V. (1952) The precipitation of iron in peat soils. *Acta Agralia Fenn.* **78**, 72.

Rabassa J., Coronato A., and Roig C. (1997) The peat bogs of Tierra del Fuego, Argentina. In *Global Peat Resources* (ed. E. Lappalainen), 261-266, International Peat Society.

Ramann E. (1895) Organogene Ablagerungen der Jetztzeit (German). *Neues Jahrbuch Mineral., Geol., Palaeontol.* **10**, 119-166.

Reeburgh W. S., Hirsch A. I., Sansone F. J., Popp B. N., and Rust T. M. (1997) Carbon kinetic isotope effect accompanying microbial oxidation of methane in boreal forest soils. *Geochim. et Cosmochim. Acta* **61**(22), 4761-4767.

Reeve A. S., Warzocha J., Glaser P. H., and Siegel D. I. (2001) Regional ground-water flow modeling of the glacial Lake Agassiz peatlands, Minnesota. *J. of Hydrology* **243**(1-2), 91-100.

Rieley J. O., Page S. E., and Setiadi B. (1997) Distribution of peatlands in Indonesia. In *Global Peat Resources* (ed. E. Lappalainen). International Peat Society.

Rigg G. B., Thompson T. G., Lorah J. R., and Williams K. T. (1927) Dissolved gases in waters of some Pudget Sound bogs. *Botanical Gazette* **84**, 264-278.

Romanowiecz E. A., Siegel D. I., and Glaser P. H. (1993) Hydraulic reversals and episodic methane emissions during drought cycles in mires. *Geology* **21**, 231-234.

Roulet N. T., Jano A., Kelly C. A., Klinger L. F., Moore T. R., Protz R., Ritter A., and Rouse W. R. (1994) Role of Hudson Bay lowland as a source of atmospheric methane. *J. Geophys. Res.* **99**(1439-1454).

Roulet N. T. and Moore T. R. (1995) The effect of forestry drainage practises on the emission of methane from northern peatlands. *Canadian J. Forestry Res.* **25**, 491-499.

Rubec C. (1997) The status of peatland resources in Canada. In *Global Peat Resources* (ed. E. Lappalainen), 243-252, International Peat Society.

Sander R. (1999) Compilation of Henry's law constants for inorganic and organic species of potential importance in environmental chemistry; http://www.mpch-mainz.mpg.de/~sander/res/henry.html

Schoell M. (1980) The hydrogen and carbon isotopic composition of methane from natural gases of various origins. *Geochim. Cosmochim. Acta* **44**, 649-661.

Schoell M. (1988) Multiple origins of methane in the Earth. In *Origins of Methane in the Earth*, Vol. 1 (ed. M. Schoell), pp. 1-10. Elsevier.

Shannon R. D. and White J. R. (1994) A three-year study of controls on methane emissions from two Michigan peatlands. *Biogeochemistry* **27**, 35-60.

Shannon R. D. and White J. R. (1996) The effects of spatial and temporal variations in acetate and sulfate on methane cycling in two Michigan peatlands. *Limnol. Oceanogr.* **41**(3), 435-443.

Shotyk W. (1986) The inorganic geochemistry of peats and the physical chemistry of waters from some *Sphagnum* bogs. PhD, University of Western Ontario, Canada, 176 pages

Shotyk W. (1987) European contributions to the geochemistry of peatland waters, 1890-1940. *Symposium '87, Wetlands / Peatlands*, 115-125.

Shotyk W. (1988) Review of the inorganic geochemistry of peats and peatland waters. *Earth Science Reviews* **25**, 95-176.

Shotyk W. (1989a) The chemistry of peatland waters. *Water Quality Bulletin* **14**(2), 47-58, 103-?

Shotyk W. (1989b) An overview of the geochemistry of methane dynamics in mires. *Int. Peat J.* **3**, 25-44.

Shotyk W. (1997) Atmospheric deposition and mass balance of major and trace elements in two oceanic peat bog profiles, northern Scotland and the Shetland Islands. *Chemical Geology* **138**(1-2), 55-72.

Shotyk W., Weiss D., Appleby P. G., Cherburkin A. K., Frei R., Gloor M., Kramers J. D., Reese S., and Van Der Knaap W. O. (1998) History of atmospheric lead deposition since 12,370 ^{14}C yr BP from a peat bog, Jura Mountains, Switzerland. *Science* **281**, 1635-1640.

Shotyk W., Weiss D., Kramers J. D., Frei R., Cherburkin A. K., Gloor M., and Reese S. (2001) Geochemistry of the peat bog at Etang de la Gruère, Jura Mountains, Switzerland, and its record of atmospheric Pb and lithogenic trace metals (Sc, Ti, Y, Zr, and REE) since 12,370 ^{14}C yr BP. *Geochim. Cosmochim. Acta* **65**, 2337-2360.

Siegel D. I., Chanton J. P., Glaser P. H., Chasar L. S., and Rosenberry D. O. (2001) Estimating methane production rates in bogs and landfills by deuterium enrichment of pore water. *Global Biogeochem. Cycles* **15**(4), 967-975.

Siegel D. I., Glaser P. H., Chanton P. J., Reeve A. S., and Romanowicz E. A. (1997) Hydrogeochemical controls over the production of greenhouse gases in peatlands. *Geological Society of America, 1997 annual meeting*, 286 pages.

Siegel D. I., Reeve A. S., Glaser P. H., and Romanowicz E. A. (1995) Climate-driven flushing of pore water in peatlands. *Nature* **374**(6522), 531-533.

Sigren L. K., Byrd G. T., Fisher F. M., and R.L. S. (1997) Comparison of soil acetate concentrations and methane production, transport, and emission in two rice cultivars. *Global Biogeochem. Cycles* **11**, 1-14.

Sims W. R., Looney B. B., and Eddy C. A. (1991) Evaluation of a rapid headspace analysis method for analysis of volatile constituents in soils and sediments. *Ground Water Management* **5**, 655-668.

Sjörs H. (1981) The zonation of northern peatlands and their importance for the carbon balance of the atmosphere. *Int. J. Ecol. Environ. Sci.* **7**, 11-14.

Stein W. D. and Lieb W. R. (1986) Transport and diffusion across cell membranes, 89-90, Academic Press.

Steinmann P. (1995) Geochemistry of atmospheric inputs and pore water genesis in two contrasting *Sphagnum* bog profiles, Jura Mountains, Switzerland. PhD, Bern University, Switzerland, 146 pages

Steinmann P., Burns S. J., and Shotyk W. (1998) Acetate accumulations in shallow and deep layers of peat bogs as a potential source of atmospheric CH_4. *Mineralog. Mag.* **62 A**, 1454-1455.

Steinmann P., Eilrich B., and Burns S. J. (2000) δ ^{13}C patterns of CO_2 and CH_4 in peatlands: The role of diffusion/advection vs. microbial reactions. In *Non-CO_2 Greenhouse Gases: Scientific Understanding, Control and Implementation* (ed. J. Van Ham, A. P. M. Baede, L. A. Meyer, and R. Ybema), pp. 151-152. Kluwer Academic Publishers.

Steinmann P. and Shotyk W. (1994) Pore-water indicators of rainwater-dominated versus groundwater-dominated peat bog profiles (Jura Mountains, Switzerland). *Chemical Geology* **116**, 137-146.

Steinmann P. and Shotyk W. (1995) Ion chromatography of organic-rich natural waters from peatlands - III.Improvements for measuring anions and cations. *J. Chromatography* **A 706**, 281-286.

Steinmann P. and Shotyk W. (1996) Sampling anoxic pore waters in peatlands using "peepers" for in situ filtration. *Fresenius J. Anal. Chem.* **354**, 709-713.

Steinmann P. and Shotyk W. (1997a) Chemical composition, pH, and redox state of sulfur and iron in complete vertical porewater profiles from two *Sphagnum* peat bogs, Jura Mountains, Switzerland. *Geochim. Cosmochim. Acta* **61**(6), 1143-1163.

Steinmann P. and Shotyk W. (1997b) Geochemistry, mineralogy, and geochemical mass balance on major elements in two peat bog profiles (Jura Mountains, Switzerland). *Chemical Geology* **138**, 25-53.

Stevenson F. J. (1985) Geochemistry of soil humic substances. In *Humic Substances in Soil, Sediment, and Water; Geochemistry, Isolation, and Characterization* (ed. G. R. Aiken, D. M. McKnight, R. L. Wershaw, and P. MacCarthy), 13-52, John Wiley and Sons.

Stumm W. and Morgan J. J. (1981) *Aquatic Geochemistry*. Wiley & Sons, 780 pages

Sugimoto A. and Wada E. (1993) Carbon isotopic composition of bacterial methane in a soil incubation experiment; contributions of acetate and CO_2 / H_2. *Geochim. Cosmochim. Acta* **57**(16), 4015-4027.

Sundh I., Mikkelä C., Nilson M., and Svensson B. H. (1995) Potential aerobic methane oxidation in a *Sphagnum*-dominated peatland - Controlling factors and relation to methane emission. *Soil Biol. Biochem.* **27**, 829-837.

Syngayevsky Y. D., Lebedev V. S., Safronova T. P., and Sushilin A. V. (1978) Study of fractionation of carbon isotopes during migration of hydrocarbons in the gas phase through rocks (in Russian). *Geol. Nefti Gaza* **1**, 53-59.

Tang Y., Perry J. K., Jenden P. D., and Schoell M. (2000) Mathematical modeling of stable carbon isotope ratios in natural gases. *Geochim. Cosmochim. Acta* **64**(15), 2673-2687.

Telmer K. and Veizer J. (1999) Carbon fluxes, pCO_2 and substrate weathering in a large northern river basin, Canada: carbon isotope perspectives. *Chem. Geol.* **159**, 61-86.

Turunen J., Tahvanainen T., Tolonen K., and Pitkänen A. (2001) Carbon accumulation in West Siberian mires, Russia. *Global Biogeochem. Cycles* **15**(2), 285-296.

Turunen J. and Tolonen K. (1997) Rate of carbon accumulation in boreal peatlands and climate change. In *Global Peat Resources* (ed. E. Lappalainen), 21-28, International Peat Society.

Tyler S. C., Zimmerman P. R., Cumberbatch C., Greenberg J. P., Westberg C., and Darlington J. P. E. C. (1988) Measurements and interpretation of $\delta\ ^{13}C$ of methane from termites, rice paddies, and wetlands in Kenya. *Global Biogeochem. Cycles* **2**(341-355).

Updegraff K., Bridgham S. D., Pastor J., and Weishampel P. (1998) Hysteresis in the temperature response of carbon dioxide and methane production in peat soils. *Biogeochemistry* **43**(3), 253-272.

Urban N. R., Eisenreich S. J., and Gorham E. (1987) Aluminum, iron, zinc, and lead in bog waters of northeastern North America. *Canadian Journal of Fisheries and Aquatic Sciences - Journal Canadien des Sciences Halieutiques et Aquatiques* **44**(6), 1165-1172.

Van Bodegom P. M., Groot T., Van den Hout B., Leffelaar P. A., and Goudriaan J. (2000) Diffusive gas transport through flooded rice systems. In *Methane Emissions from Rice Paddies; Experiments and Modelling* (ed. P. M. Van Bodegom), 113-132.

Van Bodegom P. M. and Scholten J. C. M. (2001) Microbial processes of CH_4 production in a rice paddy soil; model and experimental validation. *Geochim. Cosmochim. Acta* **65**(13), 2055-2066.

Vogt G. L. and Wargo M. J. (1993) *Microgravity - Teaching Guide With Activities for Physical Science*. National Aeronautics and Space Administration.

Voice T. C. and Kolb B. (1993) Static and dynamic headspace analysis of volatile organic compounds in soils. *Environ. Science & Techn.* **27**(4), 709-713.

Von Post L. and Granlund E. (1925) *Sveriges Geol. Undersok. Ser. C, No. 335 (Swedish)*, 127 pages

Waldron S., Fallick A. E., and Hall A. J. (1998) Comment on "Spatial distribution of microbial methane production pathways in temperate zone wetland soils: Stable carbon and hydrogen evidence" by E.R.C. Hornibrook, F.J. Longstaffe, and W.S. Fyfe. *Geochim. Cosmochim. Acta* **62**(2), 369-372.

Waldron S., Lansdown J. M., Scott E. M., Fallick A. E., and Hall A. J. (1999) The global influence of the hydrogen isotope composition of water on that of bacteriogenic methane from shallow freshwater environments. *Geochim. Cosmochim. Acta* **63**(15), 2237-2245.

Wellsbury P., Goodman K., Cragg B. A., and Parkes R. J. (2000) The geomicrobiology of deep marine sediments from Blake Ridge containing methane hydrate (Sites 994, 995, and 997). In *Proceedings of the Ocean Drilling Program, Scientific Results*, Vol. 164 (ed. C. K. Paull, R. Matsumoto, P. J. Wallace, and W. P. Dillon), 379-391.

Wermeille C. (1998) Aide mémoire pour animations sur le site. In *Fondation Les Cerlatez - étude, information et protection des tourbières (French)*, 58 pages.

Westerhoff H. V., Groen A. K., and Wanders J. A. (1984) Modern theories of metabolic control and their applications. *Biosc. Rept.* **4**, 1-22.

Weyhenmeyer C. E. (1999) Methane emissions from beaver ponds: Rates, patterns, and transport mechanisms. *Global Biochem. Cycles* **13**(4), 1079-1090.

Whigham D. F., Dykyjová D., and Hejný S. (1993) Wetlands of the World: Inventory, ecology and management. In *I. Handbook of Vegetation Science*, Vol. 15/2. Kluwer.

Whiticar M. J., Faber, E., and Schoell M. (1986) Biogenic methane formation in marine and freshwater environments: Carbon dioxide reduction versus acetate fermentation. *Geochem. Cosmochim. Acta.* **50**, 693-709.

Wind-Mulder H. L. and Vitt D. H. (2000) Comparisons of water and peat chemistries of a post-harvested and undisturbed peatland with relevance to restoration. *Wetlands* **20**(4), 616-628.

Wuebbles D. J. and Hayhoe K. (2000) Atmospheric methane: trends and impacts. In *Non-CO_2 Greenhouse Gases: Scientific Understanding, Control and Implementation* (ed. J. van Ham, A. P. M. Baede, L. A. Meyer, and R. Ybema), 1-44, Kluwer Academic Press.

.

11 APPENDICES

Appendix I
General and physical data
(AI 1 - AI 3)

Appendix II
Pore water geochemical data
(AII 1 - AII 14)

Appendix III
Posters
(NCGG-2'99; Swissed'00; CH_4-Mitigation-2'00; Goldschmidt'00; EUG '01; ACE'01; GEA-LAMUN)

Appendix IV
Model parameters and constants